

**FORMULATION OF THE PARTICLE SIZE DISTRIBUTION EFFECTS ON THE  
RHEOLOGY AND HYDRAULICS OF HIGHLY-CONCENTRATED SUSPENSIONS**

by

Turgay Dabak

Dissertation submitted to the Faculty of the  
Virginia Polytechnic Institute and State University  
in partial fulfillment of the requirements for the degree of  
Doctor of Philosophy  
in  
Civil Engineering

APPROVED:

\_\_\_\_\_  
Oner Yucel, Chairman

\_\_\_\_\_  
Walter R. Hibbard

\_\_\_\_\_  
G. V. Loganathan

\_\_\_\_\_  
Chin Y. Kuo

\_\_\_\_\_  
James M. Wiggert

June, 1986  
Blacksburg, Virginia

# FORMULATION OF THE PARTICLE SIZE DISTRIBUTION EFFECTS ON THE RHEOLOGY AND HYDRAULICS OF HIGHLY-CONCENTRATED SUSPENSIONS

by

Turgay Dabak

Oner Yuçel, Chairman

Civil Engineering

(ABSTRACT)

A formulation was developed for the rheologic characterization of highly concentrated suspensions, accounting for the physical effects of particle size distribution. A number of dimensionless parameters were developed signifying the physical characteristics of the solids and the vehicle fluid, and functionally related to the yield-stress and a flow parameter. Each of these expressions of the formulation contains an empirical dimensionless coefficient accounting for the interparticle and fluid/solid interactions that are not explained by the physical parameters involved. A formulation and a methodology were also developed for predicting the shear viscosity behavior of highly-concentrated suspensions at low and high shear-rates through the use of three parameters signifying effects of particle size distribution. A number of applications were made using various non-coal and limited coal-liquid mixture data reported in the literature to demonstrate the general validity of the formulations.

A methodology was proposed for the analysis of the particle size distribution effects on the overall optimum energy efficiency during hydraulic transportation and particle size reduction. The computer model developed for this purpose was employed to evaluate the transportation energy consumption and the energy consumed in grinding process to prepare the slurry, in pipes of various sizes and lengths for a coal slurry of various specified particle size distributions and concentrations. Correlations obtained indicated the sensitivity of transportation energy efficiency to various parameters including the

maximum packing concentration, relative concentration, specific surface area of particles, surface area mean size, pipe size and length, and annual mixture throughput. The results of combined energy calculations have shown that the particle size distribution and related physical parameters can significantly affect the energy efficiency due to both grinding and transportation, and the delivered cost of slurry fuels.

## ACKNOWLEDGEMENTS

The author would like to express sincere gratitude to his faculty advisor, Dr. Oner Yucel, for his instrumental guidance, encouragement, and invaluable suggestions, throughout the development of this research. Special thanks are also due to Dr. Walter R. Hibbard Jr., who served on the author's advisory committee, helped in obtaining the financial assistance for the study, and provided continuous, gracious support. Without the efforts and contributions of these professors, this work would not have been possible.

The author also wishes to thank Dr. Chin Y. Kuo, Dr. G. V. Loganathan and Dr. James M. Wiggert for their review of this dissertation and participation on the examining committee.

This work has been supported by the Civil Engineering Department, Virginia Mining and Minerals Resources Research Institute, and the Virginia Center for Coal and Energy Research at the Virginia Polytechnic Institute and State University.

Finally, the author humbly dedicates this work to his parents, who sacrificed much to ensure that he receive the best education possible. They continuously kept their faith, encouraged, and provided him with moral support over the years.



# TABLE OF CONTENTS

<b>INTRODUCTION</b> .....	<b>1</b>
1.1 DEFINITIONS AND GENERAL REMARKS ON SOLID-LIQUID MIXTURES ..	1
1.2 PROBLEM IDENTIFICATION AND OBJECTIVES OF THE PRESENT STUDY .	4
1.3 OUTLINE OF PRESENT STUDY .....	6
<b>BASIC CONCEPTS AND PAST STUDIES ON SOLID-LIQUID MIXTURES</b> .....	<b>8</b>
2.1 INTRODUCTORY REMARKS .....	8
2.2 FUNDAMENTAL PROPERTIES OF SOLID-LIQUID MIXTURES .....	8
2.3 PREVIOUS STUDIES ON SOLID-LIQUID SUSPENSIONS .....	16
2.3.1 Viscosity Models .....	16
2.3.2 Particle Size Distribution Models .....	22
2.3.3 Suspension Mechanics Models .....	26
<b>THEORETICAL DEVELOPMENT OF THE RHEOLOGICAL FORMULATIONS</b> ....	<b>30</b>
3.1 INTRODUCTORY REMARKS .....	30
3.2 FUNDAMENTAL SHEAR STRESS SHEAR RATE RELATION .....	31
3.3 PROPOSED FORMULATIONS .....	35

<b>SHEAR VISCOSITY BEHAVIOR AT LOW AND HIGH SHEAR RATES</b> .....	<b>45</b>
4.1 INTRODUCTORY REMARKS .....	45
4.2 THEORETICAL BASIS .....	46
4.3 DETERMINATION OF MAXIMUM PACKING CONCENTRATION .....	52
<b>ENERGY REQUIREMENT IN HYDRAULIC CONVEYANCE AND COMMINUTION OF SOLIDS</b> .....	<b>56</b>
5.1 INTRODUCTORY REMARKS .....	56
5.2 PUMPING CHARACTERISTICS OF PSEUDO-HOMOGENEOUS TIME-INDEPENDENT NON-NEWTONIAN MIXTURES IN LAMINAR FLOW ...	57
5.3 GRINDING CHARACTERISTICS OF SOLID PARTICLES .....	61
<b>COMPUTER IMPLEMENTATION</b> .....	<b>65</b>
6.1 GENERAL REMARKS .....	65
6.2 LIST OF THE MOST SIGNIFICANT VARIABLES IN THE COMPUTER PROGRAM .....	67
6.3 DESCRIPTION OF THE MAIN PROGRAM AND SUBPROGRAMS .....	69
<b>APPLICATIONS, RESULTS AND EVALUATIONS</b> .....	<b>72</b>
7.1 INTRODUCTORY REMARKS .....	72
7.2 CHARACTERISTICS OF THE DATA ANALYZED .....	73
7.3 PROCEDURE FOR ANALYSES AND CALCULATIONS .....	81
7.4 PREDICTION OF SHEAR STRESS VERSUS SHEAR RATE RELATIONSHIPS .	84
7.5 PREDICTION OF SHEAR VISCOSITY BEHAVIOR AT VARYING SHEAR RATES .....	104
7.5.1 Shear Rate Dependence of the Particle Interaction Parameter $n$ .....	106

7.6 OPTIMIZATION OF PARTICLE SIZE DISTRIBUTION .....	120
<b>CONCLUSIONS AND RECOMMENDATIONS .....</b>	<b>135</b>
8.1 CONCLUSIONS .....	135
8.2 RECOMMENDATIONS .....	137
<b>COMPUTER PROGRAM LISTING .....</b>	<b>139</b>
<b>NUMERICAL RESULTS OBTAINED FOR THE ANALYSES .....</b>	<b>157</b>
<b>REFERENCES .....</b>	<b>218</b>
<b>Vita .....</b>	<b>223</b>

## LIST OF ILLUSTRATIONS

Figure 1.	Flow curves of non-Newtonian fluids [28]	10
Figure 2.	Typical shapes of flow curves for the three rheological models of most interest [29]	11
Figure 3.	Time dependent fluids [28]	13
Figure 4.	Schematic illustration of possible sphere arrangements in a packing situation	15
Figure 5.	Typical shear stress shear rate diagram characterizing the behavior employed in the development of formulations	36
Figure 6.	Proportionality of the first dimensionless parameter to the second for each suspension	38
Figure 7.	Proportionality of the first and second dimensionless parameters to the third for each suspension	40
Figure 8.	Proportionality between the dimensionless parameters for the derivation of B (nickel/sodium suspension)	42
Figure 9.	Proportionality between the dimensionless parameters for the derivation of B (alumina/xylene suspension)	43
Figure 10.	Viscosity at low shear rates versus mobility parameter for suspensions listed in Table 2	48
Figure 11.	Viscosity at high shear rates versus mobility parameter for suspensions listed in Table 2	49
Figure 12.	Maximum packing concentrations for binary mixtures of spherical particles	54
Figure 13.	Specific comminution work $N$ vs feed particle size for a constant reduction ratio	63
Figure 14.	Block diagram of the computer model	66
Figure 15.	Particle size distribution of nickel used in nickel-sodium and nickel-xylene suspensions	77

Figure 16. Particle size distribution of alumina used in alumina-xylene and alumina-glycerin suspensions .....	78
Figure 17. Particle size distribution of coal used in coal-glycerin suspension .....	79
Figure 18. Particle size distribution of coal used in coal-oil suspension .....	80
Figure 19. Experimental and predicted behaviors of nickel-sodium suspension .....	87
Figure 20. Experimental and predicted behaviors of nickel-xylene suspension .....	88
Figure 21. Experimental and predicted behaviors of alumina-xylene suspension .....	89
Figure 22. Experimental and predicted behaviors of alumina-glycerin suspension .....	90
Figure 23. Experimental and predicted behaviors of coal-glycerin suspension .....	91
Figure 24. Experimental and predicted behaviors of coal-oil suspension .....	92
Figure 25. Flow behavior of nickel-sodium suspension .....	93
Figure 26. Flow behavior of nickel-xylene suspension .....	94
Figure 27. Flow behavior of alumina-xylene suspension .....	95
Figure 28. Flow behavior of alumina-glycerin suspension .....	96
Figure 29. Flow behavior of coal-glycerin suspension .....	97
Figure 30. Flow behavior of coal-oil suspension .....	98
Figure 31. Experimental and predicted behaviors of "as received" coal in oil .....	101
Figure 32. Experimental and predicted behaviors of 70% + 600-700 with 30% -45 micron coal in oil .....	102
Figure 33. Experimental and predicted behaviors of 50% + 600-700 with 50% -45 micron coal in oil .....	103
Figure 34. Results of predicted relative viscosity at low shear rates .....	107
Figure 35. Results of predicted relative viscosity at high shear rates .....	108
Figure 36. Correlation between measured and predicted maximum packing concentrations .	109
Figure 37. Variation of n with shear rate for nickel-sodium suspension (concentration = 0.304)	114
Figure 38. Variation of n with shear rate for nickel-sodium suspension (concentration = 0.296)	115
Figure 39. Variation of n with shear rate for nickel-sodium suspension (concentration = 0.286)	116
Figure 40. Variation of n with shear rate for coal-glycerin suspension (concentration = 0.460)	117

Figure 41. Variation of $n$ with shear rate for coal-glycerin suspension (concentration = 0.403)	118
Figure 42. Variation of $n$ with shear rate for coal-glycerin suspension (concentration = 0.384)	119
Figure 43. Energy consumption with respect to specific surface area in a stirred-ball mill	122
Figure 44. Original particle size distribution and the limits in which the distribution was varied	125
Figure 45. Variation of the percent of pumping energy with pipe size for various particle size distributions	128
Figure 46. Variation of total energy with pipe size for distributions in Figure 42	129
Figure 47. Variation of the normalized total energy with normalized specific surface area for various pipe sizes	131
Figure 48. Variation of the normalized total energy with normalized specific surface area for various pipe lengths	132
Figure 49. Variation of total energy with annual throughputs for various size distributions	134

## LIST OF TABLES

Table 1. Selected Relative Viscosity Models .....	17
Table 2. Experimental and Predicted Viscosities at Low and High Shear Rates .....	47
Table 3. Correlation of Calculated and Experimental Values of the Maximum Packing Concentration .....	55
Table 4. Physical Properties of Systems used in Applications (Raw Data) .....	74
Table 5. Calculated Physical Properties of Systems .....	75
Table 6. Parameters Characterizing Various Particle Size Distribution of a Coal-Oil Mixture	99
Table 7. Variation of viscosity and $n$ with shear rate for Sodium-Nickel Suspension .....	112
Table 8. Variation of Viscosity and $n$ with shear rate for the Coal-Glycerin Suspension ..	113
Table 9. Values of Three Parameters as Affected by the Change of the Particle Size Distribution .....	124

## NOMENCLATURE

- A : Proportionality constant in Equation (2.19)
- A : Lumped kinetic parameter in Equation (2.27)
- B : Flow parameter
- d : Diameter of solid particle
- $d_j$  : Particle size that corresponds to  $S_j$
- $d_L$  : Diameter of largest particle in a particle size distribution
- $d_m$  : Size modulus
- $d_s$  : Diameter of smallest particle in a particle size distribution
- D : Diameter of pipe
- $D_i$  : Diameter of i-th size group of particles
- $D_p$  : Geometric mean particle diameter
- $D_s$  : Surface area mean particle diameter
- e : Void fraction between solid particles
- E : Grinding energy
- f : Fanning friction factor
- $f_i$  : Fraction of i-th size group of particles
- F : Force to overcome interparticle contact
- $F_c$  : Volume fraction of coarse particles



- G : Shear-rate ( $du/dy$ )
- g : Gravitational acceleration
- k : Crowding factor in Table 2.1, Equation (2.7)
- k : Specific surface area in Equation (3.18) and (3.19)
- K : Consistency index (a power-law constant)
- m : Distribution modulus
- n : Flow index (a power-law constant)
- n : Particle interaction parameter in Equation (4.3)
- $n_c$  : Number of particle-particle contacts per unit volume
- $n_o$  : Particle interaction parameter at low shear rates
- $n_\infty$  : Particle interaction parameter at high shear rates
- N : Number of particles per unit volume
- Q : Volumetric flow rate of liquid
- $Q_m$  : Mixture flow rate
- R : Ratio between consecutive particle sizes in Equation (2.14)
- R : Radius of pipe in Equation (5.1)
- $Re_{PL1}$  : Power-law Reynolds number
- $(Re_{PL2})_c$  : Critical transition Reynolds number between laminar and turbulent regimes
- r : Radial distance from the pipe center
- $s_s$  : Specific gravity of solids
- $S_a$  : Specific surface area
- $S_j$  : Cumulative weight fraction of particles finer than  $d_j$
- $t_c$  : Time spent by one spherical particle in collision with other spheres
- u : Velocity at a radial distance r from the pipe center
- $u_y$  : Shear velocity
- V : Average velocity of flow in pipe
- $\frac{\Delta P}{\Delta L}$  : Pressure gradient along the pipe
- $\beta$  : Constant signifying the rate of contact destruction

$\beta_0$	: Rate constant for thermal rupture
$\beta_1$	: Rate constant for shear-induced rupture
$\eta$	: Apparent viscosity
$\eta_i$	: Ratio of the viscosity of i-th particle size component to the apparent liquid containing the particles other than i-th size component
$\eta_r$	: Relative apparent viscosity - ratio of the suspension viscosity to the viscosity of vehicle fluid
$\eta_0$	: Viscosity at low shear rates
$\eta_\infty$	: Viscosity at high shear rates
$\eta_{r,0}$	: Relative viscosity at low shear rates
$\eta_{r,\infty}$	: Relative viscosity at high shear rates
$[\eta]$	: Intrinsic viscosity
$\theta$	: Shear stress necessary to overcome particle interactions
$\mu$	: Absolute viscosity of liquid
$\mu_r$	: Relative viscosity
$\xi$	: Mean particle shape factor
$\pi$	: 3.141592
$\Pi_1$	: Dimensionless parameter for normalized yield stress
$\Pi_2$	: Dimensionless parameter for mobility parameter
$\Pi_3$	: Dimensionless parameter for particle size distribution effects
$\rho_l$	: Density of liquid
$\rho_m$	: Density of mixture
$\rho_s$	: Density of solids
$\sigma$	: Geometric standard deviation for particle diameter
$\tau$	: Shear stress
$\tau_y$	: Yield-stress
$\phi$	: Volumetric concentration of solids
$\phi_i$	: Volumetric concentration of i-th particle size component

- $\phi_j$  : Volumetric concentration of j-th particle size component
- $\phi_m$  : Maximum packing concentration
- $\phi_{m,c}$  : Calculated maximum packing concentration
- $\phi_{m,e}$  : Experimental or measured (actual) maximum packing concentration
- $(\phi_m)_i$  : Maximum packing concentrations for i number of possible systems
- $\Phi_{ij}$  : Coefficients to be used in relating a larger particle group to a smaller one and vice versa
- $\phi_{m0}$  : Maximum packing concentration at low shear-stresses
- $\phi_{m0}$  : Maximum packing concentration for binary mixtures
- $\phi_{m\infty}$  : Maximum packing concentration at high shear-stresses

# CHAPTER 1

## INTRODUCTION

### 1.1 DEFINITIONS AND GENERAL REMARKS ON SOLID-LIQUID MIXTURES

The mechanics of solid-liquid suspensions is regarded as a branch of science of great complexity. Depending on the components involved and their fundamental properties, solid-liquid mixtures often exhibit flow behavior that is governed by a new set of properties, which lead to entirely different responses when subjected to shear stress or motion.

Rheology deals with the determination of a relationship involving deformation and flow of matter. The relationships between the shear stress and corresponding rate of deformation (rate of shear) are referred to as the rheological behavior of the fluid or mixture.

A slurry is a mixture of solid particles in a liquid in which the solids are of sufficient size and weight that they will settle out rather quickly unless stirred or agitated by some means. A suspension, on the other hand, is a mixture of very small particles of a solid

material such as coal that "suspends" in the liquid. A "stable" suspension is one in which the solids will stay in suspension for long periods of time such as days or weeks. Various mixtures including coal-liquid mixtures are non-Newtonian fluids whose viscosity depend on shear rate. They mostly exhibit a pseudoplastic behavior (viscosity decreases with increasing shear rate) which is desirable from a handling and pumping point of view. The terms "highly concentrated" or "dense-phase", both of which refer to a solid-liquid mixture made of 70-75% of pulverized solid particles in a liquid, describe the complex fluid type that is investigated in this dissertation.

The rheological properties of highly concentrated suspensions are of interest in several applications. Industrial processes, in which large volumes of concentrated suspensions such as paint systems, reactor fuels, and coal-based fuels are handled, require understanding and control of the basic rheologic behavior of these suspensions. In spite of the differences in the physical and chemical characteristics of these mixtures, they do have one common property such that as they move through pipes or other similar transport devices, they manifest an initial shear stress. At higher shear rates the behavior of these mixtures depend on the suspension specific characteristics, such as thickening or thinning of the fluid.

In the case of coal-liquid mixtures, such as coal-oil or coal-water mixtures, each primary phase of utilization requires different desirable rheologic characteristics, not only for mixture stability during storage but also fluidity during handling, atomization and combustion. These phases of utilization can briefly be explained as follows:

a. **Stability in storage:** It is very important to produce a stable mixture which will remain in suspension with minimum or no settling for reasonably long periods of time. Stability can be directly related to the yield stress and is affected by the particle size distribution and the chemistry of the suspension.

b. **Hydraulic handling:** The resistance to flow due to the consistency of the mixture should be low. Only Bingham plastic or yield pseudoplastic flow behaviour is suitable for coal-liquid slurries. Other rheograms would yield increasing resistance with increased shear rate.

c. **Atomization:** An easy and uniform introduction of the mixture into combustion chamber should be achieved. Atomization is affected by the viscosity of the mixture and the coal particle topsize. It has also been recently reported that the quality of atomization has a major effect on the combustion performance of a coal-liquid slurry.

d. **Combustion:** Uniform and efficient combustion with minimum derating and emission problems.

Performance of the slurry in each of these utilization phases is strongly affected by its rheologic behaviour. Furthermore, even though some slurries exhibit good rheological behaviour for stability and handling, they may not atomize well and the resulting combustion could be poor. Consequently, the rheologic characteristics must be evaluated not only individually for each of these phases, but also jointly in formulating a desirable fuel.

Coal-liquid mixtures typically contain 70-75 percent by weight of pulverized coal suspended in liquid. The stability with respect to settling or separation of these mixtures permits transportation and storage for a few weeks without agitation. They can be handled and fired much like fuel oil.

Use of various appropriate chemical additives aside, the desired flow and stability characteristics and solids content can be obtained through careful control of the coal particle size distribution. The particle size distribution is designed to provide efficient particle packing so that small particles will fill the interstices between the larger particles to achieve high solids loadings.

Fluidity and stability are also largely determined by the particle size distribution. High fluidity (low viscosity) is achieved by well dispersed, efficiently packed solid particles. However, in the presence of predominating attractive forces between particles, aggregates or flocculation of particles can occur which result in poor stability and settling.

## **1.2 PROBLEM IDENTIFICATION AND OBJECTIVES OF THE PRESENT STUDY**

The design of flow systems of suspensions with high solids contents require a detailed rheological knowledge of the suspension. Mathematical models, such as Bingham-plastic model or Power-law model have been used to define the flow properties of non-Newtonian fluids. However, for most suspensions, the governing parameters have to be determined experimentally. This is mainly because of the variability in such characteristics as particle size distribution, shape of particle, solids concentration, surface condition for each suspension, and difficulties experienced in their identification and measurement.

A majority of the past studies focused on predicting the viscosity of suspensions only as a function of solids concentration, rather than attempting to develop comprehensive expressions incorporating various physical properties of solids and the carrier liquid. Each expression proposed is essentially the result of a fit to the experimental data obtained with a specific material or materials tested, and therefore can not be regarded as "general". In fact, numerous papers emphasize the uncertainty encountered in choosing the right model for their data. This is only as expected, especially for dense-phase transport, because a number of physical properties do affect the flow behavior in a rather complex manner. There are some studies which incorporate the effect of parti-

cle size distribution but none of them are directly applicable to real systems. Therefore, based on all the previous information and today's efforts in developing an alternative fuel for energy, a basic model needs to be developed to define the non-Newtonian flow behavior of coal-liquid slurries.

Literature indicates, that the majority of the efforts in the past have been towards enhancing the coal-liquid mixture properties for each utilization phase individually through the use of suitable chemical additives, with not much effort to formulate the basic rheological behavior of highly concentrated suspensions. The particle size distribution effects have been accounted for, if at all, by empirical coefficients or exponents determined for the variables obtained through a best fit procedure applied to the experimental data for a specified suspension. Few theoretical attempts have been made for various "idealized" cases and specific correlations have been developed for certain specific suspensions.

As mentioned before, one of the key parameters required to obtain highly-concentrated mixtures with desired viscosity is the particle size distribution. This parameter itself has a major influence on the rheological behavior involving the yield stress and the form of the relation between the shear stress and the shear rate. Therefore, optimization of this parameter was the main incentive in the present study for developing a basic rheologic formulation incorporating particle size distribution effects. The primary objective would be to control the particle size distribution in an effort to maximize the yield stress for stability, but at the same time to minimize the shear stress to enhance the flow during pipelining.

For this purpose the following were carried out:

- a) Review of literature
- b) Identification of the parameters that effect the microstructure of suspensions,



- c) Development of a physical formulation for the rheologic characterization of highly concentrated suspensions,
- d) Development of a formulation to predict the shear viscosity behavior at varying shear rates,
- e) Development of a methodology to determine the particle size distribution for the overall optimum energy efficiency during hydraulic transportation.

### **1.3 OUTLINE OF PRESENT STUDY**

The basic concepts in solid-liquid mixture behavior and a survey of past studies in the field of interest are explained in Chapter 2. A detailed analysis of the physical and chemical aspects of concentrated slurries, made of pulverized solid particles and a carrier liquid, is given with reference to various experimental and/or theoretical studies that have been carried out earlier.

Theoretical development of the rheological formulations is presented in Chapter 3. These formulations are used to predict the rheological behavior of solid-liquid mixtures. It is demonstrated that these formulations yield satisfactory results when applied to a specific suspension either to predict the behavior at various concentrations or to predict the effect of various particle size blends at different concentrations.

Chapter 4 outlines the predictive method developed for the shear viscosity behavior of highly concentrated suspensions at low and high shear rates. This chapter also reviews an analytical method to compute the maximum packing concentrations of a given particle size distribution. The values calculated with this method for idealized particles are compared with the actual data from measurements. This resulted in a good correlation between the analytical and measured values and was implemented in the overall analysis.

A general review is given in Chapter 5 concerning the energy requirement in hydraulic conveyance and comminution of solids. A detailed derivation of the energy requirement of a pseudo-homogeneous time-independent non-Newtonian mixtures in laminar flow is also presented in this chapter. The energy requirement for grinding of solid particles was assumed to follow a relatively basic concept, such that energy consumed in size reduction is proportional to the new surface area produced.

A brief description of the computer model developed for this study is given in Chapter 6. Description of the most significant variables in the model and the subroutines that are implemented in the computer program are presented in this chapter.

Chapter 7 provides the input data and the results of all the applications. These applications suggest that, given the necessary data characterizing a specific suspension and its solid particles, the formulations developed and the methodology presented can yield satisfactory results to achieve a desired suspension with minimal energy consumption during hydraulic conveyance.

Finally, the general conclusions of the present study and their implications are presented in Chapter 8.

## **CHAPTER 2**

# **BASIC CONCEPTS AND PAST STUDIES ON SOLID-LIQUID MIXTURES**

### **2.1 INTRODUCTORY REMARKS**

This chapter consists of a brief description of the fundamental rheologic characteristics of solid-liquid mixtures. In reviewing the previous investigations, emphasis was placed on their conceptual and methodological features, with no intention or attempt to discuss each and every one of the great number of "models" available, which can be found elsewhere [7,11,12,18,28,37,38,55,57,59,62].

### **2.2 FUNDAMENTAL PROPERTIES OF SOLID-LIQUID MIXTURES**

Rheology is defined as the study of the relationships between deformation and flow of fluids. There are two classes of fluids, in this respect: Newtonian and non-Newtonian. In Newtonian fluids, shear stress is linearly proportional to the rate of shear and therefore viscosity is constant with respect to the shear rate. Many fluids, however,

exhibit non-Newtonian behaviour. In the case of solid-liquid mixtures, for example, viscosity is not constant but dependent on the shear rate to which the fluid is subjected. A typical set of curves for both Newtonian and non-Newtonian fluids are reproduced in Figure 1 [28]. The curves which do not pass through the origin correspond to fluids displaying yield stress. They are the only ones that are capable of stability in the case of coal-water mixtures. The typical shapes of flow curves for the three rheological models of most interest in slurry work are also shown schematically, drawn on log-log axis, in Figure 2 [29].

A Bingham-plastic fluid has the simplest rheological behaviour among the non-Newtonian fluids, because after an initial yield stress is reached, the curve has the behaviour of a Newtonian fluid. A pseudoplastic fluid exhibits a curvilinear relationship with decreasing apparent viscosity with increasing shear. In contrast, a dilatant fluid demonstrates increasing viscosity as the shear rate increases.

A general mathematical description for the time-independent rheologic behavior of fluids, often referred to as the yield-power law model, is given by:

$$\tau = \tau_y + K (G)^n \quad (2.1)$$

where  $\tau$  is the shear stress,  $\tau_y$  is the yield stress,  $G$  is the shear rate (equal to velocity gradient  $du/dy$ ),  $K$  and  $n$  are empirical constants. Various types of fluids can be represented by mathematical expressions that are special forms of the preceding general formulation, as follows:

Newtonian :  $\tau = \mu G = \mu (du/dy) \quad [\tau_y = 0, n = 1, K = \mu]$

Bingham plastic :  $\tau = \tau_y + \eta (G) \quad [n = 1]$

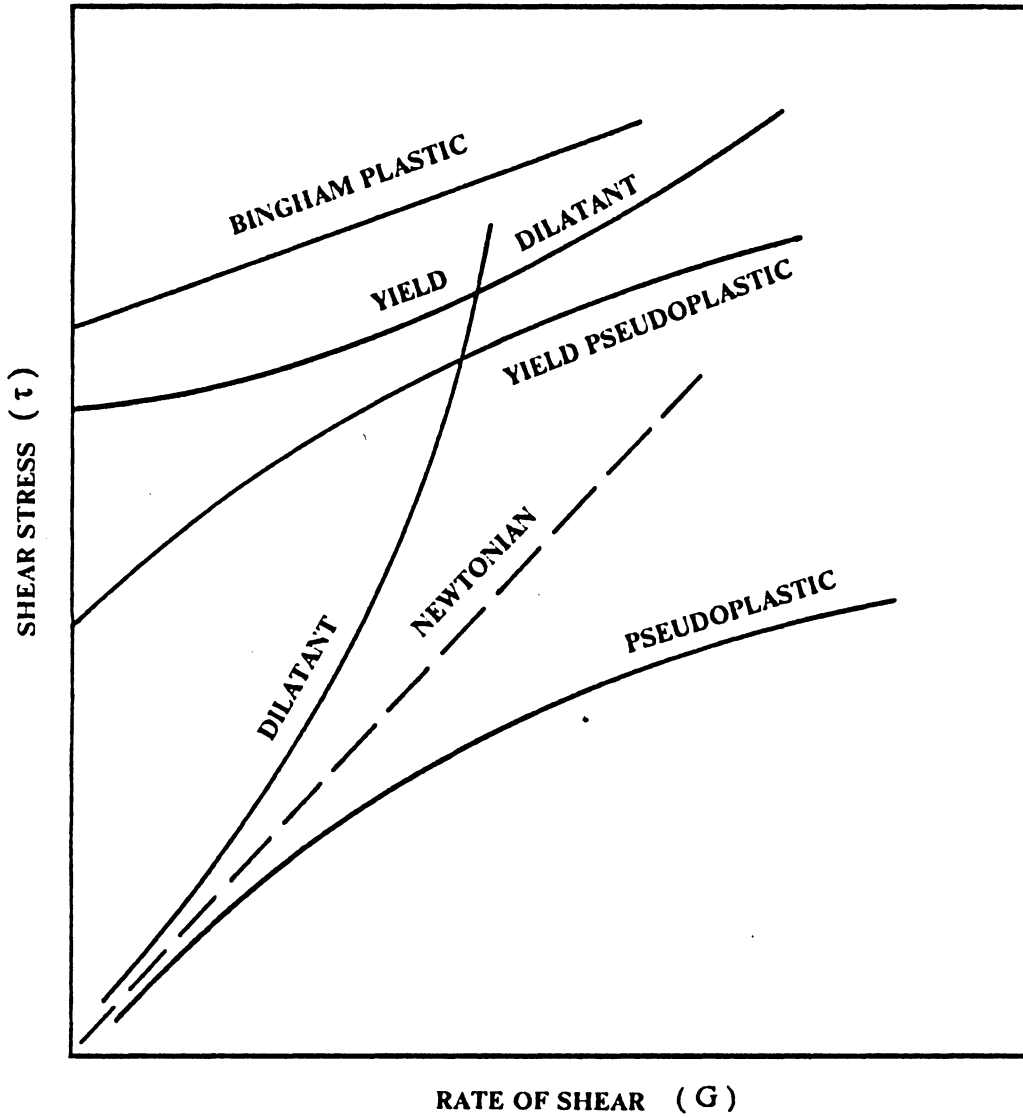


Figure 1. Flow curves of non-Newtonian fluids [28]

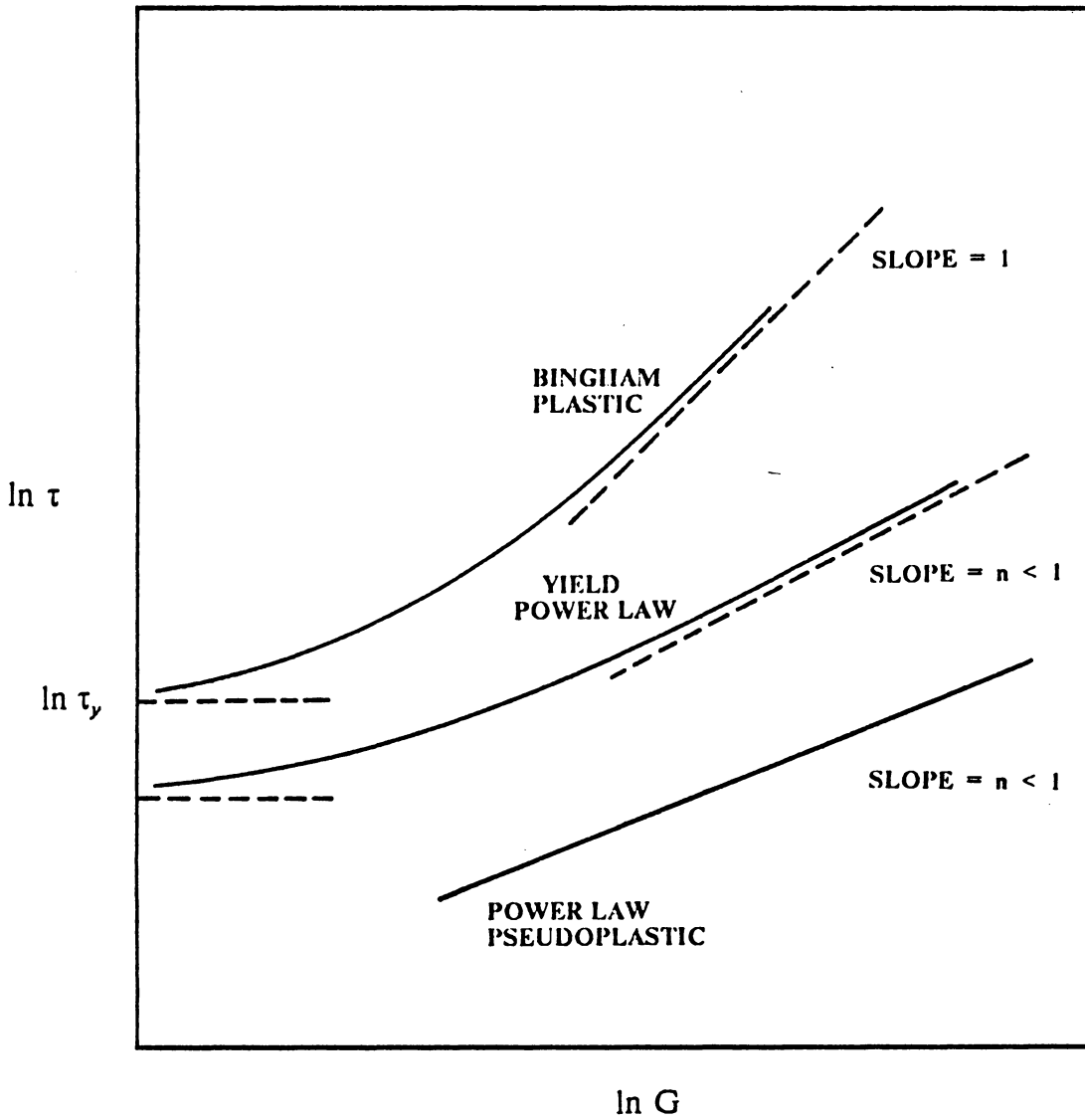


Figure 2. Typical shapes of flow curves for the three rheological models of most interest [29]

Power law :  $\tau = K(G)^n$  [ $\tau_y = 0$ ]

Yield-power law :  $\tau = \tau_y + K(G)^n$   
[  $n < 1$  rarrow yield-pseudoplastic ;  $n > 1$  rarrow yield-dilatant ]

All of these formulations represent time-independent rheologic behaviors. Some complex fluids may also exhibit time-dependent behaviors. A typical case may be explained as follows. In a liquid suspension of nonspherical solid particles, the resulting viscous fluid possesses a structure of randomly packed configuration. When this fluid is sheared and flow starts, realignment of particles takes place. The gradual change of the structural configuration and particle orientation will result in a corresponding variation of the rheological behavior of the fluid and, thus, a time-dependent viscosity relationship. Of the two primary types of time-dependent behaviors, illustrated in Figure 3, the rheopectic fluids exhibit increasing resistance to flow with time and thus also referred to as the shear-thickening fluids; whereas the thixotropic fluids exhibit decreasing resistance to flow with time, and thus also referred to as the shear-thinning fluids. Studies of coal-water mixtures based on different parent coal types have revealed the applicability of both of these properties.

The rheological properties of solid-liquid mixtures depend primarily upon the following parameters [5,10,12,50]:

- I. Physical properties of solids
  - A. Particle size distribution
  - B. Particle shape
  - C. Surface roughness of particle
  - D. Packing density

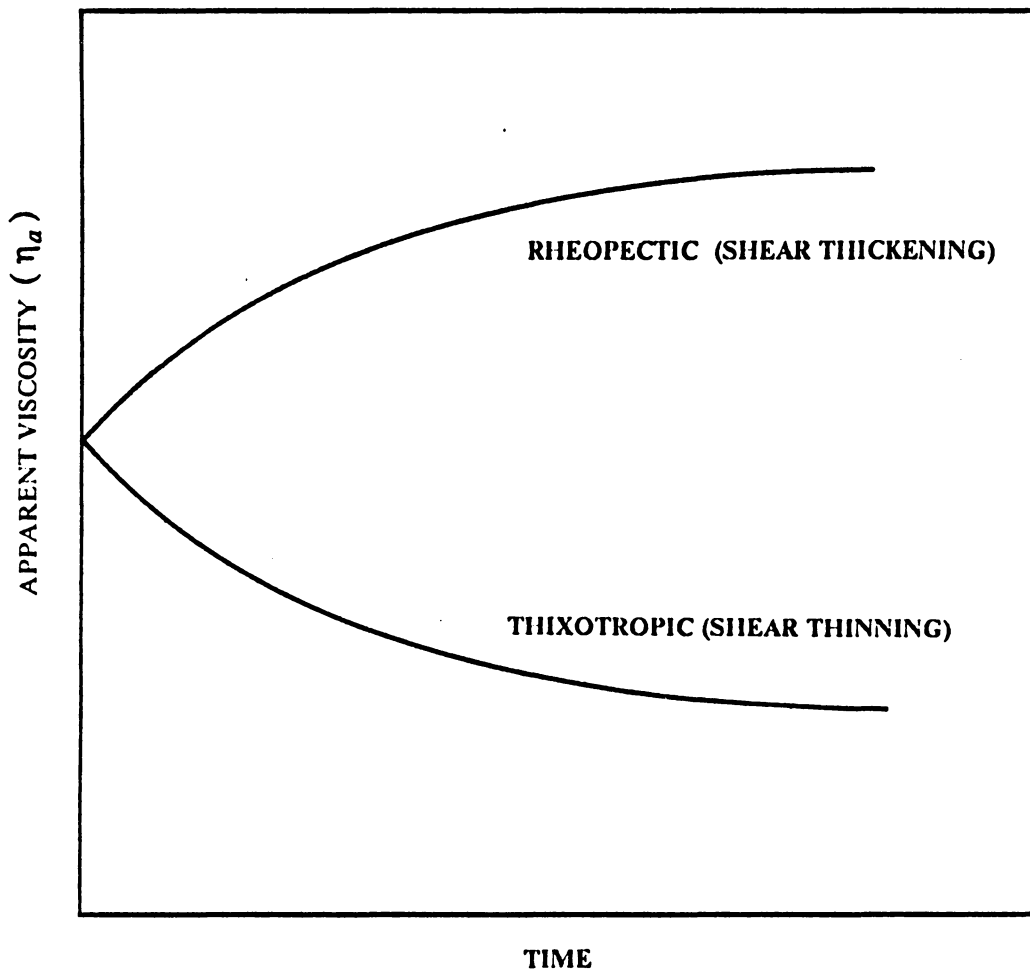


Figure 3. Time dependent fluids [28]



## II. Interparticle Interactive Forces

A. Attractive forces (Wan der Waal's intermolecular forces)

B. Repulsive forces

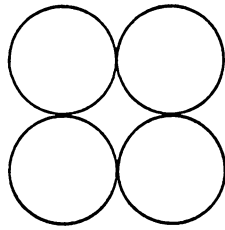
## III. Volume Concentration of Solids

## IV. Physico-chemical Properties of Suspending Vehicle

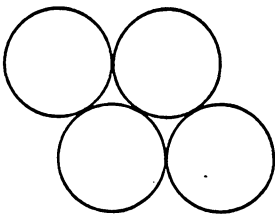
One of the most important parameters influencing the viscosity of solid-liquid mixtures is the particle size distribution. In a mixture formed of a broad distribution of particles, the void space between densely-packed coarse particles will be filled by the fluid and fine particles which will act together as a lubricant between the coarse particles [28]. This effect is very important in the resulting viscosity of the mixture, because excess of coarse particles may create an unstable suspension, and dilatancy may result due to the insufficient fines to shield settling and the excessive shear between particles.

Flow properties of mixtures will also be affected by the shape of particles, such that the greater the deviation from a uniform spherical shape the larger the viscosity will be. This difference in particle shape produces more noticeable thixotropic structure than spherical particles, thus exhibiting a better stability.

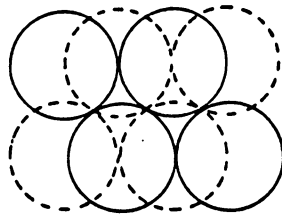
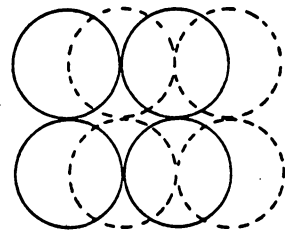
An important parameter which is closely related to the particle size distribution is the maximum packing concentration of solids. As the packing concentration is increased the viscosity will decrease, and a better lubrication between coarse particles will be achieved. It has been shown that mono-size spheres can be systematically arranged in space in four different schemes, as shown in Figure 4: simple-cubic, orthorhombic, double-nested and close-packed, which ideally pack to 53.36%, 60.46%, 69.81%, and 74.05%, respectively [43]. In reality, however, it has also been observed that the average packing concentration for mono-size spherical suspensions obtained in experiments is about 62.5%. Furthermore, the arrangements appear to be exclusively orthorhombic, although it is quite clear that these packings must be contributed by the denser packing



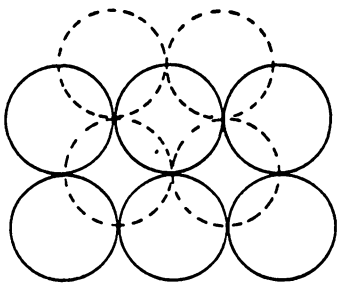
simple-cubic



orthorhombic



double-nested



close-packed

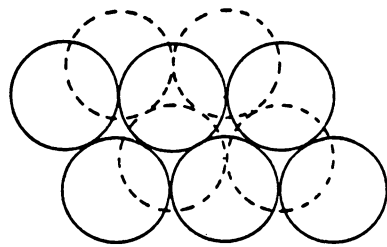


Figure 4. Schematic illustration of possible sphere arrangements in a packing situation

double-nested and close-packed arrangements, as well [43]. Packing concentrations are also found to be a function of the size ratio in binary mixtures, which will be discussed later in section 2.2.2.

## 2.3 PREVIOUS STUDIES ON SOLID-LIQUID SUSPENSIONS

There exist over 200 viscosity models in the literature [59]. Among these the most frequently used and popular ones have been selected and briefly summarized in the following section. These models show various basic forms of the viscosity equation which were used in many studies as a basis. Despite many simplifying assumptions, such as incompressibility of the suspending medium, sphericity, rigidity and smoothness of the suspended materials, no analytical solution has yet been obtained. Table 1 presents selected examples of these models.

### 2.3.1 Viscosity Models

A basic theoretical work in the rheology of suspensions is due to Einstein [7,28], who derived a formula for the relative viscosity of suspensions consisting of uniform size and rigid spherical particles. This formula is given as:

$$\mu_r = 1 + 2.5\phi + 5\phi^2 + 10\phi^3 + \dots \quad (2.2)$$

which reduces to the following for dilute concentrations of up to 2%:

**Table 1. Selected Relative Viscosity Models**

Einstein (1905)	$\mu_r = 1 + 2.5\phi$	Dilute suspensions
Guth & Simha (1936)	$\mu_r = 1 + 2.5\phi + 14.1\phi^2$	
Mooney (1951)	$\mu_r = \exp [2.5\phi/(1 + k\phi)]$ , $k = \text{crowding factor}$	
Landel (1965)	$\mu_r = [\phi/(\phi_m - \phi)]^{2.5}$	
Thomas (1965)	$\mu_r = 1 + 2.5\phi + 10.05\phi^2 + 0.00273 \exp (16.6\phi)$	
Frankel & Acrivos (1967)	$\mu_r = (9/8) \{(\phi/\phi_m)^{1/3}/[1 - (\phi/\phi_m)^{1/3}]\}$	
Chong (1971)	$\mu_r = \{1 + 0.75(\phi/\phi_m)/[1 - (\phi - \phi_m)]\}^2$	
Doherty & Krieger (1972)	$\mu_r = [1 - (\phi/\phi_m)]^{-[\eta]\phi_m}$ [ $\eta$ ] = intrinsic viscosity	

$\mu_r$  : Ratio of the suspension viscosity to the viscosity of vehicle fluid.

$\phi$  : Concentration of solids in the suspension.

$\phi_m$  : Maximum packing concentration

$$\mu_r = 1 + 2.5\phi \quad (2.3)$$

where  $\mu_r$  refers to the ratio of the suspension viscosity to the viscosity of vehicle fluid and  $\phi$  is the volumetric concentration of solids in the suspension.

Equation (2.3) is based on the classical Navier-Stokes equations. However, the derivation introduces certain simplifications which are valid only for infinitely dilute suspensions. For uniform size rigid spherical particles, Einstein showed that the constant in Equation (2.3) is indeed equal to 2.5. However, it was found that for elongated particles, the constant is greater than 2.5; and for soft or spherical liquid particles, it is less than 2.5 [7]. Equation (2.3) shows that the relative viscosity is independent of the particle size and is only a function of the solids concentration.

Guth and Simha [7] have extended Einstein's formula for higher concentrations by accounting for the interactions of the particles. The resulting equation is:

$$\mu_r = 1 + 2.5\phi + 14.1\phi^2 \quad (2.4)$$

The above formula is reported to agree with the experimental data when the volumetric concentration is between 10% and 20%. A subsequent consideration of such previously ignored factors as the possibility of direct collision of particles and mutual volume exclusion of the spheres lead to the reduction of the second coefficient in Equation (2.4) from 14.1 to 12.6 [7].

In another theoretical study carried out for uniform size spherical particles, Vand [57] used "successive reflection of the hydrodynamic disturbances from two spheres to satisfy the boundary conditions on the surface of the spheres," in an effort to account

for the mutual interaction of the particles and their collisions [57]. The resulting equation is:

$$\mu_r = \exp \frac{k_1\phi + k_3(k_2 - k_1)\phi^2}{1 - k_4\phi} \quad (2.5)$$

where  $k_1 = 2.5$  (the shape factor of particles);  $k_2 = 3.175$  (the shape factor of collision doublets);  $k_3 = 4.0$  (collision constant);  $k_4 = 0.609$  (hydrodynamic interaction constant). However, this equation takes into account neither the particle size and particle size distribution, nor the interparticle forces which give rise to non-Newtonian behavior or thixotropy.

One of the widely accepted formulations for the variation of viscosity with concentration has been given by Mooney [7,28]. The general expression for polydisperse suspensions, another terminology for nonuniform particle size distribution, proposed by Mooney is:

$$\ln \mu_r = 2.5 \sum_{i=1}^n \left[ \frac{\phi_i}{1 - \sum_{j=1}^m k_{ij} \phi_j} \right] \quad (2.6)$$

where  $k_{ij}$  is the interaction constant that is due to the crowding of the  $i$ -th group of particles by the  $j$ -th group particles. Mooney described the interaction between particles at higher concentration as essentially a crowding effect. For monodispersed systems, or suspensions with uniform size particles, Equation (2.6) reduces to:

$$\ln \mu_r = 2.5 \frac{\phi}{1 - k\phi} \quad (2.7)$$

where  $k$  varies between 1.35 and 1.91.

A study based on the concept of relating viscosity to sedimentation volume was made by Landel et al. [38]. Landel et al. were able to correlate viscosity measurements of different suspensions with the equation:

$$\eta_r = \left[ \frac{\phi_m}{\phi_m - \phi} \right]^{2.5} = \left[ \frac{1}{1 - \phi/\phi_m} \right]^{2.5} \quad (2.8)$$

where  $\phi_m$  is the maximum packing concentration at which ( when  $\phi = \phi_m$  ) the relative viscosity becomes infinite and  $\eta_r$  is the relative value of the apparent viscosity (or coefficient of rigidity). The apparent relative viscosity was found to be only a function of the packed sediment volume, and independent of the polarity of the medium, the type of particle (glass, inorganic oxide or metal), the surface area of particles, the shape of particles, the particle size and to a degree the particle size distribution. Landel observed non-Newtonian flow but confined his correlation to the region of Newtonian flow. Particle sizes ranged from 6 to 100 microns and the concentration of some suspensions were as high as 70% volume percent solids.

Many existing theoretical and empirical expressions in the form of a power series expansion have been reviewed by Thomas [55]. According to Thomas, termination of the series after quadratic term leads to errors in excess of 10% for suspensions which contain greater than 20% solids. Based on an analysis and rationalization of a large quantity of published data, Thomas [55] proposed the following closed form equation:

$$\mu_r = 1 + 2.5\phi + 10.05\phi^2 + 0.00273 \exp(16.6\phi) \quad (2.9)$$

With three terms of a power series with coefficients determined from previous theoretical analyses and an exponential term with two empirical coefficients, this equation was shown to fit the data of uniform spherical particles up to 60% volumetric concentration as well as a power series with six terms.

In another study, Frankel and Acrivos [18] assumed that the viscous dissipation of energy in highly concentrated suspensions made of uniform solid spheres arises primarily from the flow within the narrow gaps separating the solid spheres from one another; and also that within each gap this flow is due to the relative motion of the spherical particles. They obtained a theoretical equation of the following form:

$$\mu_r = \frac{9}{8} \left[ \frac{(\varphi/\varphi_m)^{1/3}}{1 - (\varphi/\varphi_m)^{1/3}} \right] \quad (2.10)$$

This equation resembles that given by Landel et al. [38], and also indicates that the relative viscosity of suspensions is a function of the ratio  $\varphi/\varphi_m$  therefore a possible reduction in viscosity is obtained by increasing the maximum packing concentration  $\varphi_m$  for a fixed concentration  $\varphi$ .

One of the studies which considered the particle size distribution effects was carried out by Chong and Chong et al. [7,8]. In this study, the viscosities of suspensions were measured with an orifice viscometer. The following equation was given to fit their data obtained at low shear rates:

$$\mu_r = \left[ 1 + 0.75 \frac{\varphi/\varphi_m}{1 - \varphi/\varphi_m} \right]^2 \quad (2.11)$$



The relative viscosities of monodispersed systems investigated were found to be independent of the particle size and temperature. This was attributed to the observation that the viscosities of monodispersed systems all tend to approach infinity asymptotically at  $\phi_m = 0.605$ . However, the value of  $\phi_m$ , at which the viscosity approaches infinity, was determined to increase for bimodal compositions. Consequently, it was stated that this equation would predict compositions of bimodal systems which would give minimum viscosity at a given total solids concentration, provided that the value of  $\phi_m$  is known for the corresponding particle size distribution. Another interesting conclusion was that there existed a limiting particle size ratio of 1/10 below which the viscosity of bimodal suspensions did not decrease significantly.

### 2.3.2 Particle Size Distribution Models

One of the key parameters required to obtain highly-loaded low-viscosity mixtures is the particle size distribution. If the distribution of particles is sufficiently broad, fines will be able to fill the interstices between the coarser particles, thus reducing the voidage and maximizing the packing efficiency. In this respect, Furnas [21] studied experimentally the voidage in binary systems of varying particle size ratios. For coarse and fines with equal densities and equal initial void ratios, he obtained the volume fraction of coarse particles at the condition of maximum density, as follows:

$$F_c = \frac{1}{1 + e} \quad (2.12)$$

where  $F_c$  is the volume fraction of coarse particles and  $e$  represents the void fraction between particles. The fraction of the fines  $F_f$  which will fill the interstices of the coarse material is then given by:

$$F_f = 1 - \frac{1}{1 + e} \quad (2.13)$$

Similarly, a third component of still finer particles could be added to fill the interstices of the second component. Theoretically, this process can be continued to an infinite number of components so that the total volume of solids may be expressed as a geometric series. A good agreement between the theory and the experimental results was obtained for binary mixtures when the ratio of the two particle sizes was greater than 50. Furnas' equation for the optimum particle size distribution of continuously varying particle diameters is as follows:

$$\frac{\text{Cumulative Percent}}{100} = \frac{R^{\log d_s} - R^{\log d_L}}{R^{\log d_L} - R^{\log d_s}} \quad (2.14)$$

where  $d_s$  and  $d_L$  refer to diameters of smallest and largest particle, respectively and  $R$  represents the ratio between consecutive sizes where "consecutive" sizes may be conveniently defined.

Another equation for the optimum packing of continuous distributions was proposed by Andreasen and Andersen given in [10], as follows:

$$\frac{\text{Cumulative Percent}}{100} = \left[ \frac{D_i}{D_L} \right]^n \quad (2.15)$$

which is further revised by Dinger et al. [10] by incorporating a finite smallest particle size as follows:

$$\frac{\text{CPFT}}{100} = \frac{D^n - D_s^n}{D_L^n - D_s^n} \quad (2.16)$$

where  $n \equiv \frac{\ln [1/(1 - \phi)]}{\ln (D_L/D_s)}$ , and CPFT stands for "cumulative percent finer than".

The form of this equation is similar to the one proposed by Furnas except for the exponent  $n$ .

An interesting theoretical approach for the optimization of the particle size distribution to obtain minimum viscosity was performed by Farris [14]. The basis of this study was the assumption, that when the size ratio of particles is 1/10 or less, the finer particles in a bimodal suspension behave essentially as a fluid so far as the coarser particles are concerned. This phenomenon was also observed by other researchers in settling experiments with uniform-sized spheres and termed by Farris as non-interacting particles. Farris proposed the following methodology. The relative viscosity of bimodal suspensions is calculated from a known relative viscosity function of a monomodal system, which is a unique function of the volume fraction of solids, such as Equation (2.11) given by Chong et al. [7,8]. The relative viscosity of a multi-modal suspension is then given as:

$$\ln \eta_r = \sum_{i=1}^N \ln \eta_i(\phi_i) \quad (2.17)$$

where  $\eta_i(\phi_i)$  is the ratio of the viscosity of i-th size component to the apparent liquid containing the particles other than i-th size component.

The optimum particle size distribution is developed by differentiating  $\eta_r$  in Equation (2.17) with respect to the concentration  $\phi_i$  and equating to zero. The primary solution for the blends that will produce the lowest possible relative viscosity for any concentration is obtained as [14]:

$$\phi_1 = \phi_2 = \phi_3 = \dots \text{ providing } \eta_1 = \eta_2 = \eta_3 = \dots \quad (2.18)$$

The equation proposed by Dinger et al. [10] was based on this result.

The preceding formulations are all based on the assumption of non-interacting particles. In reality, however, particle-particle interaction is certainly present in a system with a nonuniform particle size distribution. Furthermore, a coal-water mixture with a tetramodal distribution with the restriction of a 0.1 size ratio would not be feasible, for example, because of the top and smallest sizes would result in undesired conditions in combustion and grinding cost, respectively [31]. Farris [14] claims that the interaction between particles can be implemented in his analysis by defining a crowding factor  $f$ , which is the fraction of one size that behaves as if it were the next largest size. However, a method is presently not available for predicting the crowding factors for various particle sizes in a mixture. Therefore, this theory can only be applied to suspensions with known crowding factors, presumably to be determined experimentally.

### 2.3.3 Suspension Mechanics Models

In very few studies, attempts were made to relate the physical properties of particles to the non-Newtonian behavior. Thomas [56] correlated viscosity measurements of flocculated suspensions with the Bingham plastic model. He was able to calculate the yield stress and the coefficient of rigidity from physical properties of the constituents, but the highest concentration employed was only 23%.

Another study which has attempted to develop a mathematical model of a dense phase flow in pipes was performed by Gay et al. [23]. They started the problem with a definition of the yield stress. Yield stress was assumed to be proportional to the particle diameter  $D_p$  and inversely proportional to the space available to accommodate the displacement, namely,  $(\phi_m - \phi)$ . Thus, the yield stress was defined as follows:

$$\tau_y = A \left[ \frac{D_p}{\phi_m - \phi} \right] \quad (2.19)$$

Using data from eight different suspensions and after many trial and error attempts, the following equation was found to best represent their experimental data:

$$\tau_y = 200 \left[ \frac{D_p}{(\phi_m - \phi)} \right] \left[ \frac{\phi_m}{(1 - \phi_m)} \right]^2 \left[ \frac{1}{\xi^{1.5} \sigma^2} \right] \quad (2.20)$$

where  $\xi$  is the shape factor defined as the ratio of the surface area of a sphere of equivalent volume to the surface area of the particle and  $\sigma$  constitutes the geometric standard deviation for particle diameter.

Once the finite shear stress,  $\tau_y$ , is reached and the initial movement has started, the fluid behaves according to the following equation:

$$\tau - \tau_y = \eta_\infty G + \frac{(\eta_0 - \eta_\infty) G}{1 + \left[ \frac{(\eta_0 - \eta_\infty) G}{B} \right]} \quad (2.21)$$

where  $\eta_0$  and  $\eta_\infty$  refer to the viscosities at low and high shear rates, respectively, B is the flow parameter and G is the shear rate.

For the parameter B again after reportedly many trial and error attempts of curve fitting to their data, Gay et al. proposed the following equation:

$$B = 0.066 \tau_y \left[ \frac{\phi^2}{\phi_m - \phi} \right] \left[ \frac{\mu^2}{D_p^2 \rho_m \tau_y} \right]^{0.21} \quad (2.22)$$

where,  $\rho_m$  is the density of the mixture.

The viscosity at low shear rates was estimated from the expression given by Landel et al. [38]:

$$\eta_0 = \mu \left[ \frac{\phi_m}{\phi_m - \phi} \right]^{2.5} \quad (2.23)$$

For the viscosity of suspensions at high shear rates, on the other hand, the following expression was proposed by Gay et al. [23] based on their experimental data:

$$\eta_{\infty} = \mu \exp \left[ \left[ 2.5 + \left( \frac{\phi}{\phi_m} - \phi \right)^n \right] \frac{\phi}{\phi_m} \right] \quad (2.24)$$

A more detailed discussion of these formulations proposed by Gay et al. will be given in Chapter 3.

The approach of Wildemuth and Williams [58,59] to the characterization of the suspension microstructure resulted in a shear dependent maximum packing concentration  $\phi_m(\tau)$ . They reasoned that when the stress field alters the microstructure, the maximum packing concentration  $\phi_m$  changes and thus most non-Newtonian behavior should be characterizable by  $\phi_m(\tau)$  where  $\tau$  is a suitable invariant of the stress field. It was subsequently stated in their work that the intrinsic viscosity  $[\eta]$  also depends on  $\tau$  and a model claiming to represent the entire concentration range would have to incorporate both  $[\eta]$  and the effective volume fraction  $\phi/\phi_m$ . This was achieved by the function:

$$\eta_r = \frac{1}{(1 - \phi/\phi_m)^{[\eta]\phi_m}} \quad (2.25)$$

which was based on a derivation by Krieger and Dougherty [37]. They claim that shear effects reside in both  $\phi_m(\tau)$  and  $[\eta(\tau)]$ , and the function reduces properly to:

$$\eta_r = 1 + [\eta] \phi + \dots \quad (2.26)$$

at low concentrations which would be consistent with Einstein's formula for dilute suspensions. Their attempt to the derivation of  $\phi_m(\tau)$ , based upon stress-induced microstructural change yielded:

$$\frac{1}{\phi_m} = \frac{1}{\phi_{m0}} - \frac{\left[ \frac{1}{\phi_{m0}} - \frac{1}{\phi_{m\infty}} \right]}{(1 - A \tau^{-m})} \quad (2.27)$$

where  $\varphi_{m0}$  and  $\varphi_{m\infty}$  are the limiting values of  $\varphi_m$  at the low-  $\tau$  and high-  $\tau$  conditions, respectively, A is the lumped kinetic parameter and m is the exponent to characterize shear dependence. Equation (2.27) also carried the implication that yield stresses would arise ( $\eta \rightarrow \infty$  at  $\tau \rightarrow \tau_y$ ) when  $\varphi_{m0} \leq \varphi \leq \varphi_{m\infty}$  :

$$\tau_y(\varphi) = \left[ A \frac{\varphi/\varphi_{m0} - 1}{1 - \varphi/\varphi_{m\infty}} \right]^{1/m} \quad (2.28)$$

Extensive data on suspensions of uniform spherical particles were analyzed in the context of Equation (2.28). It was concluded that all the trends obtained for spherical particle systems were likely to be found in suspensions of coal and other irregular shaped particles, with  $[\eta_0] > 2.5$ . Accordingly, a coal-glycerin system prepared was experimentally investigated and correlated by using Equations (2.27) and (2.28).



# **CHAPTER 3**

## **THEORETICAL DEVELOPMENT OF THE RHEOLOGICAL FORMULATIONS**

### **3.1 INTRODUCTORY REMARKS**

Pumping solid-liquid mixtures in pipes needs understanding of the flow behavior of these systems not only to control the system technically but also to establish economic feasibility. Great efforts have been made to investigate the flow phenomena of suspensions, however, no concept exists to predict the flow properties of these systems.

The following theoretical analysis, as a consequence, was developed for laminar flow behavior of highly concentrated suspensions. First a detailed development of the fundamental shear stress shear rate relation is presented, then the formulations proposed for the two parameters in shear stress shear rate equation are discussed. These formulations relate mixture properties to the physical properties of the solids and liquids.

### 3.2 FUNDAMENTAL SHEAR STRESS SHEAR RATE RELATION

A general relationship between the shear stress and the shear rate for flocculated suspensions was originally advanced by Goodeve [27]. Assuming that hydrodynamic or Newtonian effects and the effects of particle interactions are cumulative, a relationship for laminar flow in a pipe was developed as follows [22,27]:

$$\tau - \tau_y = \eta G + \theta \quad (3.1)$$

where,  $\tau$  is the shear stress in axial direction,  $\tau_y$  is the yield stress,  $\eta$  represents the viscosity parameter which is descriptive of Newtonian effects,  $G$  is the shear rate and  $\theta$  defines the shear stress necessary to overcome particle interactions (particle-particle contacts). Goodeve called  $\theta$  the "coefficient of thixotropy," suggesting that it may be time dependent as well as shear dependent.

Considering uniform sized, spherical particles, the number of particle contacts per unit area in a layer one particle thick is  $(D n_c)$ , where  $D$  is the particle diameter, and  $n_c$  is the number of particle-particle contacts per unit volume. Gay et al. [23] defined the momentum transfer from one layer to the next per unit area per unit time, as follows:

$$\theta = F D n_c \quad (3.2)$$

where,  $F$  is the force necessary to overcome interparticle contact.

Thomas [56] defined the rate of formation of particle-particle contacts as a second order process, because it necessarily involves two particles, while the rate of destruction of contacts as being simply proportional to the number of contacts. Hence,

$$\frac{dn_c}{dt} = kN^2 - \beta n_c \quad (3.3)$$

where,  $k$  is the rate constant descriptive of the rate at which contacts are formed,  $N$  is the number of particles per unit volume,  $\beta$  is a constant signifying the rate of contact destruction. Under steady state conditions, the rate of formation and breaking of contacts is equal, or  $dn_c / dt = 0$ . Hence,

$$n_c = \frac{kN^2}{\beta} \quad (3.4)$$

Particles are brought into contact by Brownian movement or by their relative motion due to shear, therefore,  $k$  must be proportional to the shear rate  $G$  for particles large enough not to create any Brownian motion. In this respect, Manley and Mason [41] have proved experimentally that the two body collision frequency per unit volume is:

$$f = (2/3)D^3N^2G \quad (3.5)$$

implying,

$$k = (2/3)D^3G \quad (3.6)$$

Similarly, particle-particle contact is also destroyed by the relative motion due to shear, which again implies a direct proportionality between  $\beta$  and  $G$ . However, Gillespie [25] expressed the rate constant  $\beta$  as a linear function of  $G$ , taking the rupture of con-

tacts by thermal processes and by shear to be independent, and gave the following relationship accounting for the pseudoplastic behavior of dense-phase suspensions at low shear rates:

$$\beta = \beta_0 + \beta_1 G \quad (3.7)$$

where  $\beta_0$  and  $\beta_1 G$  are descriptive of thermal rupture and shear-induced rupture, respectively. When  $\beta_0$  is negligible, the constant  $\beta_1$  can be evaluated from the work of Manley and Mason [41], who expressed the time spent by one sphere in collision with other spheres as follows:

$$t_c = \frac{4\phi}{G} \quad (3.8)$$

On the other hand, by definition,

$$t_c = \frac{1}{\beta} \quad (3.9)$$

Therefore,

$$\beta_1 = \frac{1}{4\phi} \quad (3.10)$$

Substitution of Equations (3.10), (3.6), and (3.7) into (3.2)

$$\theta = F \frac{96 \phi^3 G}{\pi^2 D^2} \left[ \frac{1}{4 \phi \beta_o + G} \right] \quad (3.11)$$

and substitution of Equation (3.11) into (3.1) yields:

$$\tau - \tau_y = \eta G + F \frac{96 \phi^3 G}{\pi^2 D^2} \left[ \frac{1}{4 \phi \beta_o + G} \right] \quad (3.12)$$

In order to account for Newtonian effects  $\eta$  is replaced by  $\eta_\infty$ , which denotes the viscosity at very high shear rates where the flow behavior is Newtonian. Equation (3.12) can also be written in terms of suspension viscosity as follows:

$$\eta = \eta_\infty + \left[ \frac{B}{4 \phi \beta_o + G} \right] \quad (3.13)$$

where,  $\eta = (\tau - \tau_y)/G$  and  $B = 96F\phi^3/(\pi^2 D^2)$ . Gay et al. [23] defined  $\beta_o$  at very low shear rates, for which  $G \ll 4\phi\beta_o$ , as:

$$\beta_o = \frac{1}{4\phi} \left[ \frac{B}{\eta_o - \eta_\infty} \right] \quad (3.14)$$

where,  $\eta_o$  is the viscosity of suspension at the initiation of motion. Hence, the final form of shear stress shear rate equation is obtained by substituting Equation (3.14) into (3.13) as follows:

$$\tau - \tau_y = \eta_\infty G + \frac{(\eta_0 - \eta_\infty)G}{1 + \left[ \frac{(\eta_0 - \eta_\infty)G}{B} \right]} \quad (3.15)$$

The parameters to be determined in Equation (3.15) are the yield stress,  $\tau_y$ , the flow parameter,  $B$  and the viscosities at low and high shear rates. This form of shear stress shear rate equation can be represented in a more descriptive manner in Figure 5. As can be seen from the figure the whole shear rate region is divided into three regions which basically form the basis of this study provided that the behavior obeys the power law. In the low shear rate region an incipient motion is underway and therefore the yield stress and viscosity at low shear rate region have significance. At high shear rates the behavior is almost Newtonian resulting in constant slope of the shear stress curve. In between these two regions complex solid-liquid interactions are encountered exhibiting largely a pseudoplastic behavior. Consequently, the deviation from Newtonian behavior in this region is estimated by the second term on the right hand side of Equation (3.15).

### 3.3 PROPOSED FORMULATIONS

The analysis in this study was based on dimensionless parameters which were derived by careful analysis of the available data as well as physical reasoning. For the yield stress, the following parameters were obtained:

$$\begin{aligned} \Pi_1 &= \frac{\tau_y}{(s_s - 1) \rho_l g D \varphi} \\ \Pi_2 &= \frac{\varphi}{\varphi_m - \varphi} \\ \Pi_3 &= \frac{k D_s \varphi}{\xi} \end{aligned} \quad (3.18)$$

*Low Shear-Rate  
(Incipient Motion)*

*Intermediate Shear-Rate  
(Pseudoplastic)*

*High Shear-Rate  
(Largely Newtonian)*

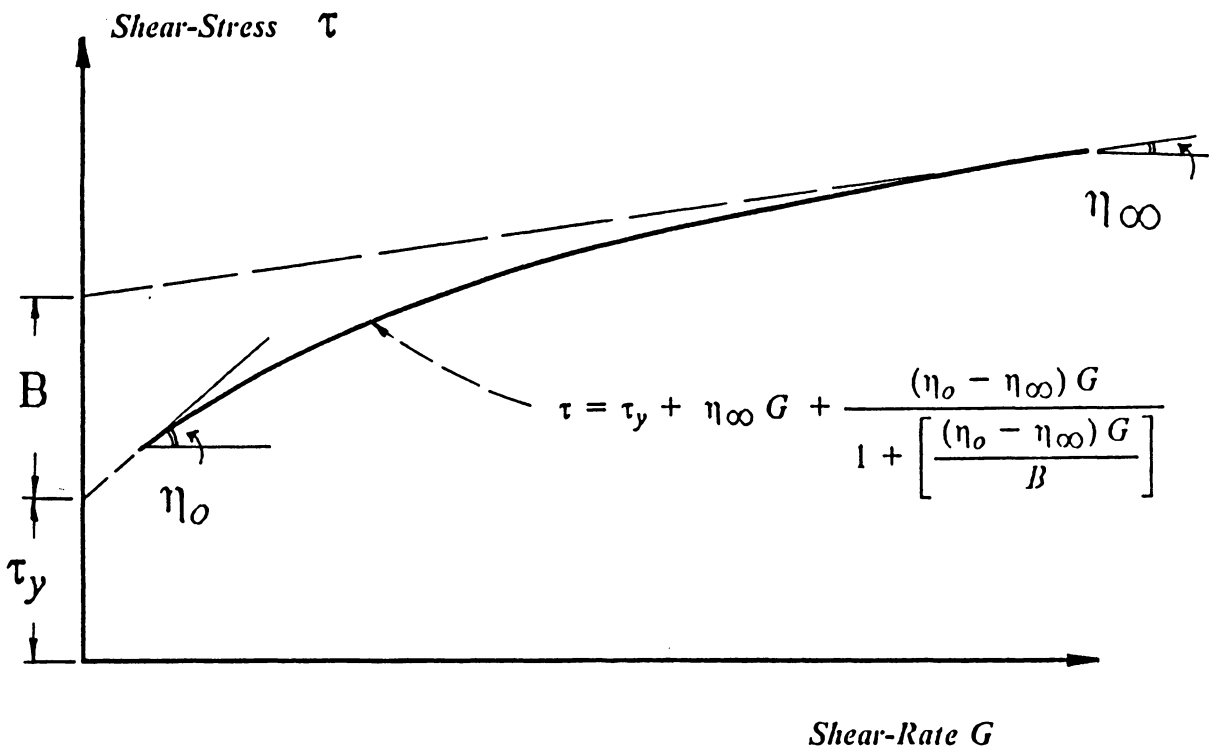


Figure 5. Typical shear-stress shear-rate diagram characterizing the behavior employed in the development of formulations.

in which,  $\phi$  is the solids concentration;  $\phi_m$  is the maximum packing concentration;  $s_s = \rho_s/\rho_f$  with  $\rho_s$  denoting the solids density and  $\rho_f$  denoting the fluid density;  $g$  is the gravitational acceleration;  $D$  is the geometric mean particle size;  $k$  is an active surface area indicator, defined as the total surface area of the particles (assumed spherical) forming the suspension per total volume of particles;  $D_s$  is the surface area mean particle size; and  $\xi$  is a mean particle shape factor, defined as the ratio of the surface area of a sphere of equivalent volume to the surface area of the actual nonspherical particle.

In the dimensionless parameters given above, the submerged unit weight of solid particles in the vehicle fluid is denoted by  $(\rho_s - \rho_f)g = (s_s - 1)\rho_f g$ , and is a significant parameter especially for static stability. The particle size  $D$  also affects the yield stress. The greater the particle size the greater the force needed to hold the particles up in suspension. The volumetric concentration  $\phi$  in the same term signifies the number of particles that are present in the suspension. Hence,  $\Pi_1$  is a physically meaningful dimensionless parameter, signifying a "normalized" yield stress.

The parameter,  $\Pi_2 = \phi/(\phi_m - \phi)$ , is a representation of the relative degree of freedom the particles have to move in the mixture. The denominator represents the effective space available for particles to disperse. When  $\phi$  is small as compared to  $(\phi_m - \phi)$ , the particles can move around easily, resulting in small values of  $\tau_y$ . As  $\phi$  approaches to  $\phi_m$ , on the other hand, the suspension will get "thicker", the relative space available will decrease, and hence,  $\tau_y$  will increase dramatically. It is reasoned physically, that the mobility of the particles should be proportional to the relative space available. This implies that the normalized yield stress should be inversely proportional to the relative space available, or  $\Pi_1 \propto \Pi_2$ . The validity of this reasoning is demonstrated in Figure 6 based on the data on various dense-phase suspensions.



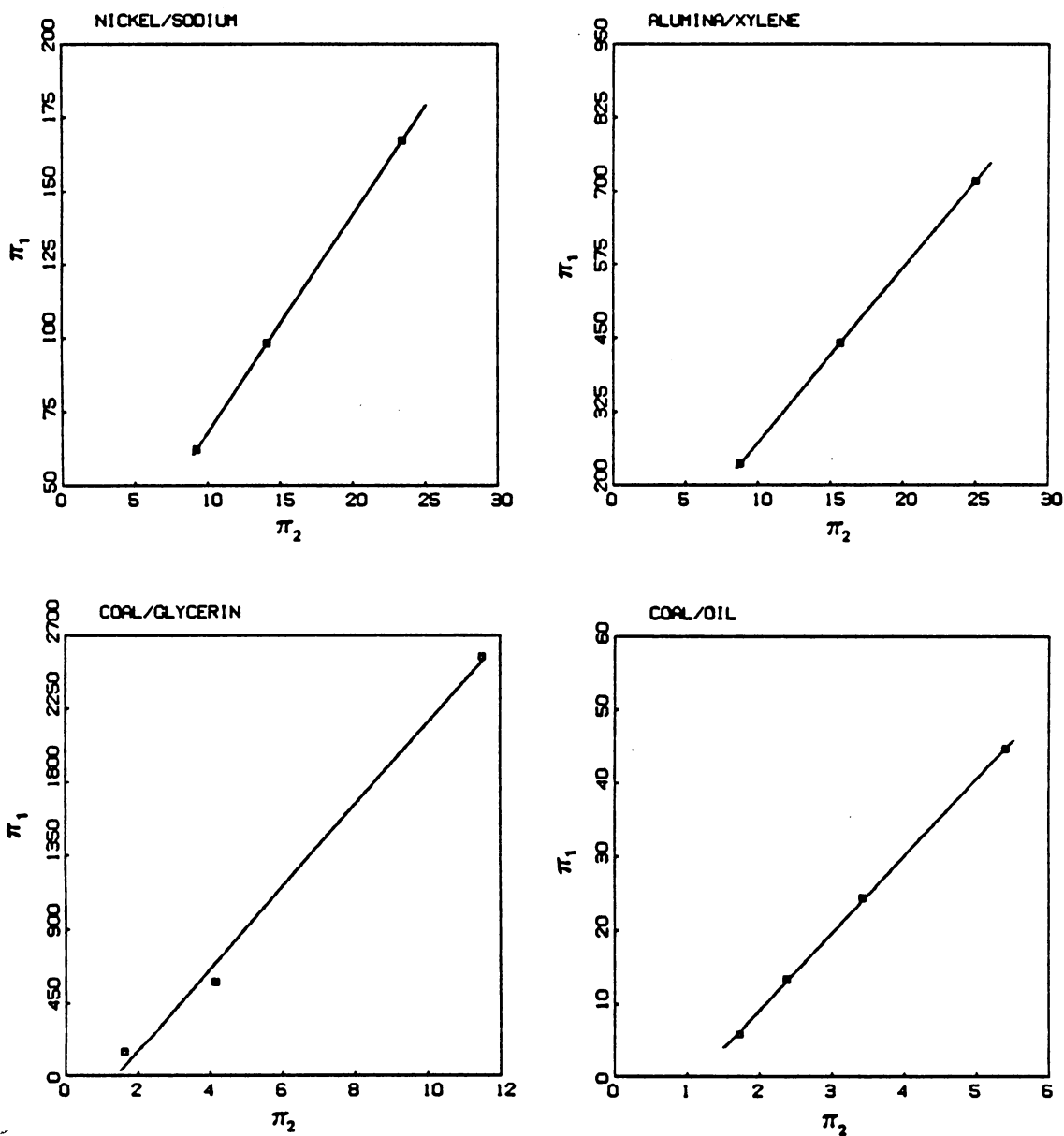


Figure 6. Proportionality of the first dimensionless parameter to the second for each suspension

The term  $\Pi_3 = (kD_s\phi/\xi)$  is a representation of the effects of particle size distribution related to the shape and surface area of the particles. While  $(kD_s\phi)$  accounts for the active surface area effects of the particle size distribution,  $\xi$  is a shape factor which corrects the assumption of spherical shape in the calculation of  $k$ . For this parameter too, it was reasoned physically, that there should be a proportionality, or  $\Pi_1 \propto \Pi_3$ , which was also confirmed with various data as exhibited in Figure 7.

The resulting formulation is the combination of these three parameters by a dimensionless constant  $C$  which is unique to each specific suspension, representing all the other fluid/solid interactions that are not accounted for physically by the above three dimensionless parameters. The final equation for the yield stress is:

$$\tau_y = C[(\rho_s - \rho_l)gD\phi] \left[ \frac{\phi}{\phi_m - \phi} \right] \left[ \frac{kD_s\phi}{\xi} \right] \quad (3.19)$$

In the given form above, the fact that the volumetric solids concentration  $\phi$  appears once in each of the three dimensionless parameters also explains as to why the yield stress  $\tau_y$  can be correlated to  $\phi^3$ , that was reported previously as an experimentally proven fact [6,55,56,59].

Also carried out was a dimensional analysis to develop a relation for  $B$  in Equation (3.15), with particular emphasis on the physical significance of eachh of the parameters involved. This analysis led to the following functional relationship:

$$B = \text{fcn} \left[ \phi, \frac{\phi}{\phi_m - \phi}, \tau_y, \rho_l, D, \mu \right] \quad (3.20)$$

where,  $\rho_l$  and  $\mu$  are the density and the viscosity of the vehicle fluid, respectively, and  $K$  is the proportionality constant. The dimensionless parameters derived were as follows:

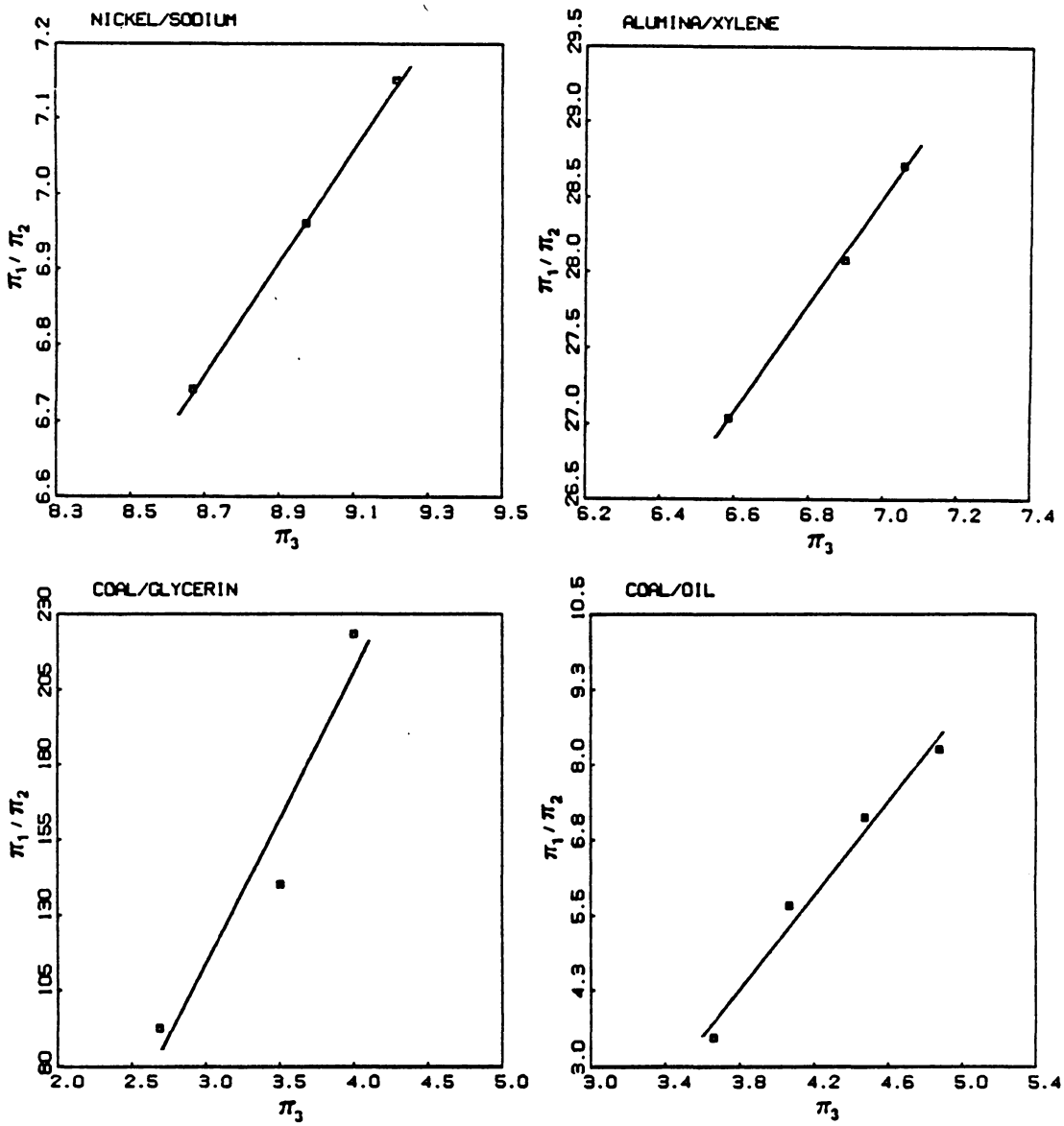


Figure 7. Proportionality of the first and second dimensionless parameters to the third for each suspension

$$P1 = \frac{B}{\tau_y}, \quad P2 = \phi, \quad P3 = \frac{\phi}{\phi_m - \phi}, \quad P4 = \frac{\sqrt{\tau_y \rho_t} D}{\mu} = Re_y \quad (3.21)$$

where,  $Re_y$  is the particle shear Reynolds number. It was physically reasoned, that because the flow parameter  $B$  reflects the resistance to flow created by the particles, it should be proportional to the concentration of solid particles  $\phi$  and the parameter  $[\phi / (\phi_m - \phi)]$ , but inversely proportional to  $Re_y$ . The concentration of solid particles is assumed to directly influence the resistance to flow together with the parameter  $[\phi / (\phi_m - \phi)]$ , which indicates the space available to accommodate the displacement of particles. On the other hand, however, the particle shear Reynolds number represents the ratio of inertia to viscous forces and would be anticipated to affect the resistance to flow directly due to increase in frictional forces as the size of particles increase or vice versa.

The validity of these assumptions are demonstrated using experimental data of Gay [22] and the proportionality of  $B/\tau_y$  to the other dimensionless numbers are illustrated in Figures 8 and 9. These figures show that an equation of the form can be written for the dimensionless flow parameter as follows:

$$\frac{B}{\tau_y} = \frac{K \phi \left[ \frac{\phi}{\phi_m - \phi} \right]}{Re_y} \quad (3.22)$$

The expressions obtained in Equations (3.19) and (3.22) are two of the parameters to be determined in Equation (3.15) which establish the beginning (using  $\tau_y$ ) and the limiting (using  $B$ ) regions of the shear stress shear rate curve as shown in Figure 5. It is necessary, however, to determine the low and high shear rate behavior of this curve in addition to  $\tau_y$  and  $B$  and this is possible by obtaining the viscosities at low and high shear

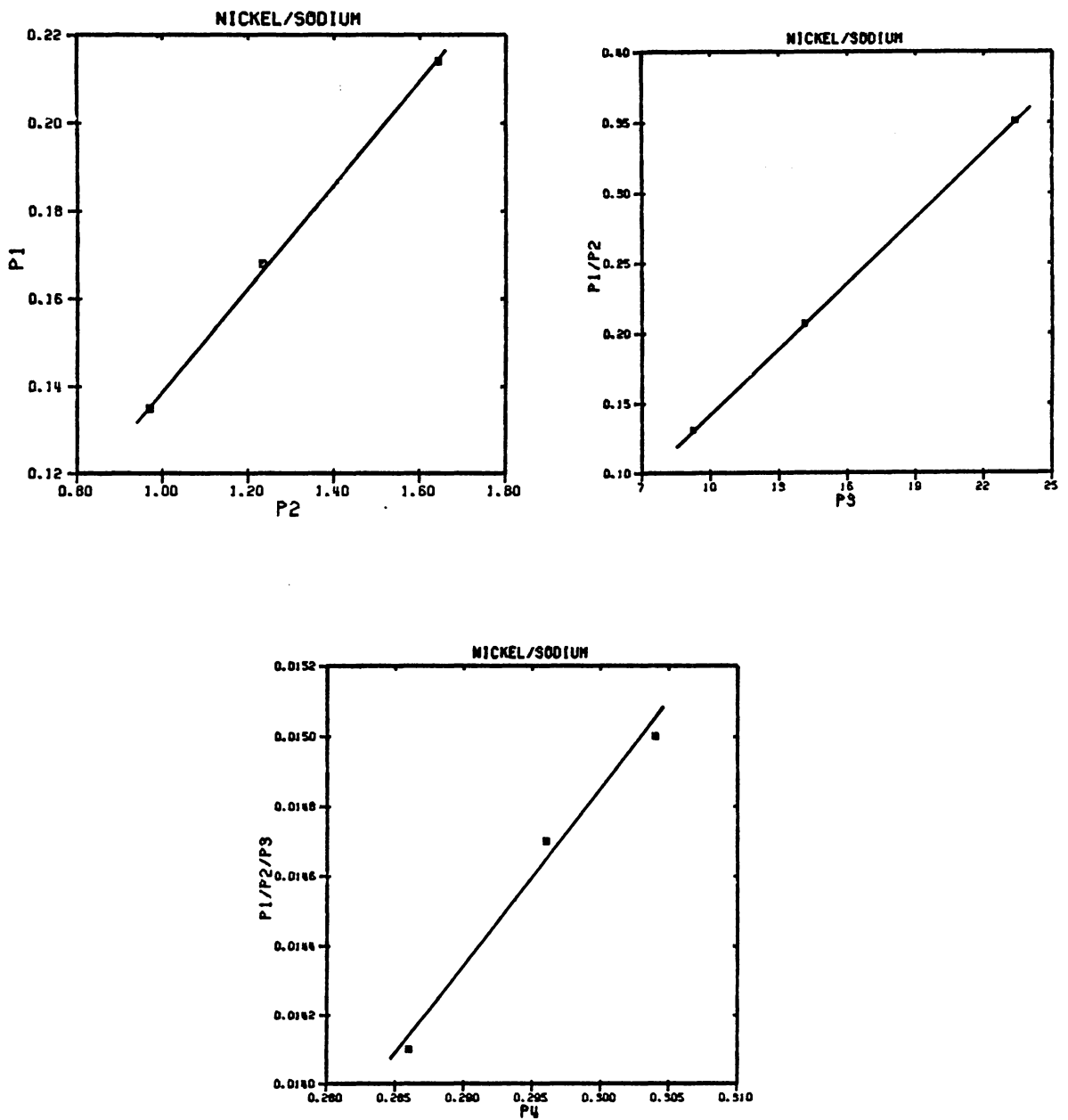


Figure 8. Proportionality between the dimensionless parameters for the derivation of B (nickel/sodium suspension)

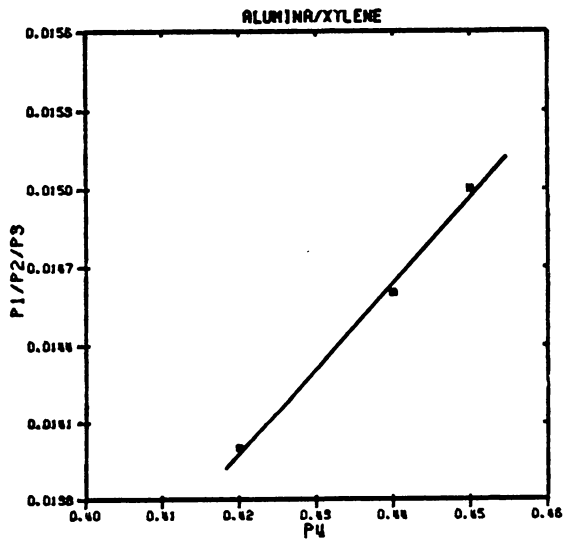
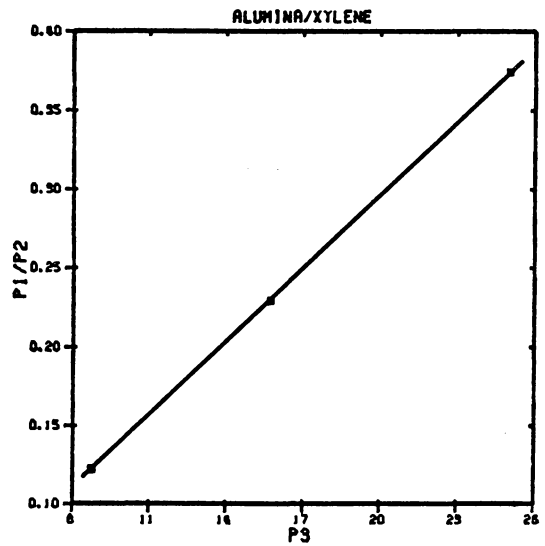
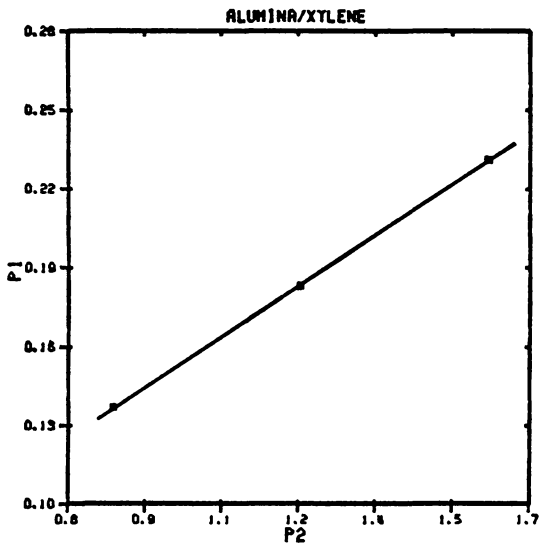


Figure 9. Proportionality between the dimensionless parameters for the derivation of B (alumina/xylene suspension)

rates. The prediction of these parameters, namely, the low shear rate viscosity  $\eta_0$  and the high shear rate viscosity  $\eta_\infty$  , will be discussed in the next chapter.

# **CHAPTER 4**

## **SHEAR VISCOSITY BEHAVIOR AT LOW AND HIGH SHEAR RATES**

### **4.1 INTRODUCTORY REMARKS**

A feature common to viscosity models presented in Chapter 2 is that any particle size distribution effects, if considered at all, have been accounted for by empirical coefficients or exponents determined for the variables, obtained by applying a best fit procedure to the data for a specified suspension. It can be argued, therefore, that it is often not plausible to generalize these formulations, because they do not facilitate further understanding of the effects of such parameters as the particle size distribution, and for that matter, for improving the rheologic characteristics of the suspension for a specified purpose other than by trial-and-error. The formulation proposed in the following sections, on the other hand, allows for predicting the shear viscosity behavior of a highly concentrated suspension through the use of three parameters signifying the effects of particle size distribution.



## 4.2 THEORETICAL BASIS

It has been generally observed, as shown in Figure 5, that three regions of flow exist in a shear stress shear rate curve of a highly concentrated suspension:

- a) a low shear rate region, in which interparticle forces are dominant;
- b) an intermediate shear rate region, in which the flow is pseudoplastic, and the viscosity is a complex function of both solid and liquid properties; and,
- c) a high shear rate region, in which the behavior is predominantly Newtonian, exhibiting well aligned particle movement, and very small interparticle effect as compared to hydrodynamic forces.

One of the physically significant parameters affecting the viscosity of a suspension is  $[\varphi/(\varphi_m - \varphi)]$  referred to herein as the mobility parameter. As mentioned earlier in the preceding chapter, the mobility parameter is a representation of the relative degree of freedom the particles have to move in the mixture.  $(\varphi_m - \varphi)$  represents the effective space available for particles to disperse. Resistance to flow is determined by the value of  $\varphi$  such that as its value approaches to  $\varphi_m$ , the suspension will get thicker, the relative space available will decrease, and hence, resistance to flow will increase dramatically. To test the validity of this reasoning, the measured viscosities of high and low shear rates were plotted versus the mobility parameter,  $[\varphi/(\varphi_m - \varphi)]$  for suspensions listed in Table 2. As can be seen from Figures 8 and 9 the correlation is very good.

Inspection of the various correlations reported in the literature [11,12] suggests that the relative viscosity of suspensions with rigid, spherical particles can well be represented by a relationship of the following form:

$$\eta_r = \left[ 1 + \frac{2.5}{n} \text{fct}(k, \varphi) \right]^n \quad (4.1)$$

**Table 2. Experimental and Predicted Viscosities at Low and High Shear-Rates**

Suspension	$\phi$	$\phi_m$	$\frac{\phi}{\phi_m - \phi}$	$\eta_{r,0}$ meas.	$\eta_{r,0}$ pred.	$\eta_{r,\infty}$ meas.	$\eta_{r,\infty}$ pred.
Nickel-Sodium Ref. [22]	0.304	0.317	23.38	2936.5	2938.5	1100.0	1109.6
	0.296		14.10	885.3	921.5	365.0	415.8
	0.286		9.23	334.4	358.1	172.0	187.5
Nickel-Xylene Ref. [22]	0.350	0.374	14.58	958.6	957.7	292.2	292.2
	0.340		10.00	401.3	383.1	197.0	144.8
Alumina-Xylene Ref. [22]	0.450	0.468	25.00	3446.9	3549.6	1110.0	1109.6
	0.440		15.71	1142.1	1185.0	420.0	454.2
	0.420		8.75	296.8	310.3	166.5	151.5
Alumina-Glycerin Ref. [59]	0.500	0.550	10.00	401.3	399.6	185.0	185.0
	0.480		6.86	173.0	173.0	86.5	92.9
Silica-Thanol Ref. [34]	0.598	0.652	11.07	534.3	529.7	187.0	180.4
	0.550		5.39	91.6	98.9	43.9	49.7
	0.500		3.29	34.4	35.1	23.8	22.0
Silica-Glycerol Ref. [34]	0.600	0.640	15.00	1150.0	1213.0	418.0	403.2
	0.582		10.03	565.0	467.0	177.0	188.0
	0.574		8.70	434.0	335.0	150.0	146.0
Coal-Glycerin Ref. [52]	0.460	0.520	7.7	200.0	206.0	70.0	70.0
	0.403		3.4	45.0	33.0	20.0	18.6
	0.384		2.8	28.0	22.2	13.0	13.8

NOTE :

- For the first four suspensions  $\phi_m$  data were reported as measured values, however, for the last three they were determined through best-fitting the viscosity data.
- For the first four suspensions,  $\eta_{r,0}$  values were calculated from the formula  $\eta_r = [\phi_m/(\phi_m - \phi)]^{2.5}$  as reported in Ref. [22]. For the remaining three suspensions, the shear-stress versus shear-rate curves were used to determine the viscosities at low shear-rates using  $\eta = \tau/G$

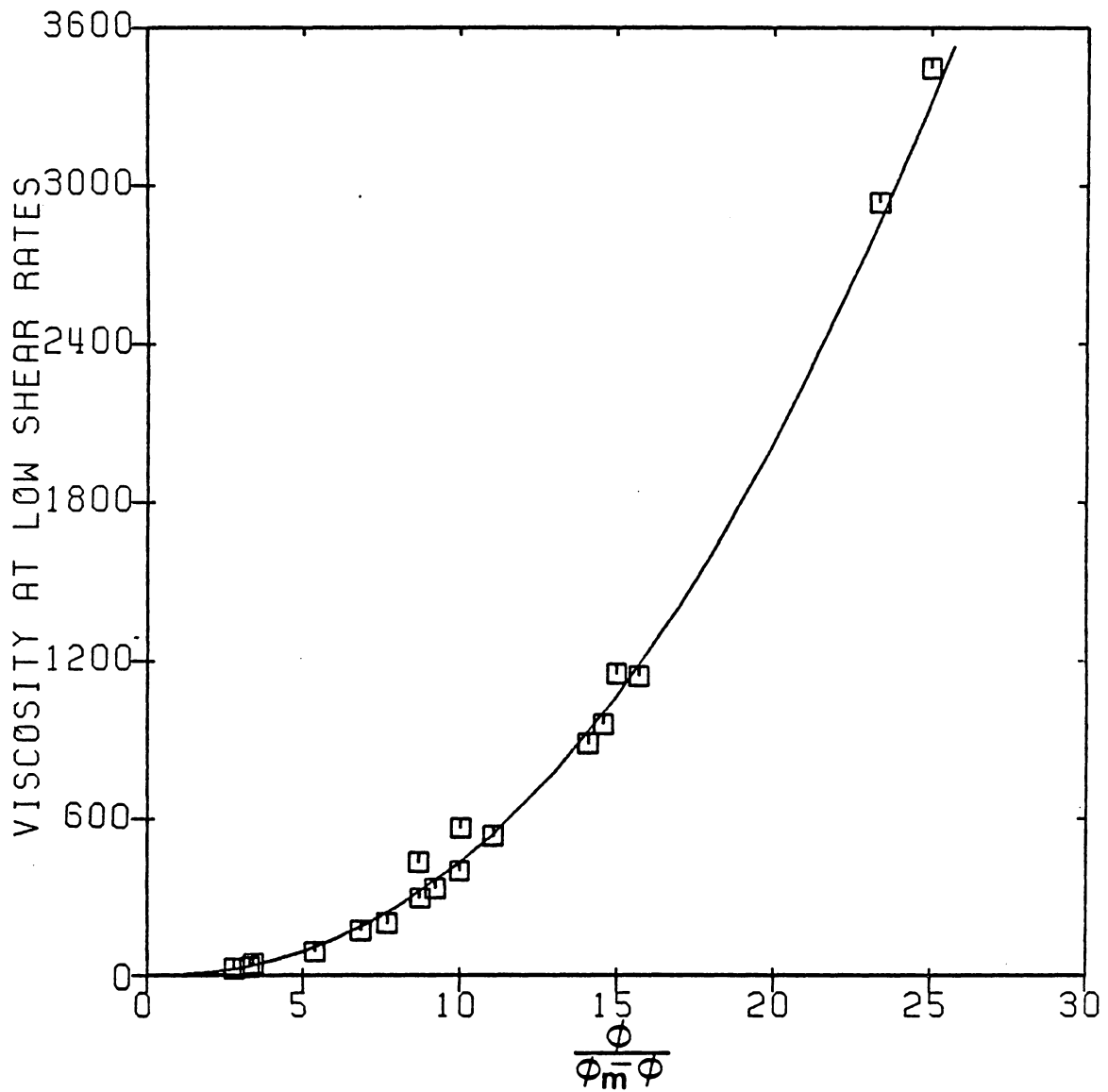


Figure 10. Viscosity at low shear rates versus mobility parameter for suspensions listed in Table 2

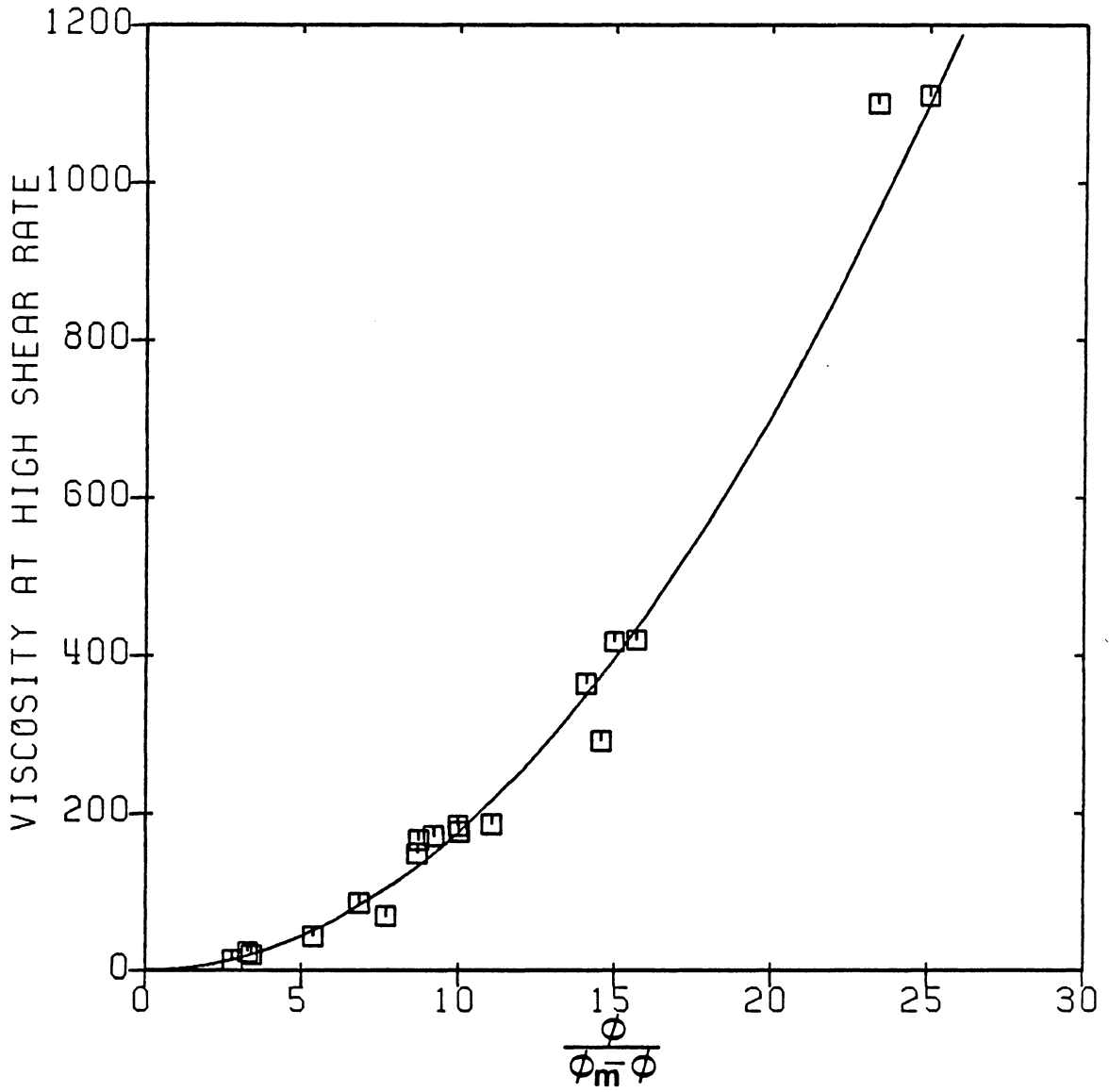


Figure 11. Viscosity at high shear rates versus mobility parameter for suspensions listed in Table 2

where  $k$  is referred to as the crowding factor,  $\phi$  is the concentration, and  $n$  is a suspension-dependent parameter.

In Equation (4.1), the constant 2.5 is a characteristic of uncharged, rigid, spherical particles. For real systems it was replaced by the intrinsic viscosity  $[\eta]$  in order to account for the effects of nonsphericity and other physical as well as nonphysical surface interactions of the solids in various fluid media [16]. Thus, the intrinsic viscosity  $[\eta]$  represents the effective shape of the particles imposed by their surface condition, and is assumed in this study to remain invariant for all shear rates for a specific material.

The parameter  $n$  in Equation (4.1) reflects the level of particle interactions in a given fluid, and varies with the shear rate. Thus,  $n$  is basically a hydrodynamic parameter related to the specific flow structure of the particle-fluid system.

The term  $fct(k, \phi)$  in Equation (4.1) implies that the parameters  $k$  and  $\phi$  have been incorporated in various functional forms in various studies on different systems. However, a widely applied representation is given by:

$$fct(k, \phi) = \frac{\phi}{(1 - k\phi)} \quad (4.2)$$

where, the crowding factor has been defined as  $k = 1/\phi_m$  in many applications [7,12]. Thus,  $k$  has a physical significance in that as  $\phi$  approaches  $\phi_m$  the suspension will get "thicker" and  $\eta_r$  in Equation (4.1) will approach infinity.

In view of the above, the general form of a viscosity equation to calculate the viscosity of suspensions at high and low shear rates is now proposed as follows:

$$\eta_{r,0} = \left[ 1 + \frac{[\eta] \phi \phi_m}{n(\phi_m - \phi)} \right]^n \quad (4.3)$$

As mentioned earlier,  $n$  is basically a flow related parameter that reflects the level of particle interactions and varies with the shear rate. At high shear rates it takes the value of  $n=2$  [11,16] and the preceding equation reduces to:

$$\eta_{r,\infty} = \left[ 1 + \frac{[\eta] \phi \phi_m}{2(\phi_m - \phi)} \right]^2 \quad (4.4)$$

This is the modified Eilers equation which appears to be capable of fitting viscosity data at high shear rates for suspensions with spherical or irregular particles better than other existing correlations [16].

At sufficiently high shear rates the behavior of suspensions tend to become Newtonian, where the shear rate versus shear rate curve tends to have a constant slope. In this region, the Newtonian viscosity of suspensions was correlated by means the intrinsic viscosity  $[\eta]$ , and the maximum packing concentration  $\phi_m$ .

The parameters to be evaluated in Equation (4.3) are  $[\eta]$ ,  $n$  and  $\phi_m$ . The value of  $[\eta]$  for uncharged particles with smooth spherical surface is reported to be 2.5, whereas particles which have irregular shape the value of  $[\eta]$  is largely uncertain. Consequently, the relative viscosity  $\eta_{r,\infty}$  at high shear rates should be known in order to calculate the value of  $[\eta]$  for that specific material.

The value of  $n$ , which represents the particle association at the initiation of motion, is difficult to obtain directly from experiments. However, the measured viscosity at low shear rates  $\eta_{r,0}$  can be used to calculate  $n$  from Equation (4.3), provided  $[\eta]$  and  $\phi_m$  are known for the suspension.

Finally, the value of the maximum packing concentration  $\phi_m$  can be obtained either experimentally or analytically. The principal methods used for measuring  $\phi_m$  are sedimentation and centrifuging. However, it is not certain as to whether either one determines the true value of  $\phi_m$ . Analytical methods, including those the ones proposed by Lee [39] and Patton [50], on the other hand, are based on ideal packing conditions and do not include the effects of surface chemistry and shape of particles. Nevertheless, it is very important to accurately evaluate the maximum packing concentration of the particles in highly concentrated suspensions, because the values of  $[\eta]$  and  $n$  in Equation (4.3) depend strongly on  $\phi_m$ .

### 4.3 DETERMINATION OF MAXIMUM PACKING CONCENTRATION

It is known that highly loaded mixtures can be achieved by blending particles of various sizes in appropriate proportions. It has also been mentioned earlier, that the viscosity of suspensions in low and high shear rate ranges can be predicted as a function of the volume concentration provided the maximum packing concentration is known. An analytical method developed by Lee [39] proposed calculation of the packing of  $n$ -component mixtures of spheres based on the idealized packing characteristics of binary mixtures, whose compositions were assumed to be independent of the size ratio of the spherical particles. This rather unrealistic assumption was improved subsequently by Patton [50], through the use of a parameter whose value varies with the size ratio. The equation derived by Patton is given as follows:

$$(\phi_m)_i = \sum_{i=1}^{nf} \sum_{j=1}^{nf} \Phi_{ij} \phi_j \quad (4.5)$$

where  $n_f$  is the number of size fractions,  $\phi_j$  refer to the respective volume fractions,  $\Phi_{ii} = \Phi_{jj} = 0.639$  and  $\Phi_{ij}$  represent the coefficients to be used in relating a larger particle group to a smaller one and vice versa. The following expression was developed for these coefficients:

$$\Phi_{ij} = 0.639 \pm \left[ \frac{\phi_{mo} - 0.639}{1.15 - 1.017\phi_{mo}} \right] \quad (4.6)$$

where,  $\phi_{mo}$  is the maximum packing concentration for binary mixtures given by Figure 10.

In Equation (4.6), positive sign applies when a coarse size fraction is blended with a finer size fraction, and the negative size applies otherwise. The lowest of the various values calculated with Equation (4.5) is selected as the correct maximum packing concentration for the given volume composition.

The maximum packing concentrations calculated for a number of suspensions with various particle size distributions are tabulated in Table 3. These calculated concentrations are then correlated to the intrinsic viscosity  $[\eta]$  and the particle interaction parameter  $n$ , as explained in Chapter 7, section 7.5.



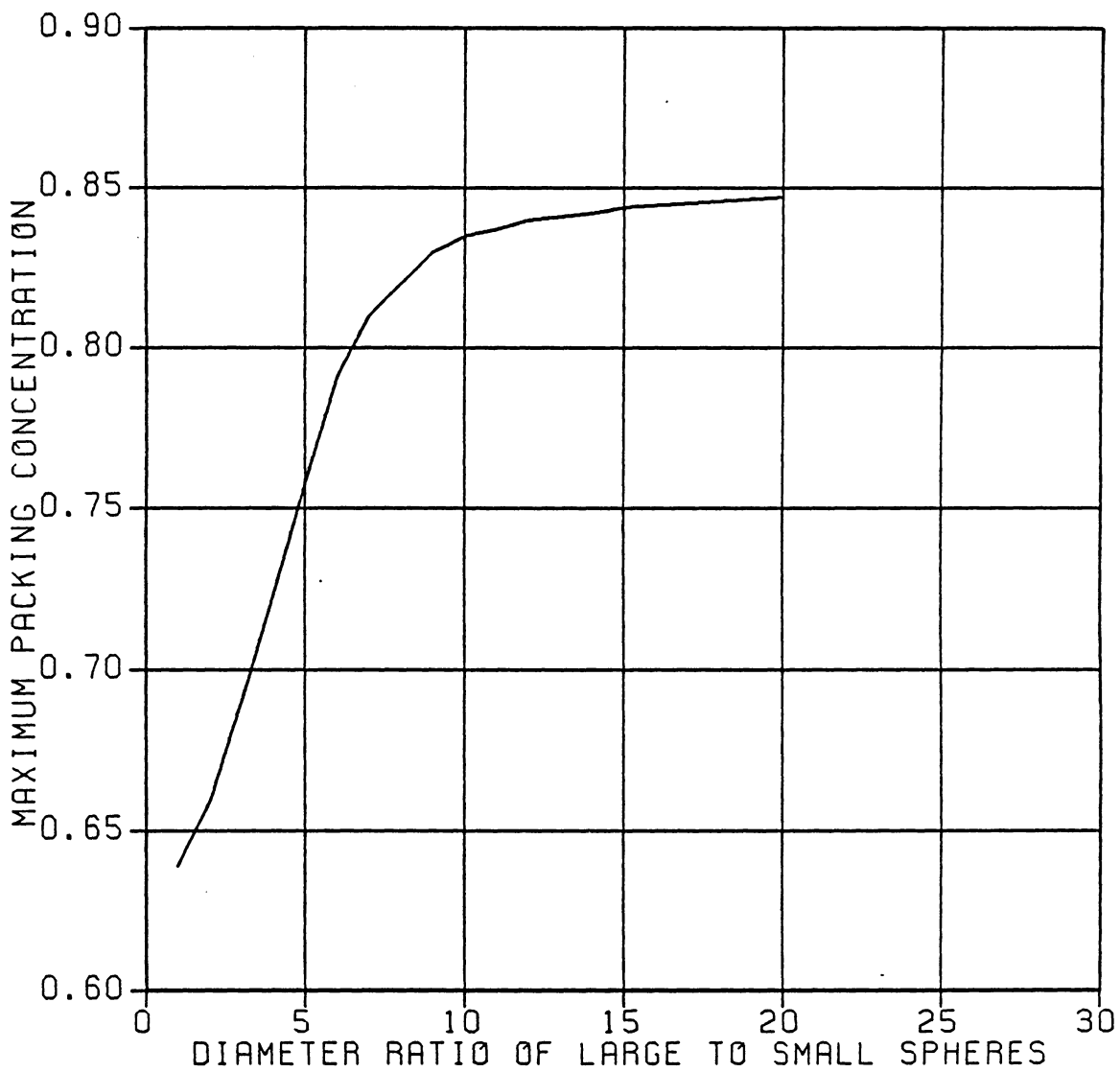


Figure 12. Maximum packing concentrations for binary mixtures of spherical particles

**Table 3. Correlation of Calculated and Experimental Values of the Maximum Packing Concentration**

Suspension	$\varphi_{m,c}$	$\varphi_{m,e}$	$[\eta]$	n	$[\eta] \frac{n_0}{n_\infty} \varphi_{m,c}$
Nickel-Sodium	0.678	0.317	8.680	2.402	7.068
Nickel-Xylene	0.678	0.374	5.901	2.673	5.347
Alumina-Xylene	0.694	0.468	5.524	2.478	4.750
Alumina-Glycerin	0.694	0.550	4.582	2.485	3.951
Silica-Thanol	0.650	0.652	3.443	2.700	3.021
Silica-Glycerol	0.650	0.640	3.975	2.570	3.320
Coal-Glycerin	0.712	0.520	3.696	3.000	3.947

NOTE :

- $\varphi_{m,c}$  values were calculated using the method of successive size fractions [39,50]
- $\varphi_{m,e}$  values for the last three suspensions were calculated by best fitting the experimental viscosity data
- $[\eta]$  and n values were calculated from Equations (4.4) and (4.3), respectively.

# **CHAPTER 5**

## **ENERGY REQUIREMENT IN HYDRAULIC CONVEYANCE AND COMMINUTION OF SOLIDS**

### **5.1 INTRODUCTORY REMARKS**

In this chapter, the technical aspects of the energy consumed, due to frictional losses during hydraulic transportation and due to reduction of particle size distribution during grinding, are discussed. In the first section, the relations describing the stabilized laminar pipe flow of both yield-power law and power law pseudoplastic fluid are derived, in a manner analogous to the Hagen-Poiseuille equation, from the fundamental momentum equation and the power law rheological equation. Subsequently, a brief presentation of the comminution theory, defined as the relationship between energy input and the product particle size obtained from a given feed size, is made for the estimation of the amount of grinding energy.

## 5.2 PUMPING CHARACTERISTICS OF PSEUDO-HOMOGENEOUS TIME-INDEPENDENT NON-NEWTONIAN MIXTURES IN LAMINAR FLOW

For steady-state laminar flow in a pipe total volumetric flow rate can be written as follows:

$$Q = 2\pi \int_0^R u r dr \quad (5.1)$$

where  $Q$  is the total volumetric flow rate,  $u$  is the velocity at a radial distance  $r$  from the pipe center line and  $R$  is the radius of the pipe. Integration of this equation by parts yields:

$$Q = \pi \left[ u r^2 - \int_0^R r^2 du \right]_0^R \quad (5.2)$$

The condition of no slip at the wall, namely,  $u=0$  when  $r=R$ , simplifies the above equation to:

$$Q = -\pi \int_0^R r^2 du \quad (5.3)$$

On the other hand the momentum equation for one dimensional flow of a cylindrical element of radius  $r$  and length  $\Delta L$  will yield:

$$-\pi r^2 \Delta P = 2\pi r \tau \Delta L \quad (5.4)$$

where  $\tau$  denotes the shear stress at a radial distance and thus,

$$\tau = -\frac{r}{2} \frac{\Delta P}{\Delta L} \quad (5.5)$$

in which  $(\Delta P/\Delta L)$  refers to the pressure gradient along the pipe.

The relation describing the stabilized laminar pipe flow of a yield-power law fluid was given previously in Equation (2.1) as follows:

$$\tau = \tau_y + KG^n \quad (2.1)$$

Combining Equation (5.5) and (2.1) yields:

$$-\frac{du}{dr} = -\left(\frac{1}{K}\right)^{1/n} \left[ \frac{r}{2} \frac{\Delta P}{\Delta L} + \tau_y \right]^{1/n} \quad (5.6)$$

where  $du/dr = G$  denotes the shear-rate. When integrated with the no-slip condition of  $u=0$  for  $r=R$ , Equation (5.6) yields the radial velocity distribution:

$$u = \left[ \frac{1}{K} \right]^{1/n} \left[ \frac{\frac{n}{1+n}}{-\frac{\Delta P}{2\Delta L}} \right] \left[ \left[ -\frac{R\Delta P}{2\Delta L} - \tau_y \right]^{(1+n)/n} - \left[ -\frac{r\Delta P}{2\Delta L} - \tau_y \right]^{(1+n)/n} \right] \quad (5.7)$$

Substituting  $u$  into Equation (5.1) and integrating the following equation is obtained for the average velocity  $V$ :

$$V = \frac{D}{2} \frac{\left(\frac{1}{K}\right)^{1/n}}{\left[\frac{D\Delta P}{4\Delta L}\right]^3} \left[ \frac{D\Delta P}{4\Delta L} - \tau_y \right]^{(1+n)/n} [\Omega] \quad (5.8)$$

$$\text{where } \Omega = \left[ \frac{\left(\frac{D\Delta P}{4\Delta L} - \tau_y\right)^2}{\frac{1+3n}{n}} + \frac{2\tau_y\left(\frac{D\Delta P}{4\Delta L} - \tau_y\right)}{\frac{1+2n}{n}} + \frac{\tau_y^2}{\frac{1+n}{n}} \right]$$

For systems exhibiting no yield stress, on the other hand, Equation (5.8) takes a less complex form:

$$V = \frac{D}{2} \left[ \frac{n}{1+3n} \right] \left[ \frac{D\Delta P}{4\Delta L} \right]^{1/n} \left( \frac{1}{K} \right)^{1/n} \quad (5.9)$$

Solving this equation for  $\Delta P/\Delta L$ , we obtain:

$$\frac{\Delta P}{\Delta L} = \frac{4V^n K}{D^{1+n}} \left[ \frac{2+6n}{n} \right]^n \quad (5.10)$$

It is possible to estimate the pressure drop for pipe flows using the Fanning equation given by [28]:

$$f = \frac{\Delta P}{\Delta L} \frac{D}{2\rho V^2} \quad (5.11)$$

where,  $\rho$  is the mass density of the suspension,  $g$  is the gravitational acceleration, and  $f$  is the Fanning friction factor. Substituting Equation (5.10) into Equation (5.11), the friction factor can be written as:

$$f = \frac{1}{8} \left[ \frac{16}{Re_{PL1}} \right] \left[ \frac{2+6n}{n} \right]^n \quad (5.12)$$

or

$$f = \frac{16}{Re_{PL2}} \quad (5.13)$$

where  $Re_{PL1}$  and  $Re_{PL2}$  are alternate forms of the "power-law Reynolds number" defined as [28]:

$$Re_{PL1} = \frac{D^n V^{2-n} \rho}{K} \quad (5.14)$$

and

$$Re_{PL2} = \frac{D^n V^{2-n} \rho}{K} 8 \left[ \frac{n}{2 + 6n} \right]^n \quad (5.15)$$

both of which reduce to the conventional Newtonian Reynolds number when  $n=1$ . Transition to turbulent flow occurs at the critical Reynolds number given as [28]:

$$(Re_{PL2})_c = \frac{6464n}{(1 + 3n)^2 \left( \frac{1}{2 + n} \right)^{(2+n)/(1+n)}} \quad (5.16)$$

In view of the above, after calculating the required average velocity of the mixture, characterized by the power-law constants  $K$  and  $n$ , the power-law Reynolds number from Equation (5.15) and the transition Reynolds number from Equation (5.16) are calculated. If the flow is laminar, meaning the value of Reynolds number is less than the critical transition value, Equation (5.12) is used for the calculation of the friction factor. If the flow is turbulent, the following friction factor equation is used:

$$\frac{1}{\sqrt{f}} = \frac{2.69}{n} - 2.95 + \frac{4.53}{n} \log_{10} [Re_{PLC} (\sqrt{f})^{2-n}] + \frac{0.68}{n} (5n - 8) \quad (5.17)$$

where  $Re_{PLC}$  is the Clapp power-law Reynolds number defined as [9,28]:

$$Re_{PLC} = \frac{Re_{PL1}}{8^{(n-1)}} \quad (5.18)$$

The energy required per unit length for transporting a non-Newtonian mixture in a pipe of certain length  $\Delta L$  is defined as:

$$\frac{\text{Energy}}{\text{Length}} = Q_m \left[ \frac{\Delta P}{\Delta L} \right] \quad (5.19)$$

Therefore, by substituting the value of  $(\Delta P/\Delta L)$  obtained from Equation (5.10) into Equation (5.19) one can obtain the energy required to pump any amount of solid-liquid mixture to any distance through pipes.

### 5.3 GRINDING CHARACTERISTICS OF SOLID PARTICLES

Fine grinding of solid particles can be achieved in many different ways. Among the most common techniques being used commercially are tumbling mill grinding, vibratory milling, impact milling and stirred ball milling [60]. The purpose of reducing the sizes of solids and thereby increasing the material's specific surface is called *comminution*. Comminution theory is concerned with the relationship between energy input and the product particle size of a given feed size. Various theories have been offered, but none is entirely satisfactory. The greatest problem lies in the fact that most of the energy input is absorbed by the machine itself in the form of heat, and therefore only a small amount of energy remains for breaking the material. In the case of plastic material, certain amount of energy will be consumed in changing shape but will never create a new surface [60]. However, this type of problem is approximated by assuming that the material used is brittle and no energy is consumed by the solid particles in themselves.

The oldest theory is that of Rittinger in [60] which states that energy consumed in the size reduction is proportional to the area of new surface produced. This can be represented as:

$$E = \text{fct}(S_a) \quad (5.20)$$

where  $E$  is the grinding energy (kWh/ton) and  $S_a$  is referred to as the specific surface area.



There are also other theories such as Kick's law and Bond's theory which again attempt to model the proportionality of the work input to some physical parameter associated with particle breakage. In general, Hukki [32] suggests that Kick's law is reasonably accurate in the crushing range above about 1 cm in diameter. Bond's theory applies reasonably in the range of conventional rod-mill and ball-mill grinding and Rittinger's law applies fairly well in the fine grinding range of 10 - 1000  $\mu$  m (microns). This is schematically represented in Figure 11 [60]. In this study, the approach of Rittinger is employed conceptually consistent with the present approach of formulating the solid-liquid mixtures.

Particle size analysis is very important in assessing the performance of grinding circuits. There are many different ways of recording the results from these circuits, the most common being that of plotting cumulative undersize (or oversize) against particle size. Many curves of cumulative oversize or undersize against particle size are S-shaped, leading to congested plots at the extremities of the graph. The two most common methods, which are often applied to comminution studies, where non-uniform size distributions are obtained are [60]:

$$\begin{array}{ll}
 \text{Schuhmann - Gaudin} & S_j = 100 (d_j/d_m)^m \\
 \text{Rosin - Rammler} & S_j = 100 [1 - e^{- (d_j/d_m)^m}]
 \end{array} \tag{5.21}$$

where,  $S_j$  is the cumulative weight fraction of particles finer than a given size  $d_j$ . Each function has two parameters,  $d_m$  and  $m$ , often called the *size modulus* and *distribution modulus*, respectively. Among these methods, Schuhmann-Gaudin method, when plotted on a log-ln scale, considerably expands the region below 50 % in the cumulative undersize. However, the region above 50 % is severely contracted which is a major disadvantage of the method. Rosin-Rammler method, often used to represent results from ball mills, expands the region below 25 % and above 75 % cumulative undersize and it

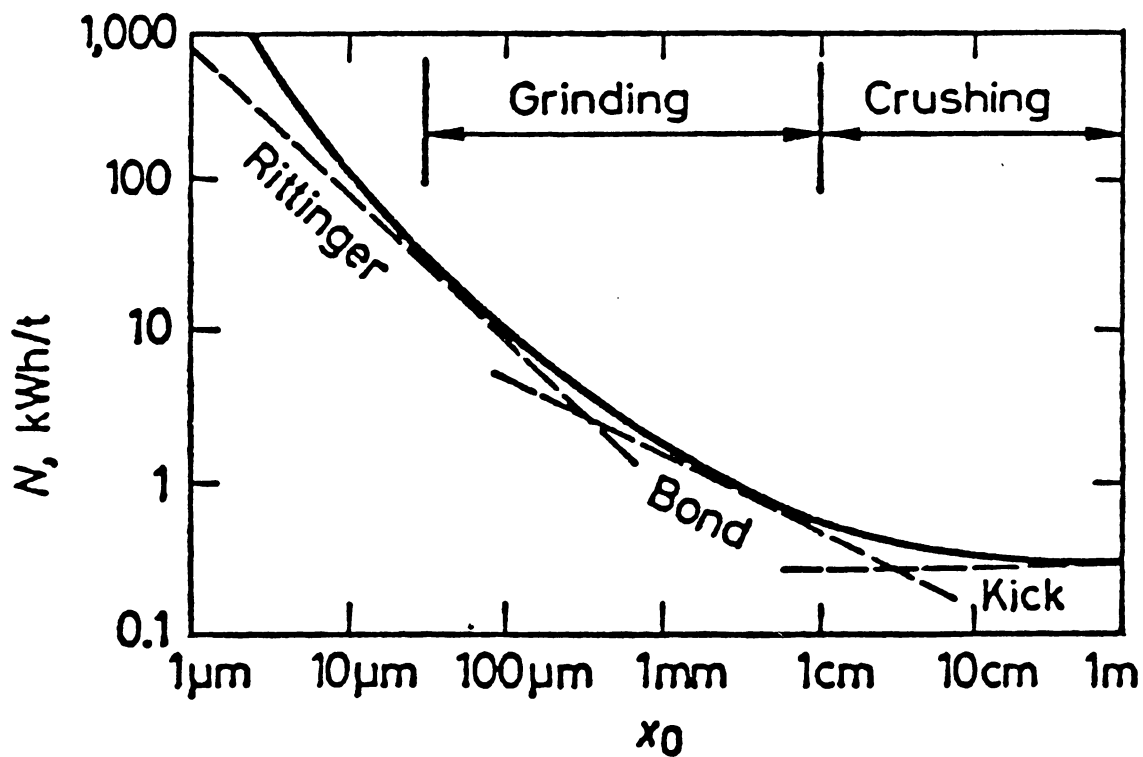


Figure 13. Specific comminution work  $N$  vs feed particle size for a constant reduction ratio

contracts the 30 - 60 % region. It has been stated, however, that this contraction does not cause adverse effects [60].

The Schuhmann-Gaudin method is often preferred to the Rosin-Rammler method in mineral processing applications, the latter being more often used in coal-preparation studies. Nevertheless, in preparation of coal- liquid mixtures the characteristic relationship or method should be used, that represents the size distribution best, estimating the results obtained by any grinding machine.

## **CHAPTER 6**

### **COMPUTER IMPLEMENTATION**

#### **6.1 GENERAL REMARKS**

A computer program was written in FORTRAN 77 to implement the formulations developed in this study and to evaluate the energy consumption of a slurry, during comminution to prepare the mixture and during hydraulic transportation, with various specified particle size distributions and concentrations. The program basically follows the computational procedure which will be outlined in the beginning of Chapter 7. The computer model consists of a main program and thirteen subprograms. The block diagram of the model is given in Figure 12.

In the following sections, a list of the most significant variables in the program and their definitions and the descriptions of all the subroutines are presented. The listing of the program is given in Appendix A.

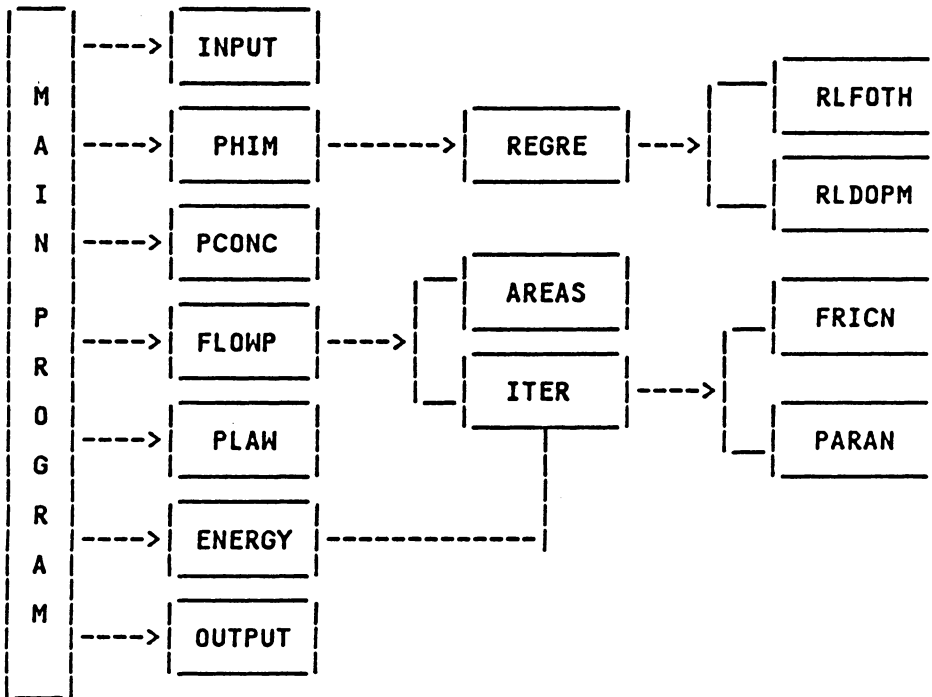


Figure 14. Block diagram of the computer model

## 6.2 LIST OF THE MOST SIGNIFICANT VARIABLES IN THE COMPUTER PROGRAM

In this section, a list of the most significant variables, variables needed for input, output and for major calculations, are presented. Definitions are kept as brief and as descriptive as possible.

BC	: Flow parameter B of Equation (3.21)
C	: Calibration coefficient in yield-stress equation [Equation (3.19)]
CENER	: Comminution energy (kWh)
CM	: Maximum packing concentration
CORR	: Desired correlation coefficient for Rosin-Rammler fit to the particle size distribution
CVOL(NCV)	: Volumetric concentrations of the suspension
D(ND)	: Pipe diameters for hydraulic transportation (inch)
DELM(IDM)	: Increments of DM
DELP	: Pressure gradient per unit length
DG	: Increment of shear-rate to be increased
DIAMR(NDR)	: Diameter ratio of large spherical particles to small ones
DIST(NDIST)	: Lengths of pipes (mile)
DP	: Geometric mean particle size (micron)
DS	: Surface area mean diameter (micron)
EFF	: Efficiency of pumps
EINF	: Relative viscosity at high shear-rates
ETA	: Intrinsic viscosity
ETA0	: Relative viscosity at low shear-rates

**F** : Friction factor  
**F0** : Input value of the friction factor for the Newton-Raphson iteration method  
**G(NG)** : Shear-rate (1/sec)  
**GA** : Gravitational acceleration (m/sec)  
**GC** : Unit conversion factor (force to mass or vice versa)  
**GI** : Conversion factor from inch to meter  
**G1** : Initial value of the shear-rate for the analysis to start from  
**IDM** : Number of increments in DELM  
**KK** : Calibration coefficient in K in Equation (3.21)  
**MU** : Dynamic viscosity (N-sec/sq-m)  
**N** : Particle interaction parameter in Equation (4.3)  
**N0** : Input value for the iteration of N  
**NCV** : Number of concentrations in CVOL  
**ND** : Number of pipe diameters  
**NDIST** : Number of lengths of pipes  
**NDR** : Number of elements in DIAMR and PMAX vector  
**NG** : Number of shear-rates  
**NSIZE** : Number of particle sizes in the particle size distribution  
**NTYPE** : Control parameter-NTYPE= 1 CM is known, NTYPE= 0 CM is not known  
**PENER** : Pumping energy (kWh/yr)  
**PK** : Power-law consistency index K in Equation (2.1) (N-sec/sq-m)  
**PMAX(NDR)** : Maximum packing concentrations that correspond to each DIAMR  
**PN** : Power-law flow index n in Equation (2.1)  
**PSIZE(NSIZE)** : Particle sizes in the input particle size distribution (micron)

QM	: Mixture volumetric flow rate (cubic-m/sec)
RE	: Power-law Reynolds number
RHOL	: Density of liquid in the suspension (kg/cubic-m)
RHOS	: Density of solid particles in the suspension (kg/cubic-m)
SF	: Shape factor of the solid particles
SSAREA	: Specific surface area of the particle size distribution (1/micron)
TAU	: Shear stress $t$ in Equation (3.1) (N/sq-m)
TAUY	: Yield stress $t_y$ in Equation (3.1) (N/sq-m)
V(NSIZE)	: Percentage of each particle size in the particle size distribution
VM	: Mixture velocity (m/sec)
W	: Annual throughput to be pumped through pipes (tons/year)

### 6.3 DESCRIPTION OF THE MAIN PROGRAM AND SUBPROGRAMS

The main program has the objective of controlling the proper execution sequence of various subprograms in accordance with the specified values of the control variables. After reading in the input data, the main program sets up a do-loop in which subroutines PHIM, PCONC, FLOWP, PLAW, OUTPUT, and ENERGY are called for every volumetric concentration specified. The execution in the main program lasts until all the particle size distribution variations specified are covered for every concentration input. If there is another set of input data following the first one then the program sets all the control variables to their initial value and carries on the same execution sequence as before.

Subroutine PHIM computes the weighted mean diameter of particles WMEAND, fits the input particle size distribution to Rosin-Rammler equation [Equation (5.21)] and varies the particle size distribution in between specified limits. The goodness of fit of



input particle size distribution to Rosin-Rammler equation is controlled with the correlation coefficient specified in the input data. When the correlation coefficient is less than the one obtained from regression then a new distribution is defined by eliminating the largest particle. This procedure is performed until an equal or better correlation is obtained. Particle size distribution is varied on a  $\log(\ln)$  versus log scale by keeping the weighted mean diameter WMEAND constant and changing the slope of the line DM. For Particle size distributions which have broader distributions than the original one, i.e. lines with smaller slope DM, the lines are extended toward the increasing size direction. The other end of the line is not extended any further than the one set by the input distribution because of the danger of getting into an area where the particle sizes are too small which generate the colloidal content that completely alters the rheological behavior.

Subroutine PCONC computes the maximum packing concentration of a specified particle size distribution. The analytical method explained in Chapter 4 is used for this computation. The calculated maximum packing concentration is then modified using Equation (7.2) to find the actual value to be used in rheologic calculations.

Subroutine FLOWP calculates the yield stress  $\tau_y$ , flow parameter B, and the shear-stresses corresponding to each shear-rate specified using given particle and fluid physical properties.

Subroutine PLAW fits a power-law curve to suspension flow data by using the method of least squares. The values of the power-law constants n and K in Equation (2.1) are determined as a result of this curve fit.

Subroutine ENERGY computes the power requirement of a yield power-law complex mixture flow in a pipe. The procedure followed was explained in Chapter 5. This subroutine also prints out the values of concentration of solids CV, power-law constants PN and PK, pipe diameter D, flow regime LAMINAR or TURBULENT, distance of

pipe DIST, and the corresponding values of the pumping, comminution and total energies in kWh/yr.

Subroutine AREAS computes the specific surface area and the surface area mean diameter of any given particle size distribution.

Subroutine ITER computes the values of the turbulent friction factor, pressure gradient of a yield power-law mixture and the particle interaction parameter using the Newton-Raphson iteration technique.

Subroutine REGRE is used for regression analysis of any specified order of a polynomial. The regression is carried out by making use of two IMSL routines that are supported by the main frame. In addition to regression analysis, this subroutine also computes the coefficient of determination that represents to the goodness of the regression.

There are three function subroutines, namely PGRAD, FRICN and PARAN, which are used for the calculation of the pressure gradient of a yield power-law fluid, friction factor of a turbulent power-law fluid and the particle interaction parameter used in viscosity equations, respectively.

## CHAPTER 7

### APPLICATIONS, RESULTS AND EVALUATIONS

#### 7.1 INTRODUCTORY REMARKS

The concepts, methodologies and formulations developed and described in the preceding sections were tested with experimental data reported in the literature for eight different solid-liquid suspensions. They all had very high relative concentrations, with calculated  $\phi/\phi_m$  values ranging from 0.738 to 0.961, each could well be represented by the yield-power-law model defined in Equation (2.1) and exhibited pseudoplastic behavior within the entire range of the shear rates measured. Many other data reported in the literature could not be used, however, due to lack of information on either the maximum packing concentration, or viscosity at low and high shear rates, or more importantly, the particle size distribution. Nevertheless, the data used pertained to suspensions formed by a variety of solids and liquids with a fairly wide range of rheologic characteristics.

This chapter describes the data characteristics used in these applications, followed by the procedures of the calculations made, the results obtained and their evaluations, for each of the three groups of analyses carried out. The first part pertains to the im-

plementation of the basic rheologic formulation developed and described in Chapter 3. The second part of calculations is about the prediction of the shear viscosities at varying shear rates using the methodology described in Chapter 4. The third group of calculations is associated with the optimization of particle size distribution for the combination of two utilization phases involving the comminution and pipeline transportation of coal-based liquid fuels as described in Chapter 5. Also presented in this chapter is an overall evaluation of the proposed approach, with emphasis on the apparent advantages and limitations deduced from these analyses.

## **7.2 CHARACTERISTICS OF THE DATA ANALYZED**

There are a number of experimental data reported in the literature on solid-liquid suspensions. However, depending on the objectives of those studies, various different parameters related to the behavior of suspensions have been focused on while neglecting others. Consequently, despite the large number of experimental data reported, only a few were found to contain the appropriate information for use in this study. The characteristics of these data, with emphasis on experimental features and physical properties of both the solid particles and the liquid, will be presented in the following.

The physical properties of the suspensions, as given in the raw data, and the particle size distributions of the solid-liquid systems used are given in Table 4 and Figures 13 through 16, respectively. The unknown properties that are calculated by using the available data are listed in Table 5. In Table 4, the first four suspensions, namely nickel-sodium, nickel-xylene, alumina-xylene and alumina-glycerin, were taken from reference [22] which had the most complete information. The maximum packing concentrations of these four suspensions were found by centrifuging the slurries. Particle surface areas were determined by measurements of nitrogen gas adsorbed by the solids.

**Table 4. Physical Properties of Systems used in Applications (Raw Data)**

Material	$\phi_m$	$\phi$	$\tau_y$	$\rho_s$ (gr/cc)	$\rho_l$ (gr/cc)	$\xi$	$\mu$ (cp)	$\eta_{r,0}$	$\eta_{r,\infty}$	Ref.
Nickel-Sodium $\tau_y$ (lb/sq.ft.)	0.317	0.304 0.296 0.286	0.700 0.400 0.245	7.32	0.92	0.118	0.54	2936.5 885.3 334.4	1100.0 365.0 172.0	[22]
Nickel-Xylene $\tau_y$ (lb/sq.ft.)	0.374	0.350 0.340	0.715 0.450	7.32	0.86	0.118	0.61	958.6 401.3	292.2 197.0	[22]
Alumina-Xylene $\tau_y$ (lb/sq.ft.)	0.468	0.450 0.440 0.420	2.08 1.25 0.245	3.48	0.86	0.164	0.61	3446.9 1142.1 296.8	1110.0 420.0 166.5	[22]
Alumina-Glycerin $\tau_y$ (lb/sq.ft.)	0.550	0.500 0.480	2.80 2.20	3.48	1.26	0.164	954	401.3 173.0	185.0 86.5	[22]
Coal-Glycerin $\tau_y$ (Pa)	—	0.460 0.430 0.384	35.00 12.70 4.85	1.48	1.248	—	954	200.0 45.0 28.0	70.0 20.0 13.0	[59]
Coal-Oil $\tau_y$ (Pa)	—	0.550 0.500 0.450	10.00 5.00 2.00	1.28	0.858	—	32.6	— — —	— — —	[52]

**Table 5. Calculated Physical Properties of Systems**

Material	$\phi_m$	$\phi$	C	K	$D_p$ ( $\mu\text{m}$ )	k ( $1/\mu\text{m}$ )	$D_s$ ( $\mu\text{m}$ )	$\xi$
Nickel-Sodium $\tau_y$ (lb/sq.ft.)	0.317	0.304 0.296 0.286	0.0241	0.0495	10.5	0.709	5.045	0.118
Nickel-Xylene $\tau_y$ (lb/sq.ft.)	0.374	0.350 0.340	0.0295	0.0486	10.5	0.709	5.045	0.118
Alumina-Xylene $\tau_y$ (lb/sq.ft.)	0.468	0.450 0.440 0.420	0.134	0.0332	12.0	0.742	3.465	0.164
Alumina-Glycerin $\tau_y$ (lb/sq.ft.)	0.550	0.500 0.480	0.508	0.0003	12.0	0.742	3.465	0.164
Coal-Glycerin $\tau_y$ (Pa)	0.520	0.460 0.430 0.384	86.00	0.00162	13.0	0.858	3.414	0.337
Coal-Oil $\tau_y$ (Pa)	0.711	0.550 0.500 0.450	1.600	1.317	180.0	0.0858	64.51	0.337

Particle diameters and size distributions were measured with a Coulter counter. The diameters measured by this instrument were equivalent spherical diameters. Laminar flow rheological properties of these suspensions were determined from pressure drop flow rate measurements using jacketed, horizontal pipe viscometers. For more information reference [22] should be consulted.

Chunks of Illinois #6 coal were ground in a ball mill for producing the coal-glycerin system [59]. No measurements were made to determine the maximum packing concentration. However, the value of 0.52 given in Table 5 was found through best fitting the experimental data to the rheological formulations proposed previously. More emphasis will be placed on this matter in the following sections. Particle size distribution was determined with a Microtrac Analyzer, a light-scattering device that records particle populations in 13 channels (sizes) over the range 1.9 - 176  $\mu$  m. Particle surface areas were not measured but information from a similar type of coal from reference [5] was used. Rheological measurements were carried out by using a Weissenberg Rheogoniometer R-17, details of which are elaborated in reference [59].

The coal type used for coal-oil mixtures was a bituminous type from Butler County, Pennsylvania [52]. This coal was dry sieved to obtain the particle size distribution and later various fractions were blended to obtain coal-oil mixtures with various size distributions. However, detailed particle size distributions were not reported for different blends. Because, no information was available on the surface area or shape characteristics of the particles, the shape factor that was used for coal in coal-glycerin suspension was assumed applicable for this coal, also. Again, no attempt was reportedly made for obtaining the maximum packing concentration. However, the particle sizes were sufficiently large and not likely to cause formation of agglomerates or significant surface condition changes. Therefore, the calculated maximum packing concentration, which

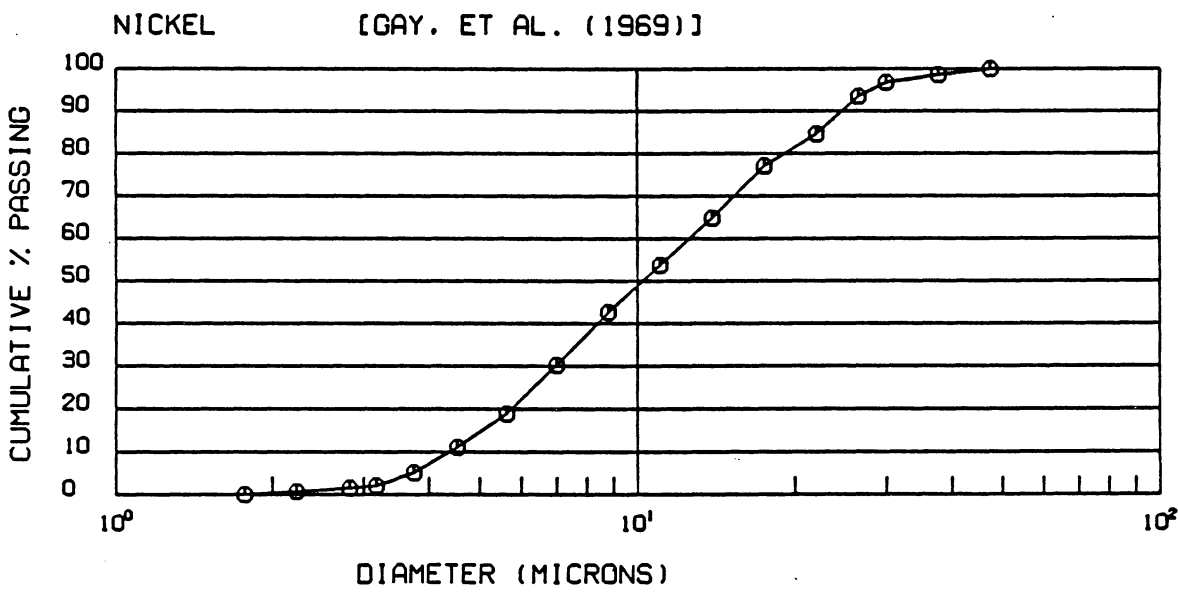


Figure 15. Particle size distribution of nickel used in nickel-sodium and nickel-xylene suspensions



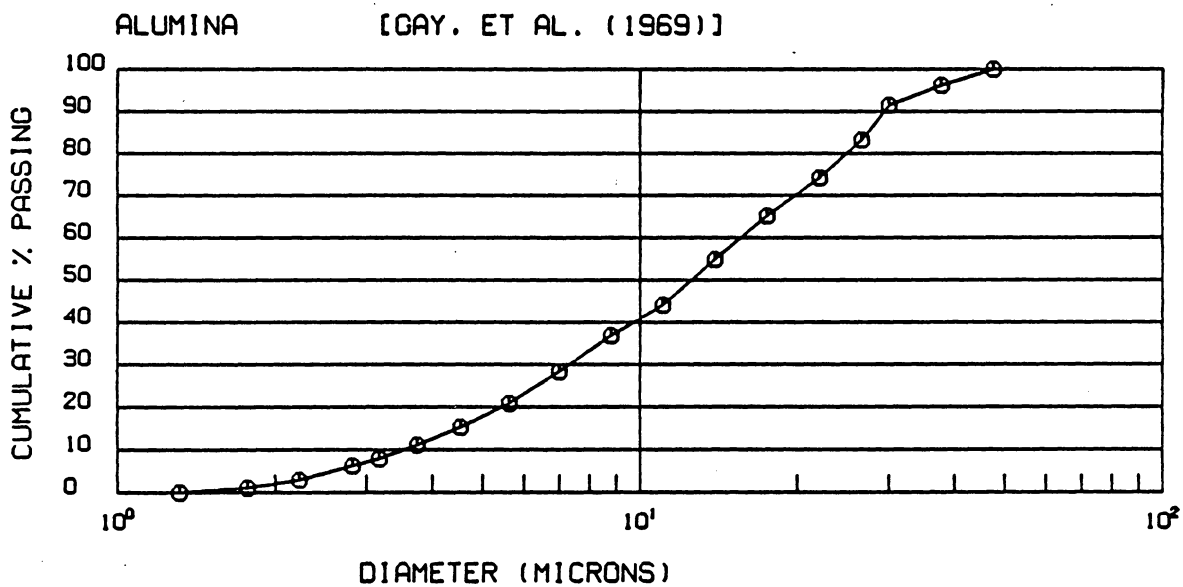


Figure 16. Particle size distribution of alumina used in alumina-xylene and alumina-glycerin suspensions

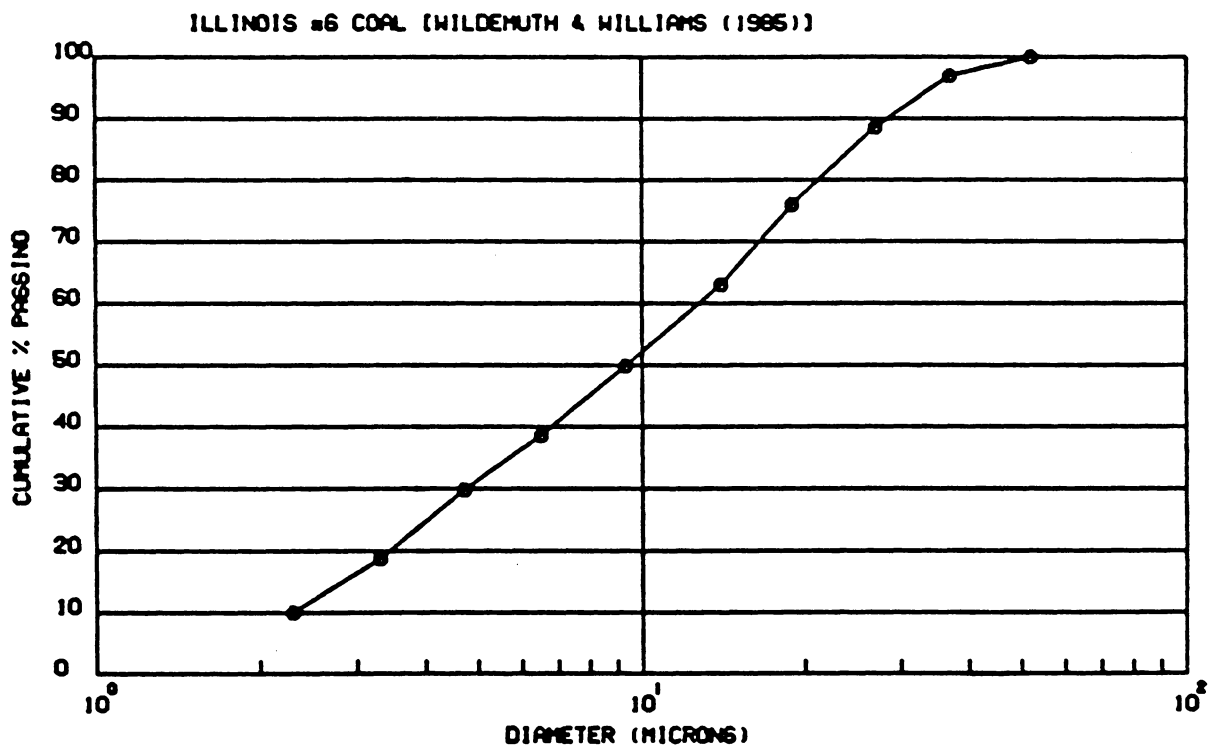


Figure 17. Particle size distribution of coal used in coal-glycerin suspension

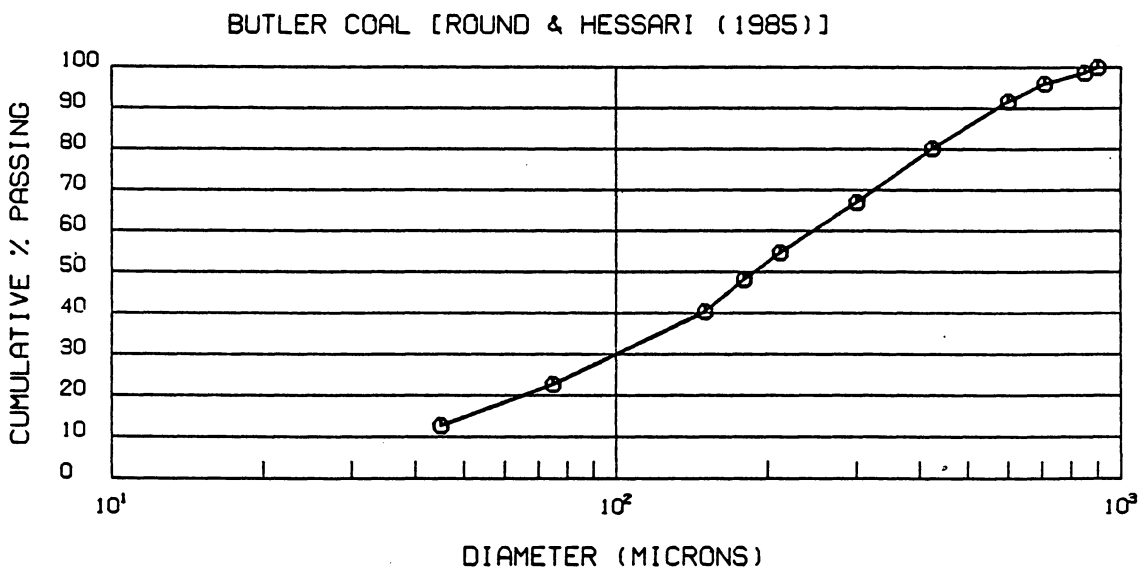


Figure 18. Particle size distribution of coal used in coal-oil suspension

will be discussed in the following section, was considered to represent the system. The rheological properties of this slurry were measured by a Haake RV12 viscometer.

### 7.3 PROCEDURE FOR ANALYSES AND CALCULATIONS

The formulations developed in this study for the prediction of the rheological behavior of solid-liquid mixtures and the formulations developed for the pressure gradient and grinding energy aspects, as discussed in Chapters 3, 4 and 5, are applied to the data given in the preceding section. The purpose was to implement the available physical properties of both the solids and liquids forming the suspension into these formulations and then see how well the experimental data were predicted by using these formulations. Hence, a systematic procedure was used in order to carry out these analyses which can be summarized as follows:

#### A- Rheologic Calculations

■ Using the given particle size distribution and assuming spherical shape, the surface area per unit volume or specific surface area  $S_a$  and surface mean diameter  $D_s$  were calculated as follows:

$$\frac{\text{Surface area}}{\text{volume}} = S_a = 6 \sum f_i / D_i \quad (7.1)$$

where  $f_i$  and  $D_i$  are the fraction and the diameter of the  $i$ -th size group of particles in the distribution, respectively.

$$\text{Surface mean diameter} = D_s = \left[ \frac{\sum (f_i / D_i)}{\sum (f_i / D_i^3)} \right]^{1/2} \quad (7.2)$$

- Using the maximum packing concentration correlation the actual maximum packing concentration  $\phi_{m,e}$  can be found. For calculating the maximum packing concentration  $\phi_{m,c}$  the method described in Chapter 4 was used together with the correlation of these values with the experimental data. The values used throughout the applications correspond to  $\phi_{m,e}$  which is referred to as the actual value, however,  $\phi_{m,c}$  is calculated only during the analysis of correlating the calculated values with experimental or actual ones.
  
- Using the experimental rheological curves the values of yield stress  $\tau_y$ , flow parameter B, viscosity at low shear rates  $\eta_o$  and viscosity at high shear rates  $\eta_\infty$  are determined. Reference should be made to Figure 5 as to how to determine these values graphically.
  
- Using the yield stress equation [Equation (3.19)] the calibration constant C, which characterizes the non-physical properties of the suspension, is calculated.
  
- Using the flow parameter equation (Equation (3.22)) the other calibration constant K is calculated.
  
- Using the viscosity equations formulated in Chapter 4 the values of the intrinsic viscosity  $[\eta]$  and the particle interaction parameter n are determined. At high shear rates, where  $n = 2$ , the value of  $[\eta]$  is calculated from Equation (4.4) which is assumed to remain constant for the same material and at low shear rates n is calculated from Equation (4.3).

- Using the general shear rate shear rate Equation (3.15) the values of shear stress for varying shear rates are calculated for any concentration.

## **B- Particle size distribution optimization**

- Assuming that the developed formulations remain valid for other particle size distributions in the same solid-liquid system from which the original parameters were calculated, the particle size related parameters  $k$ ,  $D_s$ ,  $\xi$  and  $\phi_m$  are recalculated for the new distribution.
- Using system specific characteristics  $C$ ,  $K$  and  $[\eta]$  and  $n$ , found from the relation to be presented in the following section, first the viscosities at high and low shear rates are calculated and then the yield stress, the flow parameter and finally the shear stresses as a function of shear rate again from Equation (3.15).
- Using the formulations presented in Chapter 5 together with the power-law constants obtained from the shear rate shear rate values found in the preceding step, the energy consumption of a hydraulic transportation and the particle reduction processes are determined.
- Using possible constraints and any applicable transportation scenarios, a total product optimization analysis is performed.

## 7.4 PREDICTION OF SHEAR STRESS VERSUS SHEAR RATE RELATIONSHIPS

The general rheologic formulations developed were applied to highly concentrated suspensions of nickel-sodium, nickel-xylene, alumina-xylene, alumina-glycerin, coal-glycerin, and coal-oil whose properties were given in section 7.2. Computational procedure outlined in the preceding section was followed to obtain the parameters related to particles and size distributions, such as  $\phi_m$ ,  $k$ ,  $D$ , and  $\xi$ , for each suspension [Table 5]. For nickel and alumina systems, experimentally determined values of  $\phi_m = 0.317$  and  $\phi_m = 0.468$  were used. For coal-glycerin system, however, no information on experimental  $\phi_m$  was provided and therefore,  $\phi_m = 0.52$  was utilized which yielded good results, when attempted to predict both the viscosity behavior and shear rate shear rate behavior by following the computational procedure outlined in the preceding section. For coal-oil suspensions, on the other hand, a value of  $\phi_m = 0.711$  was calculated using the analytical method explained in Chapter 4. This calculated value was assumed to represent the packing microstructure of the system since the particle sizes were large enough not to form agglomerates or cause serious surface condition changes to alter the assumed dispersed phase of the particles in the suspension.

The yield stress  $\tau_y$ , and the flow parameter  $B$  are evaluated from a measured shear rate shear rate curve of a reference concentration, which was selected to be the highest concentration available for each mixture. The dimensionless calibration constants,  $C$  and  $K$ , are then evaluated for each suspension using the yield stress and the flow parameter together with other parameters characterizing the particle size distribution. Similarly, the parameters, intrinsic viscosity  $[\eta]$  and particle interaction parameter  $n$ , needed to predict the viscosity at low and high shear rates are calculated again by using a viscosity versus shear rate curve of a reference concentration. This procedure was ex-

plained in Chapter 4. The application results, in which the validity of the formulations were proven, will be presented in the following section. Having obtained all the necessary parameters the next step is to calculate (predict) first the yield stress from Equation (3.19) and then the flow parameter from Equation (3.22) either for different concentrations or for various different particle size distributions. Finally the shear stress values at different shear rates are calculated from Equation (3.15).

There were two phases in the process of predicting the shear rate shear rate curves. In the first phase the validity of the formulations were tested by attempting to predict the shear rate shear rate curves for different concentrations of a specific suspension, with no variation in the particle size distribution. Consequently, Equations (3.19) and (3.22) were modified as follows:

$$\tau_y = C' \phi^2 \left[ \frac{\phi}{\phi_m - \phi} \right] \quad (7.3)$$

$$B = K' \tau_y \phi \left[ \frac{\phi}{\phi_m - \phi} \right] \quad (7.4)$$

where,  $C' = C[(\rho_s - \rho_l)gD][kD_s/\xi]$  and  $K' = K/Re_y$ . Equations (7.3) and (7.4) indicate that for the first phase of the prediction process, only the concentration of solids were varied keeping other parameters constant. This shows the importance of the combination of the mobility parameter  $[\phi/\phi_m - \phi]$  with the volumetric concentration of solids  $\phi$ .

Following the computational procedure outlined above the predicted variation of shear rate with shear rate for the suspensions listed in Table 5 are given in Figures 17 through 22. The agreement in all the suspensions may be considered excellent. However, in the case of coal-oil suspensions, the experimental results show that as the concentration increases, the behavior starts to deviate from the power-law at high shear rates



(approximately  $200 \text{ sec}^{-1}$  in this case). The formulations developed in this study are not intended to predict the rheologic behaviors of suspensions that do not obey the "power-law", as mentioned before in the beginning of the development of the formulations. Therefore, only the concentrations up to which the data obeys or approximates the power law were taken into consideration. The verification of the behavior of various suspensions investigated are reproduced in Figures 23 through 28, which show that all the systems predicted exhibited either a power law or yield power law behavior as schematically shown in Figure 2.

In the second phase it was attempted to predict the effect of particle size distribution on the behavior of suspensions. This was the original purpose of this study. However, no data could be found to investigate the effect of the particle size distribution on the rheology of suspensions for real systems. In other words, the experimental data obtained were apparently not meant to incorporate the physical, chemical and operational characteristics as affected by the variation of particle size distribution in real systems. Nevertheless, the formulations proposed in this study, namely Equations (3.19) and (3.22), were applied to a coal-oil mixture, which had limited data [52] on measured effects of discrete particle size distribution and no information on the maximum packing concentration, intrinsic viscosity and particle shape. In this case the unknowns were calculated indirectly from other properties of the suspension and/or solid particles. Table 6 lists all the known and calculated parameters that characterize the coal-oil system. As shown in Table 6 the only unknown needed to be estimated or computed was the real maximum packing concentrations for varying discrete particle size blends. This was taken care of by computing the maximum packing concentrations that correspond to different blends from their known apparent viscosities at low and high shear rates by rearranging Equation (4.4) as follows:

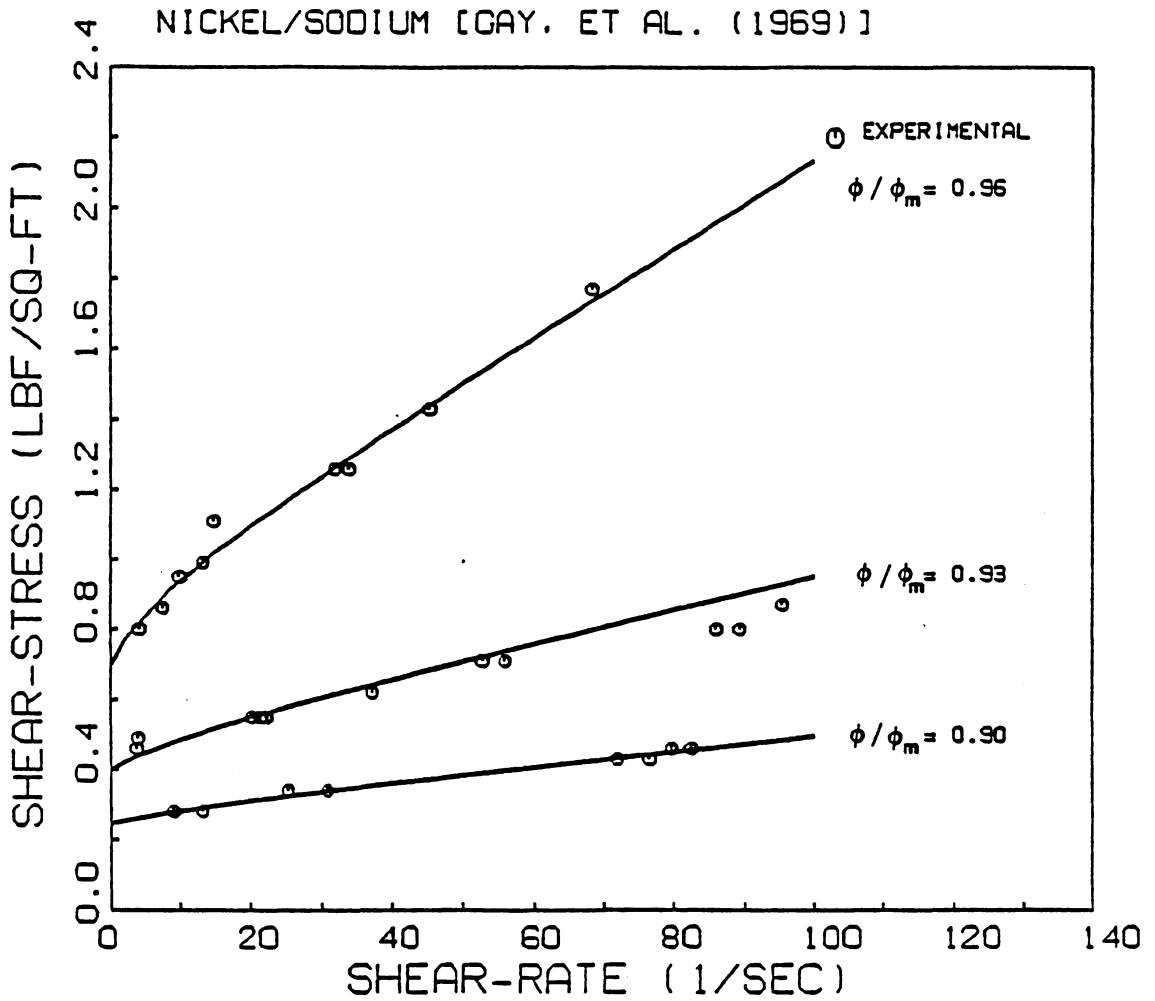


Figure 19. Experimental and predicted behaviors of nickel-sodium suspension

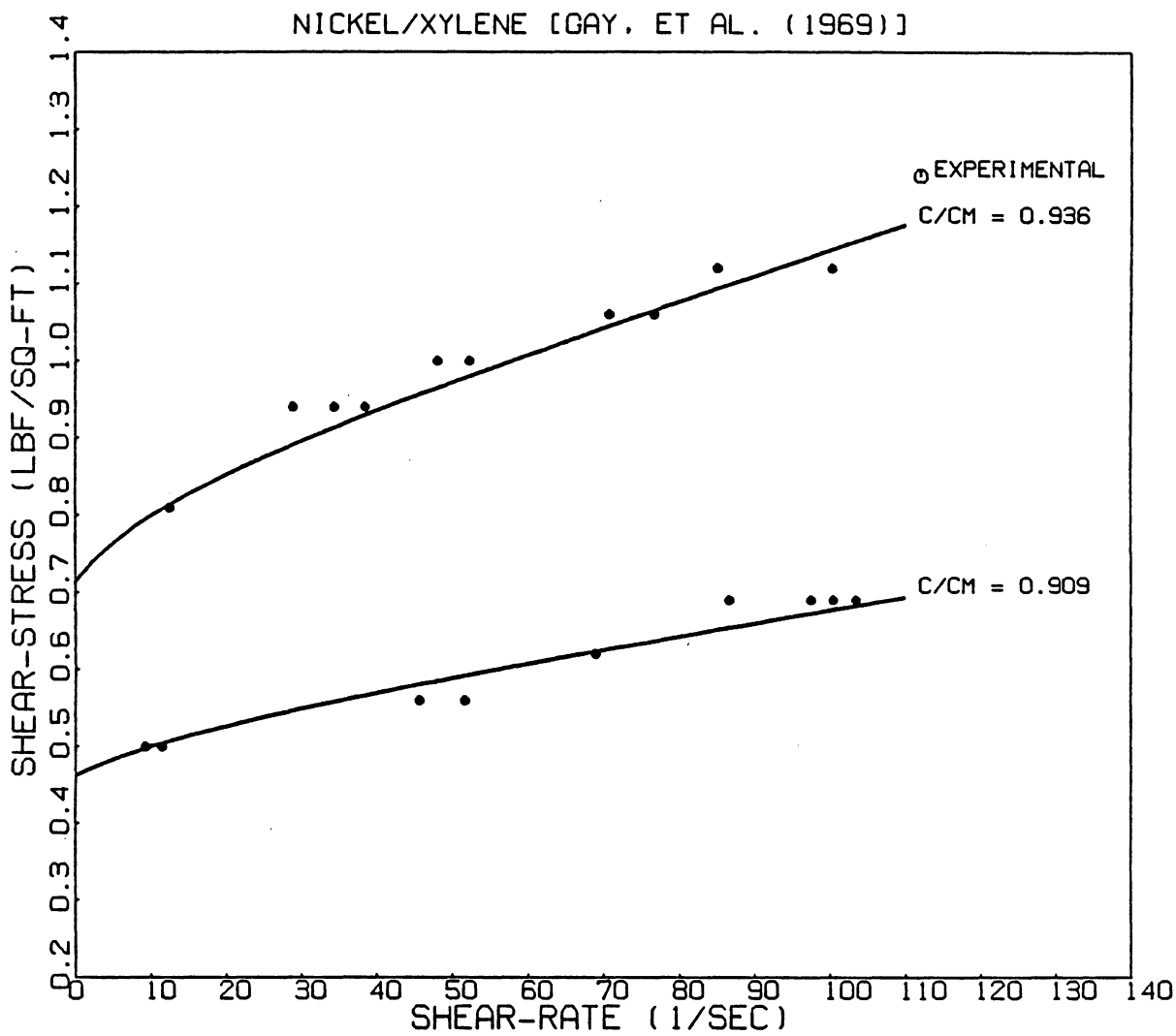


Figure 20. Experimental and predicted behaviors of nickel-xylene suspension

ALUMINA/XYLENE [GAY. ET AL. (1969)]

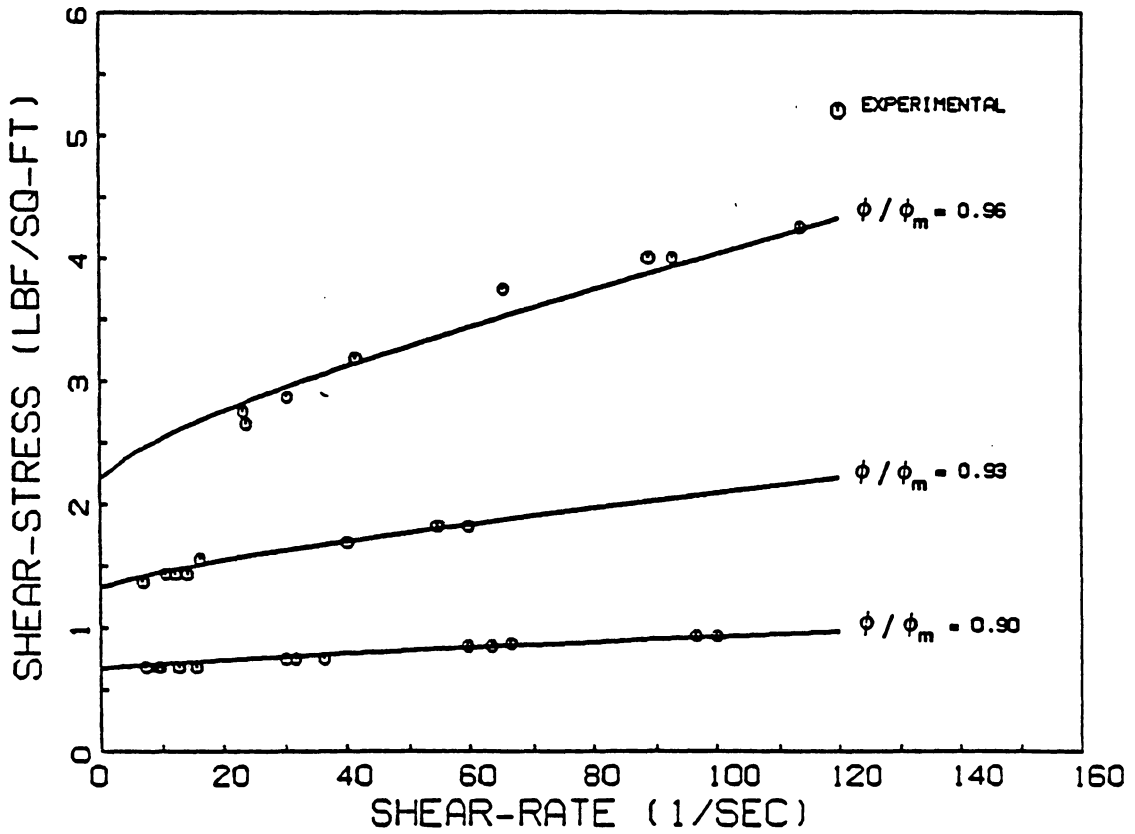


Figure 21. Experimental and predicted behaviors of alumina-xylene suspension

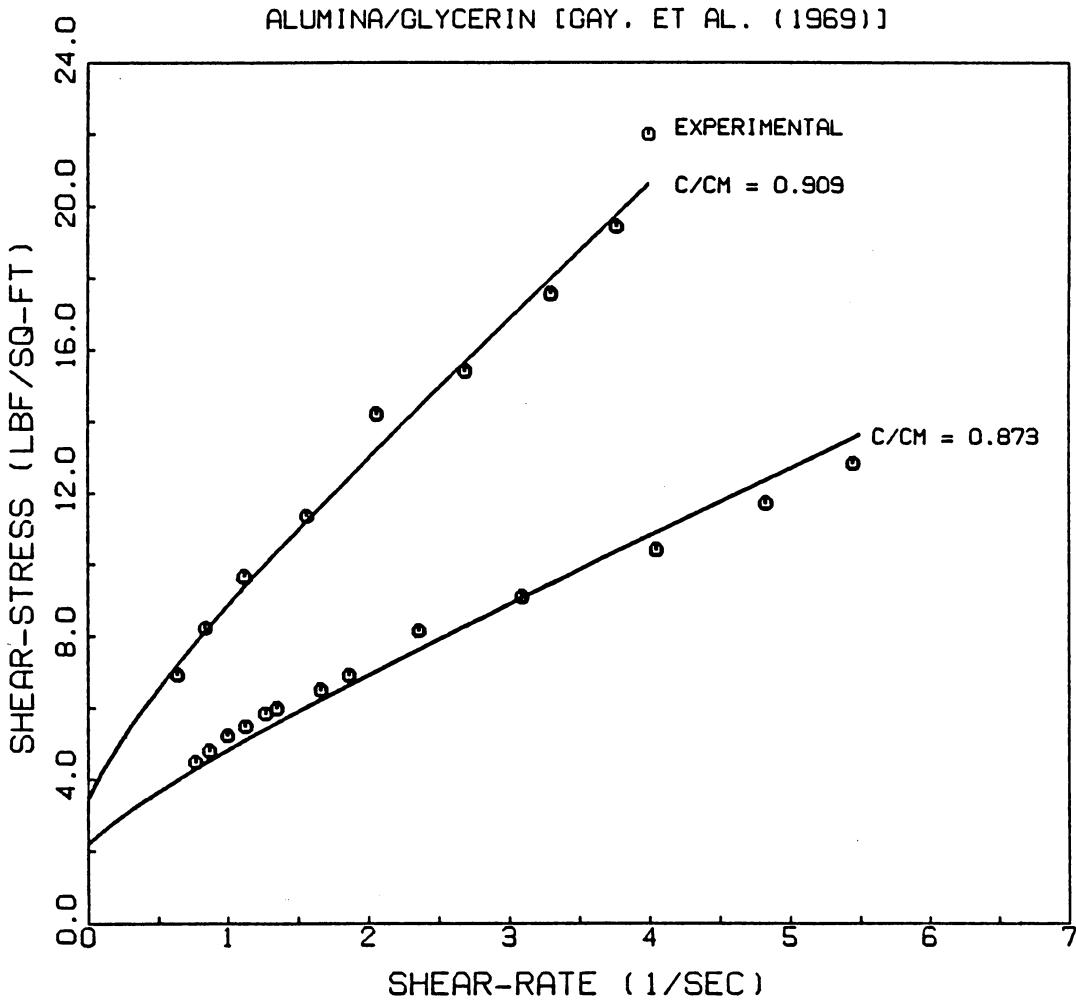


Figure 22. Experimental and predicted behaviors of alumina-glycerin suspension

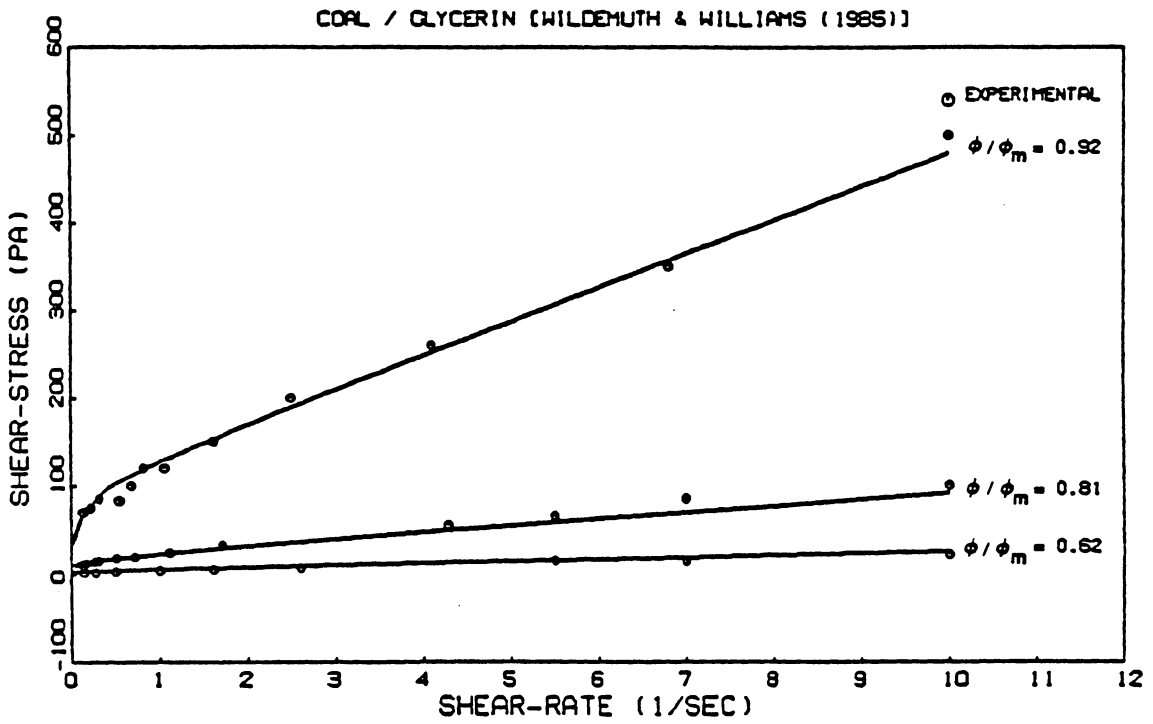


Figure 23. Experimental and predicted behaviors of coal-glycerin suspension

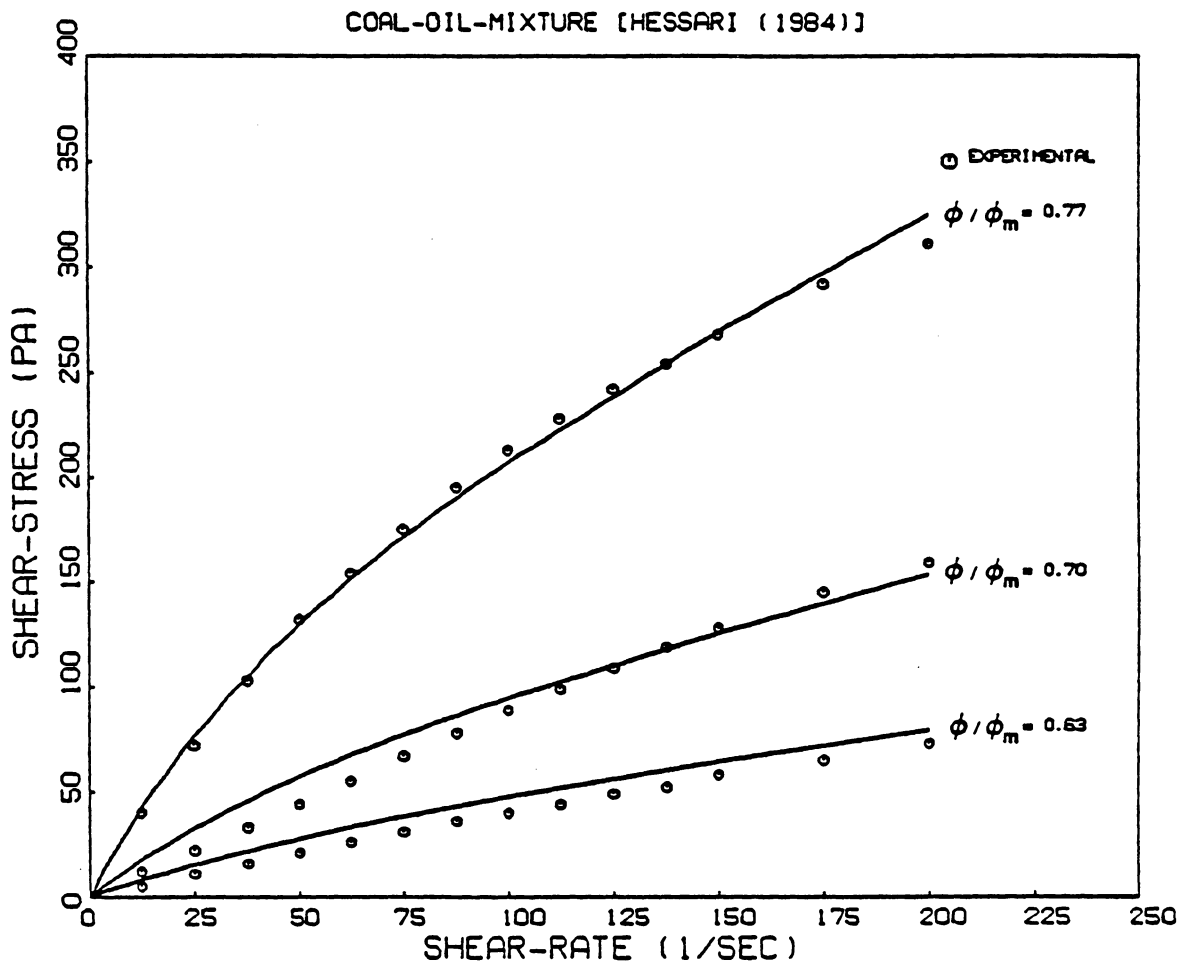


Figure 24. Experimental and predicted behaviors of coal-oil suspension

# NICKEL-SODIUM

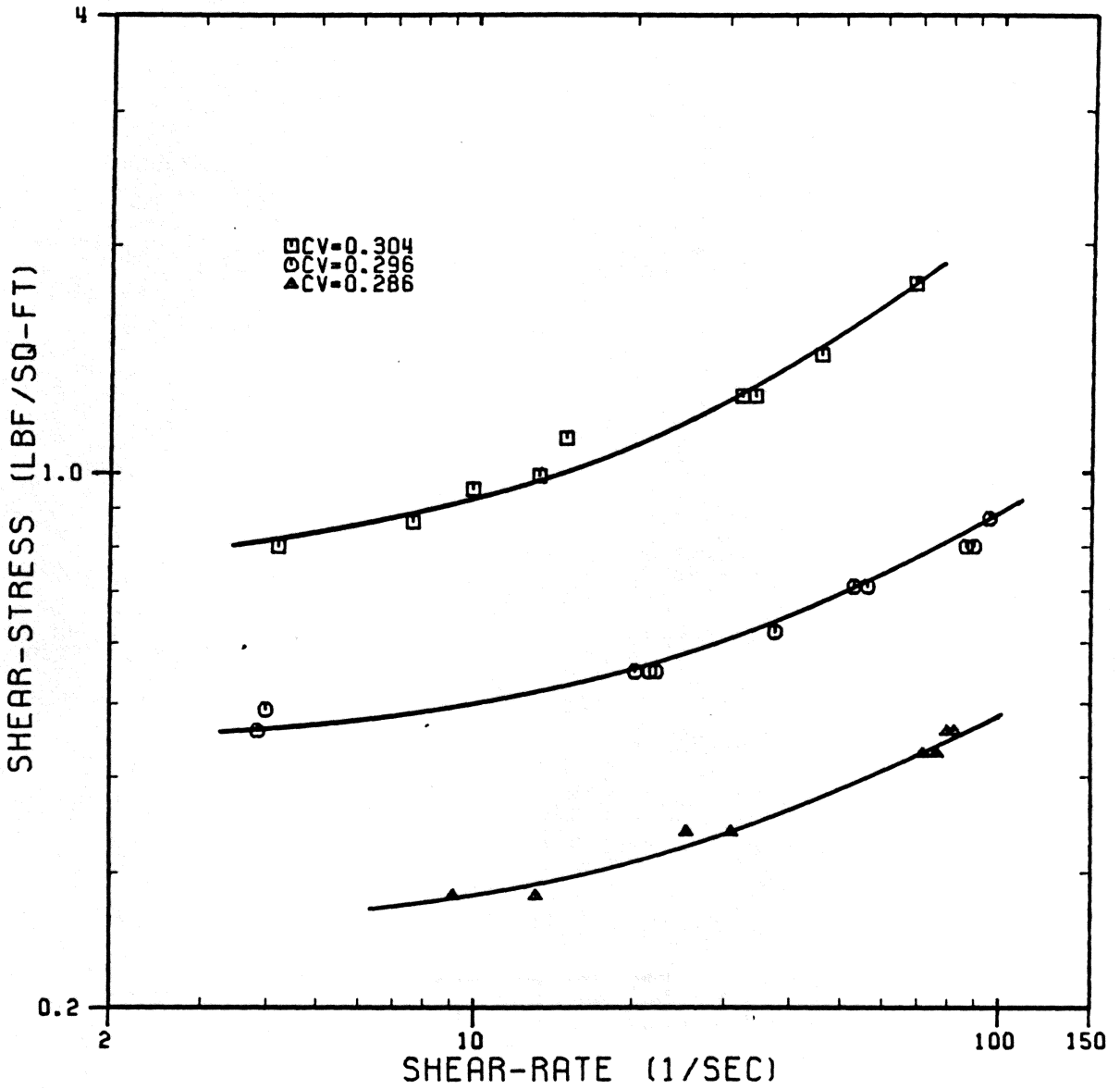


Figure 25. Flow behavior of nickel-sodium suspension



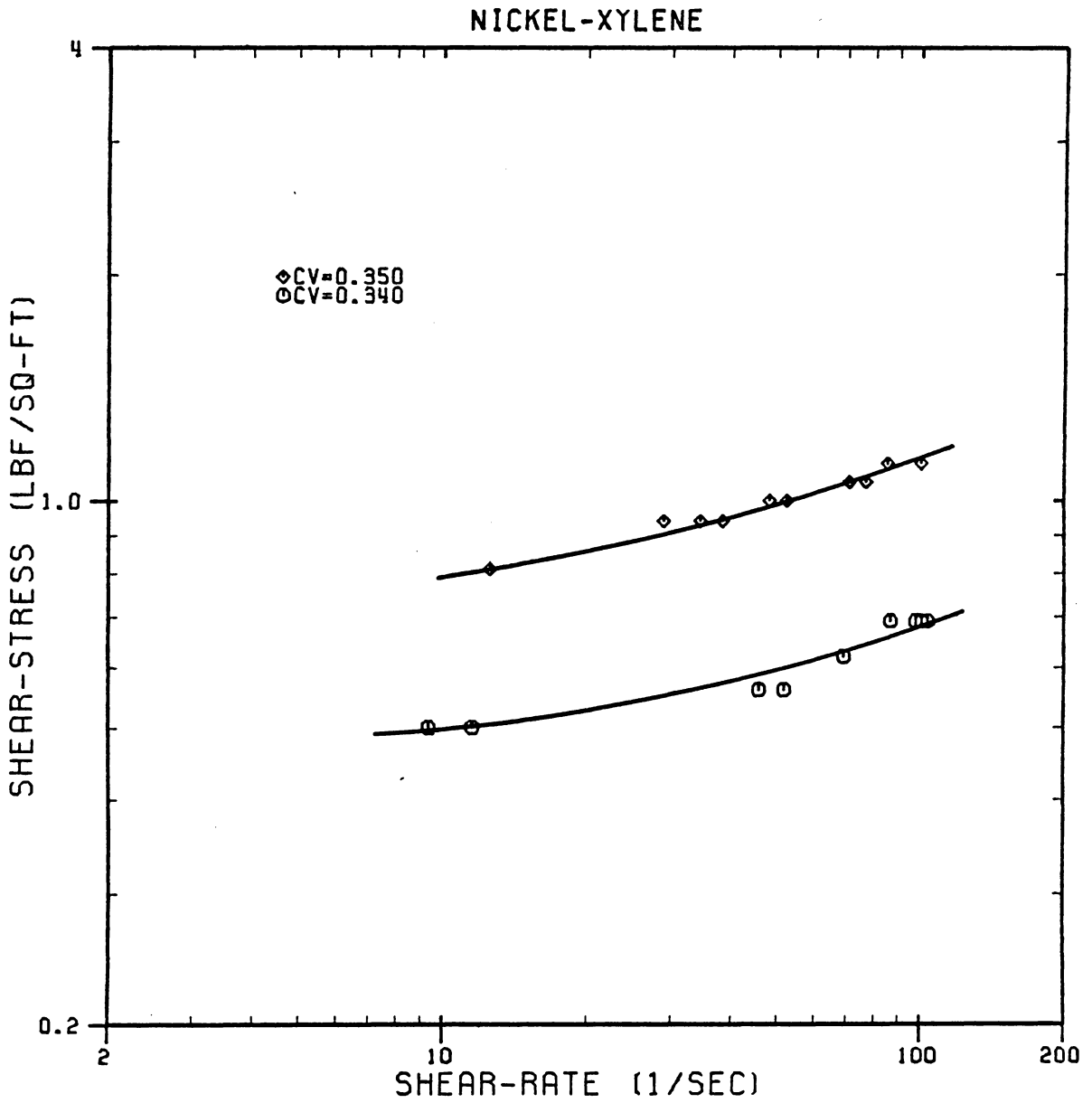


Figure 26. Flow behavior of nickel-xylene suspension

ALUMINA-XYLENE

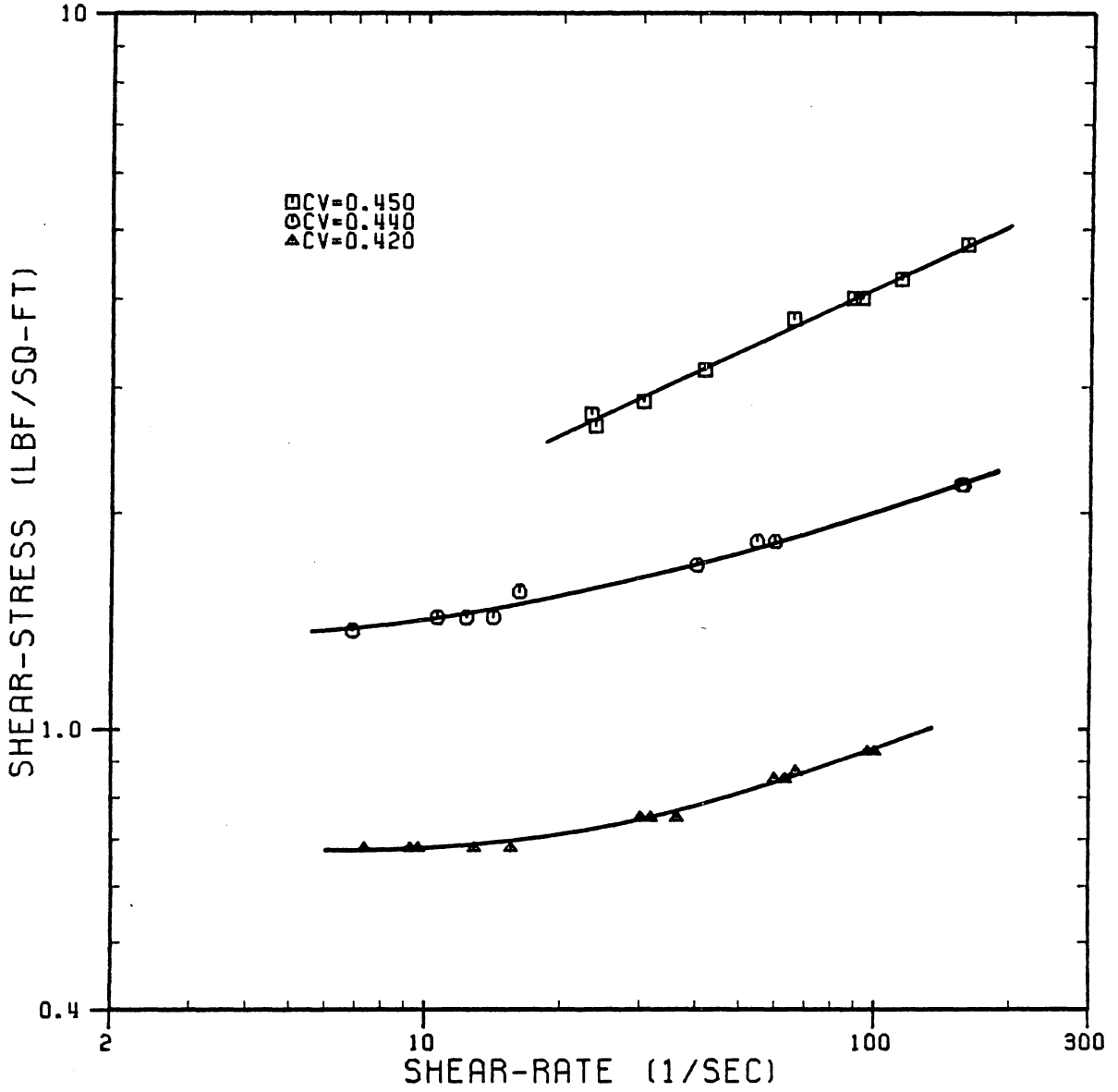


Figure 27. Flow behavior of alumina-xylene suspension

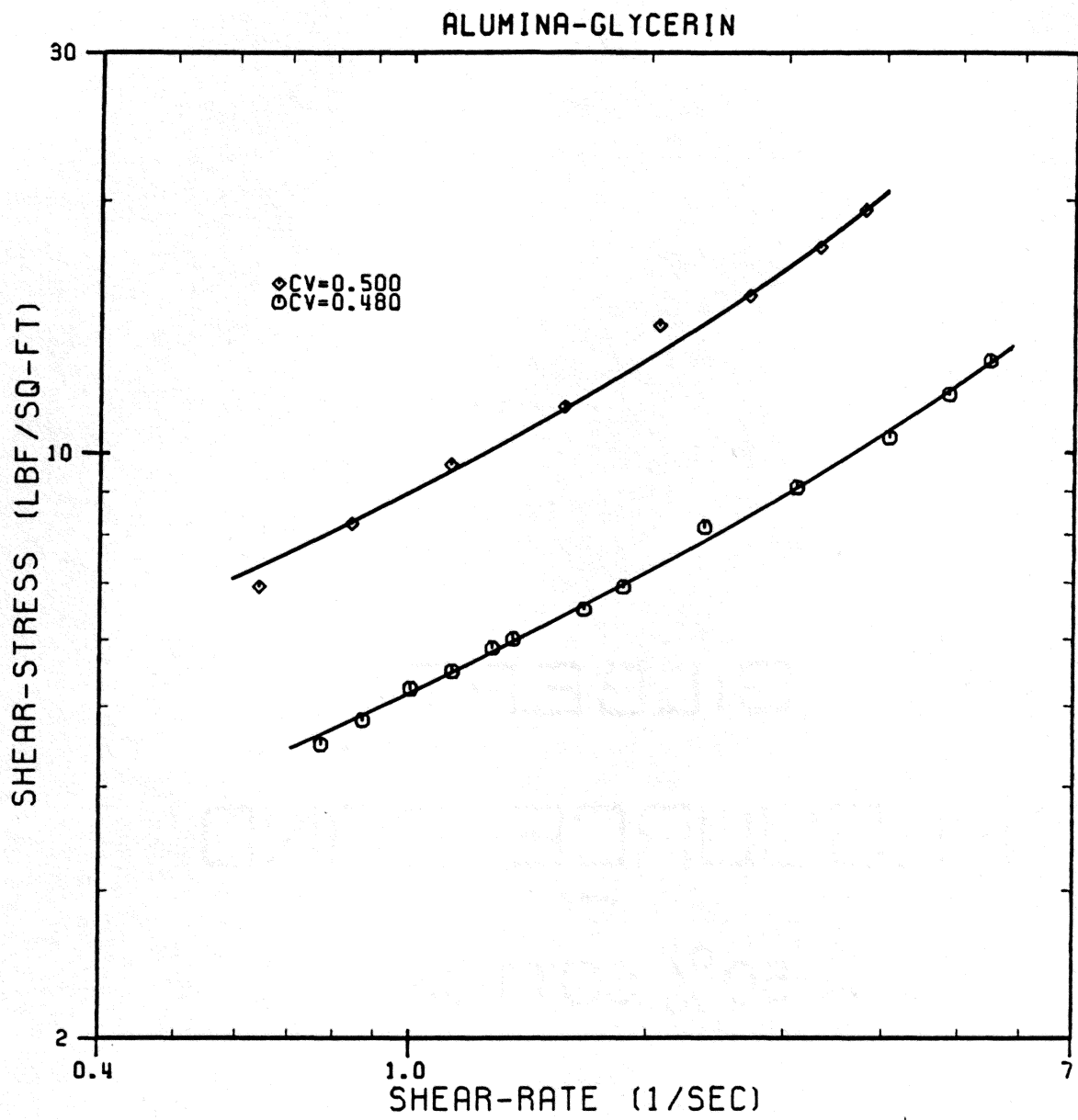


Figure 28. Flow behavior of alumina-glycerin suspension

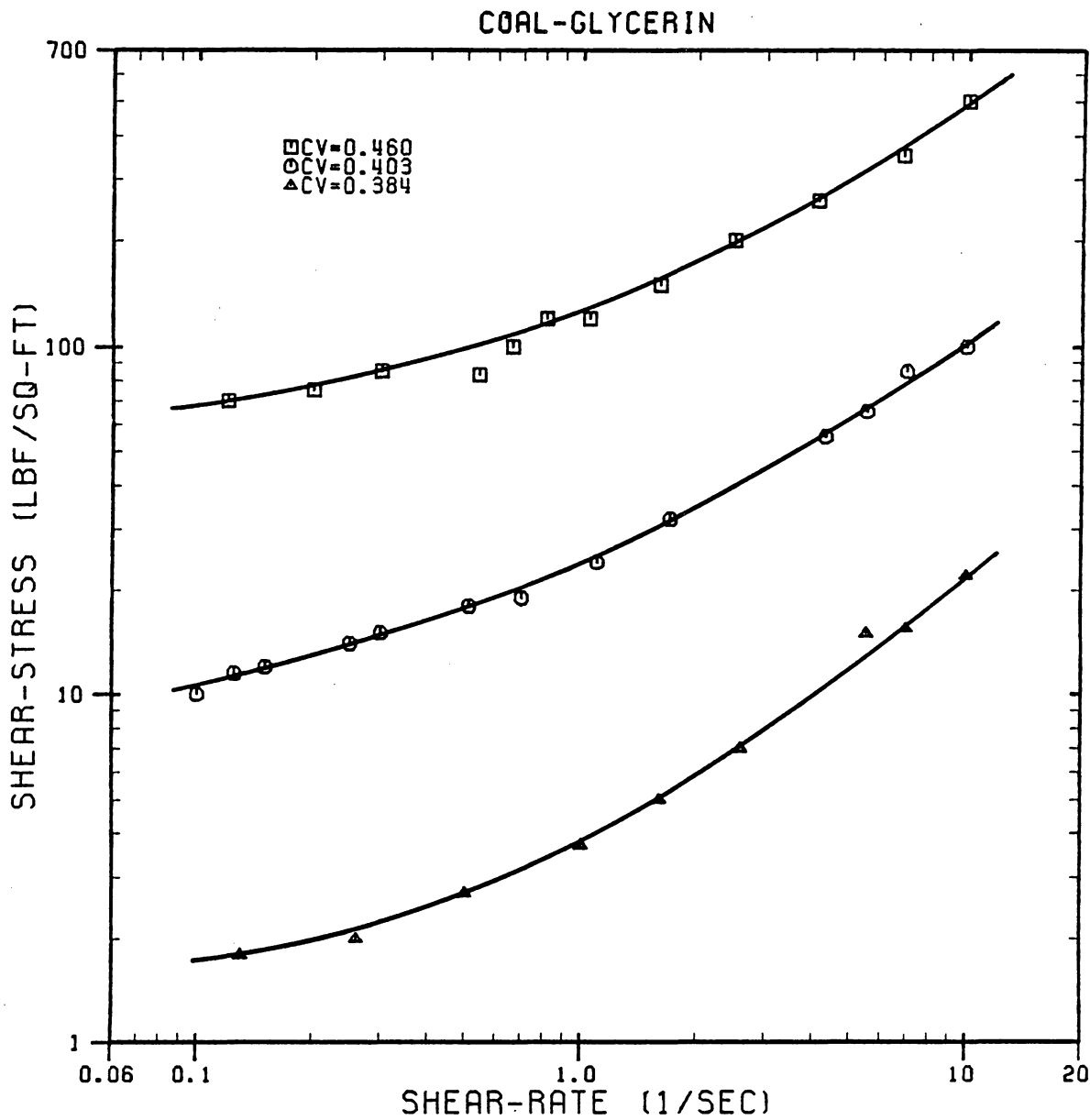


Figure 29. Flow behavior of coal-glycerin suspension

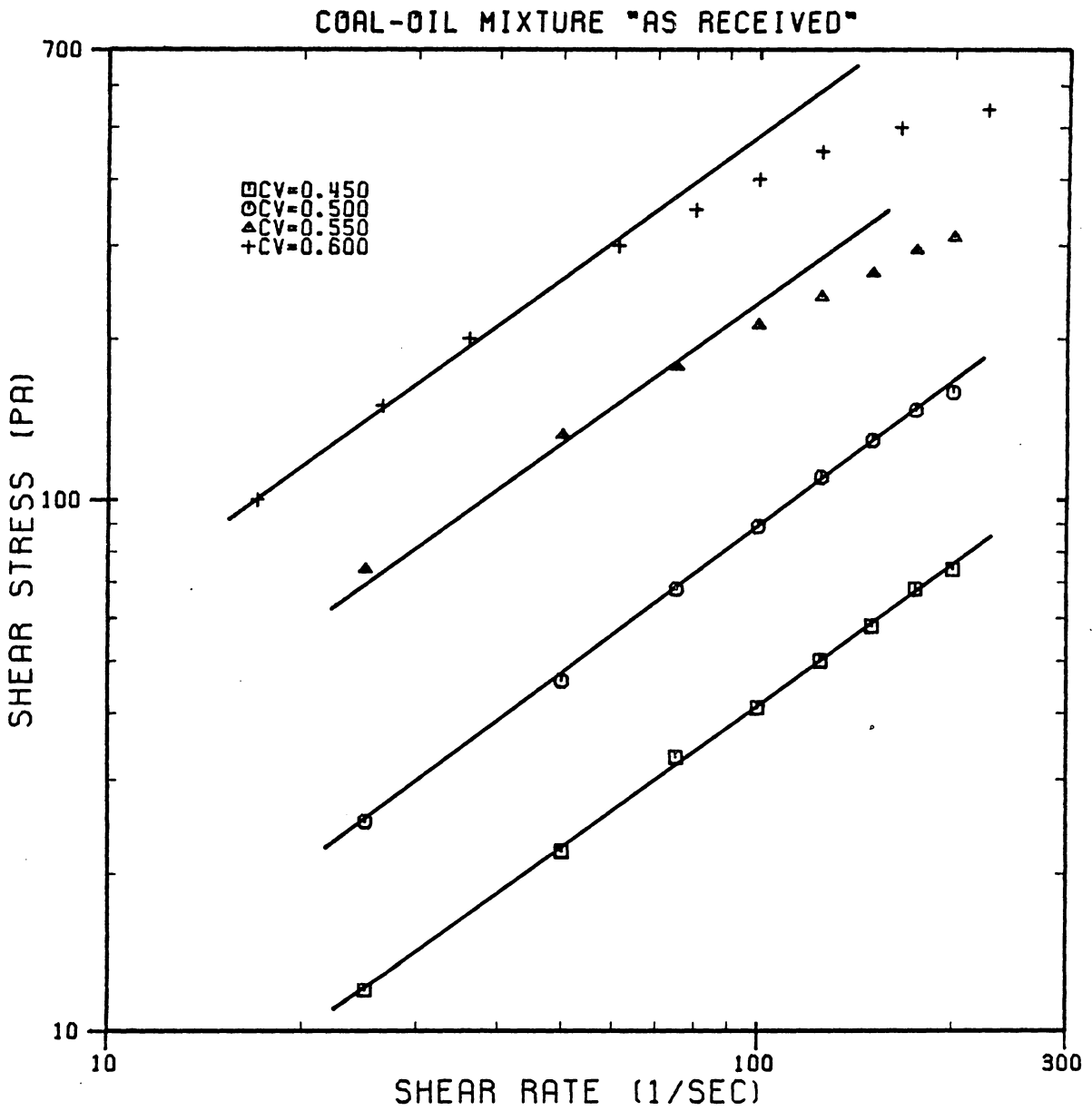


Figure 30. Flow behavior of coal-oil suspension

**Table 6. Parameters Characterizing Various Particle Size Distribution of a Coal-Oil Mixture**

Size Distribution	$\phi$	$\phi_m$	C	K	B	$D_p$ ( $\mu\text{m}$ )	k ( $1/\mu\text{m}$ )	$D_s$ ( $\mu\text{m}$ )	$\eta_{r,0}$	$\eta_{r,\infty}$
50% - A	0.450	0.680	1.60	1.317	73.710	347.5	0.058	46.5	1050	396
50% - B	0.500				153.95				2447	669
	0.550				350.14				10639	1325
70% - A	0.450	0.735	1.60	1.317	51.930	472.0	0.043	48.5	753	327
30% - B	0.500				100.28				1605	501
	0.550				200.42				4286	842
As Received	0.450	0.711	1.60	1.317	32.560	180.0	0.043	64.5	860	354
	0.500				64.810				1982	562
	0.550				135.87				6061	1004

A = + 600 - 710 (  $\mu\text{m}$  )

B = - 45 (  $\mu\text{m}$  )

$$\phi_m = \frac{1}{\frac{1}{\phi} - \frac{[\eta]}{2[\sqrt{\eta_{r,o}} - 1]}} \quad (7.5)$$

Again the particle shapes were assumed to remain the same with no apparent influence on the rheologic behavior since no information on the shapes of particles were reported.

Computational procedure followed was similar to the one outlined in the preceding section, except for the calculation of  $\phi_m$ , for the reasons explained in the previous paragraph. Hence, by using the information supplied for the "as received" particle size distribution, the flow curves of two other particle size blends were predicted as illustrated in Figures 29 through 31. For this, the calibration constants C and K and the intrinsic viscosity were kept constant as the chemical interaction parameters characterizing the non-physical reactions between the solid particles and the fluid. Figures 29 through 31 indicate that the predicted behaviors for various particle size blends and concentrations agree well with the measured values in the range 0 to 200 1/sec shear rate. This agreement was assumed to be satisfactory considering the lack of information on exact particle size distributions of various blends, maximum packing concentrations and surface condition and shape of particles.

The applications made and the results presented in this section, as a conclusion, are not obtained from a general correlation that represent the behaviors of all the suspensions, as in Gay et al. study discussed in Chapter 3. In fact, the use of such a correlation seems neither plausible nor warranted for the objectives stated in the beginning of this dissertation due to the high degree of complexity of the microstructure that give rise to highly variable rheologic behaviors of different solids with various shapes and sizes in different fluids. Once again, the objective in this study was to obtain a reliable formulation for each suspension, not for all suspensions, in such a way that the effects of variations in concentration and particle size distribution can be predicted with reason-

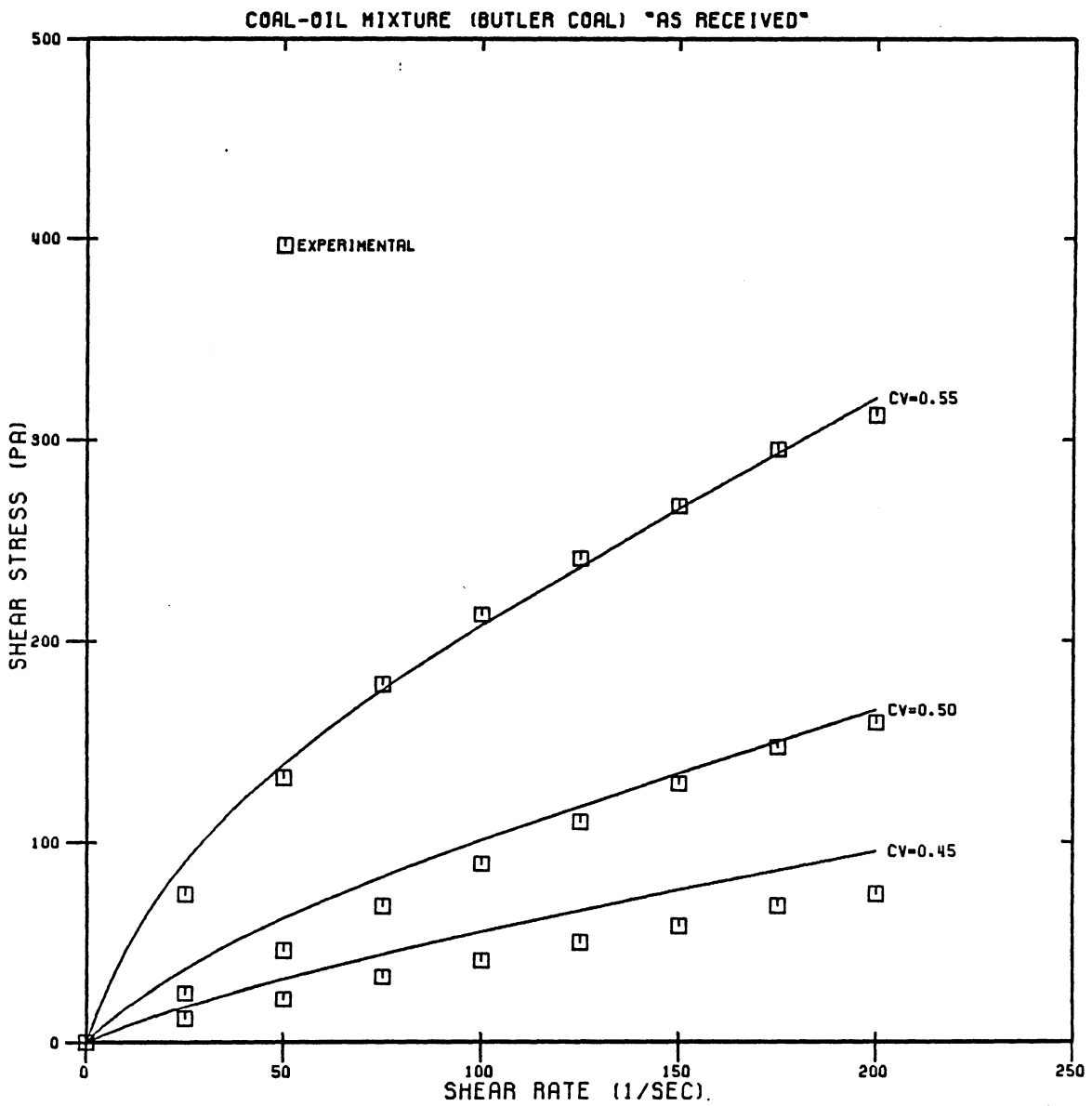
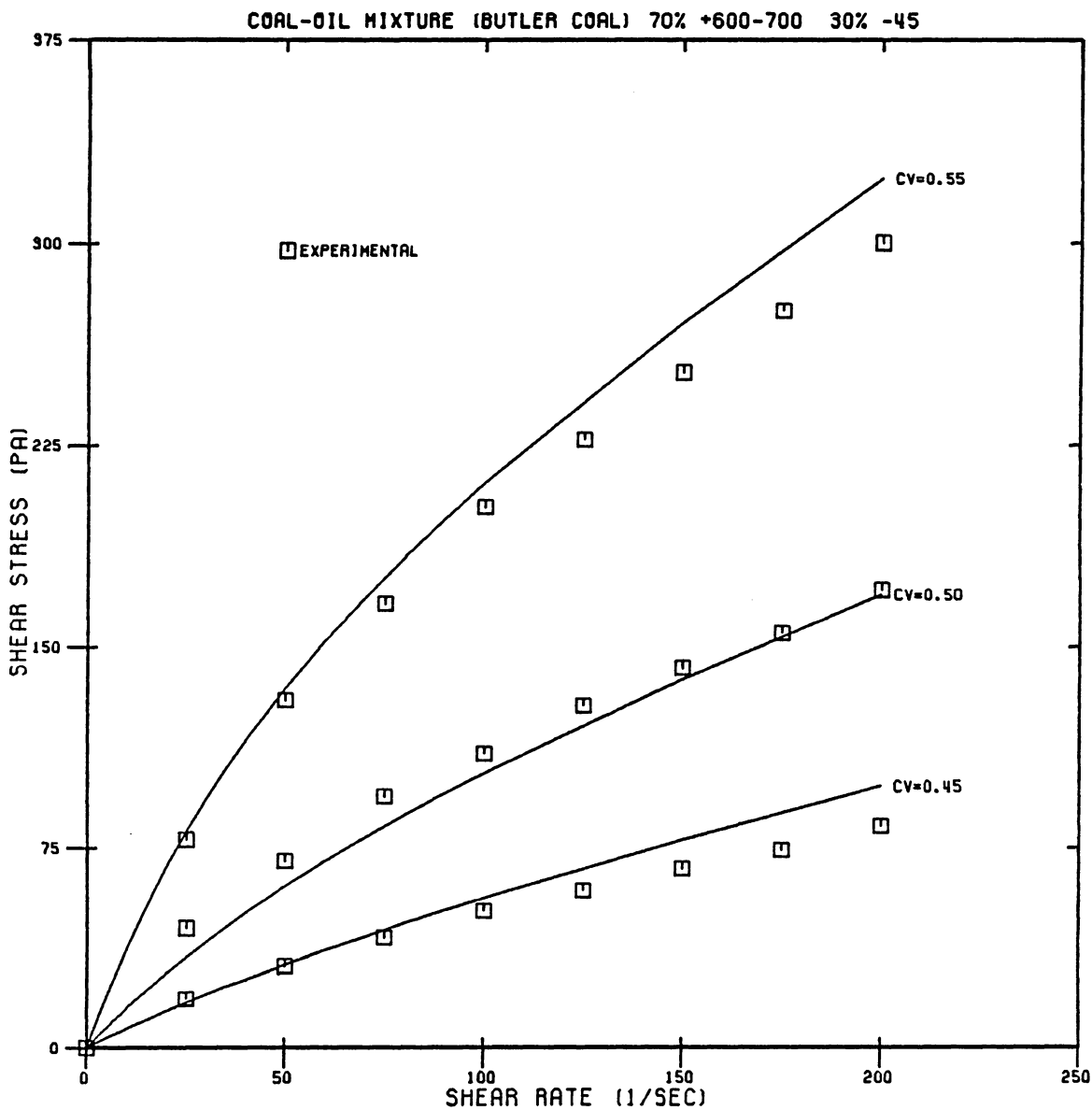
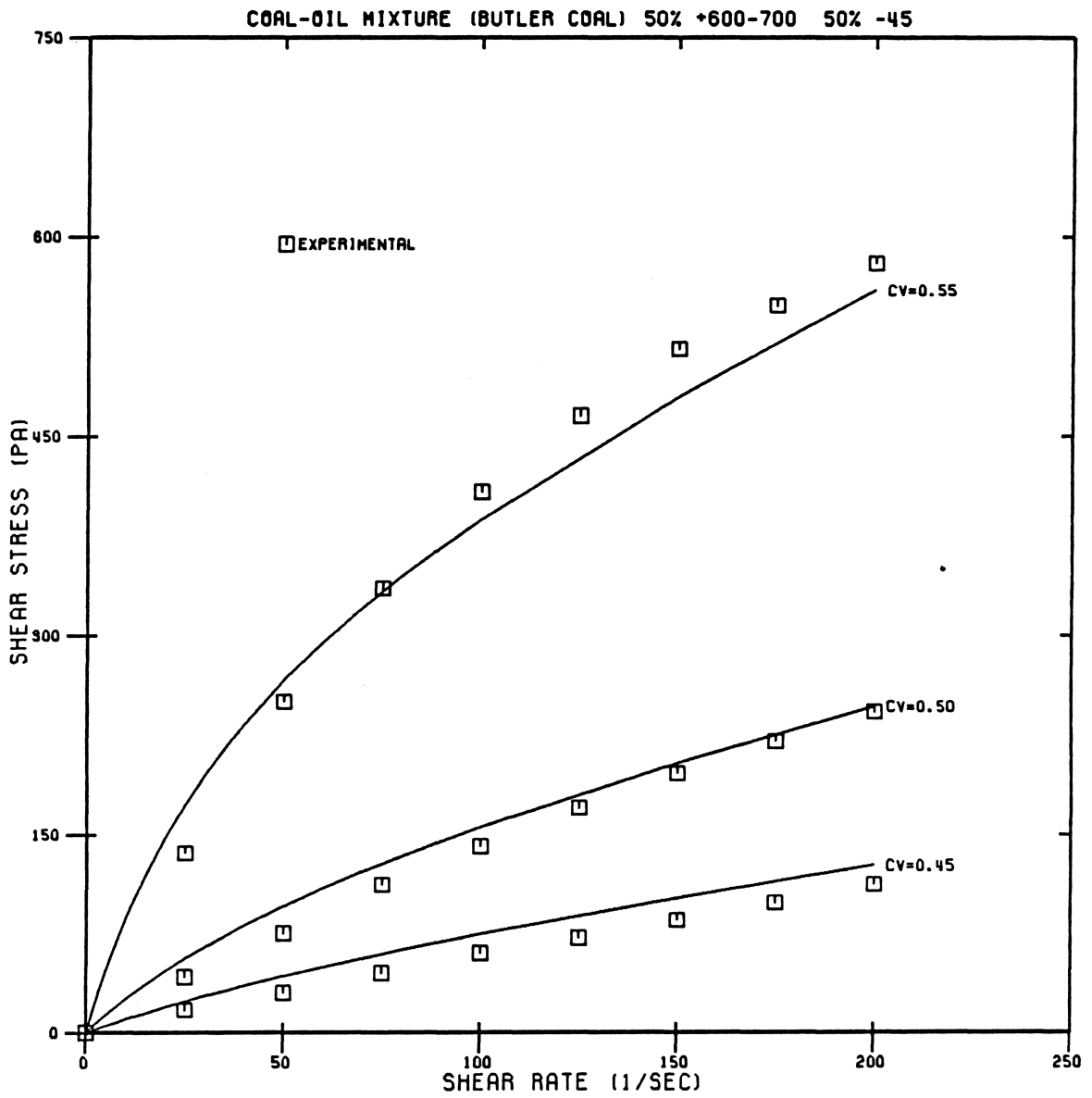


Figure 31. Experimental and predicted behaviors of "as received" coal in oil





**Figure 32. Experimental and predicted behaviors of 70% + 600-700 with 30% -45 micron coal in oil**



**Figure 33. Experimental and predicted behaviors of 50% + 600-700 with 50% -45 micron coal in oil**

able accuracy. In the case of coal-liquid mixtures prepared with a given parent coal, for example, the proposed formulations would be calibrated specifically for the material at hand, and then used to suggest the optimum particle size distribution for various utilization phases.

## **7.5 PREDICTION OF SHEAR VISCOSITY BEHAVIOR AT VARYING SHEAR RATES**

The formulations presented in Chapter 4 for the purpose of predicting viscosities at high and low shear rates, which were used in computing the shear rate shear rate variation in Equation (3.15), are applied to the suspensions listed in Table 5 to test the validity of these relationships. In Table 5 two suspensions, namely silica-glycerol and silica-ethanol, were added in addition to already existing data. However, because of the lack of information on maximum packing concentration and the deviation of the shear rate shear rate curve from power-law, the coal-oil suspension was excluded from the viscosity applications.

The intrinsic viscosity  $[\eta]$  was first calculated from Equation (4.4) for each suspension and using this value, the parameter  $n$  was calculated using Equation (4.3). As can be seen from Table 5 the intrinsic viscosities vary considerably for each suspension, whereas, the value of  $n$  ranges between 2.4 and 3.0. The intrinsic viscosity values that are different from 2.5 can be attributed to the irregular shape and the surface characteristic of the particle. Therefore, the intrinsic viscosity should either be determined experimentally or predicted for every particle fluid system by making use of extensive amount of data.

As mentioned earlier in chapter 4, the maximum packing concentrations were calculated using an analytical method proposed by Lee [39] and modified by Patton [50]. These calculated values of  $\phi_m$  are tabulated in Table 5, which indicates considerable discrepancy between the calculated and measured values of  $\phi_m$ . This is due to the failure of the analytical method to account for the packing configuration as affected by the surface condition and effective shape of the particles. The system of particles in a fluid may or may not behave as in their dry condition. Because these particles may react with the vehicle fluid, surface conditions and effective shapes may be modified and thus they either form agglomerates or tend to disperse in the flow process. Consequently, the calculated and the measured values of  $\phi_m$  may be substantially different. However, for well dispersed spherical particles of silica-ethanol and silica-glycerol suspensions [34], the calculated and measured maximum packing concentrations were found to be almost equal. This shows that the analytical method of calculating these values are realistic. Another observation made in this study was that the reported experimental methods of determining the maximum packing concentrations do not yield satisfactory results when these values are used to calculate the viscosities by using the equations proposed herein. Maximum packing concentrations for the first four suspensions in Table 5 were measured by centrifuging the slurries which gave good results when used in calculations. However, for the other two suspensions, the sedimentation technique was employed yielding the values of 0.620 and 0.600 for silica-glycerol at  $\phi = 0.600$  and silica-ethanol at  $\phi = 0.550$ , respectively. The calculated and actual values of these suspensions were found to be 0.650 and 0.640 for silica-glycerol and 0.650 and 0.652 for silica-ethanol, respectively. Therefore, it can be concluded that sedimentation technique may not provide the correct information.

As depicted by Figures 32 and 33 the measured and predicted viscosities at high and low shear rates are in good agreement with a correlation coefficient of  $R = 0.99$ .

As displayed in Table 5, experimental  $\phi_m$  values were not available for some of the suspensions. In these cases,  $\phi_m$  values were calculated by best fitting the viscosity data and then verified as plotted in Figures 8 and 9. The physical significance and consistency of the parameter  $[\phi/(\phi_m - \phi)]$  is confirmed once more, because all the data were in good agreement regardless of whether the calculations were made with measured  $\phi_m$  values or determined from measured viscosities.

Another significant result obtained in this study was the correlation between the  $\phi_m$  values calculated by using particle size distributions and the actual or measured  $\phi_m$ . This was performed by correcting the calculated  $\phi_{m,c}$  with the intrinsic viscosity as the characteristic of the particle surface condition and with the parameters  $n$  and  $n_\infty$  as follows:

$$\phi_{m,e} = \text{fct} \left\{ [\eta] \frac{n}{n_\infty} \phi_{m,c} \right\} \quad (7.6)$$

where,  $\phi_{m,e}$  is the actual value of  $\phi_m$  determined experimentally. As displayed in Figure 34, the proposed correction method appears to be successful, signified by a very high correlation coefficient which was calculated to be  $R = 0.987$ . The equation of this correlation was found to be:

$$\phi_{m,e} = \frac{1.91}{\left[ [\eta] \frac{n}{n_\infty} \phi_{m,c} \right]^{0.94}} \quad (7.7)$$

### 7.5.1 Shear Rate Dependence of the Particle Interaction Parameter $n$

In an effort to further illustrate the unique role of the particle interaction parameter  $n$  in describing the shear rate dependent rheologic behaviors, a specific methodology was developed as described subsequently.

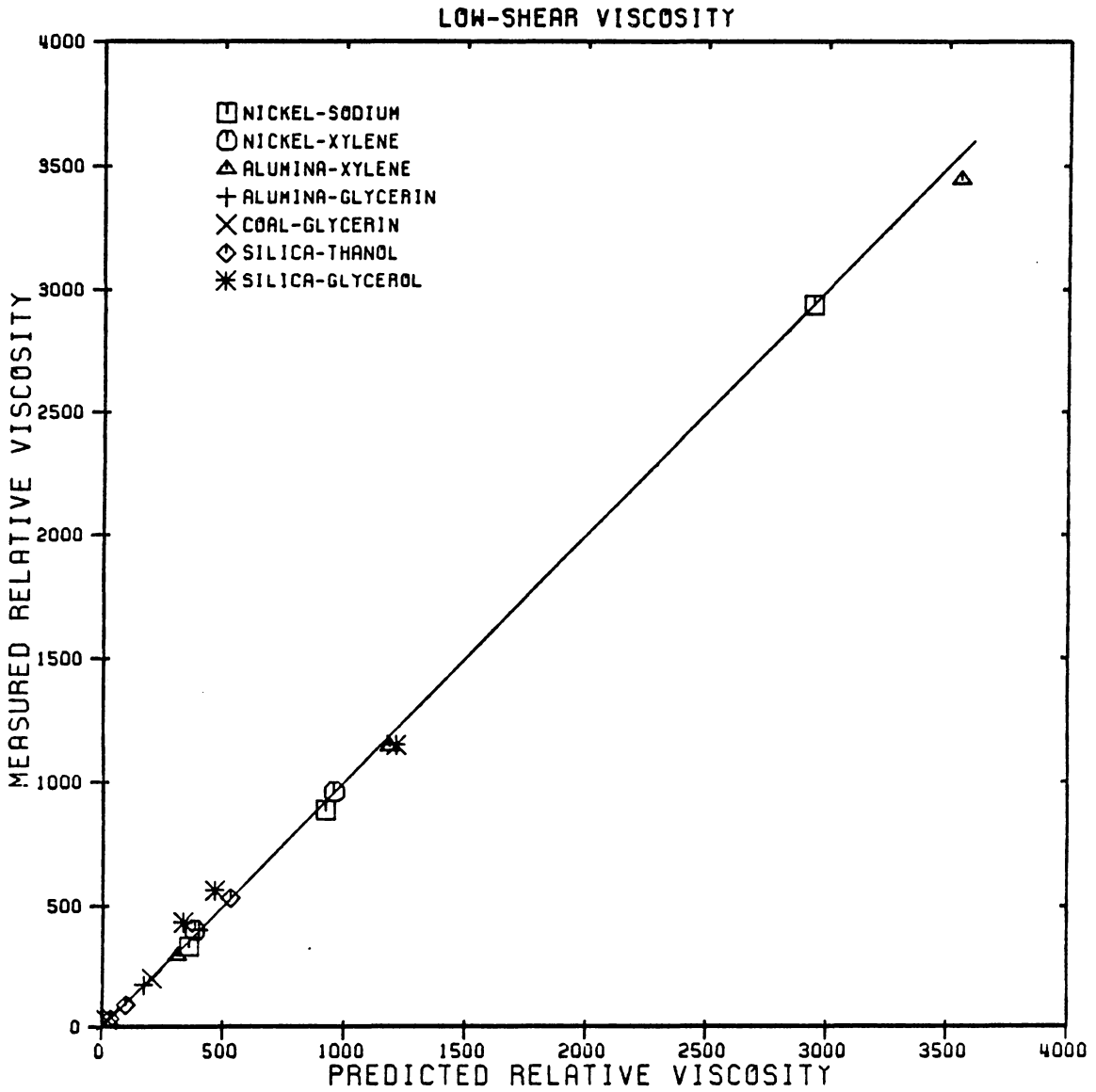


Figure 34. Results of predicted relative viscosity at low shear rates

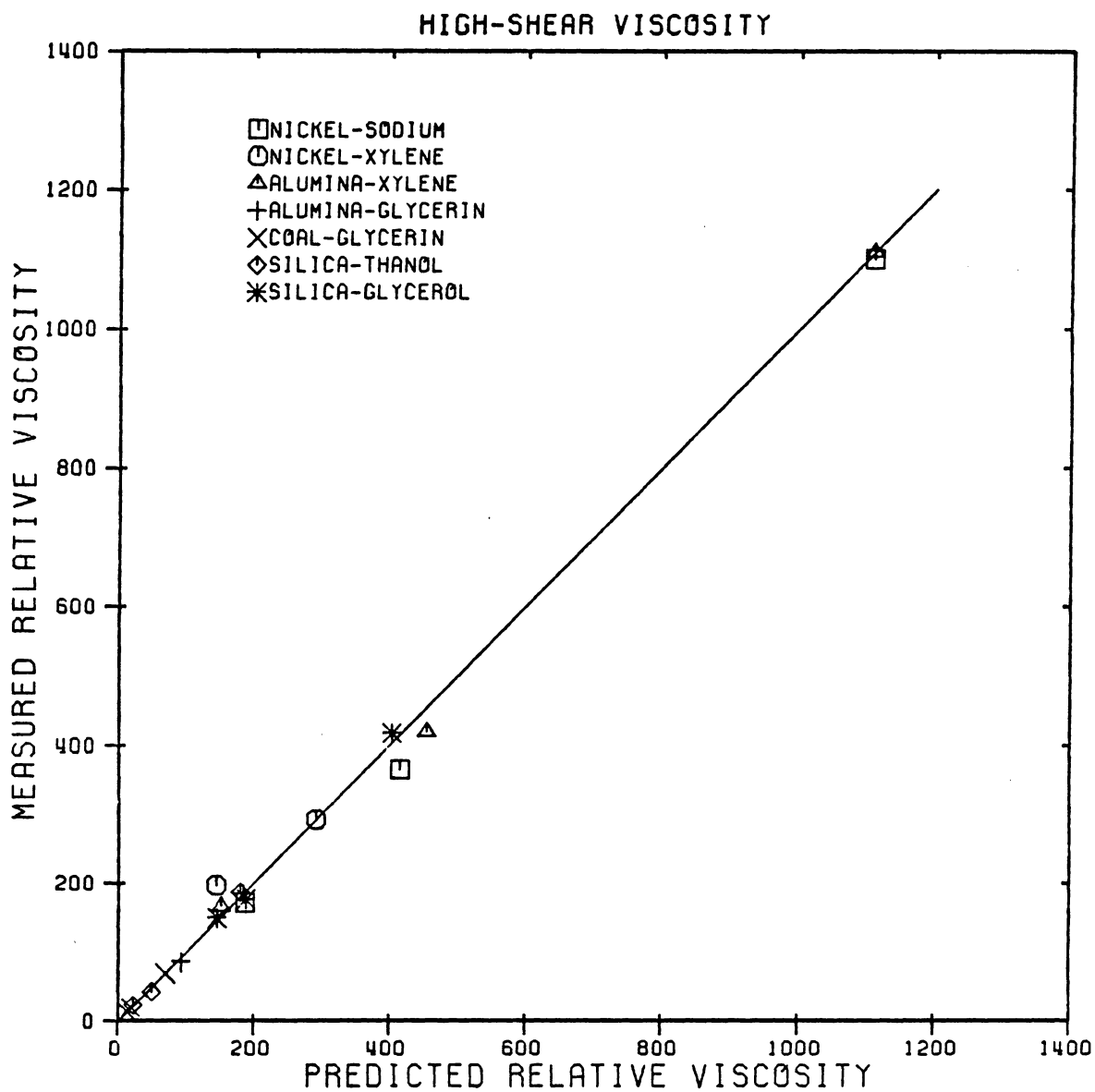


Figure 35. Results of predicted relative viscosity at high shear rates

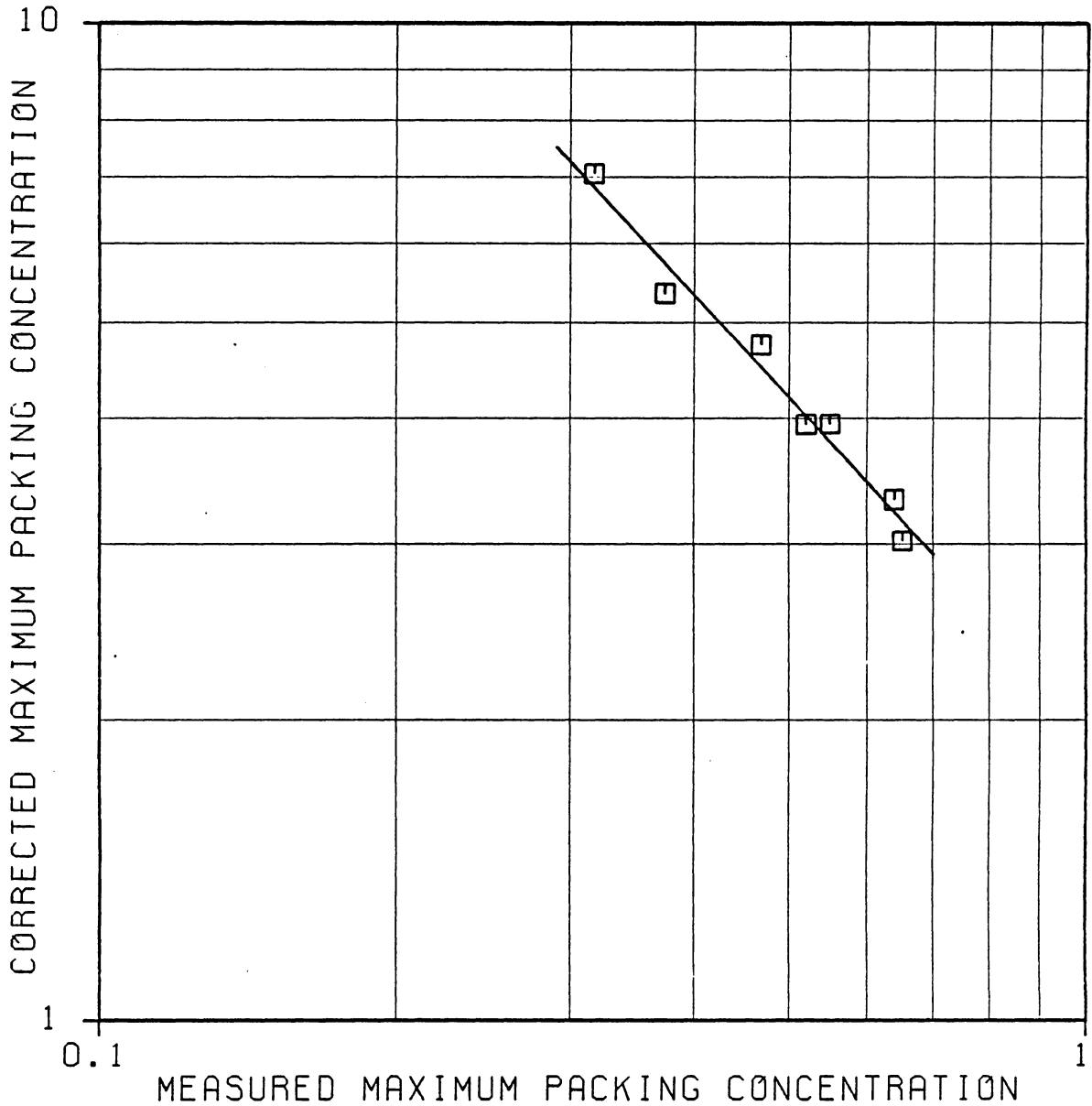


Figure 36. Correlation between measured and predicted maximum packing concentrations



The shear rate dependence of the viscosity expression given in Equation (4.3) to the shear rate can be written as:

$$\eta(G) = \mu \left[ 1 + \frac{[\eta] \phi \phi_m}{n(G) [\phi_m - \phi]} \right]^{n(G)} \quad (7.8)$$

where,  $\eta(G)$  and  $n(G)$  are the viscosity and the particle interaction parameter as a function of  $G$ , respectively. This relationship implies that at low shear rates ( $G \rightarrow 0$ ) the value of the viscosity will be equal to the value of  $\eta_o$  [ $\eta(G \rightarrow 0) = \eta_o$ ] and when  $G$  is high ( $G \rightarrow \infty$ ) then  $\eta(G \rightarrow \infty) = \eta_\infty$ .

The expression derived in Equation (3.15) can be written in a different form by dividing both sides by the shear rate  $G$  to obtain a relationship between the suspension viscosity and the shear rate:

$$\eta(G) = \eta_\infty + \frac{\eta_o - \eta_\infty}{1 + \frac{(\eta_o - \eta_\infty)G}{B}} \quad (7.9)$$

where,  $B$  is the "flow parameter" interpreted as a measure of the deviation from the suspension's Newtonian behavior as explained in Chapter 3. It can be seen from Equations (7.8) and (7.9) that first one depends on the particle interaction parameter  $n$  and the other depends on shear rate  $G$ , for a specific suspension and volumetric concentration. The value of the parameters, such as  $\eta_o, \eta_\infty$  and  $B$ , remain constant for a specific concentration and do not vary with shear rate, however, the values of  $[\eta]$  and  $\phi_m$  remain constant for all the specified concentrations and is a characteristic of the suspension. Therefore, Equation (7.9) can be used to predict the shear viscosity behavior at varying shear rates and calculate the variation of  $n(G)$  by coupling it with Equation (7.8) provided that  $\eta_o, \eta_\infty$  and  $B$  are correctly determined for each suspension and concentration from Equations (4.3), (4.4) and (3.22), respectively. In this respect,

coupling Equations (7.8) and (7.9) will yield the following expression for the particle interaction parameter  $n(G)$ :

$$n(G) = \left[ \frac{\phi}{\phi_m - \phi} \right] \frac{\phi_m[\eta]}{\left[ \frac{1}{\mu} \right]^{1/n(G)} \left[ \eta_\infty + \frac{\eta_0 - \eta_\infty}{1 + \frac{(\eta_0 - \eta_\infty)G}{B}} \right]^{1/n(G)} - 1} \quad (7.10)$$

Solving  $n$  iteratively for different shear rates  $G$  demonstrated the shear dependence of the level of particle interactions of a specific suspension with constant intrinsic viscosity  $[\eta]$  and maximum packing efficiency  $\phi_m$ . Tables 7 and 8 present the results of the application of Equations (7.9) and (7.10) to two suspensions, and Figures 35 through 40 illustrate the variation of  $n$  with respect to  $G$  calculated from Equation (7.10) and those determined indirectly from the measured data.

The preceding analysis strongly suggests that the shear viscosity variations with the shear rate can be represented solely by the particle interaction parameter  $n$ , provided the intrinsic viscosity  $[\eta]$  and the maximum packing concentration  $\phi_m$  are accurately determined for a specific suspension. In other words, it appears neither necessary nor warranted to impose shear rate dependence on  $[\eta]$  and  $\phi_m$ , as proposed in some of the recent investigations [58,59]. The present approach that  $\phi_m$  and  $[\eta]$  should remain invariant for a given suspension appears more sensible on two accounts. First of all, both of these parameters can be determined under the well-dispersed and orderly-aligned conditions implying Newtonian flow, and can thereby represent in an isolating manner the specific surface conditions arising between each particle and the carrier fluid. On the other hand, it was shown in this study at least for two of the suspensions that the parameter  $n$  has a unique variation with the shear rate for each suspension, with very good agreement between the predicted values and those determined indirectly from the measured data. Thus, the shear rate dependent variations in the suspension's shear

**Table 7. Variation of viscosity and n with shear rate for Sodium-Nickel Suspension**

(a) Experimental Values

$\phi = 0.304$	$\eta_o = 2936.5$	$\eta_\infty = 1100.0$	$B = 0.21$			
$\phi = 0.296$	$\eta_o = 885.3$	$\eta_\infty = 365.0$	$B = 0.11$			
$\phi = 0.286$	$\eta_o = 334.4$	$\eta_\infty = 172.0$	$B = 0.08$			
	<u><math>\phi = 0.304</math></u>		<u><math>\phi = 0.296</math></u>		<u><math>\phi = 0.286</math></u>	
<b>G</b>	<b><math>\eta_r</math></b>	<b>n</b>	<b><math>\eta_r</math></b>	<b>n</b>	<b><math>\eta_r</math></b>	<b>n</b>
0	2936.5	2.400	885.3	2.464	334.4	2.424
2	2634.0	2.356	835.0	2.432	327.0	2.409
5	2330.0	2.304	776.0	2.393	318.0	2.391
10	2025.0	2.247	704.0	2.340	304.0	2.359
20	1718.0	2.179	617.0	2.269	283.0	2.314
30	1564.0	2.140	565.0	2.224	268.0	2.278
40	1471.0	2.116	531.0	2.191	257.0	2.250
50	1410.0	2.099	507.0	2.167	248.0	2.228
80	1307.0	2.068	464.0	2.120	229.0	2.177
100	1269.0	2.056	447.0	2.102	221.0	2.155
200	1189.0	2.029	410.0	2.058	201.0	2.094
300	1160.0	2.021	396.0	2.041	193.0	2.070
400	1145.0	2.016	388.0	2.030	188.0	2.054
500	1136.0	2.013	384.0	2.025	185.0	2.044

(b) Predicted Values

	<u><math>\phi = 0.304</math></u>		<u><math>\phi = 0.296</math></u>		<u><math>\phi = 0.286</math></u>	
<b>n</b>	<b><math>\eta_r</math></b>	<b>G</b>	<b><math>\eta_r</math></b>	<b>G</b>	<b><math>\eta_r</math></b>	<b>G</b>
2.40	2925	0.0	918	0.0	357	0.0
2.38	2790	0.8	884	1.4	346	2.9
2.35	2598	2.2	834	3.9	330	7.9
2.32	2418	3.6	788	6.8	315	13.8
2.30	2305	5.2	758	9.1	306	18.0
2.28	2197	6.8	729	11.7	296	23.5
2.25	2043	9.5	687	16.6	282	33.2
2.23	1946	11.8	661	20.4	274	40.2
2.20	1809	16.1	623	27.7	261	54.7
2.18	1723	19.7	599	33.9	252	68.1
2.15	1600	27.0	564	46.5	240	93.3
2.12	1486	38.0	531	65.4	229	129.1
2.10	1414	49.1	510	84.3	222	163.8
2.08	1345	65.8	490	112.3	214	225.8
2.05	1248	115.6	461	197.3	204	388.1
2.02	1157	316.0	433	554.3	194	1049.4

**Table 8. Variation of Viscosity and n with shear rate for the Coal-Glycerin Suspension**

(a) Experimental Values

	$\eta_o = 203.5$	$\eta_\infty = 70.0$	$B = 135$			
	$\eta_o = 47.3$	$\eta_\infty = 20.0$	$B = 40$			
	$\eta_o = 29.7$	$\eta_\infty = 13.0$	$B = 20$			
	<u><math>\phi = 0.460</math></u>	<u><math>\phi = 0.403</math></u>	<u><math>\phi = 0.384</math></u>			
G	$\eta_r$	n	$\eta_r$	n	$\eta_r$	n
1	203.7	2.985	44.6	3.433	27.9	3.971
2	160.6	2.743	39.1	3.145	21.7	3.156
3	138.5	2.596	35.5	2.949	19.1	2.816
4	125.1	2.502	33.1	2.814	17.7	2.631
5	116.0	2.432	31.3	2.711	16.9	2.525
6	109.6	2.382	29.9	2.629	16.3	2.445
7	104.7	2.340	28.9	2.570	15.8	2.377
8	100.9	2.307	28.0	2.516	15.5	2.339
9	97.8	2.281	27.3	2.473	15.2	2.298
10	95.3	2.258	26.7	2.436	15.0	2.271
12	91.5	2.222	25.8	2.381	14.7	2.231
15	87.5	2.185	24.8	2.318	14.3	2.177
20	83.3	2.143	23.7	2.247	14.0	2.137
30	79.0	2.098	22.6	2.175	13.6	2.082
40	76.8	2.075	22.0	2.136	13.5	2.068
50	75.5	2.060	21.6	2.108	13.4	2.053
100	72.8	2.032	20.8	2.055	13.2	2.027

(b) Predicted Values

	<u><math>\phi = 0.304</math></u>		<u><math>\phi = 0.296</math></u>		<u><math>\phi = 0.286</math></u>	
n	$\eta_r$	G	$\eta_r$	G	$\eta_r$	G
3.00	206.5	1.0	32.9	1.0	22.2	1.0
2.90	187.7	1.3	31.4	2.0	21.3	1.6
2.80	170.0	1.8	29.9	3.3	20.4	2.4
2.70	153.9	2.3	28.4	5.0	19.6	3.2
2.60	138.8	3.0	26.9	7.3	18.7	4.5
2.50	124.8	4.1	25.4	10.6	17.9	6.2
2.40	111.9	5.7	24.0	15.4	17.1	8.7
2.30	100.0	8.3	22.6	23.5	16.2	13.4
2.20	89.1	13.7	21.2	40.3	15.4	22.1
2.10	79.1	29.8	19.9	88.4	14.6	48.1
2.05	74.5	61.4	19.2	200.6	14.2	100.2

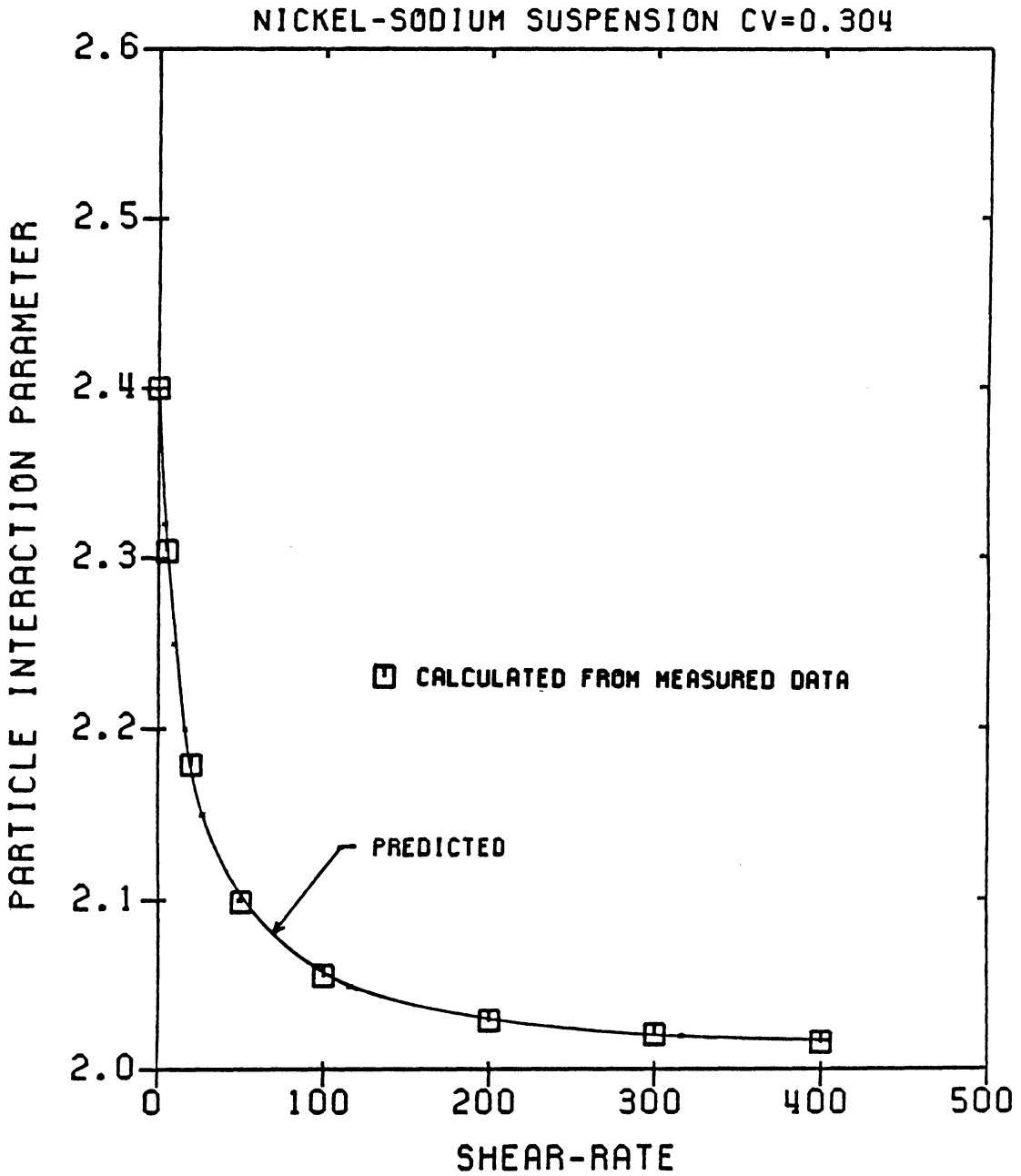


Figure 37. Variation of  $n$  with shear rate for nickel-sodium suspension (concentration = 0.304)

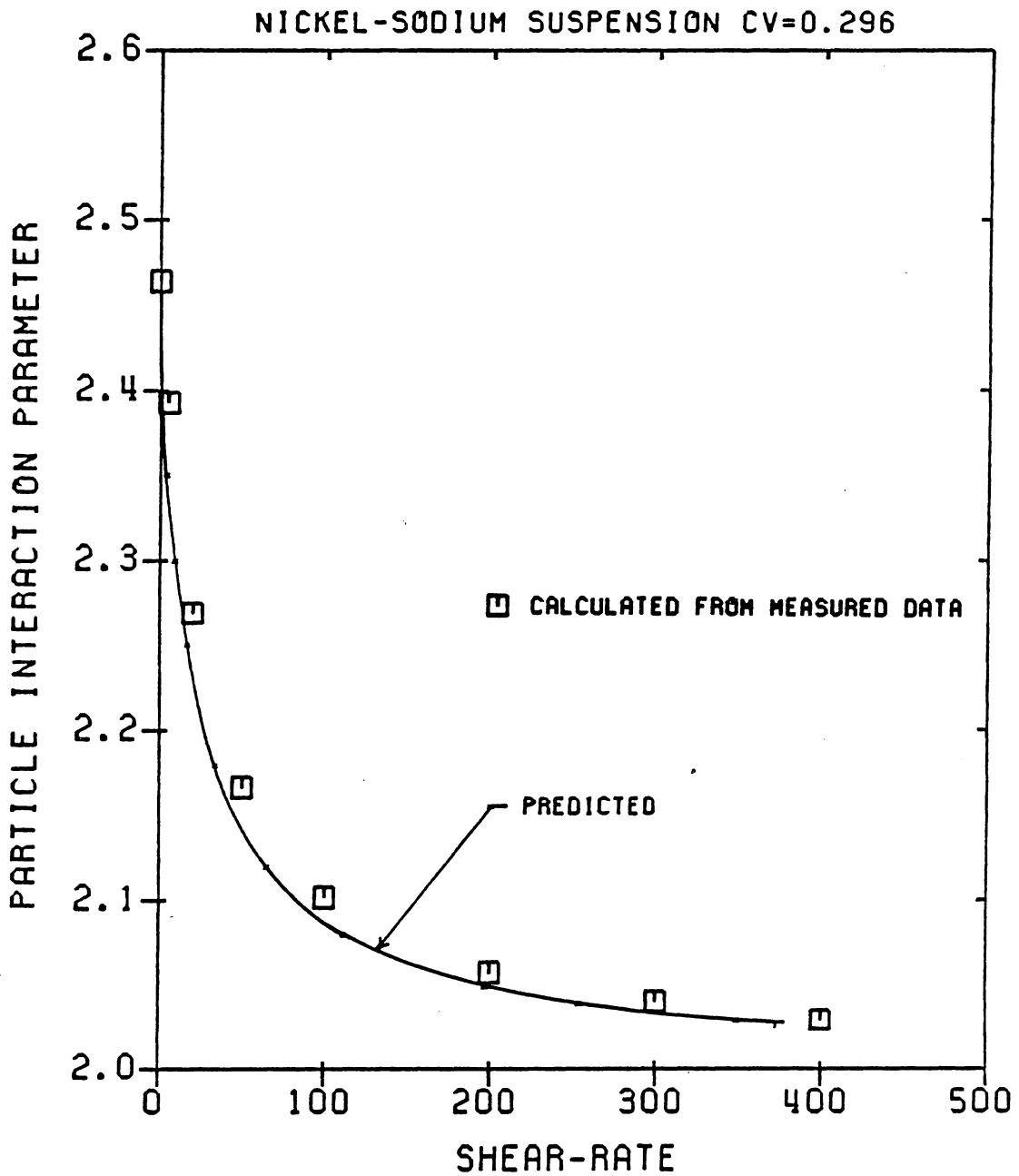


Figure 38. Variation of  $n$  with shear rate for nickel-sodium suspension (concentration = 0.296)

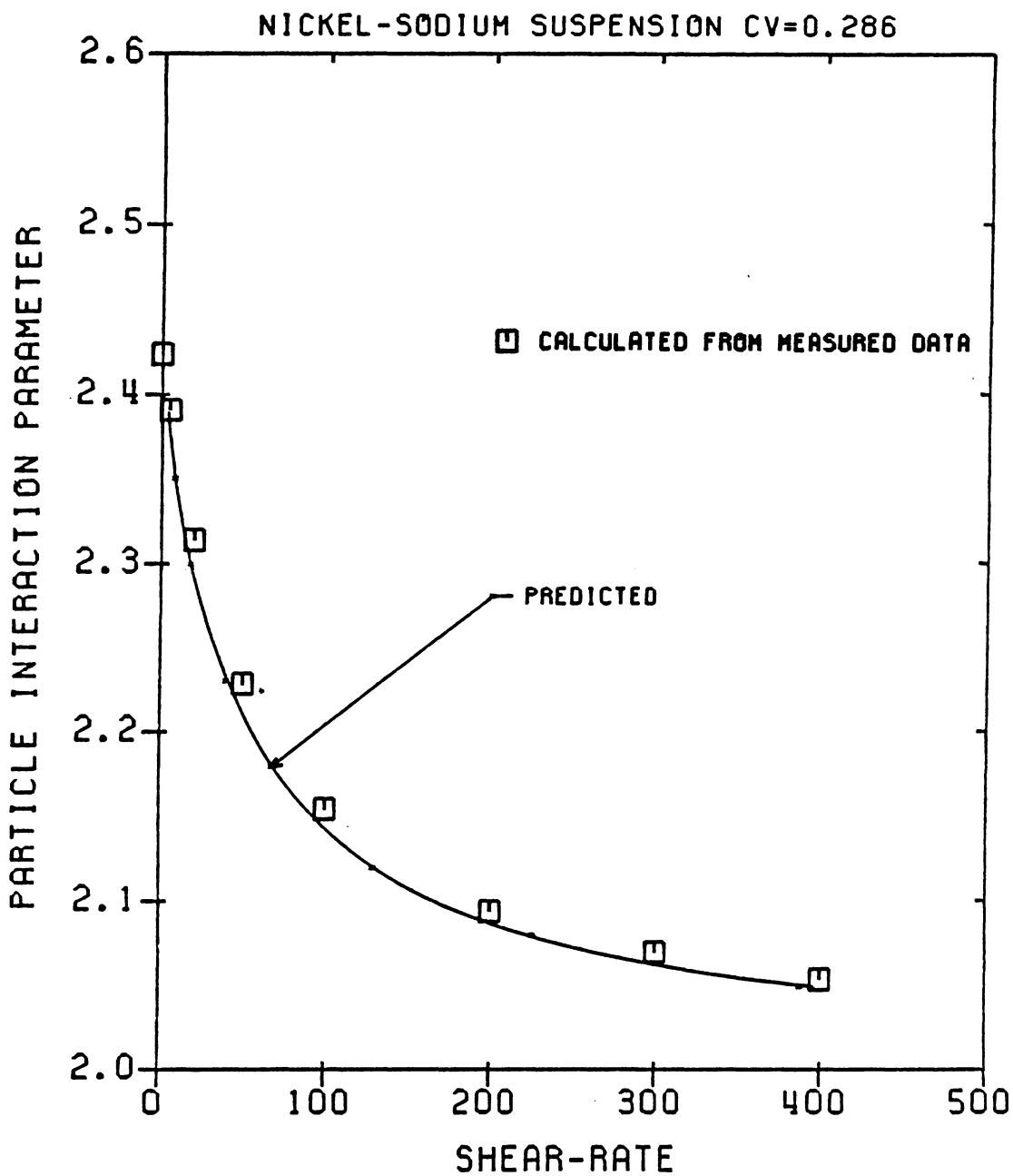


Figure 39. Variation of  $n$  with shear rate for nickel-sodium suspension (concentration = 0.286)

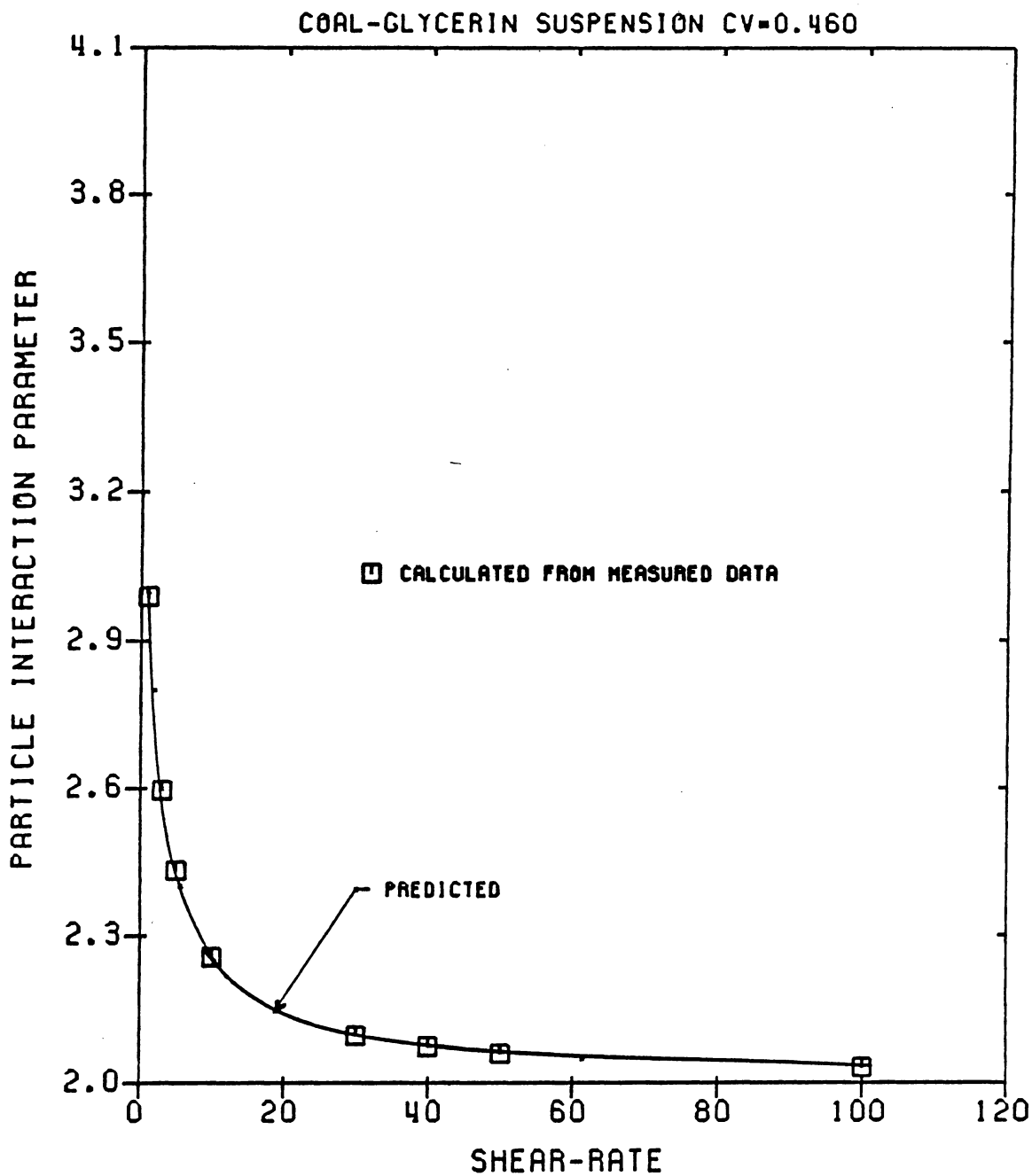


Figure 40. Variation of  $n$  with shear rate for coal-glycerin suspension (concentration = 0.460)



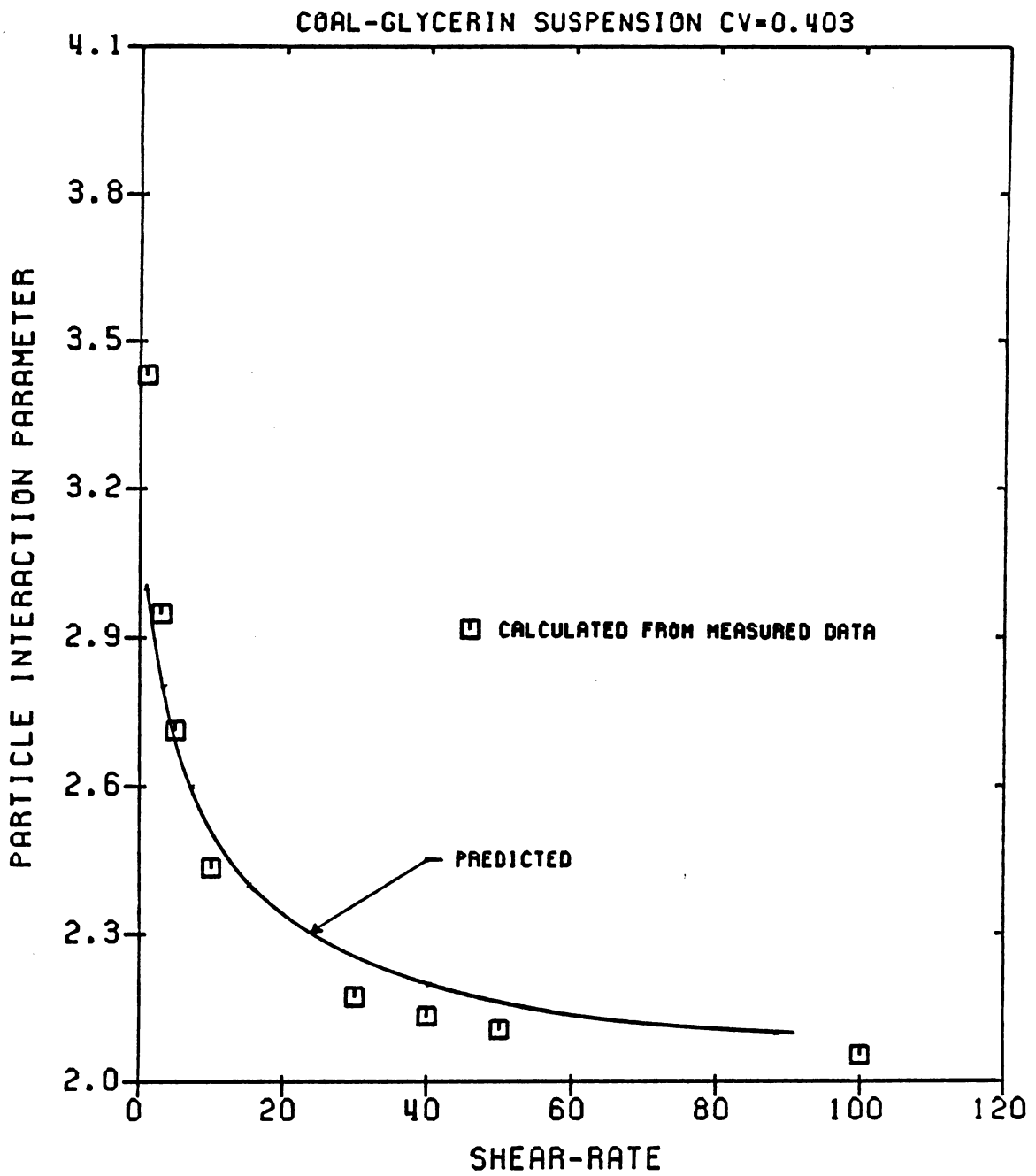


Figure 41. Variation of  $n$  with shear rate for coal-glycerin suspension (concentration = 0.403)

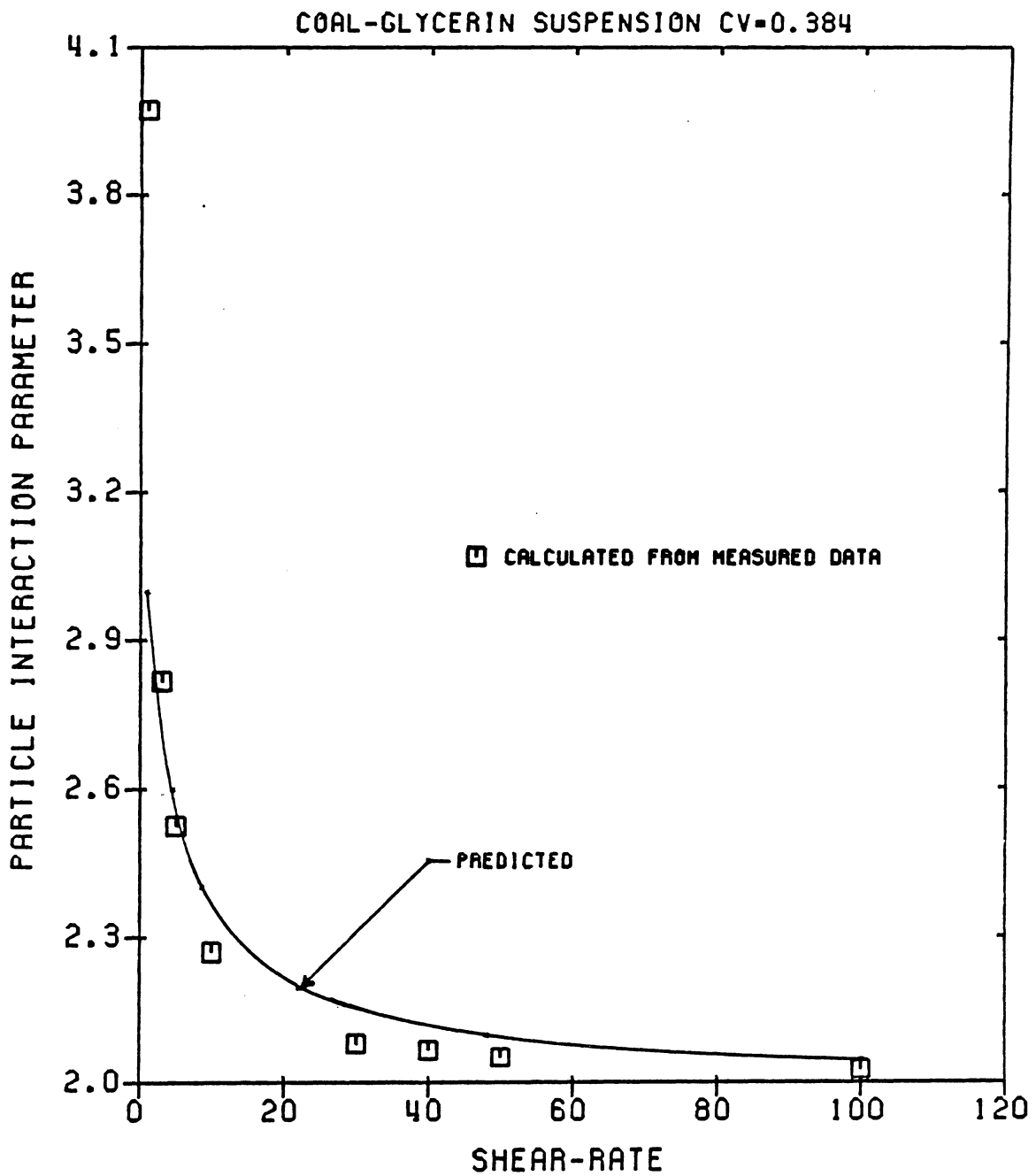


Figure 42. Variation of  $n$  with shear rate for coal-glycerin suspension (concentration = 0.384)

viscosity can apparently be attributed simply to this suspension specific behavior of the particle interaction parameter  $n$  under varying flow conditions.

Finally, it should be emphasized that any meaningful investigation on the rheologic behavior of highly concentrated suspensions must address the effects of particle size distribution. This could be achieved through experiments with systematically varied particle size distributions in an effort to evaluate the relevant effects on the primary parameters involved, which include the calculated and the measured values of the maximum packing concentration  $\phi_m$ , the intrinsic viscosity  $[\eta]$ , and the particle interaction parameter  $n$ .

## 7.6 OPTIMIZATION OF PARTICLE SIZE DISTRIBUTION

The final stage of this study involved two tasks. One of these was to develop a methodology that would incorporate all the rheologic and hydraulic formulations described so far and facilitate a physically meaningful analysis of the behavior of highly concentrated solid-liquid mixtures. The second objective was to demonstrate through a systematic application of this methodology that the particle size distribution does indeed govern the slurry behavior and lends itself for optimization to achieve a feasible slurry utilization. The specifics of the procedures and the relevant algorithm are presented subsequently.

The computational procedure of the optimization methodology requires the knowledge of the particle size distribution along with at least one experimental shear rate or one shear viscosity variation with shear rate, and can be summarized as follows:

- a) The procedure outlined in section 7.3 is performed first.
- b) The power law constants  $PN$  and  $PK$  are computed from the shear rate shear rate data [ $n$  and  $K$  in Equation (2.1)].

- c) The input particle size distribution is fit to Rosin-Rammler equation [Equation (5.21)], which is assumed to characterize the distribution of solid particles ground in ball-mill type equipment] by means of two parameters, referred to as the size modulus and the distribution modulus. Size modulus is the value of a specific particle size, such as  $d_{50}$ ,  $d_{65}$  or weighted mean diameter [61] that represents the particle size distribution best, in this study weighted mean diameter WMEAND is used in calculations. The constant DM is the slope of the Rosin-Rammler equation drawn on a log [ln (1- $S_j$ ) ] versus log (  $d_j/d_m$  ) scale and is a measure of the spread of the distribution, where  $S_j$  is the cumulative weight fraction finer than the size  $d_j$  and  $d_m$  is the weighted mean diameter WMEAND.
- d) Pumping energy is calculated next by using pressure gradient equations developed in Chapter 5. First, the flow condition is checked to find out whether it is laminar or turbulent and depending on the flow behavior appropriate equations are applied to obtain the amount of energy needed to overcome frictional losses as described in Chapter 5.
- e) Comminution energy is estimated from a given relationship between the total surface area of solid particles and the grinding energy that was provided by the Mining and Minerals Engineering Department at VPI & SU (Figure 41).
- f) Last step is to find the total energy consumption, which is the sum of pumping and comminution energy requirements, repeated for various pipe diameter and distance combinations.
- g) The particle size distribution is varied by changing the slope DM of the line on a Rosin-Rammler scale while keeping the size modulus WMEAND constant.

The computer model developed for implementing the methodology outlined above was run for the coal-glycerin system, properties of which was given in Table 4 and 5, for various particle size distributions. The numerical results obtained are tabulated in Appendix B. The particle size distributions, in which only the spread of distribution was changed keeping the size modulus constant, are shown in Figure 42 for the original, the

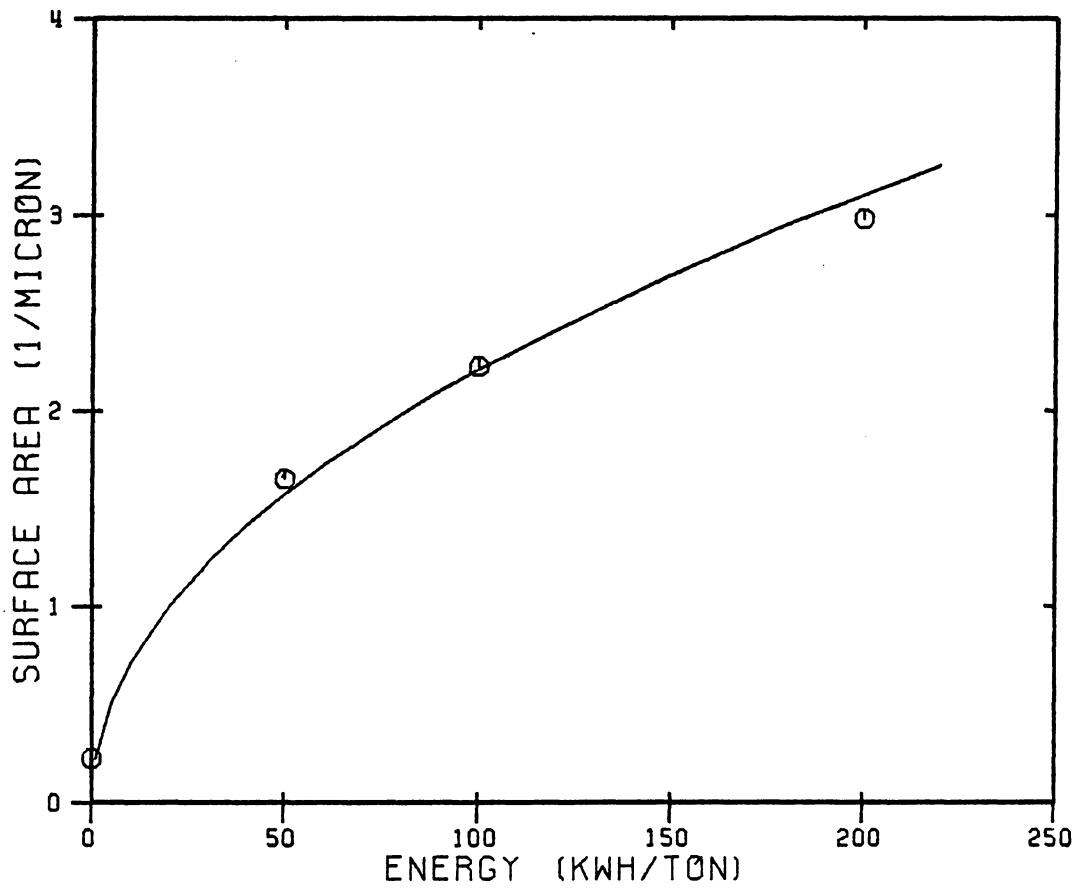


Figure 43. Energy consumption with respect to specific surface area in a stirred-ball mill

narrowest and the broadest distributions. The effects of this variation in the total surface area and the maximum packing concentration are tabulated in Table 9. As indicated in Table 9, the original distribution and the modified distribution obtained by curve fitting to Rosin-Rammler equation have the same DM, but not the same surface areas. This is because of the fact that in Rosin-Rammler equation one of the axes has a double logarithmic function which narrows the spread of data on a  $\log(\ln)$  versus  $\log$  plot. Therefore, although the correlation coefficient appears to be high the actual representation of a size distribution may not be as superior on an arithmetic scale. Consequently, either the best available correlation should be used to represent typical particle size distributions obtained from a certain grinder or various size distribution models should all be tried in the analyses.

The test runs were made for coal annual throughputs from 200,000 tons to 800,000 tons. The pipe sizes used range from 2 to 7 inches and the length of pipes analyzed were selected to be in between 0.1 and 2.5 miles. The volumetric concentrations of coal were 0.460, 0.430 and 0.384. The original particle size distribution had a slope DM of 1.36 and a specific surface area of 0.858 ( $1/\mu\text{m}$ ) as indicated in Table 9. The slope of the distributions were varied from 1.56, being the narrowest, to 0.56, being the broadest and the corresponding specific surface areas were obtained as 0.743 ( $1/\mu\text{m}$ ) and 2.711 ( $1/\mu\text{m}$ ), respectively.

The large number of parameters to be analyzed and their highly variable interdependence for different suspensions make it a formidable if not impossible task to achieve a unique design criteria for the optimization of the particle size distribution. However, when certain parameters are analyzed under various flow conditions, determined by the annual throughput, volumetric concentration and pipe size, some distinguishing features can be obtained which lead to the understanding of the effect of variation of these parameters on the total energy consumed. Therefore, the following discussion will concen-

**Table 9. Values of Three Parameters as Affected by the Change of the Particle Size Distribution**

DM	$S_a$ ( $1/\mu\text{m}$ )	$\varphi_m$	Remarks
1.56	0.743	0.503	Narrowest PSD
1.46	0.802	0.507	
1.36	0.858	0.520	Original PSD
1.36	0.875	0.511	Original PSD fit to R-R eqn.
1.26	0.964	0.516	
1.16	1.076	0.523	
1.06	1.217	0.531	
0.91	1.499	0.545	
0.81	1.750	0.556	
0.71	2.069	0.570	
0.66	2.259	0.578	
0.61	2.472	0.587	
0.56	2.711	0.596	Widest PSD

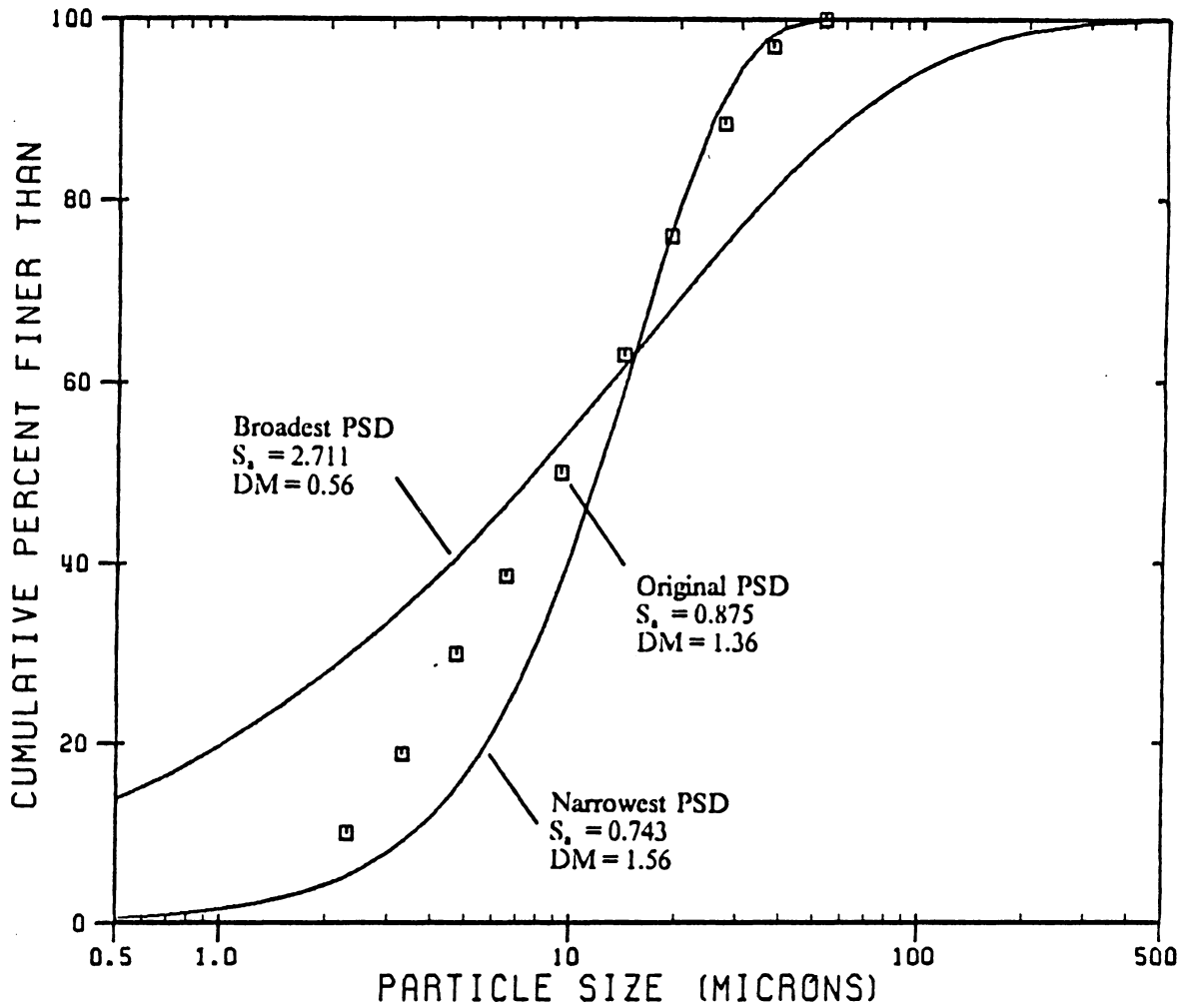


Figure 44. Original particle size distribution and the limits in which the distribution was varied



trate on certain parameters and analyze the effect of these parameters on the total energy consumed for various particle size distributions, pipe sizes and lengths, and annual throughputs.

The results that correspond to the volumetric concentration of 0.460 were presented in the following since it was the highest concentration implemented and hence, most likely the critical one in analyzing the overall suspension characteristics.

The variation of the percentages of pumping energy with respect to pipe size is given in Figure 43. As can be seen from the figure, for narrow particle size distributions, having larger fractions of coarser particles in the distribution, the specific surface area decreases, the maximum packing concentration is also reduced [Table 9]. Since the suspension with a given concentration behaves "thicker" and requires greater energy to overcome pressure losses, while the grinding energy required for the relatively coarse particles is not large. The result is then high pumping energy dominating the total energy consumption. As the particle size distribution is made broader, the surface area will be increased, the packing configuration of solid particles will be improved and as a result the pressure gradient will be lowered. On the other hand because of increasing percentage of smaller particle sizes the energy consumed in grinding will increase, the dominating percentage of the total energy will now be represented by comminution. As also depicted in Figure 43, the variation in the contribution of pumping energy depends not only on the surface areas, resulting from the change in particle size distributions, but also on the pipe sizes. This is as expected since the velocity of flow decreases as the pipe size is increased, and hence results in lower energy requirement due to lower frictional losses. The rate of decline in the amount of pumping energy becomes greater as the surface area and the pipe size are increased simultaneously. For small surface areas the pipe size does not have a significant effect on the amount of pumping energy because the comminution energy is too small as compared to the pumping energy. The

same argument is also true for small pipe sizes as depicted for example by the curves for  $D = 2$  inches in Figure 43. The velocity in such a small pipe is very high which creates a significant amount of hydraulic loss and consequently, turns out to be the dominating energy component no matter what the shape of the particle size is.

Variation of the total energy in kWh/year with pipe size is shown in Figure 44 for the original, the narrowest and the broadest particle size distributions with specific surface areas of 0.875, 0.743 and 2.711, respectively, and for three concentrations. It can be concluded from the figure that for narrow particle size distributions, the spread for different concentrations is considerably larger than that for the broadest one. For example, the analysis for  $S_a = 0.743$  revealed that the total energy varied approximately from 16 million kWh/yr in 5 inch pipe to 300 million kWh/yr in 2 inch pipe, 8 millions kWh/yr in 5 inch pipe to 140 million kWh/yr in 2 inch pipe and 6 millions kWh/yr in 5 inch pipe to 98 million kWh/yr in 2 inch pipe at concentrations of 0.460, 0.430 and 0.384, respectively. Therefore, concentration of solid particles becomes an important parameter to be watched for narrow particle size distributions. On the other hand, however, the analysis with the broadest distribution revealed that there appears to be less dependence on the concentration of solid particles, especially for pipe sizes larger than 3 inches. In the region where the pipe size is greater than 3.5 inches, the total energy consumption is slightly higher than the other two distributions. This is due to dominating comminution energy which is higher as compared to the one consumed by the narrow distribution. As a conclusion, the total energy consumed by any particle size distribution depends strongly on both the specific surface area and the pipe size, however, the volumetric concentration of solid particles may play an important role in determining the most suitable mixture.

In Figures 45 and 46, the variation of the normalized total energy with respect to the normalized specific surface area are presented, first keeping the length of pipe fixed

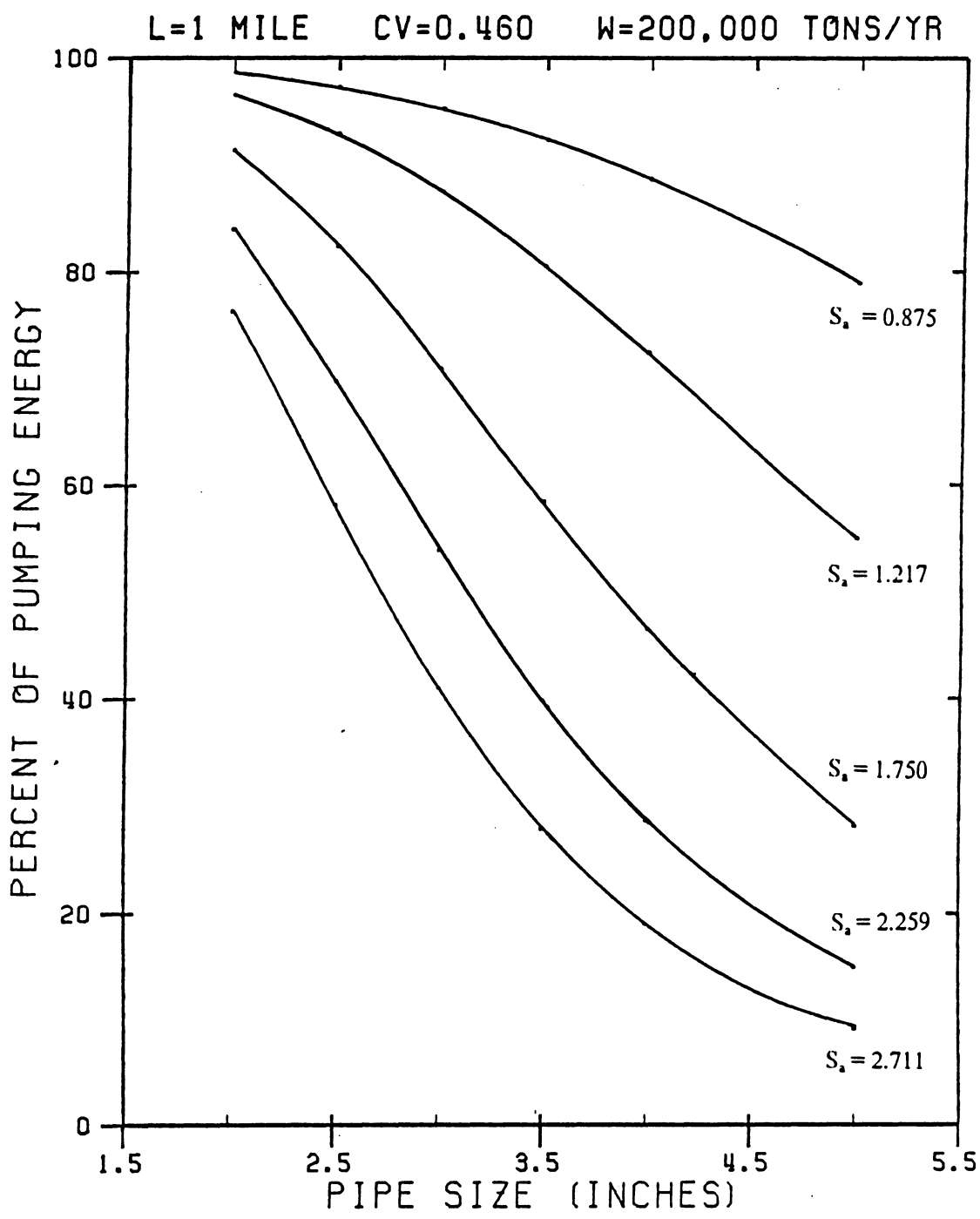


Figure 45. Variation of the percent of pumping energy with pipe size for various particle size distributions

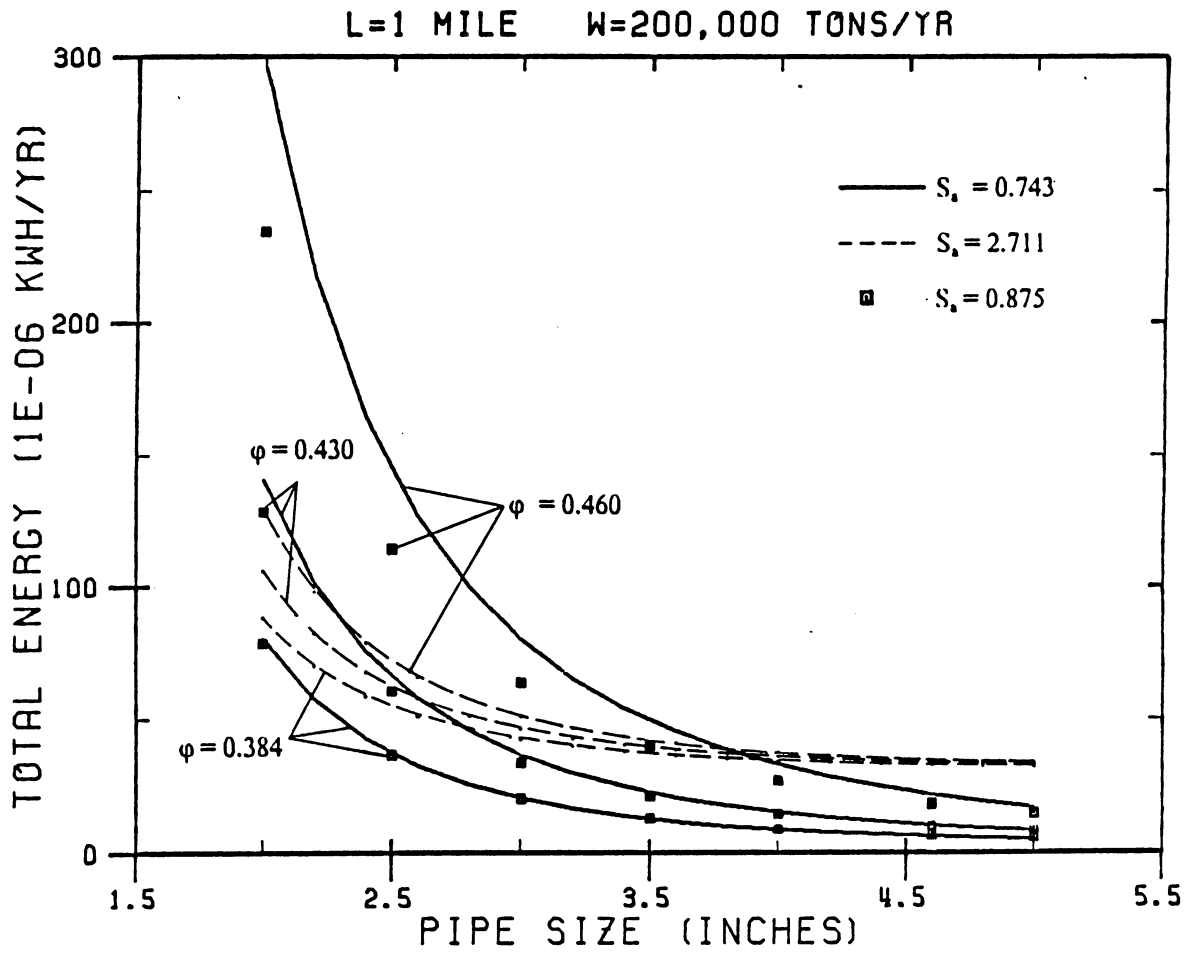


Figure 46. Variation of total energy with pipe size for distributions in Figure 42

varying the pipe diameters and then keeping the pipe size constant varying the pipe lengths, respectively. The total energy and the specific surface area were normalized by using the corresponding values from the analysis performed for the original particle size distribution that was fit to Rosin-Rammler line. These graphs reveal an important amount of information related to the effects of surface area and pipe size, and surface area and pipe length on the total energy consumed. In Figure 45, for example, the minimum total energy ratio is obtained between normalized surface areas of 1.2 and 1.3 for 5 inch pipe, 1.4 and 1.6 for 4 inch pipe, around 2 for 3 inch pipe and no minimum point for 2 inch pipe. Therefore, as the particle size distribution is made broader than the original one the suspensions' energy consumption vary depending on the pipe size and the amount of surface area created. Similarly, in Figure 46, for a constant pipe size of 4 inches the effect of various pipe lengths result in a similar behavior.

Finally, the relationship between various coal annual throughputs and total energy is plotted as given in Figure 47 for a 5 inch diameter of 1 mile long and 0.460 volumetric concentration of solids. The results indicate that starting from  $S_a = 2.711$  to  $S_a = 1.499$  the total energy consumption decreases almost parallel to each other, however, the lines corresponding to  $S_a = 0.875$  and  $S_a = 0.743$  cross these lines when the annual throughput is increased. On the other hand, as the particle size distribution is made narrower decreasing the surface area the difference between two adjacent curves decrease too until the surface area that corresponds to 1.499 is reached. After that the curves start changing behavior and increase drastically with increase in annual throughput. A possible explanation for this kind of behavior could be such that, the comminution energy consumption apparently becomes the dominant energy component for the specific pipe size and length analyzed. This is why the widest distribution, even though the pumping energy was the smallest among other distributions, appears to have the highest total energy consumption. As the shape of the distribution is altered and made narrower than there

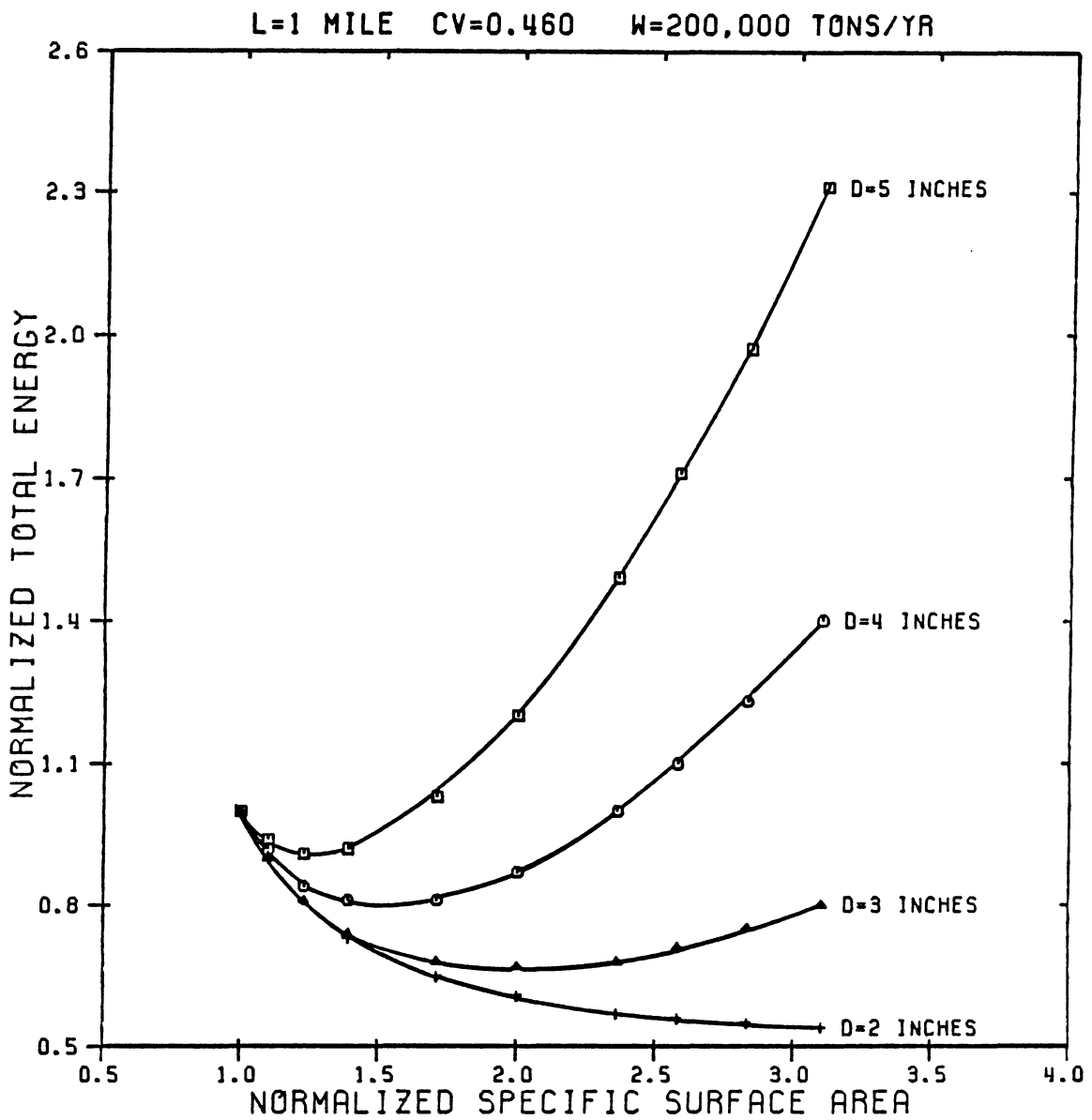


Figure 47. Variation of the normalized total energy with normalized specific surface area for various pipe sizes

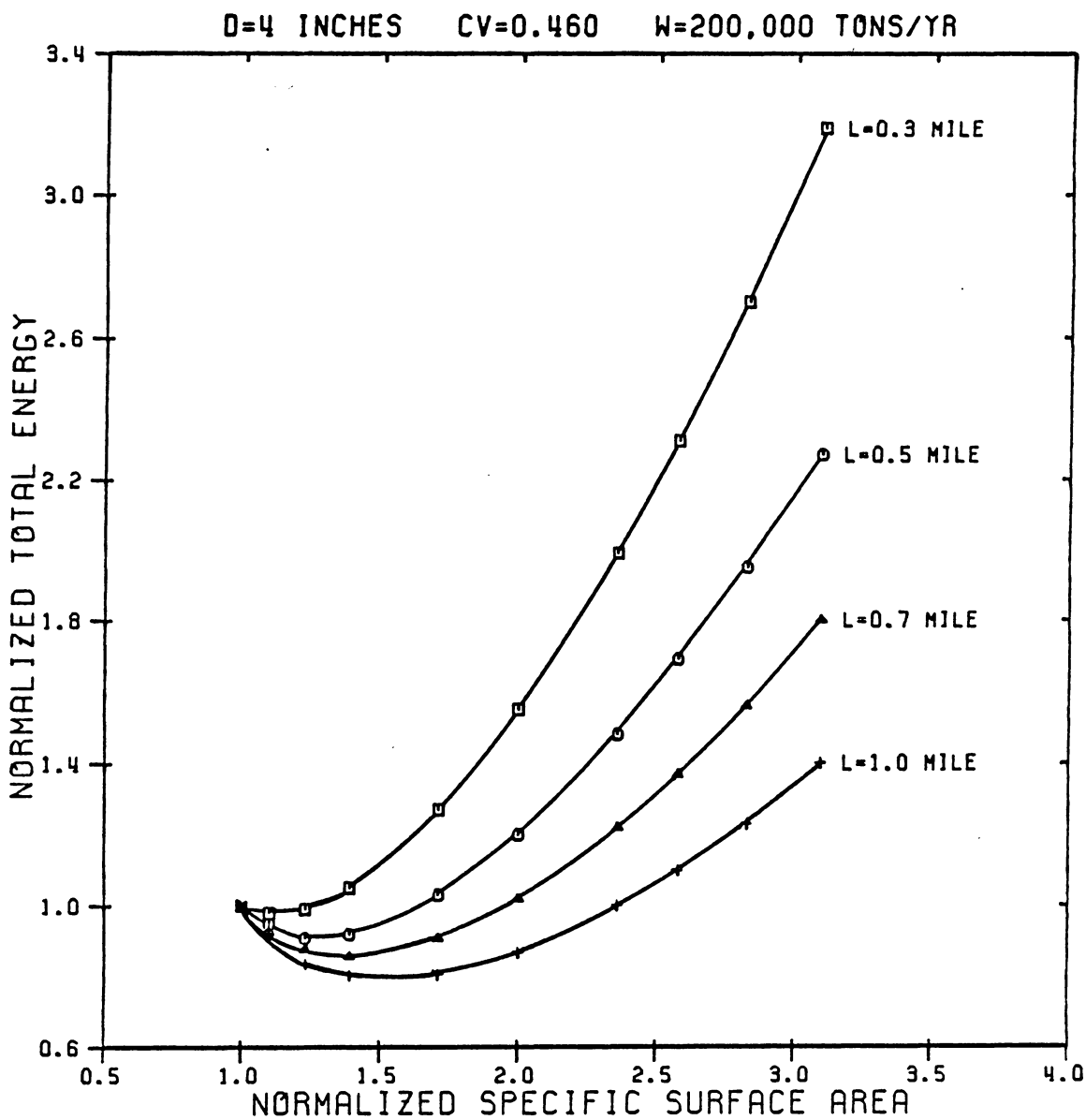


Figure 48. Variation of the normalized total energy with normalized specific surface area for various pipe lengths

is going to be a balance between the pumping and grinding energies such that a decrease in comminution energy, due to decrease in specific surface area, will be more than the increase in pumping energy due to increased frictional losses. This balance will be destroyed by further decreasing the surface area and the pumping energy will start dominating the total energy consumption. This is the reason for the behavior of the curves corresponding to surface areas of 0.875 and 0.743 which do not obey the behavior of other curves. As a conclusion, for different pipe sizes and lengths a minimum particle size distribution could be achieved for various annual coal throughputs.



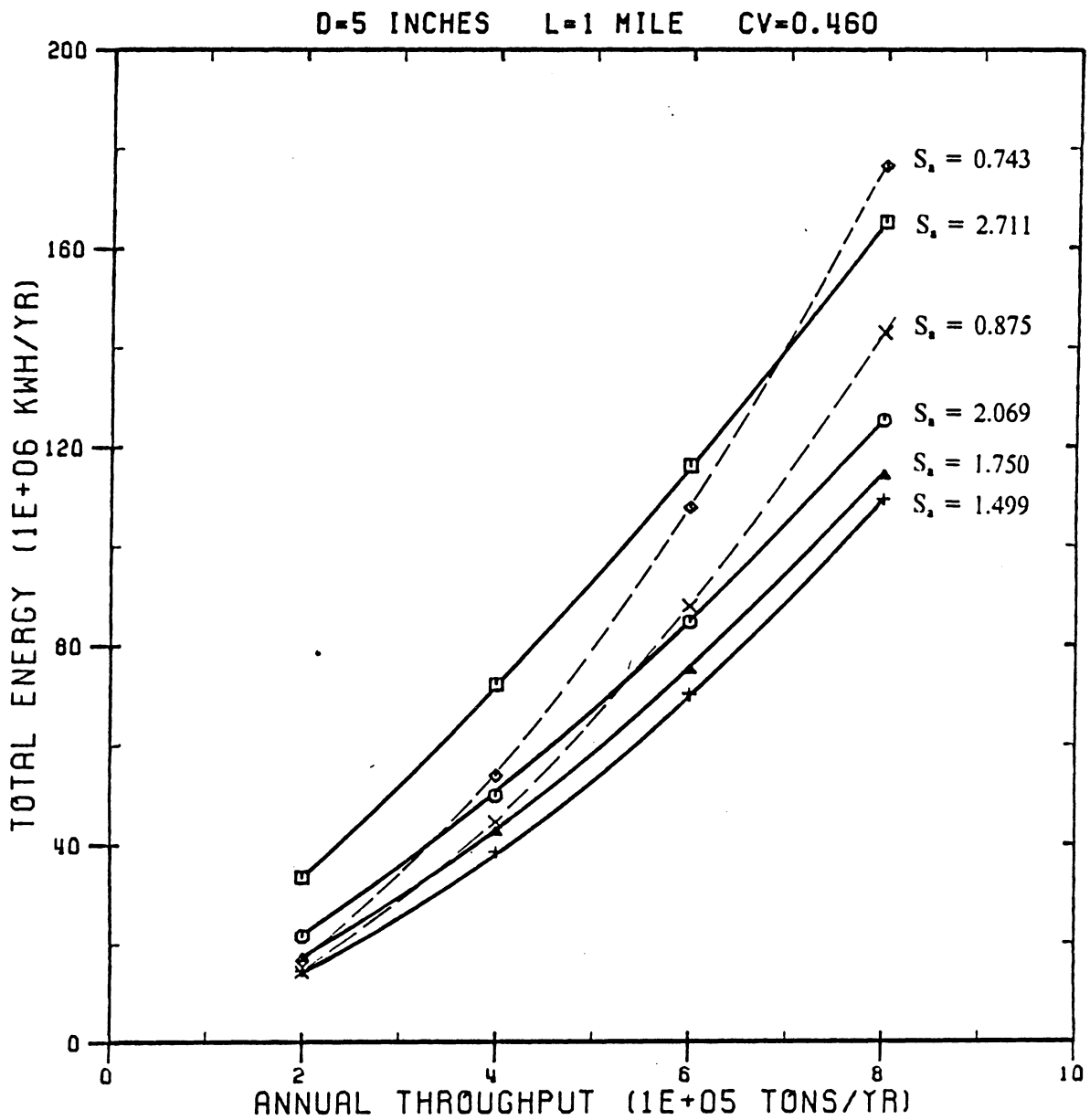


Figure 49. Variation of total energy with annual throughputs for various size distributions

## **CHAPTER 8**

# **CONCLUSIONS AND RECOMMENDATIONS**

### **8.1 CONCLUSIONS**

- A basic formulation has been developed for the rheologic behavior of highly-concentrated suspensions, using physically meaningful dimensionless parameters emphasizing the effects of variations in the particle size distribution. The variables incorporated in these dimensionless parameters were specific gravity of particles, density of carrier liquid, viscosity of carrier liquid, mean particle size, solids concentration, specific surface area of solids, surface area mean diameter, shape factor and maximum packing concentration.
  
- Shear viscosity behaviors of highly-concentrated suspensions at low and high shear rates were predicted from a formulation proposed which consists of three parameters characterizing the microstructure of the suspension. These parameters are the intrinsic viscosity that represents the effective shape of the particles imposed by their surface

condition, a parameter  $n$  that reflects the level of particle interactions between the initiation of motion and high shear rate regions, and the maximum packing concentration.

- The proposed formulations appear to correlate the data well on various limited coal and non-coal suspensions which obey both power and yield-power-laws. Once calibrated for the non-physical characteristics of a suspension with given concentration and particle size distribution, the formulations predicted shear stress shear rate behaviors for various concentrations and size distributions well. The formulation proposed for the shear viscosity behaviors at low and high shear rates also predicted the experimental data well when applied to seven different suspensions.

- A correlation between the analytically calculated and measured maximum packing concentrations has been obtained by making use of the experimental data to account for the surface induced interaction of particles with the fluid. This correlation also proved that the parameters, namely the intrinsic viscosity and the particle interaction parameter, do indeed represent the surface related interactions between solid particles and liquid.

- A methodology has been developed for the analysis of the particle size distribution effects on the overall optimum energy efficiency during hydraulic transportation and particle size reduction. A computer model developed for this methodology incorporates the rheologic and hydraulic formulations described in this study. The results obtained through a systematic application of this methodology to a coal-liquid mixture revealed that an optimum particle size distribution can be achieved by a careful analysis of the effect of various variables, such as length and size of pipe, annual throughput and concentration of solids, on the overall system energy consumption.

- Further basic research is needed using coal-liquid mixtures with systematically varied concentrations and particle size distributions, with and without chemical additives.

## 8.2 RECOMMENDATIONS

The most difficult part in this study was to find data with sufficient information to be used in applications for the verification of the formulations and the methodology. The lack of sufficient amount of data was due to differences between the methods of approach to the problem to be investigated, which was stated in Chapter 1, and the method of present approach. Therefore, the following steps should be taken into consideration as a direct extension of the present work:

1. An extensive amount of experimental research should be carried out with various coal and non-coal suspensions in order to determine a complete set of data for the characterization of each of the parameters that were identified in this study.
2. A method of measurement has to be developed to obtain various particle size groups that exist in a particle size distribution of any material as accurate as possible. In addition, the distributions obtained from these measurements should be applied to the formulations developed in this study in order to test how various size groups affect rheology. A theory needs to be developed, consequently, to achieve a physically reasonable representation of the particle size distribution that would allow simulating the actual conditions as well as other distribution related parameters, such as maximum packing concentration, specific surface area, etc., more accurately.

3. The experimental data obtained should be used to verify the validity and further improve the applicability of the proposed methodology and formulations and an overall product optimization should be established for coal slurry fuels and other highly-concentrated suspensions.

4. The change in the surface shape of particles that correspond to different size groups in a distribution needs to be investigated and the relationship between the grinding method and the change in surface shapes should be determined since the behavior of suspensions are highly dependent upon the surface characteristics of particles.

**APPENDIX A**  
**COMPUTER PROGRAM LISTING**

```

C -----
C |                               MAIN PROGRAM                               |
C -----
C
C   REAL MU, KK, N, NO, PN, PK
C   COMMON/AA/DELM(15), NSIZE, NDR, TPHIM, NTYPE, IPSD, ND, NFLOW, NCV, NSIZ
C   COMMON/BB/PSIZE(50), DIAMR(50), PMAX(50), V(50), PSIZ(50), FRACT(50)
C   COMMON/CC/C, SSAREA, AREA, RHOS, RHOL, DS, ETA, VM, WMEAND, KK, N, PN, PK, NS
C   COMMON/DD/BC, ETAU, TAU, CV, CM, SF, DP, GC, GA, GI, ETA0, EINF, MU
C   COMMON/EE/G1, NDIST, NG, DG, G(50), TAU(50)
C   COMMON/FF/D(20), DIST(20), CVOL(20), NO, F0, W, EFF, CORR, NPS, J, IDM, IM
C
C   IPSD = 0
C   IOUT = 0
C
C   1 CALL INPUT(*99)
C     J=0
C
C   11 DO 10 I=1, NCV
C     CV = CVOL(I)
C     GO TO (5), NTYPE
C
C     IF (I.NE.1) GO TO 2
C     CALL PHIM
C     IF (I.GT.1) GO TO 5
C   2 CALL PCONC
C
C
C   5 CALL FLOWP
C     CALL PLAW
C     CALL OUTPUT (IOUT)
C     CALL ENERGY
C
C   10 CONTINUE
C     NPS=1
C     J=J+1
C     IF (IDM.EQ.0) GO TO 1
C     IF (J.NE.IDM) GO TO 11
C     GO TO 1
C   99 STOP
C     END

```

```

C -----
C                               SUBROUTINE PHIM
C -----
C
C.. THIS SUBROUTINE FINDS THE WEIGHTED MEAN DIAMETER OF PARTICLES,
C.. FITS THE INPUT PARTICLE SIZE DISTRIBUTION TO ROSIN-RAMMLER
C.. EQUATION AND CHANGES THE DISTRIBUTION BY MODIFYING THE
C.. PARAMETER DM
C
COMMON/MRI/GEOM(4,64)
COMMON/AA/DELM(15),NSIZE,NDR,TPHIM,NTYPE,IPSD,ND,NFLOW,NCV,NSIZ
COMMON/BB/PSIZE(50),DIAMR(50),PMA(50),FRAC(50),PSIZ(50),FRACT(50)
COMMON/CC/C,SSAREA,AREA,RHOS,RHOL,DS,ETA,VM,WMEAND,KK,N,PN,PK,NS
COMMON/FF/D(20),DIST(20),CVOL(20),NO,F0,W,EFF,CORR,NPS,J,IDM,IM
DIMENSION DPAR(50),FRACN(50)
C
C
C   IF (NPS-1) 1,5,1
C
C.. INITIALIZE THE PARTICLE SIZE DISTRIBUTION --SET TO INPUT VALUES--
C
5 NSIZE=NSIZ
DO 222 I=1,NSIZ
PSIZE(I)=PSIZ(I)
FRAC(I)=FRACT(I)
222 CONTINUE
C
C... CHANGE PARTICLE SIZE DISTRIBUTION BY ALTERING THE VARIABLE DM
C... WHICH IS THE SLOPE IN ROSIN-RAMMLER EQUATION.
C
DM = DM+DELM(J)
IM = 0
NFRAC = 0
DO 7 I=1,NSIZE
IM = IM + 1
DPAR(I) = PSIZE (NSIZE - I + 1)
FRACN(I)=(1-EXP(-(DPAR (I)/WMEAND)**DM))
IF ( FRACN(I).GE.0.999 ) GO TO 51
7 CONTINUE
NFRAC = 1
51 NSIZE = IM
DO 55 I=1,NSIZE
PSIZE (I) = DPAR (NSIZE-I+1)
FRAC(I) = FRACN(NSIZE-I+1)
55 CONTINUE
IF(NFRAC .EQ. 1) GO TO 4
GO TO 77
C
C... EXTEND THE PARTICLE SIZE DISTRIBUTION LINE TOWARD THE LARGEST SIZE

```



C... TO INTERSECT 100% FINER LINE (ASSUME 99.9% AS THE TOP LIMIT FOR  
C... CALCULATIONS

C

```
4 NSIZE = NSIZE +1
  Y2 = 0.999 - FRAC(1)
  XY = ALOG10 ( ALOG (0.001) / ALOG (Y2) ) / DM
  XA = 10 ** XY
  PARS = PSIZE (1)* XA
  DO 6 I = 2,NSIZE
    PSIZE(I) = DPAR (IM-I+2)
    FRACN(I)=(1-EXP(-(PSIZE(I)/WMEAND)**DM))
6 CONTINUE
  PSIZE(1)=PARS
  FRACN(1) = 0.999
```

C

```
77 IF (NFRAC.EQ.1) THEN
  DO 2 I=1,NSIZE
    IF(I.EQ.NSIZE) GO TO 2
    FRAC(I) = FRACN(I) - FRACN(I+1)
2 CONTINUE
  FRAC(NSIZE) = FRACN(NSIZE)
  ELSE
  DO 23 I=1,NSIZE
    IF(I.EQ.NSIZE) GO TO 23
    FRAC(I) = FRACN(NSIZE-I+1) - FRACN(NSIZE-I)
23 CONTINUE
  FRAC(NSIZE) = FRACN(1)
  ENDIF
```

C

```
CALL AREAS
WRITE(6,8)DM,SSAREA,(PSIZE(I),FRAC(I),I=1,NSIZE)
8 FORMAT (//5X,'NEW PARTICLE SIZE DISTRIBUTION WITH DM=',F5.2/15X,
#'SURFACE AREA=',F5.3/(15X,2(F8.4,5X)))
RETURN
```

C

```
1 DO 111 I=1,NSIZE
  PSIZ(I)=PSIZE(I)
  FRACT(I)=FRAC(I)
  NSIZ=NSIZE
111 CONTINUE
```

C

```
IM = 1
DO 3 I=1,NSIZE
  IF (FRAC(I).EQ.0.) GO TO 3
  PSIZE(IM)=PSIZE(I)
  FRAC(IM)=FRAC(I)
  IM=IM+1
3 CONTINUE
NS=IM-1
JN = 1
```

```

SUMF=0
SUM = 0
DO 10 I=1,NS
  DPAR (I) =PSIZE (NS-I+1)
  SUMF = FRAC(NS-I+1)+SUMF
  FRACN(I) = SUMF
  SUM = SUM + PSIZE (I)*FRAC(I)
10 CONTINUE
C
C... WEIGHTED MEAN DIAMETER
C
  WMEAND = SUM
C
22 DO 19 I=1,NS
  GEOM(1,I)=ALOG10(DPAR (I)/WMEAND)
  GEOM(2,I)=ALOG10(ABS(ALOG(1.-FRACN(I))))
19 CONTINUE
C
C.. FIT A STRAIGHT LINE TO THE PARTICLE SIZE DISTRIBUTION BY USING
C.. ROSIN-RAMMLER PARAMETERS
C
  CALL REGRE (0,2,NS,1,CDET,DM)
  IF(CDET.LE.CORR) THEN
    NS=NS-1
    IF (NS.EQ.0) GO TO 33
    DO 11 I=1,NS
      DPAR (I) = PSIZE (I+JN)
      FRACN(I)= FRACN(I+JN)
11 CONTINUE
    JN=JN+1
    GO TO 22
  ELSE
    R2 = SQRT(CDET)
    CALL AREAS
    WRITE(6,66)DM,R2,SSAREA,(PSIZE(I),FRACN(I),I=1,NS)
  ENDIF
C
66 FORMAT(//' PARTICLE SIZE DISTRIBUTION THAT FITS ROSIN-RAMMLER EQN.
  * DM=',F5.2//15X,'CORRELATION COEFFICIENT R =',F5.3/15X,
  #'SURFACE AREA=',F5.3//(15X,2(F8.4,5X)))
C
  RETURN
C
33 WRITE (6,44) CORR
44 FORMAT (////10('*'),' NS=0 - PARTICLE SIZE DISTRIBUTION DOES NOT
  #SATISFY THE REQUIRED CORRELATION ',F5.3,10('*')//)
  STOP
  END

```

```

C -----
C                               SUBROUTINE PCONC
C -----
C
C
C... THIS SUBROUTINE CALCULATES THE MAXIMUM PACKING CONCENTRATION
C... FOR GIVEN PARTICLE SIZE DISTRIBUTION
C
  REAL LS,N,NO
  COMMON/AA/DELM(15),NSIZE,NDR,TPHIM,NTYPE,IPSD,ND,NFLOW,NCV,NSIZ
  COMMON/BB/PSIZE(50),DIAMR(50),PMAX(50),V(50),PSIZ(50),FRACT(50)
  COMMON/CC/C,SSAREA,AREA,RHOS,RHOL,DS,ETA,VM,WMEAND,KK,N,PN,PK,NS
  COMMON/DD/BC,ETAU,TAUY,CV,CM,SF,DP,GC,GA,GI,ETA0,EINF,MU
  COMMON/FF/D(20),DIST(20),CVOL(20),NO,F0,W,EFF,CORR,NPS,M,IDM,IM
C
  IF ( NPS.EQ.0 ) NSIZE = NS
  TPHIM=1.
  DO 100 I=1,NSIZE
  PHIM=0.
  DO 101 J=1,NSIZE
C
C.. RATIO OF COARSE TO FINE FOR EACH MEAN PARTICLE SIZE
C
  DRATIO=PSIZE(J)/PSIZE(I)
  IF(DRATIO.LT.1.) DRATIO=1/DRATIO
  DO 102 K=1,NDR
  IF(DRATIO.EQ.DIAMR(K)) GO TO 104
  IF(DRATIO.LT.DIAMR(K+1).AND.DRATIO.GT.DIAMR(K)) GO TO 103
102 CONTINUE
104 PHIMAX=PMAX(K)
  GO TO 105
C
C.. INTERPOLATE THE MAXIMUM PACKING CONCENTRATION
C
103 PHIMAX=(DRATIO-DIAMR(K))*(PMAX(K+1)-PMAX(K))/(DIAMR(K+1)-
  *DIAMR(K))+PMAX(K)
105 IF(I.EQ.1) GO TO 22
  IF(J.LE.I) GO TO 5
C
C.. COEFFICIENT TO BE USED IN RELATING A LARGER TO A SMALLER PARTICLE
C.. GROUP
C
  22 SL=0.639+(PHIMAX-0.639)/(1.017*PHIMAX-0.15)
  GO TO 6
C
C.. COEFFICIENT TO BE USED IN RELATING A SMALLER TO A LARGER PARTICLE
C.. GROUP
C
  5 LS=0.639+(PHIMAX-0.639)/(1.15-1.017*PHIMAX)
  SL=LS

```

```

        6 PHIM=SL*V(J)+PHIM
101 CONTINUE
C
C.. CHOOSE THE SMALLEST PHIM AS THE PACKING CONCENTRATION OF THE GIVEN
C.. PARTICLE SIZE DISTRIBUTION
C
        IF(TPHIM-PHIM) 100,100,10
        10 TPHIM=PHIM
100 CONTINUE
C
C... MODIFY THE CALCULATED PHIM AND DETERMINE THE ACTUAL PHIM
C
        IF (NPS - 1) 1,2,1
        1 PHIMC=TPHIM
        IF (IPSD.NE.0) GO TO 80
        ETA = 2*(1/CV - 1/CM) * (SQRT(EINF) - 1)
        CALL ITER (1,1.,NO,N)
80 CONTINUE
        TPHIM = 1.89/(ETA*N/2.*TPHIM)**0.94
        CM = TPHIM
        PHIME=CM
        RETURN
        2 CM = TPHIM * PHIME / PHIMC
        N = 2/(ETA*PHIMC)*(1.89/CM)**(1/0.94)
C
        RETURN
        END
C
C -----
C                               SUBROUTINE FLOWP
C -----
C
C... THIS SUBROUTINE CALCULATES THE YIELD STRESS AND SHEAR STRESS
C... FOR GIVEN PARTICLE AND FLUID PHYSICAL PROPERTIES
C
        REAL MU,NUM,KK,N,NO
        COMMON/AA/DELM(15),NSIZE,NDR,TPHIM,NTYPE,IPSD,ND,NFLOW,NCV,NSIZ
        COMMON/CC/C,SSAREA,AREA,RHOS,RHOL,DS,ETA,VM,WMEAND,KK,N,PN,PK,NS
        COMMON/DD/BC,ETAU,TAUY,CV,CM,SF,DP,GC,GA,GI,ETA0,EINF,MU
        COMMON/EE/G1,NDIST,NG,DG,G(50),TAU(50)
        COMMON/FF/D(20),DIST(20),CVOL(20),NO,F0,W,EFF,CORR,NPS,J,IDM,IM
C
C.. YIELD STRESS
C
        IPSD = 1
        TAUY = C*CV**3/(CM-CV)*(RHOS/RHOL-1)*GA*RHOL*DP*1.0E-06*(SSAREA*DS
        */SF)
C
        MU = MU/GC
        RHOL = RHOL/GC

```

```

      DS=DS*1.E-06
C
      BC = KK*TAUY*CV*(CV/(CM-CV))*MU/(DS*SQRT(RHOL*TAUY))
      MU = MU*GC
      DS = DS/1.0E-06
C
C.. VISCOSITY AT LOW SHEAR RATES
C
      ETA0 = MU*(1+ETA*CV/(N*(1-CV/CM)))*N
C
C.. VISCOSITY AT HIGH SHEAR RATES
C
      EINF = MU*(1 + 0.5*ETA/(1/CV-1/CM))*2
      G(1) = G1
      DO 90 I=1,NG
      NUM = (ETA0-EINF)*G(I)/GC
      DENUM = 1+((ETA0-EINF)/(GC*BC))*G(I)
C
C.. SHEAR STRESS
C
      TAU(I) = TAUY + EINF*G(I)/GC+NUM/DENUM
      IF ( I.EQ.NG ) GO TO 90
      G(I+1) = G(I) + DG
90 CONTINUE
C
      RETURN
      END
C
-----
                        SUBROUTINE PLAW
-----
C
C PROGRAM TO FIT A POWER-LAW CURVE TO SUSPENSION FLOW DATA BY
C THE METHOD OF LEAST SQUARES
C
      DIMENSION X(50),Y(50)
      COMMON/CC/C,SSAREA,AREA,RHOS,RHOL,DS,ETA,VM,WMEAND,KK,N,PN,PK,NS
      COMMON/DD/BC,ETAU,TAUY,CV,CM,SF,DP,GC,GA,GI,ETA0,EINF,MU
      COMMON/EE/G1,NDIST,NG,DG,GAMMA(50),TAU(50)
C
C GET THE NUMBER OF DATA POINTS FOLLOWED BY THE SHEAR RATES AND
C SHEAR STRESSES FOR EACH POINT
C
      IF(NG.GE.1.AND.NG.LE.50) GO TO 1
      WRITE (6,62) NG
62 FORMAT(' STOP - NG =',I5,'EXCEEDS DIMENSIONS')
      STOP
C
1 DO 3 I=1,NG
      IF(GAMMA(I).GT.0..AND.TAU(I).GT.0.) GO TO 2

```

```

WRITE (6,65)
65 FORMAT (////' STOP - NEGATIVE DATA')
STOP
2 X(I)=ALOG(GAMMA(I))
3 Y(I)=ALOG(TAU(I)-TAUY)

```

```

C
      XMEAN=0.
      YMEAN=0.
      SUMXX=0.
      SUMXY=0.
      DO 4 I=1,NG
      XMEAN=XMEAN+X(I)
      YMEAN=YMEAN+Y(I)
      SUMXX=SUMXX+X(I)*X(I)
4     SUMXY=SUMXY+X(I)*Y(I)
      RM=NG
      XMEAN=XMEAN/RM
      YMEAN=YMEAN/RM
      RN=(SUMXY-RM*XMEAN*YMEAN)/(SUMXX-RM*XMEAN*XMEAN)
      TAU0=EXP(YMEAN-RN*XMEAN)

```

```

C
C... POWER LAW CONSTANTS N = PN AND K = PK

```

```

C
      PN = RN
      PK = TAU0

```

```

C
      RETURN
      END

```

```

C
-----
                        SUBROUTINE ENERGY
-----

```

```

C
C... PROGRAM TO CALCULATE THE POWER REQUIREMENT OF A NON-NEWTONIAN
C... COMPLEX MIXTURE FLOW IN A PIPE WHICH OBEYS THE POWER LAW

```

```

C
      REAL N
      CHARACTER FLOW(2)*9
      COMMON/AA/DELM(15),NSIZE,NDR,TPHIM,NTYPE,IPSD,ND,NFLOW,NCV,NSIZ
      COMMON/CC/C,SSAREA,AREA,RHOS,RHOL,DS,ETA,VM,WMEAND,KK,N,PN,PK,NS
      COMMON/DD/BC,ETAU,TAUY,CV,CM,SF,DP,GC,GA,GI,ETA0,EINF,MU
      COMMON/EE/G1,NDIST,NG,DG,G(50),TAU(50)
      COMMON/FF/D(20),DIST(20),CVOL(20),NO,F0,W,EFF,CORR,NPS,J,IDM,IM
      DIMENSION RENER(10,20,20)

```

```

C
      FLOW(1)='LAMINAR'
      FLOW(2)='TURBULENT'
      PI = 3.14159265

```

```

      SS = RHOS/RHOL
C
C.... CALCULATE THE MIXTURE DESIGN VELOCITY FROM GIVEN ANNUAL TRANSPORT
C.... RATE
C
C
      WRITE (6,100)
100 FORMAT (////71X,'PUMPING',4X,'COMMUNITION',4X,'TOTAL'/
*          5X,'CV (%)',6X,'N',9X,'K',8X,'DIAMETER',7X,'FLOW',4X,
*          'DISTANCE',5X,'ENERGY',7X,'ENERGY',7X,'ENERGY'/110('-'//))
C
      DO 6 I=1,ND
      NFLOW = 1
      RHOM = RHOL * ( 1 + CV*( SS - 1))
C
C... CONVERT VM TO CM/SEC
C
      VM = 4*W*1.E+3/(CV*RHOM*GI**2*365*24*3600*PI*D(I)**2)
      QM = VM * PI * D(I) * D(I)/4*GI**2
C
C.... CHECK IF THE FLOW IS TURBULENT, FIRST CALCULATE THE TRANSITION
C REYNOLDS NUMBER.
C
      REPL2 = 8*D(I)**PN*GI**PN*VM**(2-PN)*RHOM/PK
* (PN/(2+6*PN))**PN
      REPLC = 6464 * PN /(((1+3*PN)**2*(1/(2+PN))**((2+PN)
*/(1+PN)))
      IF (REPL2.GT.REPLC) CALL ITER(2,D(I),F0,F)
      IF (REPL2.GT.REPLC) GO TO 166
C
C.... CALCULATE FLOW REYNOLDS NUMBER AND FRICTION COEFFICIENT
C
      F = 16/REPL2
C
C
C.... CALCULATE PRESSURE GRADIENT PER UNIT LENGTH
C
C 166 DELP = 2*F*RHOM*VM**2/(D(I)*GI)
166 DELP = 4*VM**PN*PK/((D(I)*GI)**(1+PN))*((2+6*PN)/PN)**PN
C
C.... COMPUTE PRESSURE GRADIENT PER UNIT LENGTH OF A YIELD POWER LAW
C.... MIXTURE
C
      CALL ITER (3,D(I),DELP,PGRAD)
C
C.... COMPUTE PUMPING POWER REQUIRED PER UNIT LENGTH (KW/MILE)
C
      P = PGRAD * QM * 1609 / ( 1000*EFF )
      DO 22 M=1,NDIST
C

```

```

C.. PUMPING ENERGY (KWH/YR)
C
PENER=P*24*365*DIST(M)
C
C... COMMINUTION ENERGY (KWH/YR)
C
CENER=W*19.97*SSAREA**2.03
C
C.. TOTAL ENERGY = PUMPING ENERGY(PENER) + COMMINUTION ENERGY (CENER)
C
TENER=PENER + CENER
C
C... NORMALIZE THE TOTAL ENERGY WITH RESPECT TO THE TOTAL ENERGY
C... COMPUTED FOR INPUT PARTICLE SIZE DISTRIBUTION (AFTER FIT TO
C... ROSIN-RAMMLER)
C
DO 111 NC=1,NCV
IF ( CV.EQ.CVOL(NC) ) GO TO 112
111 CONTINUE
112 ICV = NC
IF (J.EQ.0) RENER(ICV,I,M)=1.0
IF (J.EQ.1) THEN
RENER (ICV,I,M) = TENER
ELSE
ENRAT = TENER / RENER ( ICV,I,M )
ENDIF
C
IF(I.NE.1.OR.M.NE.1) GO TO 44
WRITE (6,10) CV,PN,PK,D(I),FLOW(NFLOW),DIST(M),PENER,CENER,TENER,
*ENRAT
GO TO 22
44 IF(M.NE.1) THEN
WRITE(6,12)DIST(M),PENER,CENER,TENER,ENRAT
GO TO 22
ELSE
WRITE(6,11) D(I),FLOW(NFLOW),DIST(M),PENER,CENER,TENER,ENRAT
ENDIF
22 CONTINUE
6 CONTINUE
10 FORMAT (/2X,F9.3,F10.3,2X,F8.3,F10.2,4X,A10,F6.2,4X,3(F14.2,3X),
*F6.2/)
11 FORMAT (32X,F10.2,4X,A10,F6.2,4X,3(F14.2,3X),F6.2/)
12 FORMAT (55X,F6.2,8X,3(F12.2,3X),F6.2/)
RETURN
END

```



```

C -----
C                   SUBROUTINE ITER (NITER,D,F0,F)
C -----
C
C... THIS SUBROUTINE COMPUTES THE TURBULENT FRICTION FACTOR AND
C... PRESSURE GRADIENT OF A YIELD POWER LAW MIXTURE USING
C...     *** NEWTON RAPHSON *** ITERATION TECHNIQUE
C
C     REAL N,NO
C     COMMON/CC/C,SSAREA,AREA,RHOS,RHOL,DS,ETA,VM,WMEAND,KK,N,PN,PK,NS
C     COMMON/DD/BC,ETAU,TAUY,CV,CM,SF,DP,GC,GA,GI,ETA0,EINF,MU
C
C     TOLER=1.E-3
C
C.... SET UP THE ITERATION LOOP
C
C     F = F0
C     DO 2 ITERA=1,50
C     GO TO (11,22,33), NITER
C
C... SET UP G0 AND G1 FOR PARAMETER N
C
C     11 G0 =PARAN ( F )
C     F = F + TOLER
C     G1 = PARAN ( F )
C     GO TO 5
C
C... SET UP G0 AND G1 FOR FRICTION FACTOR EQUATION
C
C     22 G0 = FRICN ( D,F )
C     F = F + TOLER
C     G1 = FRICN ( D,F )
C     GO TO 5
C
C... SET UP G0 AND G1 FOR PRESSURE GRADIENT EQUATION
C
C     33 G0 = PGRAD ( D,F )
C     ERR = (G0-F)/F
C     IF(ERR.LE.1.E-06) RETURN
C     F=(G0+F)/2.
C     GO TO 2
C
C
C     5 F = F - TOLER
C     DG = (G1 - G0)/TOLER
C     IF ( DG.EQ.0) RETURN
C     DELTAF = -G0/DG
C     ERROR = ABS ( DELTAF )
C     IF (ABS(F).GT.1.E-3) ERROR=ERROR/ABS(F)
C     WRITE(6,66)ERROR,F
C     66 FORMAT(2F12.4)

```

```

        IF(ERROR.LT.TOLER) RETURN
        F = F + DELTAF
    2 CONTINUE
C
C... NORMAL EXIT FROM ITERATION LOOP INDICATES FAILURE TO CONVERGE.
C
        WRITE( 6,88) F0,ITERA
    88 FORMAT ( ////20X,E12.4,I5,'-- NO CONVERGENCE --')
        RETURN
        END
C
C -----
C                               SUBROUTINE AREAS
C -----
C
C.. THIS SUBROUTINE COMPUTES THE TOTAL SURFACE AREA AND THE SURFACE MEAN
C.. DIAMETER OF ANY GIVEN PARTICLE SIZE DISTRIBUTION
C
        COMMON/AA/DELM(15),NSIZE,NDR,TPHIM,NTYPE,IPSD,ND,NFLOW,NCV,NSIZ
        COMMON/BB/PSIZE(50),D(50),PMA(50),FRAC(50),PSIZ(50),FRACT(50)
        COMMON/CC/C,SSAREA,AREA,RHOS,RHOL,DS,ETA,VM,WMEAND,KK,N,PN,PK,NS
        COMMON/FF/PD(20),DIST(20),CVOL(20),NO,F0,W,EFF,CORR,NPS,J,IDM,IM
C
        PI=3.1415927
        SAREA=0.
        VOLUME=0.
        AREA=0.
        IF (NPS .EQ. 0 ) THEN
            NSIZE = NS
        ELSE
            ENDIF
C
        DO 2 I=1,NSIZE
            SAREA=FRAC(I)/PSIZE(I)+SAREA
            VOLUME=FRAC(I)/PSIZE(I)**3+VOLUME
            AREA=FRAC(I)*(0.01*PSIZE(I))**2+AREA
    2 CONTINUE
        AREA=SQRT(AREA)
C
C... SURFACE AREA OF THE PARTICLE SIZE DISTRIBUTION
C
        SSAREA = 6*SAREA
C
C... SURFACE MEAN DIAMETER
C
        DS = SQRT(SAREA/VOLUME)
        RETURN
        END

```

C -----  
FUNCTION PGRAD(D,F)  
C -----

C  
C.. PRESSURE GRADIENT RELATIONSHIP FOR A YIELD-PSEUDOPLASTIC  
C.. FLUID  
C

REAL N,LHS  
COMMON/CC/C,SSAREA,AREA,RHOS,RHOL,DS,ETA,VM,WMEAND,KK,N,PN,PK,NS  
COMMON/DD/BC,ETAU,TAUY,CV,CM,SF,DP,GC,GA,GI,ETA0,EINF,MU

C  
C RHS1=(1./PK)\*\*(1/PN)/(D\*GI/4.)\*3\*(ABS(D\*GI\*F/4.-TAUY))\*\*((1.+PN)  
C #/PN)  
C RHS2=(ABS(D\*GI\*F/4.-TAUY))\*\*2/((1.+3.\*PN)/PN)+2\*TAUY\*  
C #(D\*GI\*F/4.-TAUY)/((1.+2.\*PN)/PN)+TAUY\*TAUY/((1.+PN)/PN)  
C LHS=D\*GI/(2.\*VM)  
C RHS=(RHS1\*RHS2\*LHS)\*\*(1./3.)  
C RHS1=4\*VM\*\*PN\*PK\*((2+6\*PN)/PN)\*\*PN/(D\*GI)\*\*(1+PN)  
C RHS2=(ABS(D\*GI/4.\*F-TAUY))\*\*((1+PN)/PN)  
C RHS3=(D\*GI/4.\*F)\*\*((3\*PN+1)/PN)  
C RHS4=(ABS(D\*GI/4.\*F-TAUY))\*\*2+((1+3\*PN)/(1+2\*PN))\*(D\*GI/4.\*F-  
C #TAUY)\*2\*TAUY+TAUY\*\*2\*(1+3\*PN)/(1+PN)  
C ALPHA=RHS2/RHS3\*RHS4  
C PGRAD=RHS1/ALPHA\*\*PN  
C RETURN  
C END

C  
C -----  
FUNCTION FRICN(D,F)  
C -----

C  
C.. FRICTION FACTOR EQUATION FOR A POWER LAW FLUID  
C

REAL N  
COMMON/AA/DELM(15),NSIZE,NDR,TPHIM,NTYPE,IPSD,ND,NFLOW,NCV,NSIZ  
COMMON/CC/C,SSAREA,AREA,RHOS,RHOL,DS,ETA,VM,WMEAND,KK,N,PN,PK,NS  
COMMON/DD/BC,ETAU,TAUY,CV,CM,SF,DP,GC,GA,GI,ETA0,EINF,MU

C  
C NFLOW = 2  
C... INPUT REYNOLDS NUMBER, INITIAL ESTIMATE OF F  
C SS=RHOS/RHOL  
C RHOM = RHOL\*(1+CV\*(SS-1))  
C REPL1 = D\*\*PN\*GI\*\*PN\*VM\*\*((2-PN)\*RHOM/PK  
C RE = REPL1/(8\*\*((PN-1))  
C IF (F.LT.0.0001) F = 0.001  
C FRICN = 1./SQRT(F) - 2.69/PN + 2.95 - 4.53/PN\*ALOG10(RE\*  
C #(SQRT(F))\*\*((2-PN))-0.68/PN\*(5\*PN-8)  
C RETURN  
C END

C

```

C
C
C -----
C                               FUNCTION PARAN(F)
C -----
C
C.. EQUATION TO CALCULATE THE PARAMETER N USED IN VISCOSITY EQUATIONS
C
COMMON/CC/C, SSAREA, AREA, RHOS, RHOL, DS, ETA, VM, WMEAND, KK, N, PN, PK, NS
COMMON/DD/BC, ETAU, TAUY, CV, CM, SF, DP, GC, GA, GI, ETA0, EINF, MU
C
PARAN = ETA0**((1./F) - ETA*CV*CM/(F*(CM - CV))) - 1
C
RETURN
END
C
C -----
C                               SUBROUTINE REGRE (IPT,K,NS,MD,CDET,DM)
C -----
C
C
C.. THIS SUBROUTINE IS FOR REGRESSION ANALYSIS BY USING IMSL ROUTINES
C.. IMSL ROUTINES USED ARE --- RLFOTH AND RLDOPM ---
C
WARNING : X ARRAY HAS VALUES CHANGED WITH IMSL
C P(2N),C(MD+3),S(MD+3),A(MD),B(MD),C(MD+3),ID(MD),A(MD),
C B(MD),T(4*(MD+1))
C
COMMON/MRI/GEOM(4,64)
INTEGER NS,MD,ID,IER
REAL XX(64),X(64),Y(64),RSQ,C(13),S(13),A(10),B(10)
DOUBLE PRECISION P(128),T(44)
RSQ=100.
C
C MD = ORDER OF POLYNOMIAL
C NS = NO. OF DATA PTS.
C CALCULATING MDTH ORDER POLY. AS F(H)
C
DO 2 I = 1,NS
C
X(I) = GEOM(1,I)
XX(I) = GEOM(1,I)
Y(I) = GEOM(K,I)
C
2 CONTINUE
C
CALL RLFOTH (X,Y,NS,RSQ,MD,ID,P,C,S,A,B,IER)
C
CALL RLDOPM (C,ID,A,B,T)
DM = C(2)

```

```

      M=MD+1
C
C CALCULATION OF REGRESSION SUM OF SQUARES (SUMSSR) AND CORRECTED TOTAL
C.... SUM OF SQUARES (SUMSY)
C
      SUMY=0.
      DO 4 I=1,NS
        SUMY=SUMY+Y(I)
4 CONTINUE
C
      YMEAN=SUMY/NS
      SUMSSR=0.
      SUM1=0.
      SUM2=0.
      DO 3 I=1,NS
        YI=C(I)
        DO 5 J=2,M
          YI=C(J)*XX(I)**(J-1)+YI
5 CONTINUE
C
      SUMSSR=(YI-YMEAN)**2+SUMSSR
      SUM1=(YI-YMEAN)**2+SUM1
      SUM2=(Y(I)-YI)**2+SUM2
C
3 CONTINUE
      SUMSY=SUM1+SUM2
C
C.. COEFFICIENT OF DETERMINATION
C
      CDET= SUMSSR/SUMSY
      RETURN
      END
C
-----
                        SUBROUTINE OUTPUT (IOUT)
-----
C
C
C
      REAL N,MU,KK
      COMMON/AA/DELM(15),NSIZE,NDR,TPHIM,NTYPE,IPSD,ND,NFLOW,NCV,NSIZ
      COMMON/BB/PSIZE(50),DIAMR(50),PMAX(50),V(50),PSIZ(50),FRACT(50)
      COMMON/CC/C,SSAREA,AREA,RHOS,RHOL,DS,ETA,VM,WMEAND,KK,N,PN,PK,NS
      COMMON/DD/BC,ETAU,TAUY,CV,CM,SF,DP,GC,GA,GI,ETA0,EINF,MU
      COMMON/EE/G1,NDIST,NG,DG,G(50),TAU(50)
      COMMON/FF/D(20),DIST(20),CVOL(20),NO,F0,W,EFF,CORR,NPS,J,IDM,IM
C
      IF(IOUT.EQ.1) GO TO 9
      IOUT = 1
C
      WRITE ( 6 , 1 ) NTYPE,NSIZE,NDR,NG,ND

```

```

WRITE ( 6 , 2 ) ( PSIZE(I),V(I),I=1,NSIZE)
WRITE ( 6 , 3 ) ( DIAMR(I),PMAX(I),I=1,NDR)
WRITE ( 6 , 4 ) C, KK, SF, MU, RHOS, RHOL, N, ETA, DP, DS

```

C

```

9 CONTINUE
DO 8 I=1,NG
IF ( I - 1 ) 7,99,7
99 WRITE ( 6 ; 6 ) CM, CV, PN, PK, ETA0, EINF, TAUY, BC, G(I), TAU(I), N
GO TO 8
7 WRITE ( 6 , 11 ) G(I), TAU(I), DS
8 CONTINUE

```

C

```

1 FORMAT (//1X, 'NTYPE', I5, 2X, 'NSIZE', I5, 2X, 'NDR', I5, 2X, 'NG', I5, 2X,
# 'ND', I5)
2 FORMAT (//7X, 'PSIZE', 11X, 'FRACTION'//(F12.4, 5X, F12.4))
3 FORMAT (//7X, 'DIAMR', 13X, 'PMAX'//(F12.4, 5X, F12.4))
4 FORMAT (//5X, 'C', 7X, 'KK', 8X, 'SF', 7X, 'MU', 7X, 'RHOS', 8X, 'RHOL',
# 9X, 'N', 8X, '[ETA]', 7X, 'DP', 9X, 'DS', 8X, 'SAREA'//4F9.4,
# 2(3X, F9.4), 5(3X, F8.3))
6 FORMAT (//5X, 'CM', 8X, 'CV', 7X, 'N', 8X, 'K', 6X, 'ETA0', 5X, 'EINF',
# 6X, 'TAUY', 6X, 'B', 9X, 'G', 7X, 'TAU'//
# 3(4X, F5.3), 6(3X, F6.2), 3X, F7.2, F5.3)
11 FORMAT (74X, 3(F7.2, 3X))
RETURN
END

```

C

C

-----  
SUBROUTINE INPUT(\*)  
-----

C

C

```

REAL MU, KK, N, NO
COMMON/AA/DELM(15), NSIZE, NDR, TPHIM, NTYPE, IPSD, ND, NFLOW, NCV, NSIZ
COMMON/BB/PSIZE(50), DIAMR(50), PMAX(50), V(50), PSIZ(50), FRACT(50)
COMMON/CC/C, SSAREA, AREA, RHOS, RHOL, DS, ETA, VM, WMEAND, KK, N, PN, PK, NS
COMMON/DD/BC, ETAU, TAUY, CV, CM, SF, DP, GC, GA, GI, ETA0, EINF, MU
COMMON/EE/G1, NDIST, NG, DG, G(50), TAU(50)
COMMON/FF/D(20), DIST(20), CVOL(20), NO, F0, W, EFF, CORR, NPS, J, IDM, IM

```

C

```

READ(5,1,END=99) NTYPE, NSIZE, NDR, NG, ND, NCV, IDM, NDIST
IF(NTYPE-1) 6,4,6
6 CONTINUE
READ(5,3) (PSIZE(I),V(I),I=1,NSIZE)
4 READ(5,3) (DIAMR(I),PMAX(I),I=1,NDR)
READ(5,2)C, KK, CM, SF, DP, RHOS, RHOL, MU, GC, GA, GI, G1, DG, EINF, ETA0
READ(5,2) NO, F0, W, EFF, CORR, (D(I), I=1, ND)
READ(5,2) (CVOL(I), I=1, NCV)
IF (IDM.EQ.0) GO TO 5
READ(5,2) (DELM(I), I=1, IDM)
5 READ(5,2) (DIST(I), I=1, NDIST)

```

C

```
NPS = 0
IPSD=0
RETURN
1 FORMAT(8I5)
2 FORMAT(7F10.0)
3 FORMAT(2F10.0)
99 RETURN 1
END
```

**APPENDIX B**

**NUMERICAL RESULTS OBTAINED FOR THE**

**ANALYSES**



NICKEL - SODIUM SUSPENSION RESULTS

INPUT DATA :

DP = 10.50 DS = 5.045 SF = 0.1180 MU = 0.00036 SAREA = 0.709

----- ETA0 = 1.06231 EINF = 0.39969 -----

----- [ETA] = 8.680 N = 2.400 -----

----- CM = 0.317 C/CM = 0.959 C = 0.776 K = 0.0494 -----

CV = 0.304  
TAUY = 0.700  
B = 0.150

CV = 0.296  
TAUY = 0.400  
B = 0.067

CV = 0.286  
TAUY = 0.244  
B = 0.033

G TAU

G TAU

G TAU

2.000	0.757	2.000	0.419	2.000	0.252
4.000	0.802	4.000	0.435	4.000	0.259
6.000	0.842	6.000	0.450	6.000	0.265
8.000	0.877	8.000	0.464	8.000	0.272
10.000	0.910	10.000	0.477	10.000	0.277
15.000	0.986	15.000	0.507	15.000	0.291
20.000	1.058	20.000	0.535	20.000	0.244
25.000	1.126	25.000	0.562	25.000	0.317
30.000	1.192	30.000	0.588	30.000	0.329
35.000	1.258	35.000	0.614	35.000	0.340
40.000	1.323	40.000	0.639	40.000	0.352
45.000	1.387	45.000	0.663	45.000	0.363
50.000	1.451	50.000	0.688	50.000	0.374
55.000	1.514	55.000	0.712	55.000	0.386
60.000	1.578	60.000	0.737	60.000	0.397
65.000	1.641	65.000	0.761	65.000	0.408
70.000	1.704	70.000	0.785	70.000	0.419
75.000	1.767	75.000	0.809	75.000	0.430
80.000	1.830	80.000	0.833	80.000	0.440
85.000	1.893	85.000	0.857	85.000	0.451
90.000	1.955	90.000	0.881	90.000	0.462
95.000	2.018	95.000	0.904	95.000	0.473
100.000	2.080	100.000	0.928	100.000	0.484

NICKEL - XYLENE SUSPENSION RESULTS

INPUT DATA :

-----

DP = 10.50 DS = 5.045 SF = 0.1180 MU = 0.00041 SAREA = 0.709

----- ETA0 = 0.39286 EINF = 0.11985 -----

----- [ETA] = 5.901 N = 2.673 -----

----- CM = 0.374 C/CM = 0.936 C = 0.952 K = 0.0486 -----

-----  
 CV = 0.350 CV = 0.340  
 TAU Y = 0.715 TAU Y = 0.462  
 B = 0.125 B = 0.067  
 G TAU G TAU  
 -----

2.000	0.738	2.000	0.473
4.000	0.757	4.000	0.481
6.000	0.774	6.000	0.489
8.000	0.790	8.000	0.496
10.000	0.804	10.000	0.503
15.000	0.835	15.000	0.518
20.000	0.862	20.000	0.532
25.000	0.888	25.000	0.545
30.000	0.911	30.000	0.557
35.000	0.934	35.000	0.569
40.000	0.956	40.000	0.580
45.000	0.978	45.000	0.591
50.000	0.999	50.000	0.602
55.000	1.019	55.000	0.613
60.000	1.040	60.000	0.623
65.000	1.060	65.000	0.633
70.000	1.080	70.000	0.643
75.000	1.100	75.000	0.653
80.000	1.119	80.000	0.663
85.000	1.139	85.000	0.673
90.000	1.158	90.000	0.683
95.000	1.178	95.000	0.693
100.000	1.197	100.000	0.703
110.000	1.236	110.000	0.722

ALUMINA - XYLENE SUSPENSION RESULTS

INPUT DATA :

-----

DP = 12.00 DS = 3.465 SF = 0.1640 MU = 0.00041 SAREA = 0.742

----- ETA0 = 1.45613 EINF = 0.45533 -----

----- [ETA] = 5.524 N = 2.478 -----

----- CM = 0.468 C/CM = 0.962 C = 4.067 K = 0.0341 -----

-----

CV = 0.450	CV = 0.440	CV = 0.420
TAUY = 2.078	TAUY = 1.249	TAUY = 0.633
B = 0.480	B = 0.229	B = 0.087

G	TAU	G	TAU	G	TAU
---	-----	---	-----	---	-----

-----

2.000	2.161	2.000	1.277	2.000	0.641
4.000	2.233	4.000	1.304	4.000	0.649
6.000	2.297	6.000	1.328	6.000	0.656
8.000	2.355	8.000	1.351	8.000	0.663
10.000	2.408	10.000	1.373	10.000	0.669
15.000	2.526	15.000	1.422	15.000	0.685
20.000	2.631	20.000	1.467	20.000	0.700
25.000	2.728	25.000	1.509	25.000	0.714
30.000	2.819	30.000	1.548	30.000	0.727
35.000	2.906	35.000	1.585	35.000	0.740
40.000	2.990	40.000	1.622	40.000	0.753
45.000	3.071	45.000	1.657	45.000	0.765
50.000	3.151	50.000	1.691	50.000	0.777
55.000	3.230	55.000	1.725	55.000	0.788
60.000	3.308	60.000	1.758	60.000	0.800
65.000	3.385	65.000	1.791	65.000	0.811
70.000	3.461	70.000	1.823	70.000	0.822
80.000	3.611	80.000	1.886	80.000	0.844
90.000	3.760	90.000	1.949	90.000	0.866
100.000	3.908	100.000	2.011	100.000	0.887
120.000	4.200	120.000	2.133	120.000	0.929
140.000	4.490	140.000	2.253	140.000	0.970
160.000	4.778	160.000	2.373	160.000	1.011

ALUMINA - XYLENE SUSPENSION RESULTS

INPUT DATA :

-----

DP = 12.00 DS = 3.465 SF = 0.1640 MU = 0.64078 SAREA = 0.742

----- ETA0 = 256.05780 EINF = 118.52630 -----

----- [ETA] = 4.582 N = 2.485 -----

----- CM = 0.550 C/CM = 0.909 C = 16.370 K = 0.0003 -----

-----

CV = 0.500	CV = 0.480
TAUY = 3.499	TAUY = 2.211
B = 2.808	B = 1.409
G	TAU
G	TAU

-----

0.100	4.238	0.100	2.540
0.200	4.890	0.200	2.843
0.300	5.483	0.300	3.127
0.400	6.034	0.400	3.396
0.600	7.048	0.600	3.900
0.800	7.985	0.800	4.373
1.000	8.874	1.000	4.825
1.200	9.730	1.200	5.261
1.400	10.563	1.400	5.686
1.600	11.379	1.600	6.102
1.800	12.182	1.800	6.512
2.000	12.974	2.000	6.916
2.200	13.759	2.200	7.315
2.400	14.538	2.400	7.711
2.600	15.311	2.600	8.104
2.800	16.080	2.800	8.495
3.000	16.845	3.000	8.883
3.200	17.608	3.200	9.270
3.400	18.367	3.400	9.655
3.600	19.125	3.600	10.039
3.800	19.881	3.800	10.422
4.000	20.635	4.000	10.803
5.000	12.699	5.500	13.642

COAL-OIL SUSPENSION RESULTS

INPUT DATA :

-----					
DP = 180.0	DS = 64.51	SF = 0.337	MU = 0.0326	SAREA = 0.043	
-----	ETA0 = 0.85810	EINF = 0.35298		-----	
-----	[ETA] = 3.737	N = 5.110		-----	
-----	CM = 0.711	C/CM = 0.633	C = 1.6000	K = 1.3170	-----
-----					
CV = 0.450	CV = 0.500		CV = 0.550		
TAUY = 3.391	TAUY = 5.753		TAUY = 10.035		
B =	B = 64.590		B = 135.278		
G	TAU	G	TAU	G	TAU
-----					
2.000	1.686	2.000	3.828	2.000	11.339
4.000	3.314	4.000	7.439	4.000	21.472
6.000	4.890	6.000	10.857	6.000	30.619
8.000	6.418	8.000	14.104	8.000	38.947
10.000	7.901	10.000	17.198	10.000	46.592
15.000	11.438	15.000	24.367	15.000	63.348
20.000	14.765	20.000	30.871	20.000	77.602
25.000	17.917	25.000	36.852	25.000	90.075
30.000	20.921	30.000	42.414	30.000	101.236
35.000	23.801	35.000	47.634	35.000	111.403
40.000	26.574	40.000	52.573	40.000	120.798
50.000	31.855	50.000	61.781	50.000	137.876
60.000	36.854	60.000	70.309	60.000	153.325
70.000	41.635	70.000	78.332	70.000	167.651
80.000	46.242	80.000	85.972	80.000	181.168
90.000	50.709	90.000	93.312	90.000	194.083
100.000	55.063	100.000	100.415	100.000	206.539
150.000	75.676	150.000	133.640	150.000	264.656
200.000	95.168	200.000	164.758	200.000	319.195

RESULTS OF THE ANALYSIS OF PSD VARIATION FOR COAL-GLYCERIN SUSPENSION

PARTICLE SIZE DISTRIBUTION THAT FITS ROSIN-RAMMLER EQN. DM= 1.36

CORRELATION COEFFICIENT R =0.972  
SURFACE AREA=0.858

PARTICLE SIZE (MICRONS)	PERCENT ( % )
52.0000	0.1000
47.0000	0.1880
42.0000	0.2980
37.0000	0.4360
32.0000	0.6090
27.0000	0.8300
22.0000	1.1100
17.0000	1.4500
14.0000	1.8500
11.0000	2.3200
9.0000	2.8700
7.0000	3.5000
5.0000	4.2200
3.0000	5.0400
2.3000	6.0000

N TYPE    0    N SIZE    10    NDR    15    NG    50    ND    6

PSIZE	FRACTION
52.0000	0.0300
47.0000	0.0850
42.0000	0.1250
37.0000	0.1300
32.0000	0.1310
27.0000	0.1130
22.0000	0.0880
17.0000	0.1100
14.0000	0.0880
11.0000	0.1000

DIAMR	P MAX
1.0000	0.6390
2.0000	0.6590
3.0000	0.6900
4.0000	0.7230
5.0000	0.7580
6.0000	0.7910
7.0000	0.8100
8.0000	0.8200
9.0000	0.8300
10.0000	0.8330
12.0000	0.8440
14.0000	0.8470
16.0000	0.8500
18.0000	0.8500
20.0000	0.8500
800.0000	0.8500

C	KK	SF	MU	RHOS	RHOL	N	[ETA]	DP	DS	SSAREA
86.0000	0.0016	0.3370	0.4800	1480.0000	1248.0000	3.000	3.696	13.000	3.414	0.8576

CM	CV	PN	PK	ETA0	EINF	TAUY	B					
0.520	0.460	0.816	70.96	99.06	33.58	35.85	136.09					
SHEAR RATE-G =		1.00	2.00	3.00	4.00	5.00	6.00	7.00	8.00	9.00	10.00	
SHEAR STRESS-TAU =		113.64	169.75	216.99	259.73	299.89	338.42	375.85	412.53	448.64	484.33	
SHEAR RATE-G =		11.00	12.00	13.00	14.00	15.00	16.00	17.00	18.00	19.00	20.00	
SHEAR STRESS-TAU =		519.71	554.82	589.74	624.48	659.09	693.59	727.99	762.31	796.56	830.75	
SHEAR RATE-G =		21.00	22.00	23.00	24.00	25.00	26.00	27.00	28.00	29.00	30.00	
SHEAR STRESS-TAU =		864.89	898.98	933.03	967.04	1001.02	1034.97	1068.90	1102.80	1136.69	1170.55	
SHEAR RATE-G =		31.00	32.00	33.00	34.00	35.00	36.00	37.00	38.00	39.00	40.00	
SHEAR STRESS-TAU =		1204.40	1238.23	1272.05	1305.85	1339.65	1373.43	1407.20	1440.96	1474.71	1508.46	
SHEAR RATE-G =		41.00	42.00	43.00	44.00	45.00	46.00	47.00	48.00	49.00	50.00	
SHEAR STRESS-TAU =		1542.19	1575.92	1609.65	1643.36	1677.08	1710.78	1744.48	1778.18	1811.87	1845.56	

CV (%)	PN	PK	DIAMETER	FLOW	DISTANCE	PUMPING ENERGY	COMMUNITION ENERGY	TOTAL ENERGY
0.460	0.816	70.957	2.00	LAMINAR	0.10	19519328.00	2924317.00	22443632.00
					0.30	58558016.00	2924317.00	61482320.00
					0.50	97596688.00	2924317.00	100520992.00
					0.70	136635360.00	2924317.00	139559664.00
					1.00	195193392.00	2924317.00	198117696.00
			2.50	LAMINAR	0.10	9058389.00	2924317.00	11982706.00
					0.30	27175152.00	2924317.00	30099456.00
					0.50	45291936.00	2924317.00	48216240.00
					0.70	63408704.00	2924317.00	66333008.00
					1.00	90583872.00	2924317.00	93508176.00
			3.00	LAMINAR	0.10	4842585.00	2924317.00	7766902.00
					0.30	14527752.00	2924317.00	17452064.00
					0.50	24212912.00	2924317.00	27137216.00
					0.70	33898080.00	2924317.00	36822384.00
					1.00	48425840.00	2924317.00	51350144.00
			3.50	LAMINAR	0.10	2855053.00	2924317.00	5779370.00
					0.30	8565158.00	2924317.00	11489475.00
					0.50	14275264.00	2924317.00	17199568.00
					0.70	19985360.00	2924317.00	22909664.00
					1.00	28550528.00	2924317.00	31474832.00
			4.00	LAMINAR	0.10	1808667.00	2924317.00	4732984.00
					0.30	5426001.00	2924317.00	8350318.00
					0.50	9043336.00	2924317.00	11967653.00
					0.70	12660670.00	2924317.00	15584987.00
					1.00	18086672.00	2924317.00	21010976.00
			5.00	LAMINAR	0.10	846636.25	2924317.00	3770953.00
					0.30	2539908.00	2924317.00	5464225.00
					0.50	4233180.00	2924317.00	7157497.00
					0.70	5926452.00	2924317.00	8850769.00
					1.00	8466361.00	2924317.00	11390678.00

CM	CV	PN	PK	ETA0	EINF	TAUY	B					
0.520	0.430	0.857	27.40	32.12	15.00	19.53	58.51					
SHEAR RATE-G =		1.00	2.00	3.00	4.00	5.00	6.00	7.00	8.00	9.00	10.00	
SHEAR STRESS-TAU =		47.77	71.13	91.88	111.07	129.28	146.80	163.83	180.51	196.92	213.12	
SHEAR RATE-G =		11.00	12.00	13.00	14.00	15.00	16.00	17.00	18.00	19.00	20.00	
SHEAR STRESS-TAU =		229.15	245.05	260.84	276.54	292.16	307.72	323.22	338.67	354.09	369.47	
SHEAR RATE-G =		21.00	22.00	23.00	24.00	25.00	26.00	27.00	28.00	29.00	30.00	
SHEAR STRESS-TAU =		384.82	400.14	415.43	430.71	445.96	461.20	476.42	491.63	506.82	522.01	
SHEAR RATE-G =		31.00	32.00	33.00	34.00	35.00	36.00	37.00	38.00	39.00	40.00	
SHEAR STRESS-TAU =		537.18	552.34	567.50	582.64	597.78	612.91	628.03	643.15	658.26	673.37	
SHEAR RATE-G =		41.00	42.00	43.00	44.00	45.00	46.00	47.00	48.00	49.00	50.00	
SHEAR STRESS-TAU =		688.47	703.57	718.66	733.75	748.84	763.92	779.00	794.07	809.14	824.21	

CV (%)	PN	PK	DIAMETER	FLOW	DISTANCE	PUMPING ENERGY	COMMUNION ENERGY	TOTAL ENERGY
0.430	0.857	27.404	2.00	LAMINAR	0.10	11178781.00	2924317.00	14103098.00
					0.30	33536336.00	2924317.00	36460640.00
					0.50	55893888.00	2924317.00	58818192.00
					0.70	78251440.00	2924317.00	81175744.00
					1.00	111787792.00	2924317.00	114712096.00
			2.50	LAMINAR	0.10	5050758.00	2924317.00	7975075.00
					0.30	15152271.00	2924317.00	18076576.00
					0.50	25253776.00	2924317.00	28178080.00
					0.70	35355296.00	2924317.00	38279600.00
					1.00	50507568.00	2924317.00	53431872.00
			3.00	LAMINAR	0.10	2642131.00	2924317.00	5566448.00
					0.30	7926393.00	2924317.00	10850710.00
					0.50	13210656.00	2924317.00	16134973.00
					0.70	18494912.00	2924317.00	21419216.00
					1.00	26421312.00	2924317.00	29345616.00
			3.50	LAMINAR	0.10	1529704.00	2924317.00	4454021.00
					0.30	4589113.00	2924317.00	7513430.00
					0.50	7648521.00	2924317.00	10572838.00
					0.70	10707929.00	2924317.00	13632246.00
					1.00	15297043.00	2924317.00	18221360.00
			4.00	LAMINAR	0.10	954191.69	2924317.00	3878508.00
					0.30	2862574.00	2924317.00	5786891.00
					0.50	4770957.00	2924317.00	7695274.00
					0.70	6679340.00	2924317.00	9603657.00
					1.00	9541915.00	2924317.00	12466232.00
			5.00	LAMINAR	0.10	435631.00	2924317.00	3359948.00
					0.30	1306892.00	2924317.00	4231209.00
					0.50	2178154.00	2924317.00	5102471.00
					0.70	3049416.00	2924317.00	5973733.00
					1.00	4356309.00	2924317.00	7280626.00



CM	CV	PN	PK	ETA0	EINF	TAUY	B					
0.520	0.384	0.905	10.02	10.63	6.62	9.20	21.20					
SHEAR RATE-G =		1.00	2.00	3.00	4.00	5.00	6.00	7.00	8.00	9.00	10.00	
SHEAR STRESS-TAU =		19.20	28.26	36.74	44.81	52.60	60.18	67.61	74.91	82.11	89.24	
SHEAR RATE-G =		11.00	12.00	13.00	14.00	15.00	16.00	17.00	18.00	19.00	20.00	
SHEAR STRESS-TAU =		96.31	103.32	110.30	117.23	124.13	131.01	137.86	144.69	151.51	158.31	
SHEAR RATE-G =		21.00	22.00	23.00	24.00	25.00	26.00	27.00	28.00	29.00	30.00	
SHEAR STRESS-TAU =		165.09	171.86	178.62	185.38	192.12	198.85	205.58	212.30	219.02	225.72	
SHEAR RATE-G =		31.00	32.00	33.00	34.00	35.00	36.00	37.00	38.00	39.00	40.00	
SHEAR STRESS-TAU =		232.43	239.13	245.82	252.51	259.20	265.88	272.56	279.24	285.92	292.59	
SHEAR RATE-G =		41.00	42.00	43.00	44.00	45.00	46.00	47.00	48.00	49.00	50.00	
SHEAR STRESS-TAU =		299.26	305.93	312.59	319.26	325.92	332.58	339.23	345.89	352.55	359.20	

CV (%)	PN	PK	DIAMETER	FLOW	DISTANCE	PUMPING ENERGY	COMBUSTION ENERGY	TOTAL ENERGY
0.384	0.905	10.018	2.00	LAMINAR	0.10	7030812.00	2924317.00	9955129.00
					0.30	21092432.00	2924317.00	24016736.00
					0.50	35154048.00	2924317.00	38078352.00
					0.70	49215664.00	2924317.00	52139968.00
					1.00	70308112.00	2924317.00	73232416.00
			2.50	LAMINAR	0.10	30755775.00	2924317.00	5999892.00
					0.30	9226723.00	2924317.00	12151040.00
					0.50	15377872.00	2924317.00	18302176.00
					0.70	21529008.00	2924317.00	24453312.00
					1.00	30755744.00	2924317.00	33680048.00
			3.00	LAMINAR	0.10	1566882.00	2924317.00	4491199.00
					0.30	4700647.00	2924317.00	7624964.00
					0.50	7834413.00	2924317.00	10758730.00
					0.70	10968178.00	2924317.00	13892495.00
					1.00	15668826.00	2924317.00	18593136.00
			3.50	LAMINAR	0.10	687123.00	2924317.00	3811440.00
					0.30	2661368.00	2924317.00	5565685.00
					0.50	4435614.00	2924317.00	7329931.00
					0.70	6209859.00	2924317.00	9134176.00
					1.00	8871228.00	2924317.00	11795545.00
			4.00	LAMINAR	0.10	5428782.69	2924317.00	3467099.00
					0.30	16283447.00	2924317.00	4552664.00
					0.50	2713913.00	2924317.00	5638230.00
					0.70	3799478.00	2924317.00	6723795.00
					1.00	5427826.00	2924317.00	83552143.00
			5.00	LAMINAR	0.10	239996.12	2924317.00	3164313.00
					0.30	719988.31	2924317.00	3644305.00
					0.50	1199980.00	2924317.00	4124297.00
					0.70	1679972.00	2924317.00	4604289.00
					1.00	2399961.00	2924317.00	5324278.00

NEW PARTICLE SIZE DISTRIBUTION WITH DM= 1.36

SURFACE AREA=0.875

PARTICLE SIZE (MICRONS)	PERCENT ( % )
80.0000	0.0046
52.0000	0.0292
37.0000	0.0759
27.0000	0.1438
19.0000	0.1502
14.0000	0.1190
9.3000	0.1318
6.5000	0.0876
4.7000	0.0666
3.3000	0.0446
2.3000	0.0324
1.5000	0.0179
1.0000	0.0152
0.5000	0.0099

CM CV PN PK ETA0 EINF TAU Y B  
 0.511 0.460 0.766 116.80 150.06 43.21 14.83 296.61

SHEAR RATE-G =	1.00	2.00	3.00	4.00	5.00	6.00	7.00	8.00	9.00	10.00
SHEAR STRESS-TAU =	136.60	225.46	298.52	362.77	421.60	476.88	529.68	580.71	630.40	679.08
SHEAR RATE-G =	11.00	12.00	13.00	14.00	15.00	16.00	17.00	18.00	19.00	20.00
SHEAR STRESS-TAU =	726.97	774.23	820.97	867.29	913.26	958.93	1004.36	1049.57	1094.60	1139.47
SHEAR RATE-G =	21.00	22.00	23.00	24.00	25.00	26.00	27.00	28.00	29.00	30.00
SHEAR STRESS-TAU =	1184.20	1228.80	1273.30	1317.70	1362.02	1406.26	1450.42	1494.53	1538.58	1582.58
SHEAR RATE-G =	31.00	32.00	33.00	34.00	35.00	36.00	37.00	38.00	39.00	40.00
SHEAR STRESS-TAU =	1626.53	1670.44	1714.31	1758.15	1801.95	1845.72	1889.46	1933.18	1976.87	2020.54
SHEAR RATE-G =	41.00	42.00	43.00	44.00	45.00	46.00	47.00	48.00	49.00	50.00
SHEAR STRESS-TAU =	2064.19	2107.82	2151.43	2195.02	2238.60	2282.16	2325.71	2369.24	2412.76	2456.27

CV (%)	PN	PK	DIAMETER	FLOW	DISTANCE	PUMPING ENERGY	COMMUNITION ENERGY	TOTAL ENERGY						
0.460	0.766	116.804	2.00	LAMINAR	0.10	23165936.00	3043148.00	26209072.00						
					0.30	69497808.00	043148.00	72540944.00						
					0.50	115829680.00	043148.00	118872816.00						
					0.70	162161536.00	043148.00	165204672.00						
					1.00	231659360.00	043148.00	234702496.00						
					2.50	LAMINAR	0.10	11105631.00	043148.00	14148779.00				
							0.30	33316880.00	043148.00	36360016.00				
							0.50	55528144.00	043148.00	58571280.00				
							0.70	77739392.00	043148.00	80782528.00				
							1.00	111056288.00	043148.00	114099424.00				
							3.00	LAMINAR	0.10	6092265.00	043148.00	9135413.00		
									0.30	18276784.00	043148.00	21319920.00		
									0.50	30461312.00	043148.00	33504448.00		
									0.70	42645840.00	043148.00	45688976.00		
									1.00	60922640.00	043148.00	63965776.00		
									3.50	LAMINAR	0.10	3668164.00	043148.00	67113312.00
											0.30	11004490.00	043148.00	14047636.00
											0.50	18340816.00	043148.00	21383952.00
											0.70	25677136.00	043148.00	28720272.00
											1.00	35816380.00	043148.00	39724768.00
4.00	LAMINAR	0.10	2264436.00	043148.00							5407625.00			
		0.30	7023380.00	043148.00							10136576.00			
		0.50	11622364.00	043148.00							14865532.00			
		0.70	16221348.00	043148.00							19594488.00			
		1.00	23644368.00	043148.00							26687904.00			
		5.00	LAMINAR	0.10	1336302.00	043148.00					4179450.00			
				0.30	4008907.00	043148.00					6452055.00			
				0.50	6681512.00	043148.00					8724660.00			
				0.70	9354116.00	043148.00					10997264.00			
				1.00	11363024.00	043148.00					14406172.00			

CM	CV	PN	PK	ETA0	EINF	TAUY	B					
0.511	0.430	0.826	37.59	40.63	17.29	7.64	117.28					
SHEAR RATE-G =		1.00	2.00	3.00	4.00	5.00	6.00	7.00	8.00	9.00	10.00	
SHEAR STRESS-TAU =		44.39	75.61	103.36	128.79	152.60	175.22	196.96	218.02	238.54	258.63	
SHEAR RATE-G =		11.00	12.00	13.00	14.00	15.00	16.00	17.00	18.00	19.00	20.00	
SHEAR STRESS-TAU =		278.38	297.83	317.05	336.06	354.90	373.60	392.17	410.62	428.98	447.26	
SHEAR RATE-G =		21.00	22.00	23.00	24.00	25.00	26.00	27.00	28.00	29.00	30.00	
SHEAR STRESS-TAU =		465.46	483.59	501.67	519.69	537.66	555.58	573.47	591.33	609.14	626.93	
SHEAR RATE-G =		31.00	32.00	33.00	34.00	35.00	36.00	37.00	38.00	39.00	40.00	
SHEAR STRESS-TAU =		644.70	662.43	680.15	697.84	715.51	733.17	750.80	768.42	786.03	803.62	
SHEAR RATE-G =		41.00	42.00	43.00	44.00	45.00	46.00	47.00	48.00	49.00	50.00	
SHEAR STRESS-TAU =		821.20	838.77	856.32	873.87	891.41	908.93	926.45	943.96	961.46	978.95	

CV (%)	PN	PK	DIAMETER	FLOW	DISTANCE	PUMPING ENERGY	COMMUNITION ENERGY	TOTAL ENERGY
0.430	0.826	37.593	2.00	LAMINAR	0.10	12524812.00	3043148.00	15567960.00
					0.30	37574416.00	3043148.00	40617552.00
					0.50	62624048.00	3043148.00	65667184.00
					0.70	87673664.00	3043148.00	90716800.00
					1.00	125248096.00	3043148.00	128291232.00
			2.50	LAMINAR	0.10	57685568.00	3043148.00	8811706.00
					0.30	17305664.00	3043148.00	20348800.00
					0.50	28842784.00	3043148.00	31885920.00
					0.70	40379888.00	3043148.00	43423024.00
					1.00	57685568.00	3043148.00	60728704.00
			3.00	LAMINAR	0.10	3062856.00	3043148.00	6106004.00
					0.30	9188568.00	3043148.00	12231716.00
					0.50	15314280.00	3043148.00	18357424.00
					0.70	21439984.00	3043148.00	24483120.00
					1.00	30628560.00	3043148.00	33671696.00
			3.50	LAMINAR	0.10	1794096.00	3043148.00	4837244.00
					0.30	5382288.00	3043148.00	8425436.00
					0.50	8970480.00	3043148.00	12013628.00
					0.70	12558671.00	3043148.00	15601819.00
					1.00	17940960.00	3043148.00	20984096.00
			4.00	LAMINAR	0.10	1129365.00	3043148.00	4172513.00
					0.30	3388096.00	3043148.00	6431244.00
					0.50	5646827.00	3043148.00	8689975.00
					0.70	7905557.00	3043148.00	10948705.00
					1.00	11293654.00	3043148.00	14336802.00
			5.00	LAMINAR	0.10	521842.06	3043148.00	3564990.00
					0.30	1565526.00	3043148.00	4608674.00
					0.50	2609210.00	3043148.00	5652358.00
					0.70	3652893.00	3043148.00	6696041.00
					1.00	5218420.00	3043148.00	8261568.00

CM	CV	PN	PK	ETA0	EINF	TAUY	B					
0.511	0.384	0.890	11.92	11.99	7.12	3.47	40.25					
SHEAR RATE - G =		1.00	2.00	3.00	4.00	5.00	6.00	7.00	8.00	9.00	10.00	
SHEAR STRESS - TAU =		14.93	25.55	35.55	45.08	54.24	63.12	71.77	80.23	88.54	96.71	
SHEAR RATE - G =		11.00	12.00	13.00	14.00	15.00	16.00	17.00	18.00	19.00	20.00	
SHEAR STRESS - TAU =		104.78	112.75	120.65	128.47	136.24	143.95	151.61	159.23	166.82	174.37	
SHEAR RATE - G =		21.00	22.00	23.00	24.00	25.00	26.00	27.00	28.00	29.00	30.00	
SHEAR STRESS - TAU =		181.90	189.39	196.87	204.32	211.75	219.16	226.56	233.94	241.31	248.66	
SHEAR RATE - G =		31.00	32.00	33.00	34.00	35.00	36.00	37.00	38.00	39.00	40.00	
SHEAR STRESS - TAU =		256.01	263.34	270.66	277.97	285.28	292.57	299.86	307.14	314.41	321.68	
SHEAR RATE - G =		41.00	42.00	43.00	44.00	45.00	46.00	47.00	48.00	49.00	50.00	
SHEAR STRESS - TAU =		328.94	336.20	343.45	350.69	357.93	365.17	372.40	379.63	386.85	394.08	

CV (%)	PN	PK	DIAMETER	FLOW	DISTANCE	PUMPING ENERGY	COMMUNION ENERGY	TOTAL ENERGY
0.384	0.890	11.925	2.00	LAMINAR	0.10	7595798.00	3043148.00	10638946.00
					0.30	22787376.00	3043148.00	25830512.00
					0.50	37978976.00	3043148.00	41022112.00
					0.70	53170576.00	3043148.00	56213712.00
					1.00	75957968.00	3043148.00	79001104.00
		2.50	LAMINAR	0.10	3350506.00	3043148.00	6393654.00	
				0.30	10051517.00	3043148.00	13094665.00	
				0.50	16752528.00	3043148.00	19795666.00	
				0.70	23453539.00	3043148.00	26496667.00	
				1.00	33505056.00	3043148.00	36548172.00	
		3.00	LAMINAR	0.10	1717326.00	3043148.00	4760474.00	
				0.30	5151979.00	3043148.00	8195127.00	
				0.50	8586632.00	3043148.00	11629780.00	
				0.70	12021284.00	3043148.00	15064432.00	
				1.00	17173264.00	3043148.00	20216400.00	
		3.50	LAMINAR	0.10	976408.81	3043148.00	4019556.00	
				0.30	2929225.00	3043148.00	5972373.00	
				0.50	48832043.00	3043148.00	7925191.00	
				0.70	6834860.00	3043148.00	9878008.00	
				1.00	9764086.00	3043148.00	12807234.00	
		4.00	LAMINAR	0.10	599003.12	3043148.00	3642151.00	
				0.30	1797009.00	3043148.00	4840157.00	
				0.50	2995015.00	3043148.00	6038163.00	
				0.70	4193020.00	3043148.00	7236168.00	
				1.00	5990030.00	3043148.00	9033178.00	
		5.00	LAMINAR	0.10	265173.06	3043148.00	3308321.00	
				0.30	795519.00	3043148.00	3838667.00	
				0.50	1325865.00	3043148.00	4369013.00	
				0.70	1856210.00	3043148.00	4899358.00	
				1.00	2651730.00	3043148.00	5694878.00	

NEW PARTICLE SIZE DISTRIBUTION WITH DM= 0.56

SURFACE AREA=2.711

PARTICLE SIZE (MICRONS)	PERCENT ( % )
453.1372	0.0041
2000.0000	0.0097
2000.0000	0.0422
1000.0000	0.0226
800.0000	0.0568
500.0000	0.0559
300.0000	0.0583
200.0000	0.0697
140.0000	0.0623
100.0000	0.0825
60.0000	0.0689
40.0000	0.0582
30.0000	0.0580
20.0000	0.0529
15.0000	0.0544
10.0000	0.0437
5.0000	0.0588
0.5000	0.1400

CM	CV	PN	PK	ETA0	EINF	TAUY	B					
0.596	0.460	0.932	16.91	16.01	10.68	8.97	166.65					
SHEAR RATE-G =		1.00	2.00	3.00	4.00	5.00	6.00	7.00	8.00	9.00	10.00	
SHEAR STRESS-TAU =		24.82	40.36	55.61	70.61	85.37	99.91	114.24	128.39	142.37	156.19	
SHEAR RATE-G =		11.00	12.00	13.00	14.00	15.00	16.00	17.00	18.00	19.00	20.00	
SHEAR STRESS-TAU =		169.86	183.40	196.80	210.08	223.25	236.32	249.29	262.16	274.95	287.65	
SHEAR RATE-G =		21.00	22.00	23.00	24.00	25.00	26.00	27.00	28.00	29.00	30.00	
SHEAR STRESS-TAU =		300.28	312.83	325.32	337.74	350.10	362.40	374.64	386.84	398.98	411.07	
SHEAR RATE-G =		31.00	32.00	33.00	34.00	35.00	36.00	37.00	38.00	39.00	40.00	
SHEAR STRESS-TAU =		423.12	435.13	447.09	459.02	470.90	482.76	494.57	506.36	518.11	529.83	
SHEAR RATE-G =		41.00	42.00	43.00	44.00	45.00	46.00	47.00	48.00	49.00	50.00	
SHEAR STRESS-TAU =		541.53	553.20	564.84	576.45	588.04	599.61	611.15	622.68	634.18	645.66	

CV (%)	PN	PK	DIAMETER	FLOW	DISTANCE	PUMPING ENERGY	COMMUNITION ENERGY	TOTAL ENERGY
0.460	0.932	16.909	2.00	LAMINAR	0.10	9754016.00	30255072.00	40009088.00
					0.30	29262032.00	30255072.00	59517104.00
					0.50	487770064.00	30255072.00	79025136.00
					0.70	68278096.00	30255072.00	98533168.00
					1.00	97540144.00	30255072.00	127795216.00
			2.50	LAMINAR	0.10	4187020.00	30255072.00	34442080.00
					0.30	12561058.00	30255072.00	42816128.00
					0.50	20935088.00	30255072.00	51190160.00
					0.70	29309120.00	30255072.00	59564192.00
					1.00	41870192.00	30255072.00	72125264.00
			3.00	LAMINAR	0.10	2099568.00	30255072.00	32354640.00
					0.30	6298704.00	30255072.00	36553776.00
					0.50	10497840.00	30255072.00	40752912.00
					0.70	14696975.00	30255072.00	44952032.00
					1.00	20995680.00	30255072.00	51250752.00
			3.50	LAMINAR	0.10	1172311.00	30255072.00	1427376.00
					0.30	3516933.00	30255072.00	3772000.00
					0.50	5861556.00	30255072.00	6116624.00
					0.70	8206178.00	30255072.00	8461248.00
					1.00	11723112.00	30255072.00	14978176.00
			4.00	LAMINAR	0.10	708327.31	30255072.00	10963392.00
					0.30	2124981.00	30255072.00	22380048.00
					0.50	3541636.00	30255072.00	3796704.00
					0.70	4958290.00	30255072.00	5213360.00
					1.00	7083272.00	30255072.00	7338336.00
			5.00	LAMINAR	0.10	306185.94	30255072.00	10561248.00
					0.30	918557.69	30255072.00	1173616.00
					0.50	1530929.00	30255072.00	1786000.00
					0.70	2143301.00	30255072.00	2398368.00
					1.00	3061859.00	30255072.00	3316928.00

CM	CV	PN	PK	ETA0	EINF	TAUY	B					
0.596	0.430	0.949	10.21	9.77	7.11	6.01	97.67					
SHEAR RATE-G =		1.00	2.00	3.00	4.00	5.00	6.00	7.00	8.00	9.00	10.00	
SHEAR STRESS-TAU =		15.71	25.28	34.73	44.06	53.28	62.41	71.44	80.38	89.25	98.04	
SHEAR RATE-G =		11.00	12.00	13.00	14.00	15.00	16.00	17.00	18.00	19.00	20.00	
SHEAR STRESS-TAU =		106.76	115.41	124.00	132.54	141.01	149.44	157.82	166.15	174.43	182.68	
SHEAR RATE-G =		21.00	22.00	23.00	24.00	25.00	26.00	27.00	28.00	29.00	30.00	
SHEAR STRESS-TAU =		190.88	199.05	207.18	215.28	223.35	231.38	239.39	247.37	255.32	263.25	
SHEAR RATE-G =		31.00	32.00	33.00	34.00	35.00	36.00	37.00	38.00	39.00	40.00	
SHEAR STRESS-TAU =		271.15	279.03	286.89	294.72	302.54	310.34	318.12	325.88	333.62	341.35	
SHEAR RATE-G =		41.00	42.00	43.00	44.00	45.00	46.00	47.00	48.00	49.00	50.00	
SHEAR STRESS-TAU =		349.06	356.75	364.43	372.10	379.75	387.39	395.02	402.63	410.23	417.83	

CV (%)	PN	PK	DIAMETER	FLOW	DISTANCE	PUMPING ENERGY	COMMUNITION ENERGY	TOTAL ENERGY
0.430	0.949	10.207	2.00	LAMINAR	0.10	7563016.00	30255072.00	37818080.00
					0.30	22689040.00	30255072.00	52944112.00
					0.50	37815072.00	30255072.00	68070144.00
					0.70	52941088.00	30255072.00	83196160.00
					1.00	75630144.00	30255072.00	105885216.00
			2.50	LAMINAR	0.10	3209650.00	30255072.00	33464720.00
					0.30	9628949.00	30255072.00	39884016.00
					0.50	16048248.00	30255072.00	46303312.00
					0.70	22467536.00	30255072.00	52722608.00
					1.00	32096496.00	30255072.00	62351568.00
			3.00	LAMINAR	0.10	1594503.00	30255072.00	31849568.00
					0.30	4783509.00	30255072.00	35038576.00
					0.50	7972515.00	30255072.00	38227584.00
					0.70	11161520.00	30255072.00	41416592.00
					1.00	15945030.00	30255072.00	46200096.00
			3.50	LAMINAR	0.10	883295.69	30255072.00	31138352.00
					0.30	2649886.00	30255072.00	32904944.00
					0.50	4416477.00	30255072.00	34671536.00
					0.70	6183068.00	30255072.00	36438128.00
					1.00	8832955.00	30255072.00	39088016.00
			4.00	LAMINAR	0.10	530050.19	30255072.00	0785120.00
					0.30	1590150.00	30255072.00	1845216.00
					0.50	2650250.00	30255072.00	2905312.00
					0.70	3710350.00	30255072.00	3965408.00
					1.00	5300501.00	30255072.00	5555568.00
			5.00	LAMINAR	0.10	226513.12	30255072.00	0481584.00
					0.30	679539.31	30255072.00	0934608.00
					0.50	1132565.00	30255072.00	1387632.00
					0.70	1585591.00	30255072.00	1840656.00
					1.00	2265131.00	30255072.00	32520192.00



CM	CV	PN	PK	ETA0	EINF	TAUY	B					
0.596	0.384	0.966	5.53	5.37	4.30	3.35	45.57					
SHEAR RATE-G =		1.00	2.00	3.00	4.00	5.00	6.00	7.00	8.00	9.00	10.00	
SHEAR STRESS-TAU =		8.69	13.99	19.24	24.45	29.62	34.76	39.86	44.93	49.98	54.99	
SHEAR RATE-G =		11.00	12.00	13.00	14.00	15.00	16.00	17.00	18.00	19.00	20.00	
SHEAR STRESS-TAU =		59.98	64.94	69.88	74.79	79.68	84.56	89.41	94.25	99.07	103.87	
SHEAR RATE-G =		21.00	22.00	23.00	24.00	25.00	26.00	27.00	28.00	29.00	30.00	
SHEAR STRESS-TAU =		108.65	113.43	118.18	122.93	127.66	132.37	137.08	141.77	146.46	151.13	
SHEAR RATE-G =		31.00	32.00	33.00	34.00	35.00	36.00	37.00	38.00	39.00	40.00	
SHEAR STRESS-TAU =		155.79	160.44	165.09	169.72	174.34	178.96	183.57	188.17	192.77	197.35	
SHEAR RATE-G =		41.00	42.00	43.00	44.00	45.00	46.00	47.00	48.00	49.00	50.00	
SHEAR STRESS-TAU =		201.93	206.51	211.07	215.64	220.19	224.74	229.28	233.82	238.35	242.88	

CV (%)	PN	PK	DIAMETER	FLOW	DISTANCE	PUMPING ENERGY	COMMUNITION ENERGY	TOTAL ENERGY
0.384	0.966	5.530	2.00	LAMINAR	0.10	5811722.00	30255072.00	36066784.00
					0.30	17435152.00	30255072.00	47690224.00
					0.50	29058608.00	30255072.00	59313680.00
					0.70	40682048.00	30255072.00	70937120.00
					1.00	58117216.00	30255072.00	88372288.00
			2.50	LAMINAR	0.10	2437763.00	30255072.00	32692832.00
					0.30	7313289.00	30255072.00	37568352.00
					0.50	12188816.00	30255072.00	42443888.00
					0.70	17064336.00	30255072.00	47319408.00
					1.00	24377632.00	30255072.00	54632704.00
			3.00	LAMINAR	0.10	1199425.00	30255072.00	31454496.00
					0.30	3598275.00	30255072.00	33853344.00
					0.50	5997125.00	30255072.00	36252192.00
					0.70	8395974.00	30255072.00	38651040.00
					1.00	11994250.00	30255072.00	42249312.00
			3.50	LAMINAR	0.10	658963.94	30255072.00	30914032.00
					0.30	1976891.00	30255072.00	32231952.00
					0.50	3294819.00	30255072.00	33549888.00
					0.70	4612746.00	30255072.00	34867808.00
					1.00	6589638.00	30255072.00	36185728.00
			4.00	LAMINAR	0.10	392563.44	30255072.00	30647632.00
					0.30	1177690.00	30255072.00	31965552.00
					0.50	1962817.00	30255072.00	33283472.00
					0.70	2747943.00	30255072.00	34601392.00
					1.00	3925634.00	30255072.00	35919312.00
			5.00	LAMINAR	0.10	165669.69	30255072.00	30420736.00
					0.30	497009.06	30255072.00	31738656.00
					0.50	828348.50	30255072.00	33056576.00
					0.70	1159687.00	30255072.00	34374496.00
					1.00	1656697.00	30255072.00	35692416.00

NEW PARTICLE SIZE DISTRIBUTION WITH DM= 0.61

SURFACE AREA=2.472

PARTICLE SIZE (MICRONS)	PERCENT ( % )
312.4597	0.0012
300.0000	0.0061
200.0000	0.0346
100.0000	0.0210
80.0000	0.0562
52.0000	0.0581
37.0000	0.0623
27.0000	0.0756
19.0000	0.0679
14.0000	0.0898
9.3000	0.0743
6.5000	0.0620
4.7000	0.0610
3.3000	0.0547
2.3000	0.0551
1.5000	0.0432
1.0000	0.0565
0.5000	0.1195

CM	CV	PN	PK	ETA0	EINF	TAUY	B					
0.587	0.460	0.919	19.47	18.36	11.67	9.05	174.72					
SHEAR RATE-G =		1.00	2.00	3.00	4.00	5.00	6.00	7.00	8.00	9.00	10.00	
SHEAR STRESS-TAU =		27.16	44.81	62.05	78.92	95.46	111.70	127.66	143.37	158.85	174.12	
SHEAR RATE-G =		11.00	12.00	13.00	14.00	15.00	16.00	17.00	18.00	19.00	20.00	
SHEAR STRESS-TAU =		189.19	204.09	218.82	233.40	247.84	262.14	276.33	290.40	304.36	318.23	
SHEAR RATE-G =		21.00	22.00	23.00	24.00	25.00	26.00	27.00	28.00	29.00	30.00	
SHEAR STRESS-TAU =		332.00	345.69	359.29	372.81	386.27	399.65	412.97	426.23	439.44	452.58	
SHEAR RATE-G =		31.00	32.00	33.00	34.00	35.00	36.00	37.00	38.00	39.00	40.00	
SHEAR STRESS-TAU =		465.68	478.73	491.73	504.68	517.60	530.47	543.31	556.11	568.87	581.61	
SHEAR RATE-G =		41.00	42.00	43.00	44.00	45.00	46.00	47.00	48.00	49.00	50.00	
SHEAR STRESS-TAU =		594.31	606.98	619.62	632.23	644.82	657.38	669.92	682.44	694.93	707.40	

CV (%)	PN	PK	DIAMETER	FLOW	DISTANCE	PUMPING ENERGY	COMMUNITION ENERGY	TOTAL ENERGY
0.460	0.919	19.471	2.00	LAMINAR	0.10	10368679.00	25077808.00	35446480.00
					0.20	31106016.00	25077808.00	56183824.00
					0.50	51843376.00	25077808.00	76921184.00
					0.70	72580736.00	25077808.00	97658544.00
					1.00	103686768.00	25077808.00	128764576.00
		2.50	LAMINAR	0.10	4487641.00	25077808.00	25077808.00	29565440.00
				0.30	13462920.00	25077808.00	25077808.00	38540720.00
				0.50	2438192.00	25077808.00	25077808.00	47516000.00
				0.70	3413472.00	25077808.00	25077808.00	56491280.00
				1.00	44876400.00	25077808.00	25077808.00	69954208.00
		3.00	LAMINAR	0.10	2265379.00	25077808.00	25077808.00	27343184.00
				0.30	6796137.00	25077808.00	25077808.00	31873936.00
				0.50	11326896.00	25077808.00	25077808.00	36404704.00
				0.70	15857654.00	25077808.00	25077808.00	40935456.00
				1.00	22653792.00	25077808.00	25077808.00	47731600.00
		3.50	LAMINAR	0.10	1271943.00	25077808.00	25077808.00	26349744.00
				0.30	3815829.00	25077808.00	25077808.00	28893632.00
				0.50	6359715.00	25077808.00	25077808.00	31437520.00
				0.70	8903601.00	25077808.00	25077808.00	33981408.00
				1.00	12719431.00	25077808.00	25077808.00	37797232.00
		4.00	LAMINAR	0.10	772160.75	25077808.00	25077808.00	25849968.00
				0.30	2316481.00	25077808.00	25077808.00	27394288.00
				0.50	3860803.00	25077808.00	25077808.00	28938608.00
				0.70	5405124.00	25077808.00	25077808.00	30482928.00
				1.00	7721606.00	25077808.00	25077808.00	32799408.00
		5.00	LAMINAR	0.10	336314.75	25077808.00	25077808.00	25414112.00
				0.30	1008944.12	25077808.00	25077808.00	26086752.00
				0.50	1681573.00	25077808.00	25077808.00	26759376.00
				0.70	2354202.00	25077808.00	25077808.00	27432000.00
				1.00	3363147.00	25077808.00	25077808.00	28440944.00

CM	CV	PN	PK	ETA0	EINF	TAUY	B					
0.587	0.430	0.940	11.31	10.78	7.57	5.98	100.36					
SHEAR RATE	$\frac{G}{\tau} =$											
SHEAR STRESS	$\tau =$	1.00	2.00	3.00	4.00	5.00	6.00	7.00	8.00	9.00	10.00	
		16.66	27.16	37.48	47.65	57.68	67.57	77.35	87.01	96.56	106.03	
SHEAR RATE	$\frac{G}{\tau} =$	11.00	12.00	13.00	14.00	15.00	16.00	17.00	18.00	19.00	20.00	
SHEAR STRESS	$\tau =$	115.40	124.69	133.90	143.04	152.11	161.12	170.07	178.96	187.80	196.59	
SHEAR RATE	$\frac{G}{\tau} =$	21.00	22.00	23.00	24.00	25.00	26.00	27.00	28.00	29.00	30.00	
SHEAR STRESS	$\tau =$	205.34	214.04	222.70	231.32	239.90	248.45	256.96	265.44	273.90	282.32	
SHEAR RATE	$\frac{G}{\tau} =$	31.00	32.00	33.00	34.00	35.00	36.00	37.00	38.00	39.00	40.00	
SHEAR STRESS	$\tau =$	290.72	299.09	307.43	315.75	324.05	332.33	340.59	348.82	357.04	365.24	
SHEAR RATE	$\frac{G}{\tau} =$	41.00	42.00	43.00	44.00	45.00	46.00	47.00	48.00	49.00	50.00	
SHEAR STRESS	$\tau =$	373.43	381.59	389.74	397.88	406.00	414.10	422.20	430.28	438.34	446.40	

CV (%)	PN	PK	DIAMETER	FLOW	DISTANCE	PUMPING ENERGY	COMBUSTION ENERGY	TOTAL ENERGY
0.430	0.940	11.307	2.00	LAMINAR	0.10	7907115.00	25077808.00	32984912.00
					0.30	23721328.00	25077808.00	48799136.00
					0.50	39535568.00	25077808.00	64613376.00
					0.70	55349792.00	25077808.00	80427600.00
					1.00	79071136.00	25077808.00	104148944.00
			2.50	LAMINAR	0.10	3375463.00	25077808.00	28453264.00
					0.30	10126387.00	25077808.00	35204192.00
					0.50	16877312.00	25077808.00	41955120.00
					0.70	23628224.00	25077808.00	48706032.00
					1.00	33754624.00	25077808.00	58832432.00
			3.00	LAMINAR	0.10	1684878.00	25077808.00	26782672.00
					0.30	5054635.00	25077808.00	30132432.00
					0.50	8424392.00	25077808.00	33502192.00
					0.70	11794148.00	25077808.00	36881952.00
					1.00	16848784.00	25077808.00	41976592.00
			3.50	LAMINAR	0.10	937054.50	25077808.00	26034848.00
					0.30	2811163.00	25077808.00	27888960.00
					0.50	4698527.00	25077808.00	29763072.00
					0.70	6629734.00	25077808.00	31637184.00
					1.00	9270192.00	25077808.00	34448336.00
			4.00	LAMINAR	0.10	564519.12	25077808.00	25642000.00
					0.30	1692585.00	25077808.00	26770384.00
					0.50	2820975.00	25077808.00	27898768.00
					0.70	3949364.00	25077808.00	29027168.00
					1.00	5644950.00	25077808.00	30719744.00
			5.00	LAMINAR	0.10	242390.34	25077808.00	25320192.00
					0.30	727170.87	25077808.00	25804976.00
					0.50	1211951.00	25077808.00	26289744.00
					0.70	1696732.00	25077808.00	26774528.00
					1.00	2423903.00	25077808.00	27501696.00

CM	CV	PN	PK	ETA0	EINF	TAUY	B					
0.587	0.384	0.960	5.90	5.71	4.47	3.29	45.93					
SHEAR RATE-G =		1.00	2.00	3.00	4.00	5.00	6.00	7.00	8.00	9.00	10.00	
SHEAR STRESS-TAU =		8.97	14.58	20.13	25.64	31.09	36.50	41.87	47.20	52.49	57.74	
SHEAR RATE-G =		11.00	12.00	13.00	14.00	15.00	16.00	17.00	18.00	19.00	20.00	
SHEAR STRESS-TAU =		62.97	68.16	73.32	78.46	83.57	88.66	93.73	98.77	103.79	108.80	
SHEAR RATE-G =		21.00	22.00	23.00	24.00	25.00	26.00	27.00	28.00	29.00	30.00	
SHEAR STRESS-TAU =		113.78	118.75	123.70	128.64	133.56	138.47	143.36	148.24	153.11	157.97	
SHEAR RATE-G =		31.00	32.00	33.00	34.00	35.00	36.00	37.00	38.00	39.00	40.00	
SHEAR STRESS-TAU =		162.81	167.65	172.47	177.28	182.09	186.88	191.67	196.45	201.22	205.98	
SHEAR RATE-G =		41.00	42.00	43.00	44.00	45.00	46.00	47.00	48.00	49.00	50.00	
SHEAR STRESS-TAU =		210.74	215.49	220.23	224.96	229.69	234.41	239.13	243.84	248.55	253.25	

CV (%)	PN	PK	DIAMETER	FLOW	DISTANCE	PUMPING ENERGY	COMMUNITION ENERGY	TOTAL ENERGY
0.384	0.960	5.899	2.00	LAMINAR	0.10	5976937.00	25077808.00	31054736.00
					0.20	17930800.00	25077808.00	43008608.00
					0.30	29884672.00	25077808.00	54962480.00
					0.40	41838544.00	25077808.00	66916352.00
					0.50	53792416.00	25077808.00	78870224.00
			2.50	LAMINAR	0.10	5976937.00	25077808.00	31054736.00
					0.20	17930800.00	25077808.00	43008608.00
					0.30	29884672.00	25077808.00	54962480.00
					0.40	41838544.00	25077808.00	66916352.00
					0.50	53792416.00	25077808.00	78870224.00
			3.00	LAMINAR	0.10	1241666.00	25077808.00	26319472.00
					0.20	3725005.00	25077808.00	28802800.00
					0.30	6208342.00	25077808.00	31286144.00
					0.40	8691679.00	25077808.00	33769472.00
					0.50	1241666.00	25077808.00	37494480.00
			3.50	LAMINAR	0.10	683846.81	25077808.00	25761648.00
					0.20	2051540.00	25077808.00	27129344.00
					0.30	3419233.00	25077808.00	28497040.00
					0.40	4786926.00	25077808.00	29864720.00
					0.50	683846.00	25077808.00	31916272.00
			4.00	LAMINAR	0.10	408227.19	25077808.00	25486032.00
					0.20	1224681.00	25077808.00	26302480.00
					0.30	2041135.00	25077808.00	27118928.00
					0.40	2857589.00	25077808.00	27935392.00
					0.50	408227.00	25077808.00	29160064.00
			5.00	LAMINAR	0.10	172841.12	25077808.00	25250640.00
					0.20	518523.31	25077808.00	25596320.00
					0.30	864205.50	25077808.00	25942000.00
					0.40	1209887.00	25077808.00	26287680.00
					0.50	172841.00	25077808.00	26806208.00

NEW PARTICLE SIZE DISTRIBUTION WITH DM= 0.66

SURFACE AREA=2.259

PARTICLE SIZE (MICRONS)	PERCENT ( % )
300.0000	0.0035
200.0000	0.0271
100.0000	0.0189
80.0000	0.0546
52.0000	0.0598
37.0000	0.0659
27.0000	0.0813
19.0000	0.0734
14.0000	0.0969
9.3000	0.0795
6.5000	0.0656
4.7000	0.0636
3.3000	0.0560
2.3000	0.0552
1.5000	0.0424
1.0000	0.0538
0.5000	0.1017

CM      CV      PN      PK      ETAO      EINF      TAUY      B  
 0.578    0.460    0.906    22.46    21.11    12.77    9.15    183.06

SHEAR RATE-G =		1.00	2.00	3.00	4.00	5.00	6.00	7.00	8.00	9.00	10.00
SHEAR STRESS-TAU =		29.90	49.98	69.48	88.46	106.98	125.09	142.83	160.24	177.35	194.19
SHEAR RATE-G =		11.00	12.00	13.00	14.00	15.00	16.00	17.00	18.00	19.00	20.00
SHEAR STRESS-TAU =		210.78	227.15	243.31	259.28	275.08	290.72	306.21	321.57	336.80	351.91
SHEAR RATE-G =		21.00	22.00	23.00	24.00	25.00	26.00	27.00	28.00	29.00	30.00
SHEAR STRESS-TAU =		366.92	381.82	396.63	411.35	425.99	440.55	455.04	469.45	483.81	498.10
SHEAR RATE-G =		31.00	32.00	33.00	34.00	35.00	36.00	37.00	38.00	39.00	40.00
SHEAR STRESS-TAU =		512.34	526.52	540.65	554.73	568.76	582.76	596.71	610.62	624.49	638.33
SHEAR RATE-G =		41.00	42.00	43.00	44.00	45.00	46.00	47.00	48.00	49.00	50.00
SHEAR STRESS-TAU =		652.14	665.91	679.65	693.37	707.05	720.71	734.34	747.95	761.53	775.10

CV (%)	PN	PK	DIAMETER	FLOW	DISTANCE	PUMPING ENERGY	COMMUNITION ENERGY	TOTAL ENERGY		
0.460	0.906	22.462	2.00	LAMINAR	0.10	10993281.00	20878368.00	31871648.00		
					0.30	32979824.00	20878368.00	53858192.00		
					0.50	54966384.00	20878368.00	75844752.00		
					0.70	76952944.00	20878368.00	97831312.00		
					1.00	109932784.00	20878368.00	130811152.00		
					2.50	LAMINAR	0.10	4799661.00	20878368.00	25678016.00
							0.30	14398982.00	20878368.00	35277344.00
							0.50	23998304.00	20878368.00	44876672.00
							0.70	33597616.00	20878368.00	54475984.00
							1.00	47996608.00	20878368.00	68874976.00
							3.00	LAMINAR	0.10	2440034.00
					0.30	7320101.00			20878368.00	28198464.00
					0.50	12200168.00			20878368.00	33078528.00
					0.70	17080224.00			20878368.00	37958592.00
					1.00	24400336.00			20878368.00	45278704.00
					3.50	LAMINAR			0.10	1378132.00
							0.30	4134395.00	20878368.00	25012752.00
							0.50	6890659.00	20878368.00	27769008.00
							0.70	9646923.00	20878368.00	30525264.00
							1.00	13781319.00	20878368.00	35405376.00
4.00	LAMINAR	0.10	840837.75	20878368.00			21719680.00			
		0.30	2522515.00	20878368.00	24400880.00					
		0.50	4204188.00	20878368.00	27082080.00					
		0.70	5885861.00	20878368.00	29763280.00					
		1.00	8408375.00	20878368.00	32444480.00					
		5.00	LAMINAR	0.10	1669321.87	20878368.00	26764224.00			
0.30	1107641.00			20878368.00	21647568.00					
0.50	1844606.00			20878368.00	22724432.00					
0.70	2584496.00			20878368.00	23801296.00					
1.00	3692138.00			20878368.00	24878160.00					

CM	CV	PN	PK	ETA0	EINF	TAUY	B				
0.578	0.430	0.931	12.53	11.91	8.07	5.96	102.96				
SHEAR RATE-G =		1.00	2.00	3.00	4.00	5.00	6.00	7.00	8.00	9.00	10.00
SHEAR STRESS-TAU =		17.73	29.24	40.52	51.59	62.48	73.19	83.75	94.16	104.44	114.61
SHEAR RATE-G =		11.00	12.00	13.00	14.00	15.00	16.00	17.00	18.00	19.00	20.00
SHEAR STRESS-TAU =		124.66	134.61	144.47	154.24	163.92	173.54	183.08	192.56	201.97	211.33
SHEAR RATE-G =		21.00	22.00	23.00	24.00	25.00	26.00	27.00	28.00	29.00	30.00
SHEAR STRESS-TAU =		220.63	229.89	239.09	248.25	257.37	266.45	275.49	284.50	293.47	302.42
SHEAR RATE-G =		31.00	32.00	33.00	34.00	35.00	36.00	37.00	38.00	39.00	40.00
SHEAR STRESS-TAU =		311.33	320.21	329.07	337.90	346.70	355.48	364.24	372.98	381.70	390.40
SHEAR RATE-G =		41.00	42.00	43.00	44.00	45.00	46.00	47.00	48.00	49.00	50.00
SHEAR STRESS-TAU =		399.08	407.74	416.39	425.02	433.63	442.23	450.81	459.38	467.94	476.49

CV (%)	PN	PK	DIAMETER	FLOW	DISTANCE	PUMPING ENERGY	COMMUNITION ENERGY	TOTAL ENERGY
0.430	0.931	12.526	2.00	LAMINAR	0.10	8245627.00	20878368.00	29123984.00
					0.30	24736864.00	20878368.00	45615232.00
					0.50	41228128.00	20878368.00	62106496.00
					0.70	57719376.00	20878368.00	78597744.00
					1.00	82456256.00	20878368.00	103334624.00
			2.50	LAMINAR	0.10	3541764.00	20878368.00	24420128.00
					0.30	10625290.00	20878368.00	31503648.00
					0.50	17708816.00	20878368.00	38587184.00
					0.70	24792336.00	20878368.00	45670704.00
					1.00	5417632.00	20878368.00	56296000.00
			3.00	LAMINAR	0.10	1776707.00	20878368.00	22655072.00
					0.30	5330121.00	20878368.00	26208480.00
					0.50	8883536.00	20878368.00	29761904.00
					0.70	12436950.00	20878368.00	33315312.00
					1.00	17767072.00	20878368.00	36868720.00
			3.50	LAMINAR	0.10	992253.19	20878368.00	18706608.00
					0.30	2976759.00	20878368.00	22855968.00
					0.50	4961235.00	20878368.00	27005328.00
					0.70	6945710.00	20878368.00	31154688.00
					1.00	9922530.00	20878368.00	35304048.00
			4.00	LAMINAR	0.10	596508.12	20878368.00	14777904.00
					0.30	1798648.00	20878368.00	22677008.00
					0.50	2997944.00	20878368.00	28576112.00
					0.70	4197240.00	20878368.00	34475216.00
					1.00	5996536.00	20878368.00	40374320.00
			5.00	LAMINAR	0.10	259042.44	20878368.00	1137408.00
					0.30	795127.19	20878368.00	1655488.00
					0.50	1212212.00	20878368.00	2173568.00
					0.70	1613226.00	20878368.00	2691648.00
					1.00	2590424.00	20878368.00	3209728.00



CM	CV	PN	PK	ETA0	EINF	TAUY	B					
0.578	0.384	0.955	6.29	6.07	4.65	3.24	46.19					
SHEAR RATE-G =		1.00	2.00	3.00	4.00	5.00	6.00	7.00	8.00	9.00	10.00	
SHEAR STRESS-TAU =		9.26	15.21	21.08	26.89	32.63	38.32	43.95	49.54	55.08	60.58	
SHEAR RATE-G =		11.00	12.00	13.00	14.00	15.00	16.00	17.00	18.00	19.00	20.00	
SHEAR STRESS-TAU =		66.05	71.47	76.86	82.22	87.55	92.85	98.13	103.38	108.61	113.81	
SHEAR RATE-G =		21.00	22.00	23.00	24.00	25.00	26.00	27.00	28.00	29.00	30.00	
SHEAR STRESS-TAU =		119.00	124.16	129.31	134.44	139.55	144.65	149.73	154.80	159.85	164.90	
SHEAR RATE-G =		31.00	32.00	33.00	34.00	35.00	36.00	37.00	38.00	39.00	40.00	
SHEAR STRESS-TAU =		169.93	174.94	179.95	184.95	189.93	194.91	199.87	204.83	209.78	214.72	
SHEAR RATE-G =		41.00	42.00	43.00	44.00	45.00	46.00	47.00	48.00	49.00	50.00	
SHEAR STRESS-TAU =		219.65	224.58	229.50	234.41	239.31	244.21	249.10	253.99	258.87	263.74	

CV (%)	PN	PK	DIAMETER	FLOW	DISTANCE	PUMPING ENERGY	COMMUNITION ENERGY	TOTAL ENERGY
0.384	0.955	6.288	2.00	LAMINAR	0.10	6135244.00	20878368.00	27013600.00
					0.30	18405728.00	20878368.00	39284096.00
					0.50	30676208.00	20878368.00	51554576.00
					0.70	42946688.00	20878368.00	63825056.00
					1.00	61352432.00	20878368.00	82230800.00
			2.50	LAMINAR	0.10	2592578.00	20878368.00	23470944.00
					0.30	7777733.00	20878368.00	28656096.00
					0.50	12962888.00	20878368.00	33841248.00
					0.70	18148032.00	20878368.00	39026400.00
					1.00	25925776.00	20878368.00	46804144.00
			3.00	LAMINAR	0.10	1283246.00	20878368.00	22161600.00
					0.30	3849738.00	20878368.00	24728096.00
					0.50	6416230.00	20878368.00	27294592.00
					0.70	8982721.00	20878368.00	29861088.00
					1.00	12832460.00	20878368.00	33710816.00
			3.50	LAMINAR	0.10	708528.12	20878368.00	21586896.00
					0.30	2125584.00	20878368.00	23003952.00
					0.50	3542640.00	20878368.00	24421008.00
					0.70	4959695.00	20878368.00	25838048.00
					1.00	7085280.00	20878368.00	27963648.00
			4.00	LAMINAR	0.10	423870.25	20878368.00	21302224.00
					0.30	1271610.00	20878368.00	22149968.00
					0.50	2119351.00	20878368.00	22997712.00
					0.70	2967091.00	20878368.00	23845456.00
					1.00	4238702.00	20878368.00	25117056.00
			5.00	LAMINAR	0.10	180076.44	20878368.00	21058432.00
					0.30	540229.19	20878368.00	21478736.00
					0.50	900382.00	20878368.00	21899040.00
					0.70	1260534.00	20878368.00	22319344.00
					1.00	1800764.00	20878368.00	22679120.00

NEW PARTICLE SIZE DISTRIBUTION WITH DM= 0.71

SURFACE AREA=2.069

PARTICLE SIZE (MICRONS)	PERCENT ( % )
300.0000	0.0018
200.0000	0.0202
100.0000	0.0165
80.0000	0.0521
52.0000	0.0607
37.0000	0.0692
27.0000	0.0869
19.0000	0.0790
14.0000	0.1040
9.3000	0.0846
6.5000	0.0689
4.7000	0.0657
3.3000	0.0569
2.3000	0.0549
1.5000	0.0412
1.0000	0.0507
0.5000	0.0865

CM	CV	PN	PK	ETA0	EINF	TAUY	B					
0.570	0.460	0.893	25.95	24.38	14.01	9.29	191.77					
SHEAR RATE-G	=	1.00	2.00	3.00	4.00	5.00	6.00	7.00	8.00	9.00	10.00	
SHEAR STRESS-TAU	=	33.14	56.02	78.08	99.43	120.15	140.32	160.01	179.27	198.14	216.68	
SHEAR RATE-G	=	11.00	12.00	13.00	14.00	15.00	16.00	17.00	18.00	19.00	20.00	
SHEAR STRESS-TAU	=	234.91	252.86	270.56	288.03	305.30	322.38	339.28	356.03	372.63	389.10	
SHEAR RATE-G	=	21.00	22.00	23.00	24.00	25.00	26.00	27.00	28.00	29.00	30.00	
SHEAR STRESS-TAU	=	405.44	421.66	437.78	453.80	469.73	485.57	501.33	517.02	532.63	548.18	
SHEAR RATE-G	=	31.00	32.00	33.00	34.00	35.00	36.00	37.00	38.00	39.00	40.00	
SHEAR STRESS-TAU	=	563.67	579.09	594.47	609.79	625.06	640.28	655.46	670.60	685.70	700.77	
SHEAR RATE-G	=	41.00	42.00	43.00	44.00	45.00	46.00	47.00	48.00	49.00	50.00	
SHEAR STRESS-TAU	=	715.80	730.79	745.75	760.68	775.58	790.46	805.31	820.13	834.93	849.70	

CV (%)	PN	PK	DIAMETER	FLOW	DISTANCE	PUMPING ENERGY	COMMUNITION ENERGY	TOTAL ENERGY
0.460	0.893	25.947	2.00	LAMINAR	0.10	11639858.00	17469552.00	29109408.00
					0.30	34919568.00	17469552.00	52389120.00
					0.50	58199280.00	17469552.00	75668832.00
					0.70	81478976.00	17469552.00	98948528.00
					1.00	116398560.00	17469552.00	133868112.00
			2.50	LAMINAR	0.10	5127817.00	17469552.00	22597360.00
					0.30	15383448.00	17469552.00	32852992.00
					0.50	25639072.00	17469552.00	43108624.00
					0.70	35894704.00	17469552.00	53364256.00
					1.00	51278160.00	17469552.00	68747712.00
			3.00	LAMINAR	0.10	2625989.00	17469552.00	20095536.00
					0.30	7877966.00	17469552.00	25347504.00
					0.50	13129944.00	17469552.00	30599488.00
					0.70	18381920.00	17469552.00	35851472.00
					1.00	26259888.00	17469552.00	43729440.00
			3.50	LAMINAR	0.10	1492254.00	17469552.00	18961792.00
					0.30	4476763.00	17469552.00	21946304.00
					0.50	7461272.00	17469552.00	24930816.00
					0.70	10445780.00	17469552.00	27915328.00
					1.00	14922544.00	17469552.00	32390296.00
			4.00	LAMINAR	0.10	915227.81	17469552.00	18384768.00
					0.30	2745562.00	17469552.00	20215232.00
					0.50	4576538.00	17469552.00	22045680.00
					0.70	6406593.00	17469552.00	23876144.00
					1.00	9152273.00	17469552.00	25706608.00
			5.00	LAMINAR	0.10	4052597.19	17469552.00	26621824.00
					0.30	1215891.19	17469552.00	18685440.00
					0.50	2026485.00	17469552.00	19476032.00
					0.70	2837079.00	17469552.00	20306624.00
					1.00	4052971.00	17469552.00	21522512.00

CM	CV	PN	PK	ETA0	EINF	TAUY	B					
0.570	0.430	0.921	13.88	13.16	8.60	5.96	105.50					
SHEAR RATE G =		1.00	2.00	3.00	4.00	5.00	6.00	7.00	8.00	9.00	10.00	
SHEAR STRESS-TAU =		18.93	31.56	43.87	55.92	67.72	79.30	90.68	101.88	112.93	123.82	
SHEAR RATE G =		11.00	12.00	13.00	14.00	15.00	16.00	17.00	18.00	19.00	20.00	
SHEAR STRESS-TAU =		134.58	145.22	155.75	166.17	176.50	186.73	196.89	206.97	216.99	226.93	
SHEAR RATE G =		21.00	22.00	23.00	24.00	25.00	26.00	27.00	28.00	29.00	30.00	
SHEAR STRESS-TAU =		236.82	246.65	256.42	266.15	275.83	285.47	295.06	304.62	314.14	323.62	
SHEAR RATE G =		31.00	32.00	33.00	34.00	35.00	36.00	37.00	38.00	39.00	40.00	
SHEAR STRESS-TAU =		333.07	342.50	351.89	361.25	370.59	379.91	389.20	398.46	407.71	416.94	
SHEAR RATE G =		41.00	42.00	43.00	44.00	45.00	46.00	47.00	48.00	49.00	50.00	
SHEAR STRESS-TAU =		426.14	435.33	444.50	453.66	462.79	471.92	481.02	490.12	499.20	508.26	

CV (%)	PN	PK	DIAMETER	FLOW	DISTANCE	PUMPING ENERGY	COMBUSTION ENERGY	TOTAL ENERGY		
0.430	0.921	13.875	2.00	LAMINAR	0.10	8581590.00	17469552.00	26051136.00		
					0.30	25744752.00	17469552.00	43214304.00		
					0.50	42907936.00	17469552.00	60377488.00		
					0.70	60071120.00	17469552.00	77540672.00		
					1.00	85815888.00	17469552.00	103285440.00		
					2.50	LAMINAR	0.10	3709560.00	17469552.00	21179104.00
							0.30	11128680.00	17469552.00	28598224.00
							0.50	18547792.00	17469552.00	36017344.00
							0.70	25966912.00	17469552.00	43436464.00
					3.00	LAMINAR	1.00	37095600.00	17469552.00	54565152.00
							0.10	1870534.00	17469552.00	19340080.00
							0.30	5611603.00	17469552.00	23081152.00
							0.50	9352672.00	17469552.00	26822224.00
					3.50	LAMINAR	0.70	13093740.00	17469552.00	30563280.00
							1.00	18705344.00	17469552.00	36174896.00
							0.10	1049154.00	17469552.00	18518704.00
							0.30	3147462.00	17469552.00	20617008.00
					4.00	LAMINAR	0.50	5245771.00	17469552.00	22715312.00
							0.70	7344079.00	17469552.00	24813616.00
							1.00	10491542.00	17469552.00	27961088.00
0.10	636262.25	17469552.00	18105308.00							
5.00	LAMINAR	0.30	1908786.00	17469552.00	19378336.00					
		0.50	3181310.00	17469552.00	20650848.00					
		0.70	4453834.00	17469552.00	21923376.00					
		1.00	6362621.00	17469552.00	23832160.00					
				LAMINAR	0.10	276541.56	17469552.00	17746080.00		
					0.30	829624.50	17469552.00	18299168.00		
					0.50	1382707.00	17469552.00	18852256.00		
					0.70	1935790.00	17469552.00	19405328.00		
					1.00	2765415.00	17469552.00	20234960.00		

CM	CV	PN	PK	ETA0	EINF	TAUY	B						
0.570	0.384	0.949	6.70	6.45	4.84	3.20	46.37						
SHEAR RATE-G =		1.00	2.00	3.00	4.00	5.00	6.00	7.00	8.00	9.00	10.00		
SHEAR STRESS-TAU =		9.59	15.88	22.08	28.20	34.24	40.21	46.12	51.97	57.76	63.51		
SHEAR RATE-G =		11.00	12.00	13.00	14.00	15.00	16.00	17.00	18.00	19.00	20.00		
SHEAR STRESS-TAU =		69.21	74.87	80.49	86.07	91.62	97.13	102.62	108.08	113.51	118.92		
SHEAR RATE-G =		21.00	22.00	23.00	24.00	25.00	26.00	27.00	28.00	29.00	30.00		
SHEAR STRESS-TAU =		124.30	129.67	135.01	140.33	145.64	150.93	156.20	161.46	166.70	171.93		
SHEAR RATE-G =		31.00	32.00	33.00	34.00	35.00	36.00	37.00	38.00	39.00	40.00		
SHEAR STRESS-TAU =		177.14	182.35	187.54	192.72	197.88	203.04	208.19	213.33	218.46	223.58		
SHEAR RATE-G =		41.00	42.00	43.00	44.00	45.00	46.00	47.00	48.00	49.00	50.00		
SHEAR STRESS-TAU =		228.70	233.80	238.90	243.99	249.07	254.15	259.22	264.29	269.35	274.40		

CV (%)	PN	PK	DIAMETER	FLOW	DISTANCE	PUMPING ENERGY	COMMUNITION ENERGY	TOTAL ENERGY
0.384	0.949	6.696	2.00	LAMINAR	0.10	6286496.00	17469552.00	23756032.00
					0.30	18859472.00	17469552.00	36329024.00
					0.50	31432464.00	17469552.00	48902016.00
					0.70	44005440.00	17469552.00	61474992.00
					1.00	62864928.00	17469552.00	80334480.00
			2.50	LAMINAR	0.10	2666789.00	17469552.00	20136336.00
					0.30	8000366.00	17469552.00	25469904.00
					0.50	13333944.00	17469552.00	30803488.00
					0.70	18667520.00	17469552.00	36137072.00
					1.00	26667888.00	17469552.00	44137440.00
			3.00	LAMINAR	0.10	1324103.00	17469552.00	18793648.00
					0.30	3972310.00	17469552.00	21441856.00
					0.50	6620518.00	17469552.00	24090064.00
					0.70	9268725.00	17469552.00	26738272.00
					1.00	13241036.00	17469552.00	30710576.00
			3.50	LAMINAR	0.10	732997.81	17469552.00	18202544.00
					0.30	2198993.00	17469552.00	19668544.00
					0.50	3664988.00	17469552.00	21134528.00
					0.70	5130983.00	17469552.00	22600528.00
					1.00	7329977.00	17469552.00	24799520.00
			4.00	LAMINAR	0.10	439484.25	17469552.00	17909024.00
					0.30	1318452.00	17469552.00	18788000.00
					0.50	2197421.00	17469552.00	19666960.00
					0.70	3076389.00	17469552.00	20545936.00
					1.00	4394842.00	17469552.00	21864384.00
			5.00	LAMINAR	0.10	187374.44	17469552.00	17656912.00
					0.30	562123.19	17469552.00	18031664.00
					0.50	936872.00	17469552.00	18406416.00
					0.70	1311620.00	17469552.00	18781168.00
					1.00	1873744.00	17469552.00	19343296.00

NEW PARTICLE SIZE DISTRIBUTION WITH DM= 0.81

SURFACE AREA=1.750

PARTICLE SIZE (MICRONS)	PERCENT ( % )
200.0000	0.0097
100.0000	0.0114
80.0000	0.0447
52.0000	0.0607
37.0000	0.0747
27.0000	0.0976
19.0000	0.0901
14.0000	0.1181
9.3000	0.0941
6.5000	0.0746
4.7000	0.0689
3.3000	0.0575
2.3000	0.0532
1.5000	0.0380
1.0000	0.0441
0.5000	0.0624

CM	CV	PN	PK	ETA0	EINF	TAUY	B					
0.556	0.460	0.865	34.70	32.87	16.94	9.70	210.50					
SHEAR RATE-G =		1.00	2.00	3.00	4.00	5.00	6.00	7.00	8.00	9.00	10.00	
SHEAR STRESS-TAU =		41.44	71.24	99.45	126.36	152.16	177.05	201.15	224.57	247.41	269.74	
SHEAR RATE-G =		11.00	12.00	13.00	14.00	15.00	16.00	17.00	18.00	19.00	20.00	
SHEAR STRESS-TAU =		291.63	313.12	334.27	355.10	375.67	395.98	416.07	435.95	455.66	475.19	
SHEAR RATE-G =		21.00	22.00	23.00	24.00	25.00	26.00	27.00	28.00	29.00	30.00	
SHEAR STRESS-TAU =		494.58	513.83	532.94	551.95	570.84	589.63	608.33	626.95	645.49	663.95	
SHEAR RATE-G =		31.00	32.00	33.00	34.00	35.00	36.00	37.00	38.00	39.00	40.00	
SHEAR STRESS-TAU =		682.34	700.67	718.94	737.15	755.31	773.42	791.49	809.50	827.48	845.42	
SHEAR RATE-G =		41.00	42.00	43.00	44.00	45.00	46.00	47.00	48.00	49.00	50.00	
SHEAR STRESS-TAU =		863.32	881.19	899.02	916.83	934.60	952.34	970.06	987.75	1005.42	1023.07	

CV (%)	PN	PK	DIAMETER	FLOW	DISTANCE	PUMPING ENERGY	COMMUNITION ENERGY	TOTAL ENERGY
0.460	0.865	34.701	2.00	LAMINAR	0.10	13011739.00	12438715.00	25450448.00
					0.30	39035200.00	12438715.00	51473904.00
					0.50	65058672.00	12438715.00	77497376.00
					0.70	91082144.00	12438715.00	103520848.00
					1.00	130117360.00	12438715.00	142556064.00
			2.50	LAMINAR	0.10	5839538.00	12438715.00	18278240.00
					0.30	17518608.00	12438715.00	29957312.00
					0.50	29197680.00	12438715.00	41636384.00
					0.70	40876752.00	12438715.00	53315456.00
					1.00	58395376.00	12438715.00	70834480.00
			3.00	LAMINAR	0.10	3035890.00	12438715.00	15474605.00
					0.30	9107669.00	12438715.00	21546384.00
					0.50	15179648.00	12438715.00	27618160.00
					0.70	21251216.00	12438715.00	33689920.00
					1.00	30358896.00	12438715.00	42797600.00
			3.50	LAMINAR	0.10	17471425.00	12438715.00	14185840.00
					0.30	2415374.00	12438715.00	17680080.00
					0.50	167355624.00	12438715.00	21174336.00
					0.70	12229873.00	12438715.00	24668576.00
					1.00	17471248.00	12438715.00	29909952.00
			4.00	LAMINAR	0.10	1083236.00	12438715.00	13521951.00
					0.30	3249708.00	12438715.00	15688423.00
					0.50	5416180.00	12438715.00	17854880.00
					0.70	7582651.00	12438715.00	20021360.00
					1.00	10832340.00	12438715.00	23271072.00
			5.00	LAMINAR	0.10	488253.31	12438715.00	12926968.00
					0.30	1464759.00	12438715.00	13903474.00
					0.50	2441266.00	12438715.00	14879981.00
					0.70	3417772.00	12438715.00	15856487.00
					1.00	4882532.00	12438715.00	17321232.00

CM	CV	PN	PK	ETA0	EINF	TAUY	B				
0.556	0.430	0.901	16.99	16.12	9.78	6.03	110.39				
SHEAR RATE-G =		1.00	2.00	3.00	4.00	5.00	6.00	7.00	8.00	9.00	10.00
SHEAR STRESS-TAU =		21.81	36.97	51.60	65.78	79.57	93.02	106.17	119.05	131.70	144.14
SHEAR RATE-G =		11.00	12.00	13.00	14.00	15.00	16.00	17.00	18.00	19.00	20.00
SHEAR STRESS-TAU =		156.39	168.47	180.41	192.20	203.88	215.44	226.89	238.25	249.53	260.73
SHEAR RATE-G =		21.00	22.00	23.00	24.00	25.00	26.00	27.00	28.00	29.00	30.00
SHEAR STRESS-TAU =		271.85	282.90	293.89	304.83	315.71	326.53	337.32	348.05	358.75	369.41
SHEAR RATE-G =		31.00	32.00	33.00	34.00	35.00	36.00	37.00	38.00	39.00	40.00
SHEAR STRESS-TAU =		380.03	390.62	401.18	411.70	422.20	432.67	443.12	453.54	463.94	474.32
SHEAR RATE-G =		41.00	42.00	43.00	44.00	45.00	46.00	47.00	48.00	49.00	50.00
SHEAR STRESS-TAU =		484.68	495.01	505.34	515.64	525.92	536.19	546.45	556.69	566.92	577.13

CV (%)	PN	PK	DIAMETER	FLOW	DISTANCE	PUMPING ENERGY	COMMUNION ENERGY	TOTAL ENERGY
0.430	0.901	16.992	2.00	LAMINAR	0.10	9249159.00	12438715.00	21687872.00
					0.30	27747456.00	12438715.00	40186160.00
					0.50	46245776.00	12438715.00	58684480.00
					0.70	64744096.00	12438715.00	77182800.00
					1.00	92491568.00	12438715.00	104980272.00
			2.50	LAMINAR	0.10	4050722.00	12438715.00	16480272.00
					0.30	12152165.00	12438715.00	26489437.00
					0.50	20252165.00	12438715.00	32590880.00
					0.70	28352165.00	12438715.00	40792744.00
					1.00	40507216.00	12438715.00	52945920.00
			3.00	LAMINAR	0.10	2064317.00	12438715.00	14503032.00
					0.30	6192350.00	12438715.00	18631664.00
					0.50	10321584.00	12438715.00	22760288.00
					0.70	14450217.00	12438715.00	26888928.00
					1.00	20643168.00	12438715.00	33081872.00
			3.50	LAMINAR	0.10	1168175.00	12438715.00	13606890.00
					0.30	3504526.00	12438715.00	15943241.00
					0.50	5840878.00	12438715.00	18279584.00
					0.70	8177229.00	12438715.00	20615936.00
					1.00	11681756.00	12438715.00	24120464.00
			4.00	LAMINAR	0.10	713841.06	12438715.00	13152556.00
					0.30	2141522.00	12438715.00	14580237.00
					0.50	3569204.00	12438715.00	16007919.00
					0.70	4996886.00	12438715.00	17435600.00
					1.00	7138409.00	12438715.00	19577120.00
			5.00	LAMINAR	0.10	314112.75	12438715.00	12752827.00
					0.30	942338.12	12438715.00	13381053.00
					0.50	1570563.00	12438715.00	14009278.00
					0.70	2198788.00	12438715.00	14637503.00
					1.00	3141127.00	12438715.00	15579842.00



CM	CV	PN	PK	ETA0	EINF	TAUY	B					
0.556	0.384	0.937	7.57	7.27	5.22	3.14	46.52					
SHEAR RATE-G =		1.00	2.00	3.00	4.00	5.00	6.00	7.00	8.00	9.00	10.00	
SHEAR STRESS-TAU =		10.33	17.35	24.24	31.00	37.65	44.19	50.65	57.03	63.34	69.57	
SHEAR RATE-G =		11.00	12.00	13.00	14.00	15.00	16.00	17.00	18.00	19.00	20.00	
SHEAR STRESS-TAU =		75.75	81.88	87.95	93.97	99.96	105.90	111.80	117.68	123.52	129.33	
SHEAR RATE-G =		21.00	22.00	23.00	24.00	25.00	26.00	27.00	28.00	29.00	30.00	
SHEAR STRESS-TAU =		135.12	140.88	146.61	152.33	158.02	163.69	169.35	174.99	180.61	186.22	
SHEAR RATE-G =		31.00	32.00	33.00	34.00	35.00	36.00	37.00	38.00	39.00	40.00	
SHEAR STRESS-TAU =		191.81	197.39	202.95	208.51	214.05	219.58	225.10	230.61	236.11	241.60	
SHEAR RATE-G =		41.00	42.00	43.00	44.00	45.00	46.00	47.00	48.00	49.00	50.00	
SHEAR STRESS-TAU =		247.09	252.56	258.03	263.49	268.94	274.39	279.83	285.26	290.69	296.11	

CV (%)	PN	PK	DIAMETER	FLOW	DISTANCE	PUMPING ENERGY	COMMUNITION ENERGY	TOTAL ENERGY
0.384	0.937	7.569	2.00	LAMINAR	0.10	6571535.00	12438715.00	19010240.00
					0.30	19714592.00	12438715.00	32153296.00
					0.50	32857664.00	12438715.00	45296368.00
					0.70	46000736.00	12438715.00	58439440.00
					1.00	65715344.00	12438715.00	78154048.00
			2.50	LAMINAR	0.10	2809632.00	12438715.00	15248347.00
					0.30	8428896.00	12438715.00	20867600.00
					0.50	14048160.00	12438715.00	26486864.00
					0.70	19667408.00	12438715.00	32106112.00
					1.00	28096320.00	12438715.00	40535024.00
			3.00	LAMINAR	0.10	1403921.00	12438715.00	13842636.00
					0.30	4211764.00	12438715.00	16650479.00
					0.50	7019606.00	12438715.00	19458320.00
					0.70	9827448.00	12438715.00	22266160.00
					1.00	14039213.00	12438715.00	26477920.00
			3.50	LAMINAR	0.10	781321.56	12438715.00	13220036.00
					0.30	2343964.00	12438715.00	14782679.00
					0.50	3906607.00	12438715.00	16345322.00
					0.70	5469249.00	12438715.00	17907952.00
					1.00	7813214.00	12438715.00	20251920.00
			4.00	LAMINAR	0.10	470582.00	12438715.00	12909297.00
					0.30	1411745.00	12438715.00	13850460.00
					0.50	2352909.00	12438715.00	14791624.00
					0.70	3294073.00	12438715.00	15732788.00
					1.00	4705819.00	12438715.00	17144528.00
			5.00	LAMINAR	0.10	202106.62	12438715.00	12640821.00
					0.30	606319.81	12438715.00	13045034.00
					0.50	1010533.00	12438715.00	13449248.00
					0.70	1414746.00	12438715.00	13853461.00
					1.00	2021066.00	12438715.00	14459781.00

NEW PARTICLE SIZE DISTRIBUTION WITH DM= 0.91

SURFACE AREA=1.499

PARTICLE SIZE (MICRONS)	PERCENT ( % )
200.0000	0.0038
100.0000	0.0068
80.0000	0.0355
52.0000	0.0582
37.0000	0.0786
27.0000	0.1077
19.0000	0.1011
14.0000	0.1319
9.3000	0.1028
6.5000	0.0792
4.7000	0.0707
3.3000	0.0568
2.3000	0.0503
1.5000	0.0343
1.0000	0.0375
0.5000	0.0448

CM	CV	PN	PK	ETA0	EINF	TAUY	B				
0.545	0.460	0.840	44.64	43.18	20.11	10.13	225.28				
SHEAR RATE-G =		1.00	2.00	3.00	4.00	5.00	6.00	7.00	8.00	9.00	10.00
SHEAR STRESS-TAU =		51.16	88.64	123.40	156.02	186.96	216.52	244.95	272.44	299.15	325.19
SHEAR RATE-G =		11.00	12.00	13.00	14.00	15.00	16.00	17.00	18.00	19.00	20.00
SHEAR STRESS-TAU =		350.66	375.64	400.18	424.36	448.20	471.76	495.06	518.13	540.99	563.67
SHEAR RATE-G =		21.00	22.00	23.00	24.00	25.00	26.00	27.00	28.00	29.00	30.00
SHEAR STRESS-TAU =		586.18	608.54	630.76	652.86	674.84	696.72	718.50	740.20	761.81	783.34
SHEAR RATE-G =		31.00	32.00	33.00	34.00	35.00	36.00	37.00	38.00	39.00	40.00
SHEAR STRESS-TAU =		804.81	826.21	847.55	868.83	890.06	911.25	932.38	953.48	974.53	995.55
SHEAR RATE-G =		41.00	42.00	43.00	44.00	45.00	46.00	47.00	48.00	49.00	50.00
SHEAR STRESS-TAU =		1016.52	1037.47	1058.38	1079.27	1100.12	1120.95	1141.76	1162.54	1183.29	1204.03

CV (%)	PN	PK	DIAMETER	FLOW	DISTANCE	PUMPING ENERGY	COMUNITION ENERGY	TOTAL ENERGY
0.460	0.840	44.637	2.00	LAMINAR	0.10	14303017.00	9078418.00	23381424.00
					0.30	42909040.00	9078418.00	51987456.00
					0.50	71515072.00	9078418.00	80593488.00
					0.70	100121088.00	9078418.00	109199504.00
					1.00	143030144.00	9078418.00	152108560.00
			2.50	LAMINAR	0.10	6524334.00	9078418.00	15602752.00
					0.30	19572992.00	9078418.00	28651408.00
					0.50	32621664.00	9078418.00	41700080.00
					0.70	45670320.00	9078418.00	54748736.00
					1.00	65243328.00	9078418.00	74321744.00
			3.00	LAMINAR	0.10	3437079.00	9078418.00	12515497.00
					0.30	10311235.00	9078418.00	19389648.00
					0.50	17185392.00	9078418.00	26263808.00
					0.70	24059536.00	9078418.00	33137952.00
					1.00	34370784.00	9078418.00	43449200.00
			3.50	LAMINAR	0.10	2000136.00	9078418.00	11078554.00
					0.30	6000408.00	9078418.00	15078826.00
					0.50	10000680.00	9078418.00	19079088.00
					0.70	14000951.00	9078418.00	23079360.00
					1.00	20001360.00	9078418.00	29079776.00
			4.00	LAMINAR	0.10	1252002.00	9078418.00	10330420.00
					0.30	3756007.00	9078418.00	12834425.00
					0.50	6260013.00	9078418.00	15338431.00
					0.70	8764018.00	9078418.00	17842432.00
					1.00	12520026.00	9078418.00	21598432.00
			5.00	LAMINAR	0.10	573229.69	9078418.00	9651647.00
					0.30	1719688.00	9078418.00	10798104.00
					0.50	2866148.00	9078418.00	11944566.00
					0.70	4012607.00	9078418.00	13091025.00
					1.00	5732296.00	9078418.00	14810714.00

CM	CV	PN	PK	ETA0	EINF	TAUY	B					
0.545	0.430	0.884	20.18	19.29	10.95	6.11	112.84					
SHEAR RATE-G =		1.00	2.00	3.00	4.00	5.00	6.00	7.00	8.00	9.00	10.00	
SHEAR STRESS-TAU =		24.82	42.54	59.43	75.65	91.30	106.47	121.23	135.63	149.73	163.56	
SHEAR RATE-G =		11.00	12.00	13.00	14.00	15.00	16.00	17.00	18.00	19.00	20.00	
SHEAR STRESS-TAU =		177.16	190.54	203.75	216.79	229.68	242.44	255.09	267.62	280.06	292.41	
SHEAR RATE-G =		21.00	22.00	23.00	24.00	25.00	26.00	27.00	28.00	29.00	30.00	
SHEAR STRESS-TAU =		304.68	316.88	329.00	341.07	353.07	365.02	376.93	388.78	400.60	412.37	
SHEAR RATE-G =		31.00	32.00	33.00	34.00	35.00	36.00	37.00	38.00	39.00	40.00	
SHEAR STRESS-TAU =		424.11	435.81	447.48	459.13	470.74	482.32	493.88	505.42	516.93	528.43	
SHEAR RATE-G =		41.00	42.00	43.00	44.00	45.00	46.00	47.00	48.00	49.00	50.00	
SHEAR STRESS-TAU =		539.90	551.35	562.79	574.21	585.61	597.00	608.38	619.74	631.08	642.42	

CV (%)	PN	PK	DIAMETER	FLOW	DISTANCE	PUMPING ENERGY	COMMUNITION ENERGY	TOTAL ENERGY
0.430	0.884	20.181	2.00	LAMINAR	0.10	9809560.00	9078418.00	18887968.00
					0.30	29428672.00	9078418.00	38507088.00
					0.50	49047792.00	9078418.00	58126208.00
					0.70	68666896.00	9078418.00	77745312.00
					1.00	98095584.00	9078418.00	107174000.00
			2.50	LAMINAR	0.10	4346191.00	9078418.00	13424609.00
					0.30	13038571.00	9078418.00	22116976.00
					0.50	21730944.00	9078418.00	30809360.00
					0.70	30423328.00	9078418.00	39501744.00
					1.00	43461904.00	9078418.00	52540320.00
			3.00	LAMINAR	0.10	2235867.00	9078418.00	11314285.00
					0.30	6707601.00	9078418.00	15786012.00
					0.50	11179336.00	9078418.00	20257744.00
					0.70	15651070.00	9078418.00	24729488.00
					1.00	22358672.00	9078418.00	34437088.00
			3.50	LAMINAR	0.10	4275289.00	9078418.00	10353707.00
					0.30	12825868.00	9078418.00	12904286.00
					0.50	26376446.00	9078418.00	15454864.00
					0.70	38927024.00	9078418.00	18005440.00
					1.00	12752892.00	9078418.00	21831296.00
			4.00	LAMINAR	0.10	2784592.12	9078418.00	9863010.00
					0.30	8353776.00	9078418.00	11432194.00
					0.50	12922960.00	9078418.00	13001378.00
					0.70	18921433.00	9078418.00	14570561.00
					1.00	28459200.00	9078418.00	16924336.00
			5.00	LAMINAR	0.10	349086.87	9078418.00	9427504.00
					0.30	1047260.44	9078418.00	10125678.00
					0.50	1745434.00	9078418.00	10823852.00
					0.70	2443607.00	9078418.00	11522025.00
					1.00	3490868.00	9078418.00	12569286.00

CM	CV	PN	PK	ETA0	EINF	TAUY	B					
0.545	0.384	0.927	8.38	8.06	5.57	3.10	45.77					
SHEAR RATE-G =		1.00	2.00	3.00	4.00	5.00	6.00	7.00	8.00	9.00	10.00	
SHEAR STRESS-TAU =		11.04	18.74	26.24	33.56	40.74	47.79	54.72	61.54	68.28	74.93	
SHEAR RATE-G =		11.00	12.00	13.00	14.00	15.00	16.00	17.00	18.00	19.00	20.00	
SHEAR STRESS-TAU =		81.51	88.02	94.47	100.87	107.22	113.52	119.78	126.00	132.19	138.35	
SHEAR RATE-G =		21.00	22.00	23.00	24.00	25.00	26.00	27.00	28.00	29.00	30.00	
SHEAR STRESS-TAU =		144.47	150.57	156.65	162.69	168.72	174.73	180.71	186.68	192.64	198.57	
SHEAR RATE-G =		31.00	32.00	33.00	34.00	35.00	36.00	37.00	38.00	39.00	40.00	
SHEAR STRESS-TAU =		204.49	210.40	216.30	222.18	228.05	233.91	239.76	245.59	251.42	257.24	
SHEAR RATE-G =		41.00	42.00	43.00	44.00	45.00	46.00	47.00	48.00	49.00	50.00	
SHEAR STRESS-TAU =		263.06	268.86	274.66	280.45	286.23	292.00	297.77	303.53	309.29	315.04	

CV (%)	PN	PK	DIAMETER	FLOW	DISTANCE	PUMPING ENERGY	COMMUNITION ENERGY	TOTAL ENERGY
0.384	0.927	8.381	2.00	LAMINAR	0.10	6788870.00	9078418.00	15867288.00
					0.30	20366592.00	9078418.00	29445008.00
			0.50		33944336.00	9078418.00	43022752.00	
			0.70		47522080.00	9078418.00	56600496.00	
			1.00		67888688.00	9078418.00	76967104.00	
			2.50		2922824.00	9078418.00	12001242.00	
			0.10		8768472.00	9078418.00	17846880.00	
			0.30		14614120.00	9078418.00	23692528.00	
			0.50		20459760.00	9078418.00	29538176.00	
			0.70		29228240.00	9078418.00	38306656.00	
		3.00	1468770.00	9078418.00	10547188.00			
		0.10	4406309.00	9078418.00	13484727.00			
		0.30	7343849.00	9078418.00	16422267.00			
		0.50	10281388.00	9078418.00	19359792.00			
		0.70	14687698.00	9078418.00	23766112.00			
		3.50	821301.94	9078418.00	9899719.00			
		0.10	2463905.00	9078418.00	11542323.00			
		0.30	4106509.00	9078418.00	13184927.00			
		0.50	5749112.00	9078418.00	14827530.00			
		0.70	8213018.00	9078418.00	17291424.00			
4.00	496668.19	9078418.00	9575084.00					
0.10	1490004.00	9078418.00	10568422.00					
0.30	2483340.00	9078418.00	11561758.00					
0.50	3476676.00	9078418.00	12555094.00					
0.70	4966681.00	9078418.00	14048509.00					
5.00	214722.25	9078418.00	9293140.00					
0.10	644166.62	9078418.00	9222584.00					
0.30	1073611.00	9078418.00	10152029.00					
0.50	1503055.00	9078418.00	10581473.00					
0.70	2147222.00	9078418.00	11225640.00					

NEW PARTICLE SIZE DISTRIBUTION WITH DM= 1.06

SURFACE AREA=1.217

PARTICLE SIZE (MICRONS)	PERCENT ( % )
100.0000	0.0023
80.0000	0.0217
60.0000	0.0507
40.0000	0.0813
20.0000	0.1216
15.0000	0.1176
14.0000	0.1520
9.5000	0.1143
6.5000	0.0841
4.7000	0.0713
3.3000	0.0539
2.3000	0.0447
1.5000	0.0284
1.0000	0.0284
0.5000	0.0271

CM	CV	PN	PK	ETA0	EINF	TAUY	B					
0.531	0.460	0.807	64.10	65.90	26.15	11.17	249.40					
SHEAR RATE-G =		1.00	2.00	3.00	4.00	5.00	6.00	7.00	8.00	9.00	10.00	
SHEAR STRESS-TAU =		71.60	123.75	170.29	212.86	252.52	289.98	325.73	360.14	393.47	425.91	
SHEAR RATE-G =		11.00	12.00	13.00	14.00	15.00	16.00	17.00	18.00	19.00	20.00	
SHEAR STRESS-TAU =		457.63	488.74	519.33	549.48	579.26	608.71	637.88	666.80	695.50	724.01	
SHEAR RATE-G =		21.00	22.00	23.00	24.00	25.00	26.00	27.00	28.00	29.00	30.00	
SHEAR STRESS-TAU =		752.34	780.52	808.57	836.48	864.28	891.98	919.59	947.11	974.56	1001.93	
SHEAR RATE-G =		31.00	32.00	33.00	34.00	35.00	36.00	37.00	38.00	39.00	40.00	
SHEAR STRESS-TAU =		1029.24	1056.49	1083.68	1110.82	1137.91	1164.96	1191.96	1218.93	1245.86	1272.76	
SHEAR RATE-G =		41.00	42.00	43.00	44.00	45.00	46.00	47.00	48.00	49.00	50.00	
SHEAR STRESS-TAU =		1299.62	1326.46	1353.27	1380.05	1406.81	1433.54	1460.25	1486.94	1513.62	1540.27	

CV (%)	PN	PK	DIAMETER	FLOW	DISTANCE	PUMPING ENERGY	COMBINATION ENERGY	TOTAL ENERGY
0.460	0.807	64.097	2.00	LAMINAR	0.10	16610642.00	5947311.00	22557952.00
					0.30	49831904.00	5947311.00	55779200.00
					0.50	83053184.00	5947311.00	89000480.00
					0.70	116274464.00	5947311.00	122221760.00
					1.00	166106384.00	5947311.00	172053680.00
			2.50	LAMINAR	0.10	7745438.00	5947311.00	13692749.00
					0.30	23236304.00	5947311.00	29183600.00
					0.50	38727184.00	5947311.00	44674480.00
					0.70	54218048.00	5947311.00	60165344.00
					1.00	77454368.00	5947311.00	83401664.00
			3.00	LAMINAR	0.10	4154117.00	5947311.00	10101428.00
					0.30	12462350.00	5947311.00	18409648.00
					0.50	20770576.00	5947311.00	26717872.00
					0.70	29078816.00	5947311.00	35026112.00
					1.00	41541168.00	5947311.00	47488464.00
			3.50	LAMINAR	0.10	2454059.00	5947311.00	8401370.00
					0.30	7362177.00	5947311.00	13309488.00
					0.50	12270296.00	5947311.00	18217600.00
					0.70	17178400.00	5947311.00	23125696.00
					1.00	24540592.00	5947311.00	30487888.00
			4.00	LAMINAR	0.10	1556176.00	5947311.00	7503487.00
					0.30	4668528.00	5947311.00	10615839.00
					0.50	7780880.00	5947311.00	13728191.00
					0.70	10893231.00	5947311.00	16840528.00
					1.00	15561760.00	5947311.00	21509056.00
			5.00	LAMINAR	0.10	727868.44	5947311.00	6675179.00
					0.30	2183604.00	5947311.00	8130915.00
					0.50	3639341.00	5947311.00	9586652.00
					0.70	5095078.00	5947311.00	11042389.00
					1.00	7278683.00	5947311.00	13225994.00

CM	CV	PN	PK	ETA0	EINF	TAUY	B					
0.531	0.430	0.860	25.69	25.18	12.92	6.40	115.86					
SHEAR RATE-G =		1.00	2.00	3.00	4.00	5.00	6.00	7.00	8.00	9.00	10.00	
SHEAR STRESS-TAU =		30.41	52.47	73.07	92.53	111.08	128.90	146.13	162.86	179.18	195.15	
SHEAR RATE-G =		11.00	12.00	13.00	14.00	15.00	16.00	17.00	18.00	19.00	20.00	
SHEAR STRESS-TAU =		210.82	226.23	241.42	256.42	271.25	285.93	300.47	314.90	329.22	343.44	
SHEAR RATE-G =		21.00	22.00	23.00	24.00	25.00	26.00	27.00	28.00	29.00	30.00	
SHEAR STRESS-TAU =		357.58	371.64	385.63	399.56	413.43	427.24	441.01	454.73	468.41	482.05	
SHEAR RATE-G =		31.00	32.00	33.00	34.00	35.00	36.00	37.00	38.00	39.00	40.00	
SHEAR STRESS-TAU =		495.65	509.22	522.76	536.27	549.76	563.22	576.65	590.07	603.46	616.84	
SHEAR RATE-G =		41.00	42.00	43.00	44.00	45.00	46.00	47.00	48.00	49.00	50.00	
SHEAR STRESS-TAU =		630.20	643.54	656.86	670.17	683.46	696.74	710.01	723.27	736.51	749.74	

CV (%)	PN	PK	DIAMETER	FLOW	DISTANCE	PUMPING ENERGY	COMMUNITION ENERGY	TOTAL ENERGY
0.430	0.860	25.685	2.00	LAMINAR	0.10	10675684.00	5947311.00	16622995.00
					0.30	32027040.00	5947311.00	37974336.00
					0.50	53378400.00	5947311.00	59325696.00
					0.70	74729760.00	5947311.00	80677056.00
					1.00	106756816.00	5947311.00	112704112.00
			2.50	LAMINAR	0.10	4806441.00	5947311.00	10753752.00
					0.30	14419320.00	5947311.00	20366624.00
					0.50	24032192.00	5947311.00	29979488.00
					0.70	33645072.00	5947311.00	39592368.00
					1.00	48064400.00	5947311.00	54011696.00
			3.00	LAMINAR	0.10	2505165.00	5947311.00	8452476.00
					0.30	7515494.00	5947311.00	13462805.00
					0.50	12525824.00	5947311.00	18473120.00
					0.70	17536144.00	5947311.00	23483440.00
					1.00	25051648.00	5947311.00	30998944.00
			3.50	LAMINAR	0.10	1444695.00	5947311.00	7392006.00
					0.30	4334086.00	5947311.00	10281397.00
					0.50	7223477.00	5947311.00	13170788.00
					0.70	10112868.00	5947311.00	16060179.00
					1.00	14446955.00	5947311.00	20394256.00
			4.00	LAMINAR	0.10	897235.19	5947311.00	6844546.00
					0.30	2691705.00	5947311.00	8639016.00
					0.50	4486175.00	5947311.00	10433486.00
					0.70	6280644.00	5947311.00	12227955.00
					1.00	8972350.00	5947311.00	14919661.00
			5.00	LAMINAR	0.10	405446.94	5947311.00	6352757.00
					0.30	1216340.00	5947311.00	7163651.00
					0.50	2027234.00	5947311.00	7974545.00
					0.70	2838128.00	5947311.00	8785439.00
					1.00	4054469.00	5947311.00	10001780.00



CM	CV	PN	PK	ETA0	EINF	TAUY	B					
0.531	0.384	0.912	9.64	9.34	6.11	3.13	44.35					
SHEAR RATE - G =		1.00	2.00	3.00	4.00	5.00	6.00	7.00	8.00	9.00	10.00	
SHEAR STRESS - TAU =		12.25	20.99	29.42	37.58	45.52	53.28	60.87	68.33	75.67	82.91	
SHEAR RATE - G =		11.00	12.00	13.00	14.00	15.00	16.00	17.00	18.00	19.00	20.00	
SHEAR STRESS - TAU =		90.05	97.12	104.11	111.04	117.91	124.73	131.50	138.24	144.93	151.59	
SHEAR RATE - G =		21.00	22.00	23.00	24.00	25.00	26.00	27.00	28.00	29.00	30.00	
SHEAR STRESS - TAU =		158.22	164.81	171.38	177.93	184.45	190.96	197.44	203.91	210.35	216.79	
SHEAR RATE - G =		31.00	32.00	33.00	34.00	35.00	36.00	37.00	38.00	39.00	40.00	
SHEAR STRESS - TAU =		223.21	229.61	236.00	242.38	248.75	255.11	261.46	267.80	274.13	280.45	
SHEAR RATE - G =		41.00	42.00	43.00	44.00	45.00	46.00	47.00	48.00	49.00	50.00	
SHEAR STRESS - TAU =		286.76	293.07	299.37	305.66	311.95	318.23	324.51	330.77	337.04	343.30	

CV (%)	PN	PK	DIAMETER	FLOW	DISTANCE	PUMPING ENERGY	COMMUNITION ENERGY	TOTAL ENERGY
0.384	0.912	9.637	2.00	LAMINAR	0.10	7088198.00	5947311.00	13035509.00
					0.30	21264576.00	5947311.00	27211872.00
					0.50	35440976.00	5947311.00	41388272.00
					0.70	49617376.00	5947311.00	55564672.00
					1.00	70881968.00	5947311.00	76829264.00
			2.50	LAMINAR	0.10	3081517.00	5947311.00	9028828.00
					0.30	9244550.00	5947311.00	15191861.00
					0.50	15407584.00	5947311.00	21354880.00
					0.70	21570608.00	5947311.00	27517904.00
					1.00	30815168.00	5947311.00	36762464.00
			3.00	LAMINAR	0.10	1560786.00	5947311.00	7508097.00
					0.30	4682359.00	5947311.00	10629670.00
					0.50	7803933.00	5947311.00	13751244.00
					0.70	10925506.00	5947311.00	16872816.00
					1.00	15607866.00	5947311.00	21555168.00
			3.50	LAMINAR	0.10	878567.75	5947311.00	6825878.00
					0.30	2635702.00	5947311.00	8583013.00
					0.50	4392838.00	5947311.00	10340149.00
					0.70	6149973.00	5947311.00	12097284.00
					1.00	8785676.00	5947311.00	14732987.00
			4.00	LAMINAR	0.10	534341.19	5947311.00	6481652.00
					0.30	1603023.00	5947311.00	7550334.00
					0.50	2671705.00	5947311.00	8619016.00
					0.70	3740387.00	5947311.00	9687698.00
					1.00	5343411.00	5947311.00	11290722.00
			5.00	LAMINAR	0.10	233176.81	5947311.00	6180487.00
					0.30	699530.37	5947311.00	6646841.00
					0.50	1165884.00	5947311.00	7113195.00
					0.70	1632237.00	5947311.00	7579548.00
					1.00	2331768.00	5947311.00	8279079.00

NEW PARTICLE SIZE DISTRIBUTION WITH DM= 1.16

SURFACE AREA=1.076

PARTICLE SIZE (MICRONS)	PERCENT ( % )
100.0000	0.0009
80.0000	0.0141
60.0000	0.0439
40.0000	0.0810
20.0000	0.1299
10.0000	0.1285
5.0000	0.1651
3.0000	0.1209
1.5000	0.0861
0.7000	0.0704
0.3000	0.0512
0.1000	0.0406
0.0500	0.0246
0.0000	0.0233
0.5000	0.0194

CM	CV	PN	PK	ETA0	EINF	TAUY	B					
0.523	0.460	0.790	79.69	87.00	31.02	12.12	265.18					
SHEAR RATE-G =		1.00	2.00	3.00	4.00	5.00	6.00	7.00	8.00	9.00	10.00	
SHEAR STRESS-TAU =		89.36	152.88	208.00	257.60	303.38	346.42	387.41	426.83	465.03	502.25	
SHEAR RATE-G =		11.00	12.00	13.00	14.00	15.00	16.00	17.00	18.00	19.00	20.00	
SHEAR STRESS-TAU =		538.69	574.48	609.73	644.53	678.94	713.03	746.84	780.40	813.75	846.91	
SHEAR RATE-G =		21.00	22.00	23.00	24.00	25.00	26.00	27.00	28.00	29.00	30.00	
SHEAR STRESS-TAU =		879.90	912.74	945.46	978.05	1010.54	1042.94	1075.24	1107.47	1139.63	1171.72	
SHEAR RATE-G =		31.00	32.00	33.00	34.00	35.00	36.00	37.00	38.00	39.00	40.00	
SHEAR STRESS-TAU =		1203.75	1235.73	1267.65	1299.53	1331.37	1363.16	1394.92	1426.65	1458.34	1490.00	
SHEAR RATE-G =		41.00	42.00	43.00	44.00	45.00	46.00	47.00	48.00	49.00	50.00	
SHEAR STRESS-TAU =		1521.63	1553.24	1584.82	1616.38	1647.92	1679.44	1710.93	1742.41	1773.88	1805.32	

CV (%)	PN	PK	DIAMETER	FLOW	DISTANCE	PUMPING ENERGY	COMMUNITION ENERGY	TOTAL ENERGY
0.460	0.790	79.694	2.00	LAMINAR	0.10	18436416.00	4638086.00	23074496.00
					0.30	55709248.00	4638086.00	59947328.00
					0.50	92182080.00	4638086.00	96820160.00
					0.70	129054912.00	4638086.00	133692992.00
					1.00	184364176.00	4638086.00	189002256.00
			2.50	LAMINAR	0.10	8698430.00	4638086.00	13336516.00
					0.30	26095280.00	4638086.00	30733360.00
					0.50	43492144.00	4638086.00	48130224.00
					0.70	60888992.00	4638086.00	65527072.00
					1.00	86984288.00	4638086.00	91622368.00
			3.00	LAMINAR	0.10	4710145.00	4638086.00	9348231.00
					0.30	14130432.00	4638086.00	18768512.00
					0.50	23550720.00	4638086.00	28188800.00
					0.70	32970992.00	4638086.00	37609072.00
					1.00	47101440.00	4638086.00	51739520.00
			3.50	LAMINAR	0.10	2805103.00	4638086.00	7443189.00
					0.30	8415307.00	4638086.00	13053393.00
					0.50	14025512.00	4638086.00	18663584.00
					0.70	19635712.00	4638086.00	24273792.00
					1.00	28051024.00	4638086.00	32689104.00
			4.00	LAMINAR	0.10	1791179.00	4638086.00	6429265.00
					0.30	5373537.00	4638086.00	10011623.00
					0.50	8955896.00	4638086.00	13593982.00
					0.70	12538254.00	4638086.00	17176336.00
					1.00	17911792.00	4638086.00	22549872.00
			5.00	LAMINAR	0.10	847450.56	4638086.00	5485536.00
					0.30	2542351.00	4638086.00	7180437.00
					0.50	4237252.00	4638086.00	8875338.00
					0.70	5932152.00	4638086.00	10570238.00
					1.00	8474504.00	4638086.00	13112590.00

CM	CV	PN	PK	ETA0	EINF	TAUY	B					
0.523	0.430	0.846	29.59	29.76	14.32	6.71	116.92					
SHEAR RATE-G =		1.00	2.00	3.00	4.00	5.00	6.00	7.00	8.00	9.00	10.00	
SHEAR STRESS-TAU =		34.67	59.78	82.85	104.41	124.81	144.31	163.11	181.33	199.07	216.43	
SHEAR RATE-G =		11.00	12.00	13.00	14.00	15.00	16.00	17.00	18.00	19.00	20.00	
SHEAR STRESS-TAU =		233.46	250.21	266.73	283.04	299.17	315.15	331.00	346.72	362.34	377.87	
SHEAR RATE-G =		21.00	22.00	23.00	24.00	25.00	26.00	27.00	28.00	29.00	30.00	
SHEAR STRESS-TAU =		393.31	408.67	423.97	439.20	454.38	469.51	484.59	499.62	514.62	529.58	
SHEAR RATE-G =		31.00	32.00	33.00	34.00	35.00	36.00	37.00	38.00	39.00	40.00	
SHEAR STRESS-TAU =		544.51	559.40	574.27	589.11	603.93	618.72	633.50	648.25	662.98	677.70	
SHEAR RATE-G =		41.00	42.00	43.00	44.00	45.00	46.00	47.00	48.00	49.00	50.00	
SHEAR STRESS-TAU =		692.40	707.08	721.75	736.41	751.05	765.68	780.30	794.91	809.51	824.10	

CV (%)	PN	PK	DIAMETER	FLOW	DISTANCE	PUMPING ENERGY	COMMUNITION ENERGY	TOTAL ENERGY						
0.430	0.846	29.588	2.00	LAMINAR	0.10	11260996.00	4638086.00	15899082.00						
					0.30	33782976.00	4638086.00	38421056.00						
					0.50	56304960.00	4638086.00	60943040.00						
					0.70	78826944.00	4638086.00	83465024.00						
					1.00	112609936.00	4638086.00	117248016.00						
					2.50	LAMINAR	0.10	5115991.00	4638086.00	9754077.00				
							0.30	15347971.00	4638086.00	19986048.00				
							0.50	25579952.00	4638086.00	30218032.00				
							0.70	35811920.00	4638086.00	40450000.00				
							1.00	51159904.00	4638086.00	55797984.00				
							3.00	LAMINAR	0.10	2686229.00	4638086.00	7324315.00		
									0.30	8058686.00	4638086.00	12696772.00		
									0.50	13431144.00	4638086.00	18069216.00		
									0.70	18803600.00	4638086.00	23441680.00		
									1.00	26862288.00	4638086.00	31500368.00		
									3.50	LAMINAR	0.10	1558741.00	4638086.00	6196827.00
											0.30	4676223.00	4638086.00	9314309.00
											0.50	7793705.00	4638086.00	12431791.00
											0.70	10911186.00	4638086.00	15549272.00
											1.00	15587410.00	4638086.00	20225488.00
4.00	LAMINAR	0.10	973272.87	4638086.00							5611358.00			
		0.30	2919818.00	4638086.00							7557904.00			
		0.50	4866363.00	4638086.00							9504449.00			
		0.70	6812908.00	4638086.00							11450994.00			
		1.00	9732727.00	4638086.00							14370813.00			
		5.00	LAMINAR	0.10	443697.56	4638086.00					5081783.00			
				0.30	1331092.00	4638086.00					5969178.00			
				0.50	2218487.00	4638086.00					6856573.00			
				0.70	3105882.00	4638086.00					7743968.00			
				1.00	4436975.00	4638086.00					9075061.00			

CM	CV	PN	PK	ETA0	EINF	TAUY	B					
0.523	0.384	0.904	10.44	10.22	6.46	3.20	43.11					
SHEAR RATE-G =		1.00	2.00	3.00	4.00	5.00	6.00	7.00	8.00	9.00	10.00	
SHEAR STRESS-TAU =		13.12	22.52	31.51	40.18	48.57	56.75	64.73	72.57	80.26	87.84	
SHEAR RATE-G =		11.00	12.00	13.00	14.00	15.00	16.00	17.00	18.00	19.00	20.00	
SHEAR STRESS-TAU =		95.32	102.72	110.03	117.28	124.47	131.61	138.69	145.74	152.74	159.71	
SHEAR RATE-G =		21.00	22.00	23.00	24.00	25.00	26.00	27.00	28.00	29.00	30.00	
SHEAR STRESS-TAU =		166.65	173.56	180.45	187.31	194.15	200.96	207.76	214.54	221.31	228.06	
SHEAR RATE-G =		31.00	32.00	33.00	34.00	35.00	36.00	37.00	38.00	39.00	40.00	
SHEAR STRESS-TAU =		234.79	241.52	248.23	254.93	261.62	268.30	274.97	281.63	288.28	294.93	
SHEAR RATE-G =		41.00	42.00	43.00	44.00	45.00	46.00	47.00	48.00	49.00	50.00	
SHEAR STRESS-TAU =		301.57	308.20	314.82	321.44	328.06	334.66	341.27	347.86	354.46	361.04	

CV (%)	PN	PK	DIAMETER	FLOW	DISTANCE	PUMPING ENERGY	COMMUNION ENERGY	TOTAL ENERGY
0.384	0.904	10.443	2.00	LAMINAR	0.10	7264888.00	4638086.00	11902974.00
					0.30	21794656.00	4638086.00	26432736.00
					0.50	363224432.00	4638086.00	409622512.00
					0.70	508554192.00	4638086.00	554922272.00
					1.00	726488664.00	4638086.00	77286944.00
			2.50	LAMINAR	0.10	3176099.00	4638086.00	7814185.00
					0.30	9528297.00	4638086.00	14166383.00
					0.50	15880494.00	4638086.00	20518576.00
					0.70	222232688.00	4638086.00	26870776.00
					1.00	31760999.00	4638086.00	36399072.00
			3.00	LAMINAR	0.10	1616095.00	4638086.00	6254181.00
					0.30	4848286.00	4638086.00	9486372.00
					0.50	8080477.00	4638086.00	12718563.00
					0.70	11312666.00	4638086.00	15950754.00
					1.00	16160995.00	4638086.00	2079040.00
			3.50	LAMINAR	0.10	2719249.19	4638086.00	5551299.00
					0.30	2737627.00	4638086.00	7377725.00
					0.50	43566065.00	4638086.00	9204151.00
					0.70	63392490.00	4638086.00	110330576.00
					1.00	9132130.00	4638086.00	13770216.00
			4.00	LAMINAR	0.10	557258.12	4638086.00	5195344.00
					0.30	1671774.00	4638086.00	6309860.00
					0.50	2786290.00	4638086.00	7424376.00
					0.70	3008005.00	4638086.00	8538891.00
					1.00	5572580.00	4638086.00	10210666.00
			5.00	LAMINAR	0.10	244516.62	4638086.00	4882602.00
					0.30	733549.81	4638086.00	5371635.00
					0.50	1222583.00	4638086.00	5860669.00
					0.70	1711616.00	4638086.00	6349702.00
					1.00	2445166.00	4638086.00	7083252.00

NEW PARTICLE SIZE DISTRIBUTION WITH DM= 1.26

SURFACE AREA=0.964

PARTICLE SIZE (MICRONS)	PERCENT ( % )
80.0000	0.0084
52.0000	0.0366
37.0000	0.0792
27.0000	0.1373
19.0000	0.1894
14.0000	0.1778
9.3000	0.1268
6.5000	0.0873
4.7000	0.0688
3.3000	0.0480
2.3000	0.0365
1.5000	0.0211
1.0000	0.0189
0.5000	0.0158

CM	CV	PN	PK	ETA0	EINF	TAUY	B					
0.516	0.460	0.775	98.29	115.89	36.95	13.39	282.91					
SHEAR RATE-G =		1.00	2.00	3.00	4.00	5.00	6.00	7.00	8.00	9.00	10.00	
SHEAR STRESS-TAU =		112.06	188.62	253.15	310.41	362.93	412.20	459.15	504.37	548.27	591.15	
SHEAR RATE-G =		11.00	12.00	13.00	14.00	15.00	16.00	17.00	18.00	19.00	20.00	
SHEAR STRESS-TAU =		633.22	674.63	715.50	755.93	795.98	835.71	875.18	914.41	953.44	992.29	
SHEAR RATE-G =		21.00	22.00	23.00	24.00	25.00	26.00	27.00	28.00	29.00	30.00	
SHEAR STRESS-TAU =		1030.99	1069.55	1107.99	1146.32	1184.55	1222.70	1260.77	1298.77	1336.70	1374.58	
SHEAR RATE-G =		31.00	32.00	33.00	34.00	35.00	36.00	37.00	38.00	39.00	40.00	
SHEAR STRESS-TAU =		1412.40	1450.18	1487.90	1525.59	1563.24	1600.85	1638.43	1675.98	1713.50	1751.00	
SHEAR RATE-G =		41.00	42.00	43.00	44.00	45.00	46.00	47.00	48.00	49.00	50.00	
SHEAR STRESS-TAU =		1788.47	1825.92	1863.34	1900.75	1938.14	1975.51	2012.86	2050.20	2087.52	2124.83	

CV (%)	PN	PK	DIAMETER	FLOW	DISTANCE	PUMPING ENERGY	COMMUNITION ENERGY	TOTAL ENERGY
0.460	0.775	98.295	2.00	LAMINAR	0.10	20703232.00	3711356.00	24414576.00
					0.30	62109712.00	7111356.00	65821056.00
					0.50	103516208.00	7111356.00	107227552.00
					0.70	144922688.00	7111356.00	148624032.00
					1.00	207032416.00	7111356.00	210743760.00
			2.50	LAMINAR	0.10	9863344.00	7111356.00	13574700.00
					0.30	29590016.00	7111356.00	33301360.00
					0.50	49316704.00	7111356.00	53028048.00
					0.70	69043392.00	7111356.00	72754736.00
					1.00	98633424.00	7111356.00	102344768.00
			3.00	LAMINAR	0.10	5383420.00	7111356.00	9094776.00
					0.30	16150258.00	7111356.00	19861600.00
					0.50	26917088.00	7111356.00	30628432.00
					0.70	37683920.00	7111356.00	41395264.00
					1.00	53834192.00	7111356.00	57545536.00
			3.50	LAMINAR	0.10	3227525.00	7111356.00	6938881.00
					0.30	9682574.00	7111356.00	13393930.00
					0.50	16137624.00	7111356.00	19848976.00
					0.70	22592672.00	7111356.00	26304016.00
					1.00	32275248.00	7111356.00	35986592.00
			4.00	LAMINAR	0.10	2072779.00	7111356.00	5784135.00
					0.30	6218337.00	7111356.00	9929693.00
					0.50	10363896.00	7111356.00	14075252.00
					0.70	14509454.00	7111356.00	18220800.00
					1.00	20727792.00	7111356.00	24439136.00
			5.00	LAMINAR	0.10	990061.19	7111356.00	4701417.00
					0.30	2970183.00	7111356.00	6681539.00
					0.50	4950305.00	7111356.00	8661661.00
					0.70	6930426.00	7111356.00	10641782.00
					1.00	9900610.00	3711356.00	13611966.00

CM	CV	PN	PK	ETA0	EINF	TAUY	B				
0.516	0.430	0.834	33.79	35.16	15.85	7.14	117.92				
SHEAR RATE-G =		1.00	2.00	3.00	4.00	5.00	6.00	7.00	8.00	9.00	10.00
SHEAR STRESS-TAU =		39.58	67.93	93.53	117.20	139.46	160.66	181.05	200.79	220.01	238.82
SHEAR RATE-G =		11.00	12.00	13.00	14.00	15.00	16.00	17.00	18.00	19.00	20.00
SHEAR STRESS-TAU =		257.28	275.45	293.37	311.09	328.64	346.03	363.28	380.42	397.46	414.40
SHEAR RATE-G =		21.00	22.00	23.00	24.00	25.00	26.00	27.00	28.00	29.00	30.00
SHEAR STRESS-TAU =		431.26	448.05	464.78	481.45	498.06	514.63	531.15	547.64	564.08	580.50
SHEAR RATE-G =		31.00	32.00	33.00	34.00	35.00	36.00	37.00	38.00	39.00	40.00
SHEAR STRESS-TAU =		596.88	613.24	629.57	645.87	662.15	678.42	694.66	710.88	727.09	743.28
SHEAR RATE-G =		41.00	42.00	43.00	44.00	45.00	46.00	47.00	48.00	49.00	50.00
SHEAR STRESS-TAU =		759.46	775.62	791.78	807.91	824.04	840.16	856.26	872.36	888.45	904.53

CV (%)	PN	PK	DIAMETER	FLOW	DISTANCE	PUMPING ENERGY	COMMUNITION ENERGY	TOTAL ENERGY
0.430	0.834	33.793	2.00	LAMINAR	0.10	11908868.00	3711356.00	15620224.00
					0.30	55726592.00	7113356.00	39437936.00
					0.50	9544320.00	7113356.00	63255664.00
					0.70	83362048.00	7113356.00	87073392.00
					1.00	11908868.00	7113356.00	122800000.00
			2.50	LAMINAR	0.10	5453329.00	7113356.00	9164685.00
					0.30	16359984.00	7113356.00	20071328.00
					0.50	27266640.00	7113356.00	30977984.00
					0.70	38173280.00	7113356.00	41884624.00
					1.00	54533280.00	7113356.00	58244624.00
			3.00	LAMINAR	0.10	2881843.00	7113356.00	6593199.00
					0.30	8645529.00	7113356.00	12356885.00
					0.50	14409216.00	7113356.00	18120560.00
					0.70	20172896.00	7113356.00	23884240.00
					1.00	28818432.00	7113356.00	32529776.00
			3.50	LAMINAR	0.10	1681371.00	7113356.00	5392727.00
					0.30	5044113.00	7113356.00	8755469.00
					0.50	8406856.00	7113356.00	12118212.00
					0.70	11769598.00	7113356.00	15480954.00
					1.00	16813712.00	7113356.00	20525056.00
			4.00	LAMINAR	0.10	1054768.00	7113356.00	4766124.00
					0.30	3164303.00	7113356.00	6875659.00
					0.50	5273839.00	7113356.00	8985195.00
					0.70	7383374.00	7113356.00	11094730.00
					1.00	10547678.00	7113356.00	14259034.00
			5.00	LAMINAR	0.10	484599.69	7113356.00	4195951.00
					0.30	1453798.00	7113356.00	5165154.00
					0.50	2422998.00	7113356.00	6134454.00
					0.70	3392197.00	7113356.00	7103754.00
					1.00	4845996.00	7113356.00	8557352.00



CM	CV	PN	PK	ETA0	EINF	TAUY	B						
0.516	0.384	0.896	11.25	11.14	6.81	3.32	41.85						
SHEAR RATE-G =		1.00	2.00	3.00	4.00	5.00	6.00	7.00	8.00	9.00	10.00		
SHEAR STRESS-TAU =		14.05	24.12	33.66	42.81	51.64	60.21	68.57	76.75	84.79	92.70		
SHEAR RATE-G =		11.00	12.00	13.00	14.00	15.00	16.00	17.00	18.00	19.00	20.00		
SHEAR STRESS-TAU =		100.50	108.21	115.85	123.41	130.91	138.36	145.76	153.12	160.44	167.72		
SHEAR RATE-G =		21.00	22.00	23.00	24.00	25.00	26.00	27.00	28.00	29.00	30.00		
SHEAR STRESS-TAU =		174.97	182.20	189.40	196.58	203.73	210.87	217.99	225.09	232.18	239.25		
SHEAR RATE-G =		31.00	32.00	33.00	34.00	35.00	36.00	37.00	38.00	39.00	40.00		
SHEAR STRESS-TAU =		246.31	253.36	260.39	267.42	274.44	281.44	288.44	295.43	302.42	309.39		
SHEAR RATE-G =		41.00	42.00	43.00	44.00	45.00	46.00	47.00	48.00	49.00	50.00		
SHEAR STRESS-TAU =		316.36	323.33	330.28	337.24	344.18	351.12	358.06	364.99	371.92	378.85		

CV (%)	PN	PK	DIAMETER	FLOW	DISTANCE	PUMPING ENERGY	COMMUNITION ENERGY	TOTAL ENERGY
0.384	0.896	11.247	2.00	LAMINAR	0.10	7443950.00	3711356.00	11155306.00
					0.30	22331840.00	7113556.00	26043184.00
					0.50	37219744.00	7113556.00	40931088.00
					0.70	52107632.00	7113556.00	55818976.00
					1.00	74439488.00	7113556.00	78150832.00
			2.50	LAMINAR	0.10	3270819.00	7113556.00	6982175.00
					0.30	9812457.00	7113556.00	13523813.00
					0.50	16354096.00	7113556.00	20065440.00
					0.70	22895728.00	7113556.00	26607072.00
					1.00	32708192.00	7113556.00	36419536.00
			3.00	LAMINAR	0.10	1671140.00	7113556.00	5382496.00
					0.30	5013421.00	7113556.00	8724777.00
					0.50	8355703.00	7113556.00	12067059.00
					0.70	11697984.00	7113556.00	15409340.00
					1.00	16711406.00	7113556.00	20422752.00
			3.50	LAMINAR	0.10	947599.00	7113556.00	465589.00
					0.30	2842796.00	7113556.00	6554152.00
					0.50	4737994.00	7113556.00	8449350.00
					0.70	6633191.00	7113556.00	10344547.00
					1.00	9475989.00	7113556.00	13187344.00
			4.00	LAMINAR	0.10	579977.62	7113556.00	4291333.00
					0.30	1739932.00	7113556.00	5451288.00
					0.50	2899887.00	7113556.00	6611243.00
					0.70	4059842.00	7113556.00	7771198.00
					1.00	5799775.00	7113556.00	9511153.00
			5.00	LAMINAR	0.10	255752.75	7113556.00	3967108.00
					0.30	767259.12	7113556.00	447866.14.00
					0.50	1278763.00	7113556.00	4990119.00
					0.70	1790268.00	7113556.00	5501624.00
					1.00	2557527.00	7113556.00	6268883.00

NEW PARTICLE SIZE DISTRIBUTION WITH DM= 1.36

SURFACE AREA=0.875

PARTICLE SIZE (MICRONS)	PERCENT ( % )
80.0000	0.0046
52.0000	0.0292
37.0000	0.0759
27.0000	0.1438
19.0000	0.1502
14.0000	0.1902
9.3000	0.1318
6.5000	0.0876
4.7000	0.0666
3.3000	0.0446
2.3000	0.0324
1.5000	0.0179
1.0000	0.0152
0.5000	0.0099

CM	CV	PN	PK	ETA0	EINF	TAUY	B					
0.511	0.460	0.766	116.81	150.06	43.21	14.83	296.61					
SHEAR RATE-G =		1.00	2.00	3.00	4.00	5.00	6.00	7.00	8.00	9.00	10.00	
SHEAR STRESS-TAU =		136.60	225.46	298.52	362.76	421.60	476.87	529.68	580.70	630.40	679.08	
SHEAR RATE-G =		11.00	12.00	13.00	14.00	15.00	16.00	17.00	18.00	19.00	20.00	
SHEAR STRESS-TAU =		726.97	774.22	820.96	867.28	913.25	958.93	1004.35	1049.56	1094.59	1139.46	
SHEAR RATE-G =		21.00	22.00	23.00	24.00	25.00	26.00	27.00	28.00	29.00	30.00	
SHEAR STRESS-TAU =		1184.19	1228.79	1273.29	1317.69	1362.01	1406.25	1450.41	1494.52	1538.57	1582.57	
SHEAR RATE-G =		31.00	32.00	33.00	34.00	35.00	36.00	37.00	38.00	39.00	40.00	
SHEAR STRESS-TAU =		1626.52	1670.43	1714.30	1758.14	1801.94	1845.71	1889.45	1933.16	1976.86	2020.52	
SHEAR RATE-G =		41.00	42.00	43.00	44.00	45.00	46.00	47.00	48.00	49.00	50.00	
SHEAR STRESS-TAU =		2064.17	2107.80	2151.41	2195.00	2238.58	2282.14	2325.69	2369.22	2412.74	2456.25	

CV (%)	PN	PK	DIAMETER	FLOW	DISTANCE	PUMPING ENERGY	COMMUNITION ENERGY	TOTAL ENERGY
0.460	0.766	116.805	2.00	LAMINAR	0.10	23165184.00	3043153.00	26208336.00
					0.30	69495568.00	3043153.00	72538720.00
					0.50	115825952.00	3043153.00	118869104.00
					0.70	162156336.00	3043153.00	165199488.00
					1.00	231651920.00	3043153.00	234695072.00
			2.50	LAMINAR	0.10	11105377.00	3043153.00	14148530.00
					0.30	33316112.00	3043153.00	36349264.00
					0.50	55526864.00	3043153.00	58570016.00
					0.70	77737616.00	3043153.00	80780768.00
					1.00	111053744.00	3043153.00	114096896.00
			3.00	LAMINAR	0.10	6092142.00	3043153.00	9135295.00
					0.30	18276416.00	3043153.00	21319568.00
					0.50	30440704.00	3043153.00	33473856.00
					0.70	42644976.00	3043153.00	45688128.00
					1.00	60921408.00	3043153.00	63964560.00
			3.50	LAMINAR	0.10	3668092.00	3043153.00	6711245.00
					0.30	11004274.00	3043153.00	14047427.00
					0.50	18340448.00	3043153.00	21383600.00
					0.70	25676624.00	3043153.00	28719776.00
					1.00	36680912.00	3043153.00	39724064.00
			4.00	LAMINAR	0.10	2364454.00	3043153.00	5407607.00
					0.30	7093363.00	3043153.00	10136516.00
					0.50	11822272.00	3043153.00	14865425.00
					0.70	16551180.00	3043153.00	19594320.00
					1.00	23644544.00	3043153.00	26687696.00
			5.00	LAMINAR	0.10	1136792.00	3043153.00	4179445.00
					0.30	3408878.00	3043153.00	6452031.00
					0.50	5681463.00	3043153.00	8724616.00
					0.70	7954048.00	3043153.00	10997201.00
					1.00	11362927.00	3043153.00	14406080.00

CM	CV	PN	PK	ETA0	EINF	TAUY	B					
0.511	0.430	0.826	37.59	40.63	17.29	7.64	117.28					
SHEAR RATE-G =		1.00	2.00	3.00	4.00	5.00	6.00	7.00	8.00	9.00	10.00	
SHEAR STRESS-TAU =		44.39	75.61	103.36	128.79	152.60	175.22	196.96	218.02	238.54	258.63	
SHEAR RATE-G =		11.00	12.00	13.00	14.00	15.00	16.00	17.00	18.00	19.00	20.00	
SHEAR STRESS-TAU =		278.38	297.83	317.05	336.06	354.90	373.60	392.17	410.62	428.98	447.26	
SHEAR RATE-G =		21.00	22.00	23.00	24.00	25.00	26.00	27.00	28.00	29.00	30.00	
SHEAR STRESS-TAU =		465.46	483.59	501.66	519.68	537.66	555.58	573.47	591.32	609.14	626.93	
SHEAR RATE-G =		31.00	32.00	33.00	34.00	35.00	36.00	37.00	38.00	39.00	40.00	
SHEAR STRESS-TAU =		644.69	662.43	680.14	697.84	715.51	733.16	750.80	768.42	786.03	803.62	
SHEAR RATE-G =		41.00	42.00	43.00	44.00	45.00	46.00	47.00	48.00	49.00	50.00	
SHEAR STRESS-TAU =		821.20	838.77	856.32	873.87	891.40	908.93	926.44	943.95	961.45	978.95	

CV (%)	PN	PK	DIAMETER	FLOW	DISTANCE	PUMPING ENERGY	COMMUNITION ENERGY	TOTAL ENERGY
0.430	0.826	37.593	2.00	LAMINAR	0.10	12524662.00	3043153.00	15567815.00
					0.30	37573968.00	3043153.00	40617120.00
					0.50	62623296.00	3043153.00	65666448.00
					0.70	87672608.00	3043153.00	90715760.00
					1.00	125246592.00	3043153.00	128289744.00
			2.50	LAMINAR	0.10	5768521.00	3043153.00	8811674.00
					0.30	17305552.00	3043153.00	20348704.00
					0.50	28842592.00	3043153.00	31885744.00
					0.70	40379632.00	3043153.00	43422784.00
					1.00	57685200.00	3043153.00	60728352.00
			3.00	LAMINAR	0.10	3062837.00	3043153.00	6105990.00
					0.30	9188510.00	3043153.00	12231663.00
					0.50	15314184.00	3043153.00	18357328.00
					0.70	21439856.00	3043153.00	24483008.00
					1.00	30628368.00	3043153.00	33671520.00
			3.50	LAMINAR	0.10	1794083.00	3043153.00	4837236.00
					0.30	5382249.00	3043153.00	8425402.00
					0.50	8970416.00	3043153.00	12013599.00
					0.70	12558582.00	3043153.00	15601785.00
					1.00	17940832.00	3043153.00	20983984.00
			4.00	LAMINAR	0.10	1129357.00	3043153.00	4172510.00
					0.30	3388072.00	3043153.00	6431925.00
					0.50	5646787.00	3043153.00	8689940.00
					0.70	7905501.00	3043153.00	10948654.00
					1.00	112937574.00	3043153.00	14336727.00
			5.00	LAMINAR	0.10	1565522.06	3043153.00	3564995.00
					0.30	4699210.00	3043153.00	4608679.00
					0.50	76552893.00	3043153.00	5652363.00
					0.70	10618420.00	3043153.00	6696046.00
					1.00	5218420.00	3043153.00	8261573.00

CM	CV	PN	PK	ETA0	EINF	TAUY	B					
0.511	0.384	0.890	11.92	11.99	7.12	3.47	40.25					
SHEAR RATE-G =		1.00	2.00	3.00	4.00	5.00	6.00	7.00	8.00	9.00	10.00	
SHEAR STRESS-TAU =		14.93	25.55	35.55	45.08	54.24	63.12	71.77	80.23	88.54	96.71	
SHEAR RATE-G =		11.00	12.00	13.00	14.00	15.00	16.00	17.00	18.00	19.00	20.00	
SHEAR STRESS-TAU =		104.78	112.75	120.65	128.47	136.24	143.95	151.61	159.23	166.82	174.37	
SHEAR RATE-G =		21.00	22.00	23.00	24.00	25.00	26.00	27.00	28.00	29.00	30.00	
SHEAR STRESS-TAU =		181.90	189.39	196.87	204.32	211.75	219.16	226.56	233.94	241.31	248.66	
SHEAR RATE-G =		31.00	32.00	33.00	34.00	35.00	36.00	37.00	38.00	39.00	40.00	
SHEAR STRESS-TAU =		256.01	263.34	270.66	277.97	285.27	292.57	299.86	307.14	314.41	321.68	
SHEAR RATE-G =		41.00	42.00	43.00	44.00	45.00	46.00	47.00	48.00	49.00	50.00	
SHEAR STRESS-TAU =		328.94	336.20	343.45	350.69	357.93	365.17	372.40	379.63	386.85	394.07	

CV (%)	PN	PK	DIAMETER	FLOW	DISTANCE	PUMPING ENERGY	COMMUNITION ENERGY	TOTAL ENERGY
0.384	0.890	11.925	2.00	LAMINAR	0.10	7595696.00	3043153.00	10638849.00
					0.30	22787072.00	0433153.00	25830224.00
					0.50	37978464.00	0433153.00	41021616.00
					0.70	53169856.00	0433153.00	56213008.00
					1.00	75956944.00	0433153.00	79000096.00
			2.50	LAMINAR	0.10	3350503.00	0433153.00	6393656.00
					0.30	10051507.00	0433153.00	13094660.00
					0.50	16752512.00	0433153.00	19795664.00
					0.70	23453504.00	0433153.00	26496668.00
					1.00	33505024.00	0433153.00	36548176.00
			3.00	LAMINAR	0.10	1717307.00	0433153.00	4760460.00
					0.30	5151921.00	0433153.00	8195074.00
					0.50	8586536.00	0433153.00	11629689.00
					0.70	12021150.00	0433153.00	15064303.00
					1.00	17173072.00	0433153.00	20216924.00
			3.50	LAMINAR	0.10	976395.81	0433153.00	4016956.81
					0.30	2929188.00	0433153.00	5972347.81
					0.50	4686198.00	0433153.00	7922511.81
					0.70	6834776.00	0433153.00	9877722.00
					1.00	9763958.00	0433153.00	12807109.00
			4.00	LAMINAR	0.10	1598999.31	0433153.00	3642152.00
					0.30	4793699.00	0433153.00	4840150.00
					0.50	7934896.00	0433153.00	6038142.00
					0.70	11329994.00	0433153.00	7236147.00
					1.00	15989992.00	0433153.00	9033145.00
			5.00	LAMINAR	0.10	265173.06	0433153.00	330833.06
					0.30	795519.00	0433153.00	383867.00
					0.50	1322586.00	0433153.00	4369018.00
					0.70	18556210.00	0433153.00	4899343.00
					1.00	2651730.00	3043153.00	5694883.00

NEW PARTICLE SIZE DISTRIBUTION WITH DM= 1.46

SURFACE AREA=0.802

PARTICLE SIZE . (MICRONS)	PERCENT ( % )
80.0000	0.0023
52.0000	0.0223
37.0000	0.0715
27.0000	0.1494
19.0000	0.1609
14.0000	0.2023
9.3000	0.1361
6.5000	0.0873
4.7000	0.0639
3.3000	0.0412
2.3000	0.0286
1.5000	0.0151
1.0000	0.0121
0.5000	0.0070

CM	CV	PN	PK	ETA0	EINF	TAUY	B				
0.507	0.460	0.760	136.34	192.73	50.24	16.59	309.59				
SHEAR RATE-G =		1.00	2.00	3.00	4.00	5.00	6.00	7.00	8.00	9.00	10.00
SHEAR STRESS-TAU =		164.41	265.46	346.86	418.16	483.59	545.30	604.51	661.96	718.11	773.29
SHEAR RATE-G =		11.00	12.00	13.00	14.00	15.00	16.00	17.00	18.00	19.00	20.00
SHEAR STRESS-TAU =		827.73	881.57	934.93	987.91	1040.57	1092.96	1145.13	1197.10	1248.91	1300.58
SHEAR RATE-G =		21.00	22.00	23.00	24.00	25.00	26.00	27.00	28.00	29.00	30.00
SHEAR STRESS-TAU =		1352.13	1403.57	1454.91	1506.17	1557.35	1608.47	1659.52	1710.52	1761.47	1812.38
SHEAR RATE-G =		31.00	32.00	33.00	34.00	35.00	36.00	37.00	38.00	39.00	40.00
SHEAR STRESS-TAU =		1863.25	1914.08	1964.87	2015.64	2066.38	2117.09	2167.78	2218.44	2269.08	2319.71
SHEAR RATE-G =		41.00	42.00	43.00	44.00	45.00	46.00	47.00	48.00	49.00	50.00
SHEAR STRESS-TAU =		2370.31	2420.90	2471.48	2522.04	2572.58	2623.11	2673.64	2724.14	2774.64	2825.13

CV (%)	PN	PK	DIAMETER	FLOW	DISTANCE	PUMPING ENERGY	COMMUNITION ENERGY	TOTAL ENERGY
0.460	0.760	136.339	2.00	LAMINAR	0.10	26051808.00	2552041.00	28603840.00
					0.30	78155440.00	2552041.00	80707472.00
					0.50	130259088.00	2552041.00	132811120.00
					0.70	182322720.00	2552041.00	184914752.00
					1.00	260518176.00	2552041.00	263070208.00
			2.50	LAMINAR	0.10	12537329.00	2552041.00	15089370.00
					0.30	37611968.00	2552041.00	40164000.00
					0.50	62686624.00	2552041.00	65238656.00
					0.70	87761280.00	2552041.00	90313312.00
					1.00	125373264.00	2552041.00	127925296.00
			3.00	LAMINAR	0.10	6899364.00	2552041.00	9451405.00
					0.30	20698080.00	2552041.00	23250112.00
					0.50	34496816.00	2552041.00	37048848.00
					0.70	48295536.00	2552041.00	50847568.00
					1.00	68993632.00	2552041.00	71545664.00
			3.50	LAMINAR	0.10	4165154.00	2552041.00	6717195.00
					0.30	12495461.00	2552041.00	15047502.00
					0.50	20825760.00	2552041.00	23377792.00
					0.70	29156064.00	2552041.00	31708096.00
					1.00	41651536.00	2552041.00	44203568.00
			4.00	LAMINAR	0.10	2690979.00	2552041.00	5243020.00
					0.30	8072937.00	2552041.00	10624978.00
					0.50	13454896.00	2552041.00	16006937.00
					0.70	18836848.00	2552041.00	21388880.00
					1.00	26909792.00	2552041.00	29461824.00
			5.00	LAMINAR	0.10	1298108.00	2552041.00	3850149.00
					0.30	3894325.00	2552041.00	6446366.00
					0.50	6490541.00	2552041.00	9042582.00
					0.70	9086757.00	2552041.00	11638798.00
					1.00	12981083.00	2552041.00	15533124.00

CM	CV	PN	PK	ETA0	EINF	TAUY	B					
0.507	0.430	0.819	41.24	46.50	18.76	8.25	116.10					
SHEAR RATE-G =		1.00	2.00	3.00	4.00	5.00	6.00	7.00	8.00	9.00	10.00	
SHEAR STRESS-TAU =		49.40	83.31	113.00	140.02	165.25	189.20	212.22	234.55	256.33	277.69	
SHEAR RATE-G =		11.00	12.00	13.00	14.00	15.00	16.00	17.00	18.00	19.00	20.00	
SHEAR STRESS-TAU =		298.71	319.44	339.95	360.26	380.42	400.43	420.33	440.12	459.82	479.45	
SHEAR RATE-G =		21.00	22.00	23.00	24.00	25.00	26.00	27.00	28.00	29.00	30.00	
SHEAR STRESS-TAU =		499.01	518.50	537.95	557.34	576.69	596.00	615.28	634.52	653.73	672.92	
SHEAR RATE-G =		31.00	32.00	33.00	34.00	35.00	36.00	37.00	38.00	39.00	40.00	
SHEAR STRESS-TAU =		692.09	711.23	730.35	749.45	768.53	787.60	806.66	825.69	844.72	863.74	
SHEAR RATE-G =		41.00	42.00	43.00	44.00	45.00	46.00	47.00	48.00	49.00	50.00	
SHEAR STRESS-TAU =		882.74	901.73	920.71	939.69	958.65	977.61	996.56	1015.50	1034.43	1053.36	

CV (%)	PN	PK	DIAMETER	FLOW	DISTANCE	PUMPING ENERGY	COMMUNITION ENERGY	TOTAL ENERGY
0.430	0.819	41.241	2.00	LAMINAR	0.10	13174583.00	2552041.00	15726624.00
					0.30	39523728.00	2552041.00	42075760.00
					0.50	65872896.00	2552041.00	68424928.00
					0.70	92222064.00	2552041.00	94774096.00
			1.00	131745808.00	2552041.00	134297840.00		
			2.50	LAMINAR	0.10	6094198.00	2552041.00	8646239.00
					0.30	18282576.00	2552041.00	20834608.00
					0.50	30470976.00	2552041.00	33023008.00
					0.70	42659376.00	2552041.00	45211408.00
			1.00	60941968.00	2552041.00	63494000.00		
			3.00	LAMINAR	0.10	3247235.00	2552041.00	5799276.00
					0.30	9741705.00	2552041.00	12293746.00
		0.50			16236176.00	2552041.00	18788208.00	
		0.70			22730640.00	2552041.00	25282672.00	
		1.00	32472352.00	2552041.00	35024384.00			
		3.50	LAMINAR	0.10	1907819.00	2552041.00	4459860.00	
				0.30	5723457.00	2552041.00	8275498.00	
				0.50	9539096.00	2552041.00	12091137.00	
				0.70	13354734.00	2552041.00	15906775.00	
		1.00	19078192.00	2552041.00	21630224.00			
		4.00	LAMINAR	0.10	1204064.00	2552041.00	3756105.00	
				0.30	3612193.00	2552041.00	6164234.00	
				0.50	6020322.00	2552041.00	8572363.00	
				0.70	8428451.00	2552041.00	10980492.00	
		1.00	12040645.00	2552041.00	14592686.00			
		5.00	LAMINAR	0.10	558778.69	2552041.00	3110819.00	
				0.30	1676335.00	2552041.00	422837.00	
				0.50	2793893.00	2552041.00	534593.00	
				0.70	3911450.00	2552041.00	6463491.00	
		1.00	5587786.00	2552041.00	8139827.00			



CM	CV	PN	PK	ETA0	EINF	TAUY	B					
0.507	0.384	0.886	12.54	12.81	7.42	3.67	38.60					
SHEAR RATE-G =		1.00	2.00	3.00	4.00	5.00	6.00	7.00	8.00	9.00	10.00	
SHEAR STRESS-TAU =		15.82	26.94	37.33	47.19	56.64	65.78	74.68	83.39	91.94	100.35	
SHEAR RATE-G =		11.00	12.00	13.00	14.00	15.00	16.00	17.00	18.00	19.00	20.00	
SHEAR STRESS-TAU =		108.65	116.86	125.00	133.06	141.07	149.02	156.94	164.81	172.64	180.45	
SHEAR RATE-G =		21.00	22.00	23.00	24.00	25.00	26.00	27.00	28.00	29.00	30.00	
SHEAR STRESS-TAU =		188.23	195.98	203.71	211.42	219.12	226.79	234.46	242.10	249.74	257.36	
SHEAR RATE-G =		31.00	32.00	33.00	34.00	35.00	36.00	37.00	38.00	39.00	40.00	
SHEAR STRESS-TAU =		264.97	272.57	280.17	287.75	295.33	302.90	310.46	318.01	325.56	333.11	
SHEAR RATE-G =		41.00	42.00	43.00	44.00	45.00	46.00	47.00	48.00	49.00	50.00	
SHEAR STRESS-TAU =		340.65	348.18	355.71	363.23	370.76	378.27	385.79	393.30	400.80	408.31	

CV (%)	PN	PK	DIAMETER	FLOW	DISTANCE	PUMPING ENERGY	COMMUNITION ENERGY	TOTAL ENERGY
0.384	0.886	12.539	2.00	LAMINAR	0.10	7742864.00	2552041.00	10294905.00
					0.30	23228576.00	2552041.00	25780608.00
					0.50	38714304.00	2552041.00	41266336.00
					0.70	54200032.00	2552041.00	56752064.00
					1.00	77428624.00	2552041.00	79980656.00
			2.50	LAMINAR	0.10	3426216.00	2552041.00	5978257.00
					0.30	10278648.00	2552041.00	12830689.00
					0.50	17131072.00	2552041.00	19683104.00
					0.70	23983504.00	2552041.00	26535536.00
					1.00	34262160.00	2552041.00	36814192.00
			3.00	LAMINAR	0.10	1760672.00	2552041.00	4312713.00
					0.30	5282016.00	2552041.00	7834057.00
					0.50	8803360.00	2552041.00	11355401.00
					0.70	12324703.00	2552041.00	14876744.00
					1.00	17606720.00	2552041.00	20158752.00
			3.50	LAMINAR	0.10	1003251.31	2552041.00	3555292.00
					0.30	3009753.00	2552041.00	5571794.00
					0.50	5016255.00	2552041.00	7568296.00
					0.70	7022757.00	2552041.00	9574798.00
					1.00	10032511.00	2552041.00	12584553.00
			4.00	LAMINAR	0.10	616651.62	2552041.00	3168693.00
					0.30	1849954.00	2552041.00	4401993.00
					0.50	3083257.00	2552041.00	5635293.00
					0.70	4316560.00	2552041.00	6868601.00
					1.00	6166515.00	2552041.00	8718556.00
			5.00	LAMINAR	0.10	871866.94	2552041.00	3225907.00
					0.30	273866.69	2552041.00	3373641.00
					0.50	436933.40	2552041.00	3921375.00
					0.70	5917068.00	2552041.00	4469109.00
					1.00	2738669.00	2552041.00	5290710.00

NEW PARTICLE SIZE DISTRIBUTION WITH DM= 1.56

SURFACE AREA=0.743

PARTICLE SIZE (MICRONS)	PERCENT ( % )
80.0000	0.0010
52.0000	0.0163
37.0000	0.0661
27.0000	0.1540
19.0000	0.1715
14.0000	0.2140
9.3000	0.1396
6.5000	0.0864
4.7000	0.0609
3.3000	0.0377
2.5000	0.0251
1.5000	0.0127
1.0000	0.0096
0.5000	0.0050

CM	CV	PN	PK	ETA0	EINF	TAUY	B					
0.503	0.460	0.758	156.14	244.52	57.94	18.69	321.16					
SHEAR RATE-G =		1.00	2.00	3.00	4.00	5.00	6.00	7.00	8.00	9.00	10.00	
SHEAR STRESS-TAU =		194.65	307.17	396.57	474.98	547.29	615.88	682.02	746.48	809.72	872.06	
SHEAR RATE-G =		11.00	12.00	13.00	14.00	15.00	16.00	17.00	18.00	19.00	20.00	
SHEAR STRESS-TAU =		933.70	994.80	1055.48	1115.80	1175.84	1235.65	1295.25	1354.68	1413.97	1473.14	
SHEAR RATE-G =		21.00	22.00	23.00	24.00	25.00	26.00	27.00	28.00	29.00	30.00	
SHEAR STRESS-TAU =		1532.19	1591.16	1650.04	1708.84	1767.58	1826.27	1884.90	1943.48	2002.03	2060.53	
SHEAR RATE-G =		31.00	32.00	33.00	34.00	35.00	36.00	37.00	38.00	39.00	40.00	
SHEAR STRESS-TAU =		2119.00	2177.44	2235.85	2294.23	2352.59	2410.92	2469.24	2527.53	2585.81	2644.08	
SHEAR RATE-G =		41.00	42.00	43.00	44.00	45.00	46.00	47.00	48.00	49.00	50.00	
SHEAR STRESS-TAU =		2702.32	2760.56	2818.78	2876.98	2935.18	2993.36	3051.54	3109.70	3167.86	3226.01	

CV (%)	PN	PK	DIAMETER	FLOW	DISTANCE	PUMPING ENERGY	COMMUNITION ENERGY	TOTAL ENERGY
0.460	0.758	156.141	2.00	LAMINAR	0.10	29376544.00	2184432.00	31560976.00
					0.30	88129616.00	2184432.00	90314048.00
					0.50	146882688.00	2184432.00	149067120.00
					0.70	205635744.00	2184432.00	207820176.00
					1.00	293765376.00	2184432.00	295949568.00
			2.50	LAMINAR	0.10	14160209.00	2184432.00	16344641.00
					0.30	42480608.00	2184432.00	44665040.00
					0.50	70801024.00	2184432.00	72985456.00
					0.70	99121440.00	2184432.00	101305872.00
					1.00	141602064.00	2184432.00	143786496.00
			3.00	LAMINAR	0.10	7802576.00	2184432.00	9987008.00
					0.30	23407712.00	2184432.00	25592144.00
					0.50	39012864.00	2184432.00	41197296.00
					0.70	54618016.00	2184432.00	56802448.00
					1.00	78025744.00	2184432.00	80210176.00
			3.50	LAMINAR	0.10	4715631.00	2184432.00	6900063.00
					0.30	14146891.00	2184432.00	16331323.00
					0.50	23578144.00	2184432.00	25762576.00
					0.70	33009408.00	2184432.00	35193840.00
					1.00	47156304.00	2184432.00	49340736.00
			4.00	LAMINAR	0.10	3049543.00	2184432.00	5233975.00
					0.30	9148627.00	2184432.00	11333059.00
					0.50	15247712.00	2184432.00	17432144.00
					0.70	21346784.00	2184432.00	23531216.00
					1.00	30495424.00	2184432.00	32679856.00
			5.00	LAMINAR	0.10	1473395.00	2184432.00	3657827.00
					0.30	4420184.00	2184432.00	6604616.00
					0.50	7366974.00	2184432.00	9551406.00
					0.70	10313764.00	2184432.00	12498196.00
					1.00	14733949.00	2184432.00	16918368.00

CM	CV	PN	PK	ETA0	EINF	TAUY	B						
0.503	0.430	0.815	44.62	52.64	20.21	8.97	114.33						
SHEAR RATE-G =		1.00	2.00	3.00	4.00	5.00	6.00	7.00	8.00	9.00	10.00		
SHEAR STRESS-TAU =		54.45	90.77	122.16	150.57	177.06	202.22	226.45	249.98	272.97	295.56		
SHEAR RATE-G =		11.00	12.00	13.00	14.00	15.00	16.00	17.00	18.00	19.00	20.00		
SHEAR STRESS-TAU =		317.81	339.81	361.58	383.18	404.63	425.95	447.16	468.27	489.31	510.28		
SHEAR RATE-G =		21.00	22.00	23.00	24.00	25.00	26.00	27.00	28.00	29.00	30.00		
SHEAR STRESS-TAU =		531.18	552.03	572.83	593.59	614.30	634.99	655.64	676.26	696.86	717.44		
SHEAR RATE-G =		31.00	32.00	33.00	34.00	35.00	36.00	37.00	38.00	39.00	40.00		
SHEAR STRESS-TAU =		737.99	758.53	779.04	799.54	820.02	840.49	860.95	881.40	901.83	922.25		
SHEAR RATE-G =		41.00	42.00	43.00	44.00	45.00	46.00	47.00	48.00	49.00	50.00		
SHEAR STRESS-TAU =		942.67	963.07	983.46	1003.85	1024.23	1044.60	1064.97	1085.33	1105.69	1126.03		

CV (%)	PN	PK	DIAMETER	FLOW	DISTANCE	PUMPING ENERGY	COMMUNITION ENERGY	TOTAL ENERGY
0.430	0.815	44.617	2.00	LAMINAR	0.10	13845184.00	2184432.00	16029616.00
					0.30	41535536.00	2184432.00	43719968.00
					0.50	69225904.00	2184432.00	71410336.00
					0.70	96916256.00	2184432.00	99100688.00
					1.00	138451808.00	2184432.00	140636240.00
			2.50	LAMINAR	0.10	6423670.00	2184432.00	8608102.00
					0.30	19270992.00	2184432.00	21455424.00
					0.50	32118336.00	2184432.00	34302768.00
					0.70	44965680.00	2184432.00	47150112.00
					1.00	64236688.00	2184432.00	66421120.00
			3.00	LAMINAR	0.10	3431282.00	2184432.00	5615714.00
					0.30	10293845.00	2184432.00	12478277.00
					0.50	17156400.00	2184432.00	19340832.00
					0.70	24018960.00	2184432.00	26203392.00
					1.00	34312816.00	2184432.00	36497248.00
			3.50	LAMINAR	0.10	2020165.00	2184432.00	4204597.00
					0.30	6060494.00	2184432.00	8244926.00
					0.50	10100824.00	2184432.00	12285256.00
					0.70	14141153.00	2184432.00	16325585.00
					1.00	20201648.00	2184432.00	22386080.00
			4.00	LAMINAR	0.10	1277293.00	2184432.00	3461725.00
					0.30	3831880.00	2184432.00	6016312.00
					0.50	6386468.00	2184432.00	8570900.00
					0.70	8941055.00	2184432.00	11125487.00
					1.00	12772936.00	2184432.00	14957368.00
			5.00	LAMINAR	0.10	594579.19	2184432.00	2779011.00
					0.30	1783737.00	2184432.00	3968169.00
					0.50	2972895.00	2184432.00	5157327.00
					0.70	4162053.00	2184432.00	6346485.00
					1.00	5945791.00	2184432.00	8130223.00

## REFERENCES

1. Alessandrini, A., I. Kikic and R. Lapasin, "Rheology of Coal Suspensions," *Rheologica Acta*, Vol. 22, pp. 500-504, 1983.
2. Batra, S.K., R. B. Kenney, R. K. Batra and A. O'Toole, "Stability and Rheological Characteristics of Coal-Water Slurry Fuels," Proceedings of the Eight International Technical Conference on Slurry Transportation, pp. 415-422, 1983.
3. Borghesani, A.F., "Concentration-Dependent Behavior of the Shear Viscosity of Coal-Fuel Oil Suspensions," *Rheologica Acta* Vol. 24, No. 2, pp. 189-197, 1985.
4. Botsaris, G. D. and K. N. Astill, "Effect of The Interaction Between Particles On The Viscosity of Coal-Water Slurries," Proceedings of the Sixth International Symposium on Coal Slurry Combustion, 1984.
5. Casassa, E. Z., G. D. Parfitt, A. S. Rao and E. W. Toor, "Rheology of Coal/Water Slurries," Proceedings of the Fifth International Symposium on Coal Slurry Combustion and Technology, April 25-27, 1983.
6. Castillo, C. and M. C. Williams, "Rheology of Very Concentrated Coal Suspensions," *Chemical Engineering Communications*, Vol. 3, pp. 529-547, 1979.
7. Chong, J. S., "The Rheology of Concentrated Suspensions", Ph.D. Dissertation, University of Utah, August 1964.
8. Chong, J. S., E. B. Christiansen and A. D. Baer, " Rheology of Concentrated Suspensions," *Journal of Applied Polymer Science*, Vol. 15, pp. 2007-2021, 1971.
9. Davis, P. K. and P. Shrivastava, "Rheological and Pumping Characteristics of Coal-Water Suspensions," *Journal of Pipelines*, Vol. 3, pp. 97-107, 1982.
10. Dinger, D. R., J. E. Funk Jr. and J. E. Funk Sr., " Rheology of a High Solids Coal-Water Mixture : CO-AL," Proceedings of the Fourth International Symposium on Coal Slurry Combustion, May 10-12, 1982.
11. Eilers, H., "Die Viskositat von Emulsionen Hochviskoser Stoffe als Funktion der Konzentration," *Kolloid-Zeitschrift* Band 97, Heft 3, 1941.
12. Eirich, F. R., Editor, *Rheology* , 1, Academic Press, New York, 1956.
13. Ekmann, J. M., "Stability and Flow Properties of Alternate Fuel Mixtures - A Review," Proceedings of the 21. Annual Meeting, Society of Engineering Science Inc., Virginia Polytechnic Institute and State University, October 15-17, 1984.

14. Farris, R. J., "Prediction of The Viscosity of Multimodal Suspensions From Unimodal Viscosity Data," *Transactions of the Society of Rheology*, Vol. 12, No. 2, pp. 281-301, 1968.
15. Fedors, R. F., "A relationship Between Maximum Packing of Particles and Particle Size," *Powder Technology*, Vol. 22, pp. 71-76, 1979.
16. Ferrini, F., D. Ercolani, B. de Cindio, L. Nicodemo, L. Nicolais and S. Ranaudo, "Shear Viscosity of Settling Suspensions," *Rheologica Acta*, Vol. 18, No. 2, pp.289-296, 1979.
17. Ferrini, F., V. Battarra, E. Donati and C. Piccinini, "Optimization of Particle Grading for High Concentration Coal Slurry," *Hydrotransport 9*, Paper B2, October 1984.
18. Frankel, N. A. and A. Acrivos, "On The Viscosity of a Concentrated Suspension of Solid Spheres," *Chemical Engineering Science*, Vol. 22, pp. 847-853, 1967.
19. Funk, J. E., D. R. Dinger, J. E. Funk Jr. and D. F. Funk, "Preparation and Combustion of a High Solids Coal Water Fuel/CO-AL," DoE Workshop on Coal-Water Fuel Technology, March 19-20, 1981.
20. Funk, J. E., D. R. Dinger, J. E. Funk Jr. and D. R. Dinger, "Measurement of Stability of Highly Loaded CWM," Proceedings of the Sixth International Symposium on Coal Slurry Combustion and Technology, Orlando, Florida, June 25-27, 1984.
21. Furnas, C. C., "Grading Aggregates," *Industrial and Engineering Chemistry*, Vol. 23, No. 9, pp. 1052-1058, September 1931.
22. Gay, E. C., "Flow Properties of Liquid Sodium Suspensions With High Solid Concentration" , Ph.D. Dissertation, Washington University, St. Louis, Missouri, June 1967.
23. Gay, E. C., P. A. Nelson and W. P. Armstrong, "Flow Properties of Suspensions With High Solids Concentration," *AIChE Journal*, Vol 15, No. 6, November 1969.
24. Ghosh, A. K. and S. N. Bhattacharya, "Rheological Study of Black Coal-Oil Suspensions," *Rheologica Acta*, Vol. 23, No. 2, pp. 195-206, 1984.
25. Gillespie, T., "An Extension of Goodeve's Impulse Theory of Viscosity to Pseudoplastic Systems," *Journal of Colloid Science*, Vol. 15, pp. 219-231, 1960.
26. Gleissle, W. and M. K. Baloch, "Flow Behaviour of Concentrated Suspensions At High Shear Stresses and Shear Rates," Proceedings of the Eight International Technical Conference on Slurry Transportation, pp. 103-109, 1983.
27. Goodeve, C. F., "A General Theory of Thixotropy and Viscosity," *Transactions of the Faraday Society*, Vol. 35, 1939.
28. Govier, G. W and K. Aziz, The Flow of Complex Mixtures in Pipes , Van Nostrand Reinhold Co., 1972.
29. Hanks, R. W. and Aude, T. C., Slurry Pipeline Hydraulics and Design , Published Jointly by R. W. Hanks Associates, Inc. and Pipeline Systems Incorporated, 1982.

30. Henderson, C. B. and R. S. Scheffee, "The Optimum Particle Size Distribution of Coal for Coal-Water Slurries," Preprints Vol. 28, No. 2, Division of Fuel Chemistry, American Chemical Society, 1983.
31. Henderson, C. B., R. S. Scheffee and E. T. McHale, "Coal- Water Slurries--A Low cost Liquid Fuel For Boilers," *Energy Progress*, Vol. 3, No. 2, June 1983.
32. Hukki, R.T., "The Principles of Comminution: An Analytical Summary," *Engineering and Mining Journal*, Vol. 176, pp. 106-110, May 1985.
33. Jiang, L., H. Yun and L. Zhang, "Role of Shape and Size of Particles In The Preparation of Highly Loaded Coal-Water Slurry," Proceedings of the Sixth International Symposium on Coal Slurry Combustion and Technology, Orlando, Florida, June 25-27, 1984.
34. Kao, V. S., L. E. Nielsen and C. T. Hill, "Rheology of Concentrated Suspensions of Spheres-1. Effect of the Liquid-Solid Interface," *Journal of Colloid and Interface Science*, Vol. 53, No. 3, pp. 358-366, December 1975.
35. Klimpel, R. R., "Laboratory Studies of The Grinding and Rheology of Coal-Water Slurries," Proceedings of the Fourth International Symposium on Coal Slurry Combustion, Orlando, Florida, May 10-12, 1982.
36. Krieger, I. M., "Rheology of Monodisperse Latices," *Advances in Colloid and Interface Science*, Vol. 3, pp. 111-136, 1972.
37. Krieger, I. M. and T. J. Dougherty, "A Mechanism for non-Newtonian Flow in Suspensions of Rigid Spheres," *Transactions of the Society of Rheology*, Vol. 3, pp.137-152, 1959.
38. Landel, R. F., B. G. Moser and A. J. Bauman, "Rheology of Concentrated Suspensions: Effect of a Surfactant," Proceedings of the Fourth International Congress on Rheology, 663, 1965.
39. Lee, D. I., "Packing of Spheres And Its Effect On the Viscosity of Suspensions," *Journal of Paint Technology*, Vol. 42, No. 550, pp. 579-587, November 1970.
40. Lewis, T. B. and L. E. Nielsen, "Viscosity of Dispersed and Aggregated Suspensions of Spheres," *Transactions of the Society of Rheology*, Vol. 12, No. 3, pp. 421-443, 1968.
41. Manley, R. St. J. and S. G. Mason, "Particle Motions in Sheared Suspensions. II. Collisions of Uniform Spheres," *Journal of Colloid Science* Vol. 7, pp. 354-369, 1952.
42. Marvin, D. C. and T. C. Frankiewicz, "CWS Rheology: The Role of The Coal Particle," Preprints Vol. 28, Division of Fuel Chemistry, American Chemical Society, 1983.
43. McGeary, R. K., "Mechanical Packing of Spherical Particles," *Journal of the American Ceramic Society*, Vol. 44, No. 10, October 1961.
44. Metzner, A. B., "Non-Newtonian Fluid Flow," *Industrial and Engineering Chemistry*, Vol. 49, No. 9, pp. 1429-1432, September 1957.

45. Metzner, A. B. and J. C. Reed, "Flow of non-Newtonian Fluids - Correlation of the Laminar, Transition and Turbulent Flow Regimes," *A.I.Ch.E. Journal*, Vol. 1, No. 4, pp. 434-440, December 1955.
46. Moreland, C., "Viscosity of Suspensions of Coal in Mineral Oil," *Canadian Journal of Chemical Engineering*, pp. 24-28, February 1963.
47. Nicodemo, L. and L. Nicolais, "Viscosity of Concentrated Fiber Suspensions," *Chemical Engineering Journal*, Vol. 8, pp. 155-156, 1974.
48. Nicodemo, L., L. Nicolais and R. F. Landel, "Shear Rate Dependent Viscosity of Suspensions in Newtonian and Non-Newtonian Liquids," *Chemical Engineering Science*, Vol. 29, pp. 729-735, 1974.
49. Pal, R. and E. Rhodes, "A Novel Viscosity Correlation for non-Newtonian Concentrated Emulsions," *Journal of Colloid and Interface Science*, Vol. 107, No. 2, pp. 301-307, October 1985.
50. Patton, T. C., Paint Flow and Pigment Dispersion, John Wiley & Sons, 1979.
51. Priggen, K. S., R. S. Scheffee and E. T. McHale, "Pipelining of High-Density Coal-Water Slurry," Proceedings of the Ninth International Technical Conference on Slurry Transportation, pp. 141-146, March 1984.
52. Round, G. F. and A. R. Hessari, "The effect of Size Distribution and pH on the Rheology of Coal slurries," Proceedings of the Tenth International Technical Conference on Slurry Technology, Lake Tahoe, March 1985.
53. Smith, T.L., "Rheological Properties of Dispersions of Particulate Solids in Liquid Media," *Journal of Paint Technology*, Vol. 44, No. 575, December 1972.
54. Sweeny, K. H. and R. D. Geckler, "The Rheology of Suspensions," *Journal of Applied Physics*, Vol. 25, No. 9, September 1954.
55. Thomas, D. G., "Transport Characteristics of Suspension: VIII. A Note on The Viscosity of Newtonian Suspensions of Uniform Spherical Particles," *Journal of Colloid Science*, Vol. 20, pp. 267-277, 1965.
56. Thomas, D. G., "Transport Characteristics of Suspensions: VII. Relation of Hindered-Settling Floc Characteristics to Rheological Parameters," *AICHE Journal*, pp. 310-316, May 1963.
57. Vand, V., "Viscosity of Solutions and Suspensions," *Journal of Physical and Colloidal Chemistry*, Vol. 52, 277, 1948.
58. Wildemuth, C. R. and M. C. Williams, "Viscosity of Suspensions Modeled with a Shear-Dependent Maximum Packing Fraction," *Rheologica Acta*, Vol. 23, No. 6, pp. 627-635, 1984.
59. Wildemuth, C. R. and M. C. Williams, "A New Interpretation of Viscosity and Yield Stress in Dense Slurries: Coal and Other Irregular Particles," *Rheologica Acta*, Vol. 24, No. 1, pp. 75-91, 1985.
60. Williams, P. S., "Flow of Concentrated Suspensions," *Journal of Applied Chemistry*, Vol. 3, pp. 120-128, March 1953.



61. Wills, B. A., Mineral Processing Technology , 3rd Edition, Pergamon Press, New York, 1985
62. Zenz, F. A. and D. F. Othmer, Fluidization and Fluid-Particle Systems, Reinhold Publication Corp., New York, 1960.

**The vita has been removed from  
the scanned document**